BEHAVIOUR OF HIGH PERFORMANCE CONCRETE EXPOSED TO ELEVATED TEMPERATURES

Ph.D. THESIS

by

ABDUL RAHIM. A

DEPARTMENT OF CIVIL ENGINEERING
INDIAN INSTITUTE OF TECHNOLOGY ROORKEE
ROORKEE – 247 667 (INDIA)
AUGUST, 2013

BEHAVIOUR OF HIGH PERFORMANCE CONCRETE EXPOSED TO ELEVATED TEMPERATURES

A THESIS

Submitted in partial fulfilment of the requirements for the award of the degree of

DOCTOR OF PHILOSOPHY
in
CIVIL ENGINEERING

by

ABDUL RAHIM. A

DEPARTMENT OF CIVIL ENGINEERING
INDIAN INSTITUTE OF TECHNOLOGY ROORKEE
ROORKEE - 247667 (INDIA)
AUGUST, 2013

INDIAN INSTITUTE OF TECHNOLOGY ROORKEE
ROORKEE

CANDIDATE'S DECLARATION

I hereby certify that the work which is being presented in the thesis entitled **"BEHAVIOUR OF HIGH PERFORMANCE CONCRETE EXPOSED TO ELEVATED TEMPERATURES"** in partial fulfilment of the requirements for the award of the Degree of Doctor of Philosophy and submitted in the Department of Civil Engineering of the Indian Institute of Technology Roorkee is an authentic record of my own work carried out during a period from July, 2009 to August, 2013 under the supervision of Dr. Umesh Kumar Sharma, Associate Professor, Department of Civil Engineering and Dr. Krishnan Murugesan, Associate Professor, Department of Mechanical and Industrial Engineering, Indian Institute of Technology Roorkee, Roorkee, India.

The matter presented in this thesis has not been submitted by me for the award of any other degree of this or any other Institute.

(**ABDUL RAHIM. A**)

This is to certify that the above statement made by the candidate is correct to the best of our knowledge.

(Krishnan Murugesan) Supervisor

(Umesh Kumar Sharma) Supervisor

Date: _____

The Ph.D. Viva-Voice examination of **Mr. ABDUL RAHIM. A**, Research Scholar, has been held on_____

Signature of Supervisors Chairman, SRC Signature of External Examiner

Head of the Deptt./Chairman, ODC

ABSTRACT

When the concrete is submitted to high temperatures, a series of physical and chemical changes take place, which result in a complex thermal behaviour in the multi-phase nature of hardened concrete. The unwanted heating may cause large volume changes due to thermal dilation, shrinkage due to moisture migration, eventual spalling due to high thermal stresses. The differential thermal volume changes produce stresses that results micro cracking and large fractures which may finally lead to structural failure. Previous studies indicate that the properties of concrete at high temperatures are influenced by many internal and external parameters, such as properties of mix constituents, mineral and chemical admixtures, type of aggregates, concrete strength and grade, mixture constituents, heating rate, cooling rate, peak temperature, size and shape of member and testing methods. Among the notable revolutionary developments in the field of concrete technology over the last few decades, high performance concrete (HPC) is considered to be a construction material with variety of applications. The HPC has found its use in concrete structures such as nuclear reactor vessels, clinker silos of cement plants, metallurgical and chemical industrial structures, glass making industrial structures, storage tanks for hot crude oils, coal gasification and liquefaction vessels, reinforced concrete chimneys, high rise buildings etc. Often these modern concrete structures may get subjected to elevated temperatures due to exposure to an aggressive fire or other heat source. A review of the existing literature indicates that only few studies were undertaken on the influence of elevated temperature on the behaviour of HPC and the research in this area is inconclusive.

It is now well established that the inclusion of mineral admixtures in a concrete mix is generally an essential condition for obtaining high performance concrete (HPC). However, a review of the existing literature shows that the behaviour of HPC is more sensitive to high temperature conditions than a normal concrete mix, though there are conflicting conclusions about the role of mineral admixture on the performance of heated high performance concrete. While some studies report that the inclusion of mineral admixtures, especially silica fume, enhances the chances of sudden explosive spalling during heating, some other studies report that the addition of fly ash, ground granulated blast furnace slag (GGBFS) etc. may be beneficial to the post-fire strength properties of HPC. Most of the earlier investigations related to fire induced spalling of concrete were

undertaken on small scale un-reinforced cubes or cylinders without any pre-load. It may be mentioned here that the presence of a pre-load and the reinforcing bars, especially confining reinforcement, are expected to influence the spalling and other mechanical properties of concrete exposed to fire scenarios. Thus there is a need to investigate the spalling and mechanical properties of high performance concrete under stressed residual conditions.

This study was aimed to investigate the role of various concrete mix parameters on the residual compressive strength of pozzolanic concretes after exposing to various elevated temperatures. The experimental variables of the study were the type of high performance concrete (plain HPC, silica fume HPC, fly ash HPC and GGBFS HPC), their mix constituents and five different target temperatures (room temperature, 200 °C, 400 °C, 600 °C and 800 °C). A large number of trial experiments are usually required to deal with such cases where the number of variables and mix combinations become worth investigating. However, a good mix proportioning procedure has to minimize the number of trial mixes and achieve an economical and satisfactory mixture with desired properties. In view of this the design of experiment (DoE) methods and optimization tools are generally used to fix-up a suitable mixture combination for getting the targeted requirements. For this purpose, the design of experiments based on Taguchi method was formulated considering four parameters (mix constituents) at three levels with an aim to achieve maximum compressive strength using larger-the-better criterion. A total of 756 cubic specimens (100 mm × 100 mm × 100 mm) of different types of high performance concretes were cast and tested under this study. The cubic specimens were first exposed to temperatures ranging from room temperature to 800 °C and then they were tested under axial compression after complete cooling. Using the resulting mix parameter design, the experiments were carried out and the results were analyzed statistically by analysis of variance (ANOVA) to find out the significant factors affecting the residual compressive strength of HPC. While the best mono mix combination for each target temperature was established by Taguchi's technique, an overall most excellent single concrete mix combination was obtained by using the utility concept. The results show that the residual strength of HPC largely remains unaffected and rather it increases up to a temperature of exposure of 400 °C irrespective of the type of pozzolana and other mix parameters considered in this study. It is only in the temperature range of 600 to 800 °C that a noticeable degradation in the compressive strength of high performance concrete is

observed. The results also showed that the mix parameters change their influence with the change in temperature of exposure on the residual compressive strength. The results of this study would help in designing HPC mixes for concrete structures liable to be exposed to elevated temperatures.

The experimental program was planned to explore the effects of high temperatures on the spalling, residual strength and deformation behaviour of reinforced high performance concrete short columns exposed to elevated temperatures ranging from room temperature to 800 °C. A total of 108 numbers of tie confined short cylindrical column specimens of size 150 mm diameter and 450 mm height were cast and tested. The three pozzolanic HPC mixes and one non-pozzolanic high performance concrete mix optimized in the study as reported in the previous section were used here to cast confined cylindrical concrete specimens. The experimental variables included type of HPC based on mineral admixture (silica fume (SF), fly ash (FA) and ground granulated blast furnace slag (GGBFS) and control plain HPC), the different target temperatures of exposures (Room temperature, 200 °C, 400 °C, 600 °C and 800 °C) and the two test methods (unstressed residual and stressed residual strength test). The effects of variables were studied and quantified in terms of spalling, residual strength and ductility. The results indicate that the detrimental effects of temperature on the spalling behaviour of pozzolanic and non-pozzolanic reinforced HPC do not matter much up to a temperature of 400 °C. However, an exposure to further higher temperatures such as 600 °C and 800 °C, the thermal spalling of HPC occurs irrespective of the type of pozzolana. The silica fume HPC is more vulnerable to spalling than fly ash and GGBFS HPC. Non-pozzolanic HPC is least influenced by thermal spalling. The presence of axial load on HPC during heating results in to more severe spalling compared to the HPC specimens with no load during heating. The results show that though the severe explosive spalling of core concrete is saved by providing the confining reinforcement, the cover is still liable to be spalled. The results indicate that the exposure of up to 400 °C temperature does not affect much the residual strength of HPC irrespective of type of HPC and type of test (unstressed or stressed). Rather a strength gain of about 6 to 16% was noted in this temperature range in some of the specimens. Beyond the temperature of 400 °C, most of the concretes showed thermal spalling of cover concrete and resulting drop in compressive strength of specimens. The reinforced HPC specimens exposed to 800 °C temperatures showed 0.34 to 0.42 times of original unheated concrete strength. The influence of pre-load during heating was to

reduce the residual load carrying capacity of reinforced HPC short columns, especially at temperatures of more than 400 °C. The results indicated that the strain ductility of HPC specimens also got influenced when the temperature was increased from room temperature to 800 °C. The influence of high temperature was more pronounced at temperatures more than 400 °C. The specimens tested under unstressed residual test conditions showed higher average strains than those tested under preloaded test conditions. The fly ash HPC had shown highest strain values among all the HPCs, on the other hand the silica fume HPC showed the lowest strain values.

The part of this study presents effects of high temperatures on the thermal properties of different types of high performance concretes. The thermal properties namely thermal conductivity, specific heat, thermal expansion and mass loss were employed in this study. For thermal conductivity test, a total of 12 sets of three different types of pozzolanic high performance concretes and one plain HPC were cast. The specimens were in the shape of rectangular prisms of size 200 mm ×100 mm × 75 mm. For coefficient of thermal expansion test, cylindrical cores of 8 mm diameter and 25 mm length were cut from 100 mm cubes using special core cutting tool. Twelve samples were prepared from these cylindrical cores for evaluating thermal expansion using the dilatometric apparatus. The differential scanning calorimetry (DSC) and thermo gravimetric analysis test (TGA) were used for measuring the specific heat capacity and mass loss of HPC mixes at elevated temperatures. The above said experiments were performed from room temperature to pre-defined target high temperatures. While the specific heat capacity, thermal expansion and mass loss tests were carried out up to 1000 °C temperature, the thermal conductivity experiments could be performed up to 700 °C. The results indicate that the thermal properties of high performance concrete change with the increase in temperature. With the gradual increase of temperature up to 400 °C, all HPC mixes indicated continuously decreasing thermal conductivity values. Further increase of the temperatures, ranging between 400 °C and 700 °C, all the pozzolanic and non-pozzolanic high performance concretes showed an increase in thermal conductivity. The differential scanning calorimetry plots of plain HPC and pozzolanic high performance concretes revealed that the specific heat capacity of all types of concretes indicated almost similar trend up to 750 °C, however above 750 °C, all types of concretes varied widely. Silica fume based HPC showed maximum specific heat in this temperature range up to 1000 °C. The dilatometric curves showed steady increase of thermal strain

from room temperature to 550 °C; thereafter the thermal expansion became constant from 600 °C to 900 °C before rising again up to 1000 °C. The thermal expansion results show that the GGBFS HPC had the highest thermal expansion and the fly ash HPC exhibited lowest thermal strain values. When the temperature was increased to 1000 °C, all concretes showed rising trend and maximum thermal strain and expansion coefficients were found in this temperature range. The results of gravimetric analysis showed that the loss in mass increased and the resulting mass decreased as the temperature increased. All the four HPC mixes showed almost similar kind of trends and sudden loss in mass was observed in temperatures ranges of 100-200 °C, 400- 440 °C and 600-700 °C. The mass gradually decreased with the increase in temperature up to 700 °C and thereafter remained stable at higher temperatures.

CHAPTER - 1

INTRODUCTION

The concrete structures may be subjected to elevated temperatures due to a destructive fire or thermal accident. Generally, the reinforced concrete structures behave well in fire and exhibit reasonably high thermal resistance to thermal attack. However, an unwanted heating either from heat or fire sources may sometimes cause serious deterioration of concrete properties such as large volume changes due to thermal dilation, shrinkage because of moisture movement and thermal stresses due to temperature gradients. Significant changes may occur in the composition of concrete due to high temperature that may lead to degradation of mechanical properties and durability. Many material parameters such as constituents of concrete mix, properties of the constituents, grade of concrete and shape and size of member, and fire parameters such as heating rate, peak temperature, cooling rate, methods of heating and cooling etc. influence the behavior of concrete at high temperatures. The majority of concrete structures are not destroyed in a fire or under thermal exposure, and so one of the major advantages of using concrete is that it can usually be repaired and reused afterwards. The evaluation of structure after the fire or high temperature is necessary to ascertain the residual strength capacity level and sustainability in spite of the mechanical decay of materials. After the fire, it is important to ascertain the residual structural capacity of structural members and thus knowing the residual mechanical and thermal properties of concrete becomes important.

Among the notable revolutionary developments in the field of concrete technology, varieties of specialized series of concretes have been developed over the last few decades to enhance the durability and functional requirements of concrete. One such relatively recently developed concrete known as high performance concrete (HPC) is considered to be a construction material with variety of applications. The HPC has found its use in concrete structures such as nuclear reactor vessels (Basu et al. 1999), clinker silos of cement plants, metallurgical and chemical industrial structures, glass making industrial structures, storage tanks for hot crude oil, coal gasification and liquefaction vessels, reinforced concrete chimneys, high rise buildings, bridges etc (Kamita 2000). All these modern HPC structures are liable to be exposed to high temperatures.

1.1 HIGH PERFORMANCE CONCRETE

Basically concrete is not simply a mixture of cement, water and aggregates, rather it is a heterogeneous composite construction material. The modern concrete is more complex and very often contains various mineral admixtures and chemical admixtures to improve certain specific characteristics of concrete. Such admixture based concretes possess better properties compared to normal concrete in many aspects at ambient temperature. In recent times, the construction industry is showing significant interest in the usage of High Performance Concrete (HPC) for added fast track construction practices. High performance concrete means concrete with high strength or low permeability and higher durability. The high strength requires lesser volume of pores. The only way to have lesser volume of pore is to have the mix containing particles graded down to the finest size. According to the definition of American Concrete Institute (ACI), "High performance concrete is a concrete meeting special combinations of performance and uniformity requirements that cannot be achieved routinely using conventional constituents and normal mixing, placing, and curing practices" (Aitcin, 1998). HPC is not fundamentally different from the concrete that we have been using since the time immemorial. The ingredients of concrete are the same in both cases, but HPC is made with appropriately and carefully selected high quality ingredients combined with selected mix design of lower water-cementitious materials or water-binder ratio, with inclusion of high binder content including pozzolanas (fly ash, silica fume, blast furnace slag, rice husk, metakaolin and natural pozzolanas) and chemical admixtures (Aitcin, 1998, Russell 1999). HPC possesses superior performance characteristics than normal strength concrete (NSC) in many aspects namely higher compressive strength, higher modulus of elasticity and thinner paste - aggregate zone, better durability and workability and hence provides good durable long lasting and serviceable concrete.

1.2 BEHAVIOUR OF CONCRETE STRUCTURES SUBJECTED TO HIGH TEMPERATURES

Under an unexpected event of accidental fire or thermal exposure on concrete buildings or structural systems, the concrete would suffer from degradation of mechanical properties and durability, which is attributed to serious physical, complex chemical changes in composition and micro structural changes in the concrete. The extent of deterioration in material properties of concrete and loosening of the structural integrity of structural elements has increased the attention on thermal behavior of residential and

industrial structures. For evaluating the fire resistance of structural members the temperature distributions within the members is to be established. The temperature distribution within the member is mainly dependent on the thermal properties of concrete namely; thermal conductivity, specific heat capacity, thermal diffusivity, thermal expansion and mass loss and these are being used as function of temperature dependent properties. These temperature dependent mechanical and material specific properties are most important for understanding, establishing and evaluating the fire response of RC structural members exposed to fire.

It is now known that the fire performance of high performance concrete (HPC) is different from the normal strength concrete (NSC) and the HPC exhibits poor performance than NSC under fire situations. The behaviour of HPC is more sensitive to high temperature conditions and HPC is expected to get explosive spalling because of highly dense micro-structure and reduced porosity. The penetration of heat towards the core may result in high thermal gradients due to high and rapid rising temperature on the surface of structural members and is responsible for quick increase in internal thermal stresses and the pore pressure. The quick development of thermal gradients depends upon different thermal properties of concrete mix constituents. When the developed pore pressure exceeds the maximum allowable tensile strength of concrete, it could result in explosive spalling. Explosive spalling of concrete is the most complex and critical phenomenon and is poorly understood. The explosive spalling may seriously affect the physical strength of structural elements by reducing its cross-sections and results in the reduction of its load carrying capacity. This may lead to severe reduction in fire resistance of the structural members and also create the threat on the integrity of the whole structure. Eventually, the whole structural collapse may occur. Some studies have indicated that the effects of loading influence significantly the spalling and thus reduce the fire endurance of structural members during heating. The structural capacity of RC member decreases with increase of fire exposure duration and loss of integrity occurs when the imposed service load becomes comparable or exceeds the reduced strength of the member due to fire. The thermal performance of high performance concrete under elevated temperature exposure is very complicated and difficult to characterize. At high temperatures, deterioration in mechanical properties is highly influenced by the composition of mix constituents. The mix parameters of concrete influence the residual compressive strength of concrete considerably after exposure to elevated temperatures. The inclusion of

mineral admixtures in concrete is well established to improve the mechanical properties, performance characteristics and durability of high performance and high strength concretes. However, a review of the existing literature shows that the behaviour of HPC is more sensitive to high temperature conditions than a normal concrete mix, though there are conflicting conclusions about the role of mineral admixture on the performance of heated high performance concrete. While some studies report that the inclusion of mineral admixtures, especially silica fume, enhances the chances of sudden explosive spalling during heating, some other studies report that the addition of fly ash, ground granulated blast furnace slag (GGBFS) etc. may be beneficial to the post-fire strength properties of HPC. A detailed literature review presented in the next chapter brings out the key issues concerning the behavior of HPC exposed to elevated temperatures. The literature review shows that the research in this area is still not conclusive and there are many unresolved issues. In view of this, the present study attempts to investigate conclusively the residual material and structural behavior of high performance concrete subjected to elevated temperatures.

1.3 OBJECTIVES

The following are the key objectives of the present research work:

(i) To investigate the influence of high temperatures on the residual mechanical properties of high performance concrete containing different mineral admixtures namely silica fume, fly ash, and GGBFS.

(ii) To determine the most influential mix parameters affecting the residual compressive strength of HPC and there-by to propose optimum HPC mixes.

(iii) To investigate the spalling and residual mechanical behaviour of reinforced high performance concrete under unstressed and stressed residual test conditions.

(iv) To establish the thermal properties of HPC exposed to elevated temperatures.

1.4 SCOPE AND METHODOLOGY

The proposed research work planned in the present study primarily involves casting and testing of cubes and short columns of reinforced high performance concrete under thermal loading and subsequently testing for axial compression loads. The experimental work reported in this thesis has been undertaken in the following phases:

Multi-response optimization of residual compressive strength of heated high performance concrete:

This study is aimed to investigate the role of various concrete mix parameters on the residual compressive strength of pozzolanic concretes (silica fume, fly ash, and ground granulated blast furnace slag etc.) after exposing to various elevated temperatures. The design of experimental techniques like Taguchi method and Utility concept are proposed to be employed for optimizing the HPC mix proportions.

The following procedure was employed to achieve the objectives of the proposed research in the first part:

(i) The concrete was made with ordinary Portland cement, siliceous aggregate with nominal size of 12.5 mm, and natural graded river sand as fine aggregates.

(ii) The experimental variables of the study were the types of high performance concrete, plain HPC, silica fume HPC, fly ash HPC and GGBFS HPC, their mix constituents and five different target temperatures, room temperature, 200 °C, 400 °C, 600 °C and 800 °C.

(iii) A total of 756 numbers of three different HPC's with plain control concrete of 100 mm × 100 mm ×100 mm cube specimens were cast to investigate and maximize the residual compressive strength of concrete exposed to different target temperatures. Each specimen was cast in triplicate in order to reduce statistical uncertainties associated with testing of concrete.

(iv) After aging of 28 days, the specimens were heated in an electrical high temperature furnace of size (600 × 600 × 450 mm) in groups of four and subjected to temperatures ranging from 200 °C to 800 °C in the increment of 200 °C. For each specimen exposed to high temperature, the target temperature was maintained for 2 hours to obtain steady state condition. After that cooling was allowed to take place in natural condition without any restriction or control.

(v) After complete cycle of heating and cooling, the specimens were tested under uni-axial compression testing machine. Then the significant factors that affect residual compressive strength of HPC were identified. Again, the specimens were cast with identified factors to confirm the results.

Behaviour of reinforced high performance concrete under stressed residual test conditions:

This section describes the experimental program planned to explore the effects of elevated temperature on spalling, residual strength and uni-axial load-displacement behaviour of reinforced and confined high performance concrete (HPC) short columns to elevated temperatures ranging from room temperature to 800 °C. The above objective was achieved by using the following procedure:

(i) The present investigation was formulated using the results of statistically optimized HPC mixes. Short column specimens of reinforced HPC were cast and tested.

(ii) The specimens were instrumented with sufficient numbers of thermocouples before the casting in order to determine the temperature changes in the specimens throughout the tests.

(iii) A total of 108 number of tie confined short cylindrical column specimens of size 150 mm diameter and 450 mm height were cast and tested. The three pozzolanic HPC mixes and one non-pozzolanic high performance concrete mix optimized in the study reported in the previous section were used here to cast confined cylindrical concrete specimens.

(iv) The experimental variables included the type of HPC based on mineral admixture (silica fume (SF), fly ash (FA) and ground granulated blast furnace slag (GGBFS) and control plain HPC), the different target temperatures of exposures (room temperature, 200 °C, 400 °C, 600 °C and 800 °C) and the two test methods (unstressed residual and stressed residual strength test).

(v) After that, at the completion of 90 days age, the specimens were exposed to a complete cycle of thermal loading from room temperature to 800 °C and then subsequent axial compressive testing after cooling to investigate complete residual and residual stressed load-displacement behaviour of confined HPC. The specimens were exposed to five different temperatures ranging from room temperature to 800 °C, room temperature, 200 °C, 400 °C, 600 °C and 800 °C. In this study, heating rate of 5 °C/min was maintained throughout the experimental trials. To reduce statistical uncertainties associated with testing of concrete, each specimen was cast in triplicate.

(vi) The specimens were heated in an electrical high temperature vertical split type muffle furnace of size (230 mm × 230 mm × 600 mm) and subjected to various temperatures ranging up to 800 °C. Before heating, the specimen was loaded with 25% of ultimate load of respective confined HPC specimens; subsequently the load level was maintained to simulate the stressed condition, then the specimen was heated under the same conditions to attain the target temperatures and maintained to obtain steady state, after that the specimen was allowed to cool to normal room temperature. Then the specimens were tested under uni-axial compression testing machine.

Thermal properties of high performance concrete at elevated temperature:

This part of the study presents the effects of high temperatures on the thermal properties of different types of high performance concretes. The following procedure was employed:

(i) For thermal conductivity test, a total of 12 sets of three different types of pozzolanic high performance concretes and one plain HPC were cast.

(ii) The thermal conductivity was measured by hot wire method by using rectangular prisms of size 200 mm × 100 mm × 75 mm. The hot-wire method (parallel) is a transient measuring procedure based on the measurement of the temperature rise at a certain location and at a specified distance from a linear heat source embedded between the two test specimens. The thermal conductivity was measured from room temperature to 700 °C and slow heating rate of 1.67 °C/min was maintained for all the four types of high performance concretes.

(iii) Thermal expansion of high performance concrete was obtained by the dilatometric apparatus. The test samples were cored from concrete cubes of a cylinder size 8 mm diameter and 25 mm long. The test samples were exposed to high temperatures to measure the thermal expansion of HPC concrete from room temperature to 1000 °C.

(iv) Specific heat capacity and mass loss of concrete were measured by differential scanning calorimeter (DSC) and thermogravimetric analyzer (TGA). In this study, 75 micron powder samples were exposed to high temperatures to determine the thermal capacity of concrete from room temperature to 1000 °C.

1.5 ORGANIZATION OF THE THESIS

The entire thesis is divided into six chapters. The **Chapter 1** presents the introduction to the behavior of high performance concrete (HPC) exposed to elevated temperatures and objectives of the dissertation work.

Chapter 2 presents a detailed literature review in the relevant fields of the existing research study. A detailed review on the thermo-mechanical properties and reinforced HPC concrete subjected to elevated temperatures in reference is presented and critically evaluated to establish the need for the present study.

Chapter 3 presents the experimental investigation carried out to optimize the parameters of mix proportion for high performance concrete for post fire residual compressive strength of different pozzolans incorporated high performance concrete exposed to high temperatures. A concise examination of the existing literature on the optimization of mix proportion of HPC using Taguchi method followed by utility concept has been presented. The properties of various constituent materials used and details of the casting and test procedure are presented. The test results have been analyzed and discussed.

Chapter 4 discusses the experimental investigations carried out on the reinforced high performance concrete specimens exposed to elevated temperatures. The details regarding the experimental program undertaken, relevant material properties, specimens details, instrumentation and testing procedure are explained in detail. The residual load-displacement behavior of heated reinforced high performance concrete under uni-axial compression have been presented and analyzed.

Chapter 5 presents the experimental studies on thermal properties of four types of HPC concretes (plain and three different types of mineral admixture based) at elevated temperatures. The main aim of this study is to investigate the thermal behavior of HPC and to formulate the empirical relationships for the thermal properties at elevated temperatures.

Chapter 6 presents the main conclusions of the study.

CHAPTER - 2

LITERATURE REVIEW

2.1 INTRODUCTION

The behavior of high performance concrete exposed to fire is understood to a lesser extent as compared to normal strength concrete. In the recent past, variety of buildings and structures has been constructed using reinforced high performance concrete due to its better mechanical properties and durability. It becomes important to examine the behavior of high performance concrete structures subjected to elevated temperatures due to exposure to an aggressive fire or heat source. This chapter provides a critical review of available literature related to the mechanical and thermal properties of concrete, especially high performance concrete when exposed to high temperatures. Based on the review of the available literature, gaps have been identified and need for the present investigation is highlighted.

2.2 MECHANICAL PROPERTIES OF CONCRETE SUBJECTED TO ELEVATED TEMPERATURES

The heterogeneous nature of porous medium of concrete is very sensitive to unwanted fire or high temperatures conditions. Basically concrete is a multiphase composite material consisting of cement paste and aggregates. The thermal behavior of concrete up to quite high temperatures has been investigated by various researchers and a brief discussion on these literatures is given in the following sections.

2.2.1 Material properties

The initial research activities on high temperature of concrete was coined by Lea and Straddling (Lea 1920, Lea and Straddling 1922) and later this domain was explored by a number of researchers from 1940 onwards (Malhotra 1956, Abrams 1971, Mohamedbhai 1986, Castillo and Durani 1990, Papayianni et al. 1991, Khoury 1992, Sullivan and Sharshar 1992, Sharahar and Khoury 1993, Chan et al. 1996, Felicetti and Gambarova 1998, Kodur and sultan 1998, Phan et al. 1998, Poon et al. 2001, Husem 2006, Arioz 2007, Kodur et al. 2010 and Sharma et al. 2012). However, the initial stage of research had particularly paid attention on the mechanical properties (resistance properties of concrete) and material behavior (chemical and physical changes) of concrete when exposed to high temperature conditions (Malhotra 1956). The existing literature

indicated that the primary changes in the hardened cement matrix and to some extent in aggregates when exposed to high temperatures. At low temperatures, between room temperature to 105 °C, the evaporable water from capillary pores may go off from saturated concrete. Above 105 °C, adsorbed water and chemically bound or hygroscopic water are gradually lost from the cement paste. During heating, the dehydration of the calcium hydroxide starts at about 400 °C, which increases rapidly around 535 °C, and escapes out completely at about 600 °C. A further decomposition of the hardened cement paste takes place between 600 °C and 700 °C mainly due to the phase transformation of the calcium-silicate-hydrate gel (CSH). Commonly, all types of aggregates are thermally stable up to 300 °C to 350 °C. On further increase of the temperature, the siliceous aggregates, especially quartzite, experience phase transformation at approximately 570 °C from α-quartz to β-quartz and on the other hand the calcium carbonate aggregates remain stable up to 850 °C (Harmathy et al. 1973, Hertz 2005, Naus et al. 2006, Seleem et al. 2011). Figure 2.1 shows the physical and chemical deterioration of plain concrete as a function of temperature.

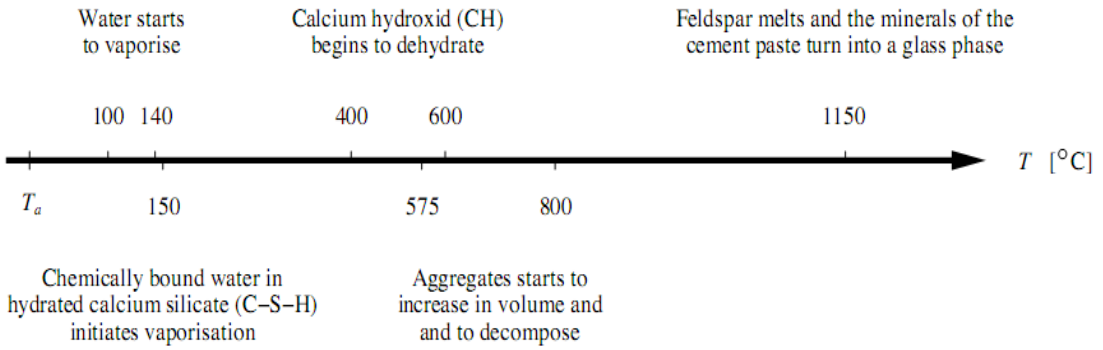

Fig. 2.1 Schematic view of physical and chemical deterioration of plain concrete as a function of temperature (Hertz 2005)

Majority of studies noted that at high temperatures the material parameters and environmental factors are highly influential on the on-fire and post-fire performance of concrete. Small changes in the material composition of concrete also become more sensitive to the performance of concrete at high temperatures (Gustaferro 1966, Khoury 1992, Sarshar and Khoury 1993, Saad et al. 1996, Balendran et al. 2002, Sharma et al. 2013). The main inference from a number of past studies is that the degradation of mechanical properties of concrete exposed to elevated temperatures are affected by a

number of factors such as the constituents of concrete mix, binder materials (cement and mineral admixtures), chemical admixtures, type of aggregates, grade of concrete, size and shape of sections, moisture condition, environmental factors (heating and cooling rate, thermal gradients, duration and maximum temperature), load level, testing condition and number of repeated thermal cycles (Sarshar and Khoury 1993, Khoury 1992, Laskar et al. 2008).

Generally, a few damage mechanisms play vital role on the deterioration of the mechanical properties as well as durability of concrete when subjected to elevated temperatures (Khoury 2000, Hertz 2005, Kaspar et al. 2009). The mechanisms can be categorized as (i) physical-chemical changes taking place in the cement matrix due to dehydration of moisture and other different forms of water; (ii) physical-chemical changes taking place in the aggregates because of movement of moisture at low temperature and phase changes at high temperatures due to mineral composition (Haramathy et al. 1973); (iii) existing thermal incompatibility between the aggregates and cement paste. The differential thermal expansion between the cement paste and the aggregate would cause cracking in the week transition zone around the aggregate and aggravates spalling.

2.2.2 Test methods

Generally, the assessment of fire resistance of concrete can be done using three types of testing methods, which are stressed test, unstressed test and unstressed residual strength test method (Abrams 1971, Sullivan et al. 1992, Phan et al. 1996, Phan et al. 1998, Phan et al. 2001, Phan et al. 2002, Kim et al. 2009, Zaidi 2011). These test methods have been used for determining mechanical properties and their behavior under high temperature conditions. The stressed and unstressed test methods are suitable for assessing the strength during high temperature while the later is most suitable for finding the residual properties of post-fire conditions. The schematic view of the three test methods are shown in Figure 2.2 (a)-(c).

In a stressed test method, a preload, often 20 to 40% of the ultimate compressive load at room temperature is applied on the test specimen prior to heating and the load is sustained during the heating period until the target temperature is reached, and it is further maintained until a thermal steady state is achieved. Then, the axial load or strain is increased at a prescribed rate until the test sample fails (Abrams 1971, Phan et al. 1996,

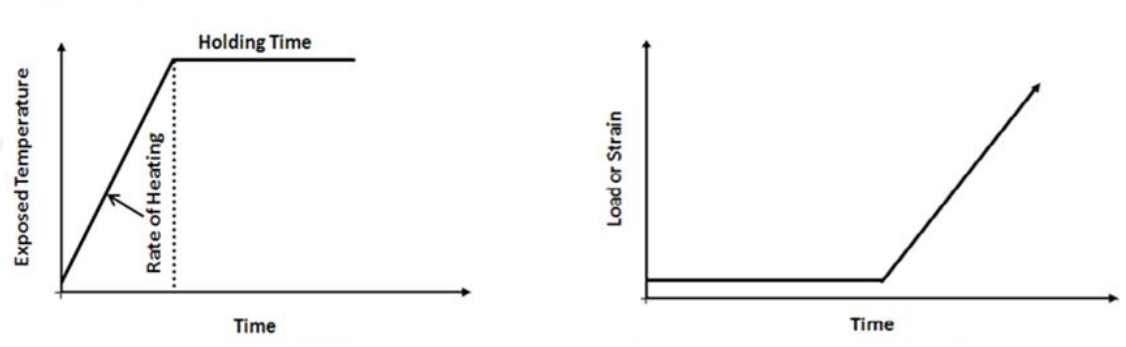

(a) Stressed test method

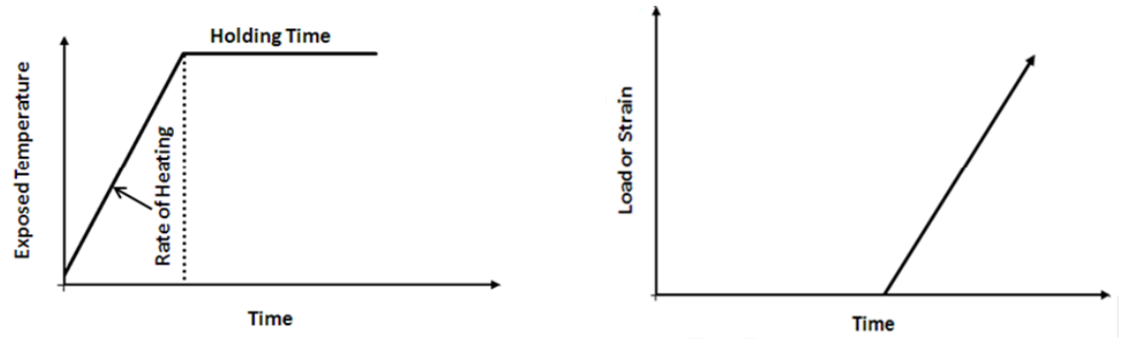

(b) Unstressed test method

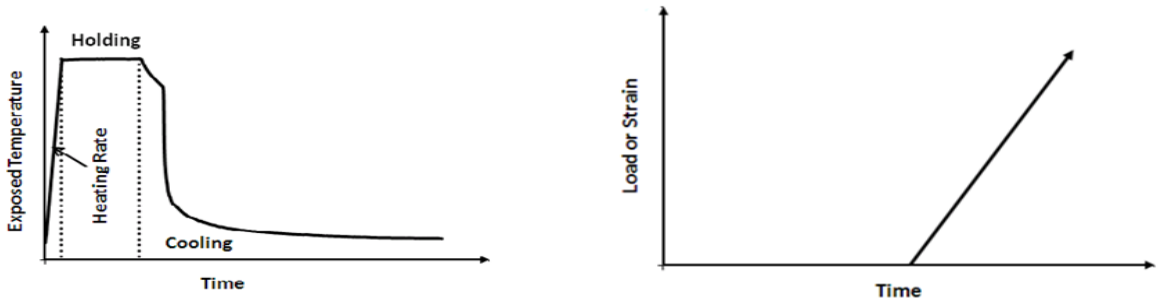

(c) Unstressed residual test Method

Fig. 2.2 (a)-(c) Schematic view of different testing methods under loading histories for concrete at elevated temperatures (Phan et al. 1998, Phan et al. 2001)

Phan et al. 1998, Kim et al. 2005). The results of stressed test are most suitable for representing the fire performance of concrete in a column or in the compression zone of beam.

In the unstressed test method, the specimen is heated without preload, at a constant rate until the target temperature is reached, which is maintained until a thermal steady state is achieved within the specimen. The load or strain is increased at a prescribed rate until the test sample failure occurs. The test result is most appropriate for

representing the fire performance of concrete in the tension zone of a beam or concrete element which has a small compressive load.

In the unstressed residual strength test method, the concrete specimen is heated without preload at a prescribed rate to the target temperature, which is maintained until the steady state is reached. The specimen is then allowed to cool to room temperature. The load or strain is applied at room temperature until the test sample failure occurs. The results of this method differ from the test methods described above, and the results are more suitable for assessing the post-fire (residual) properties of concrete. Several researchers investigated concrete of various strength grades, different mix constituents and tested these under different thermal and mechanical protocol.

Abrams attempted all three types of test methods and revealed the influence of aggregate type and test methods on the compressive strengths of specimens. The stressed tests reported in general 5 to 25% of higher strength gain than the results of unstressed tests because the preload helps to close the existing cracks in concrete. Further, at elevated temperature condition, the unstressed residual strength test method showed lowest compressive strength compared to other test methods. Figure 2.3 shows the plots of high temperature effects of three different test methods on stressed, unstressed and residual properties of concrete (Abrams 1971).

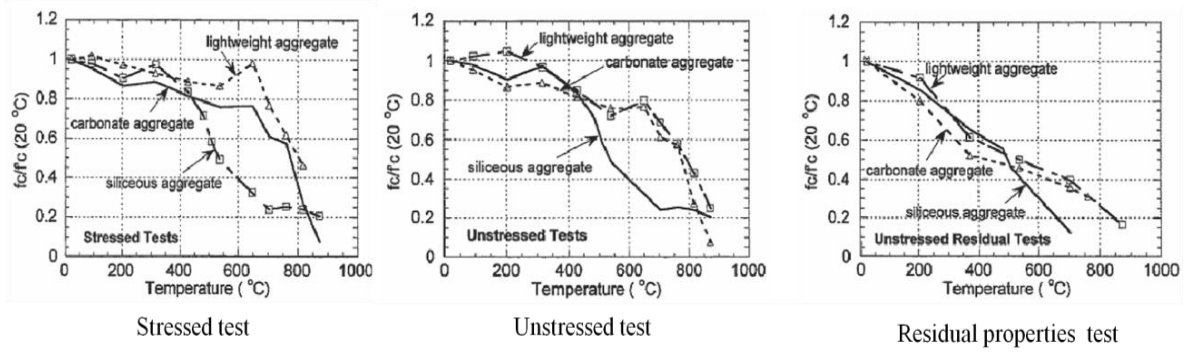

Fig. 2.3 The stressed, unstressed and residual properties test data of high temperatures (Abrams 1971)

2.2.3 Compressive strength of concrete

The degradation of residual compressive strength of concrete was investigated for long time (Malhotra 1956, Abrams 1971, Khoury 1992, Phan 1996, Chan et al. 1999, Peng 2000, Lao et al. 2000, Phan et al. 2001, Poon et al. 2004, Xiao and Falkner 2006,

Suresh 2006, Xiao et al. 2006, Ghandehari et al. 2010, Demirel et al. 2010, Yaragal et al. 2010). At elevated temperatures, the loss of compressive strength of concrete depends on many internal and external factors such as properties of the constituents, various concrete grade, aggregate types (Campbell-Allen et al. 1967, Abrams 1971, Phan 1996), inclusion of mineral admixtures (Poon et al. 2001, Ravindrarajah et al. 2002, Xiao et al. 2004, Xiao et al. 2006, Ghandehari et al. 2010), environmental factors, heating rate, peak temperature, cooling rate, methods of heating and cooling rates (Mohammedbhai 1986, Phan et al. 2001, Lao et al. 2000), size, shape and cover thickness of structural member (Hager 2005, Arioz 2009, Lixian, 2010), test methods (Abrams 1973, Phan et al. 1998) and level of applied load (Khoury 2002, Kodur 2003)

Aggregate is a major fraction in concrete and mostly occupy 65 to 75 % of total volume of concrete (Naus et al. 2006, Yan et al. 2007). According to the structural requirement or application, the concretes are prepared by normal weight, light weight (Sancak et al. 2008) and heavy weight aggregates (Sakr et al. 2005). Usually, normal weight aggregates of siliceous and carbonates are used for making concrete in large quantity. This type of aggregate has a significant influence on mechanical properties of concrete at elevated temperature (Hull et al. 1925, Malhotra 1956, Campbell-Allen et al. 1967, Abrams 1971, Phan 1996, Janotka et al. 2000, Felicetti et al. 1998, Yan et al. 2007, Robert et al. 2009, Xing et al. 2010, Netinger et al. 2011). The literatures have reported that, the dominant effect of higher temperatures is the physical and chemical changes that occur in aggregates due to the different mineral composition (Yan et al. 2007). The experimental results showed that the test specimens made of siliceous aggregate concrete had greater strength loss than carbonate aggregates (Phan 1996, Janotka et al. 2000, Hertz 2005, Arioz et al. 2007, Fletcher et al. 2007). A few studies show that the concrete made of carbonate aggregate provides higher fire resistance and better spalling resistance than the siliceous aggregates (Felicetti et al. 1998, Fletcher et al. 2007, Kodur et al. 2010). During heating, the siliceous aggregate expands more compared to other types of aggregates and phase changes of silica from α to β, are responsible for the largest damage of the concrete at elevated temperature, while the calcareous aggregates will start to decompose at about 800 °C (Harmathy et al. 1973, Fletcher et al. 2007, Naus et al. 2006). Table 2.1 shows the physical and chemical changes offered by different aggregates at elevated temperatures.

Table 2.1 Changes due to effects of elevated temperatures on aggregates

Temperature (°C)	Transformation and decomposition reaction of aggregates
30-120	Evaporation as well as vaporization of free an physically tied water
100-300	Gel reduction, beginning of dehydration
250-600	Depositing of the chemically bound water
450-550	Decomposition of portlandite; $Ca(OH)_2 \rightarrow CaO + H_2O$
573	Only with quartz: quartz conversion; $\alpha \rightarrow \beta SiO_2$
600-700	Begin of the decomposition of the CSH –phases; formation of β-C_2S
600-900	Only with limestone: decalcination; $CaCO_3 \rightarrow CaO + CO_2$
1200-1300	Beginning of the melting of cement stone
>1400	Cement stone is available as vitreous glasses

The literature indicates that large body of the data are available on the effect of elevated temperature on the residual compressive strength of normal strength and high strength concrete exposed to elevated temperatures (Khoury 1992, Sarshar et al. 1993, Poon et al. 2001, Phan et al. 2001, Phan et al. 2002, Poon et al. 2004, Suresh 2002, Ghandehari et al. 2010). Most of the experimental results have shown that concrete loses their compressive strength when heated to 200 °C to 800 °C progressively. The temperature between room temperature and 200 °C, the pozzolanic high strength concrete had shown higher strength gain of about 15 to 20% compared to room temperature strength (Poon et al. 2001, Li et al. 2008). On the other hand in the same temperature range the silica fume based concretes suffered strength reduction of about 20 to 25% (Castillo and Durani 1990). With further rise in temperature from 200 °C to 400 °C, the high strength concretes retained their original room temperature strength (Poon et al. 2001, Li et al. 2008) and some test stressed results had shown strength gain of about 10 to 20% of unheated concrete strength (Castillo and Durani 1990, Kim et al. 2009). Further, it can be observed from experimental results that the drop of residual strength was noticed at an average of 30 to 45 of residual strength compared to unheated concrete strength after exposure to 600 °C. In the next higher temperature level of 800 °C, the available compressive strength is only 20 to 25% of room temperature strength for both cases of normal and high strength concretes (Poon et al. 2001, Poon et al. 2004).

Preloading during heating has positive effects on both compressive strength and elasticity modulus of concrete (Dotreppe et al. 1996, Khoury 2000[b]). The application of 20% preload of ultimate strength reduces the strains significantly due to the influence of temperature on unstressed concrete. Figure 2.4 shows the effect of preloading and

temperature behavior of unsealed concrete specimens under uni-axial compression (Castillo and Durani 1990).

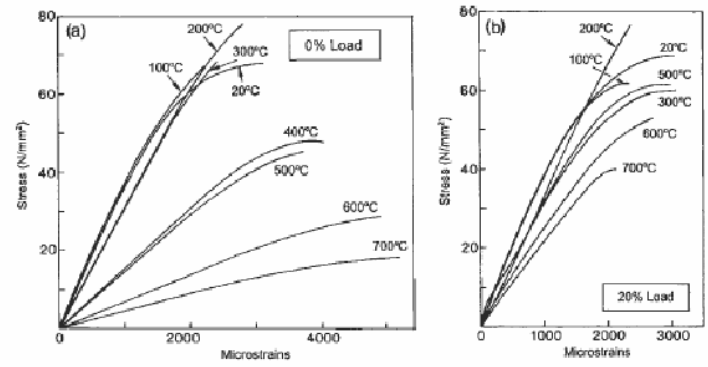

(a) For 0% load (b) For 20% load

Fig. 2.4 The effect of preloading and temperature behaviour under uni-axial compression on unsealed specimens (Khoury et al. 2000)

2.2.4 Thermal Spalling

The unpredictable event of spalling is not well understood because it is a coupled function of many different parameters involved in the concrete subjected to rapidly rising temperatures. Available information (Phan et al. 2001, Chan et al. 1999[b]) shows that concrete with strength grade higher than 60 MPa are more susceptible for spalling and may result in lower fire resistance. Spalling refers to the sudden separation or violent breaking away of cover layers from structural concrete elements when it is subjected to high and rapidly elevating temperatures during fires (Khoury 2000[a]). The results of fire tests have shown the occurrence of explosive spalling on impermeable and highly compacted dense concrete during rapidly rising temperature (Hertz 1984, Hertz 1992, Sanjayan and Stocks 1993, Bazant 1997, Phan 1996, Khoury et al. 2000, Khoury 2000[a], Kalifa et al. 2000, Bentz 2000, Hertz 2003, Peng et al. 2006, Xiangjun et al. 2008, Han et al 2008, Ko et al. 2011, Fu et al. 2011). The above literature also gives details about the mechanism of concrete spalling. The explosive spalling may be categorized under three categories i.e. pore pressure spalling (Figure 2.5 (a)-(b)), thermal spalling (Figure 2.6) and combination of both (Figure 2.7).

Generally, the spalling of concrete is associated with the migration of mass (air, vapor and liquid phase of water) in the discontinued porous network, which results in building-up high pore pressure and severe thermal gradients. The generation of pore pressure in the heat exposed concrete's cross section is shown in Figure 2.5 (a)-(b). Occasionally the spalling is also attributed to excessive thermal stress generated by rapid

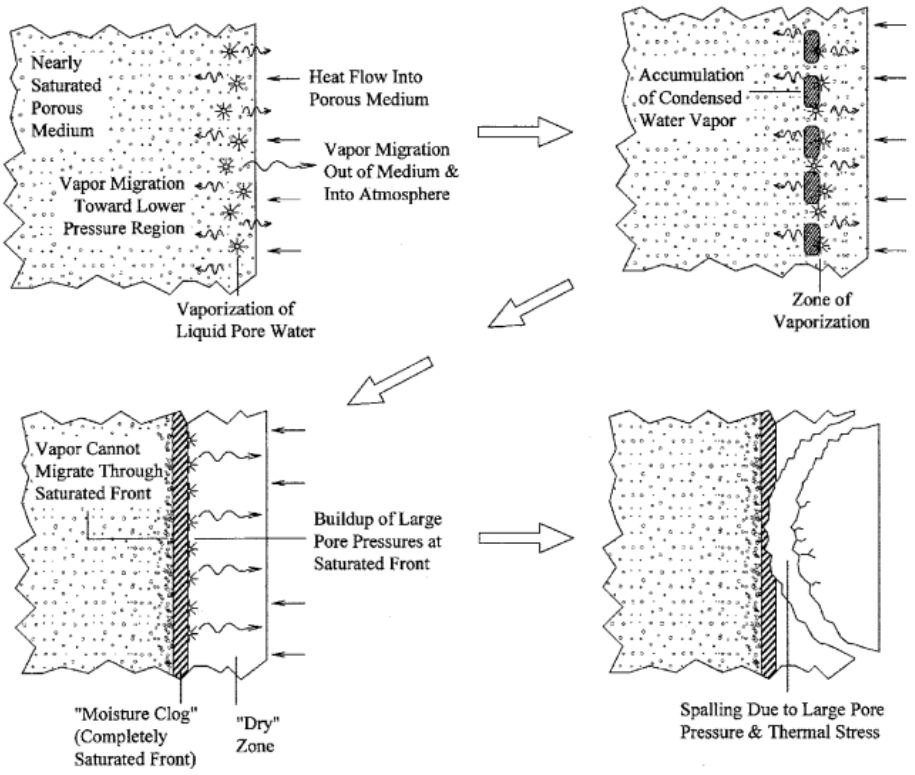

(a)

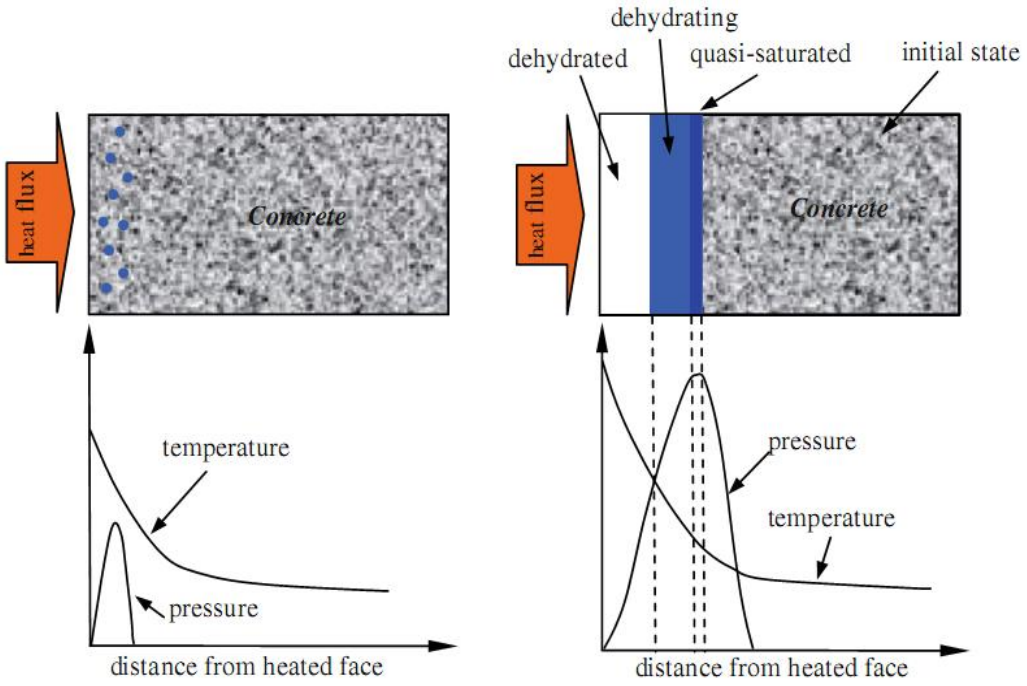

(b)

Fig. 2.5 (a)-(b) Sequential steps of pore pressure spalling

(Consolazioet al. 1998, Kalifa et al. 2000, Zeiml et al. 2006)

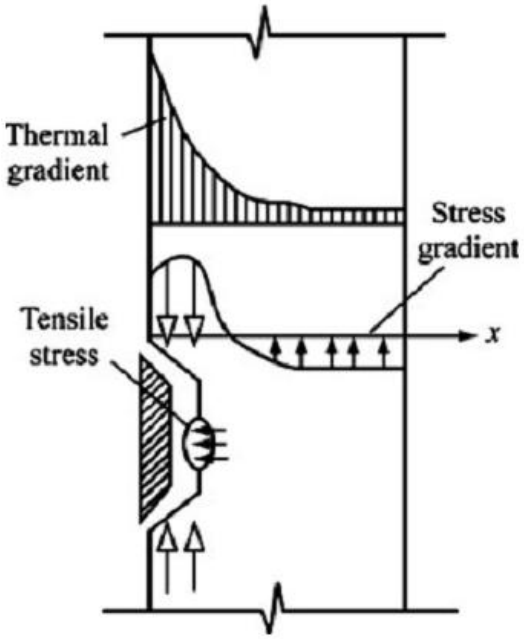

Fig. 2.6 Mechanism of thermal stress spalling (Bazant 1997)

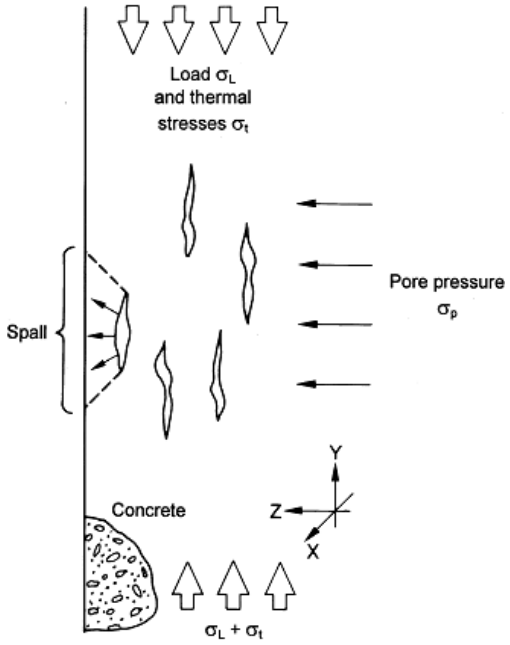

Fig. 2.7 Coupled action of Thermal stress, external load and pore pressure acting simultaneously in heated concrete (Khoury 2000[a])

heating. The rapid thermal heating resulting on the surface of concrete may generate severe thermal gradients, which induces high compressive stresses close to heated surface and tensile stresses in the cooler inner core regions (Khoury 2000[a], Fu et al. 2011).

The experiments have revealed that the increased susceptibility of spalling is affected by many key factors, material properties (e.g. type size of aggregate and size of aggregate (Pan et al. 2012), higher grade concretes added with mineral admixtures (> 60 MPa), geometric factors (e.g. section size and shape), environmental factors (moisture level, rate of heating, heating profile) and load level (Kodur et al. 1998, Chan et al. 1999, Khoury 2000[a], Buchanan 2001, Hertz 2003, Peng et al. 1996, Phan 2006, Kodur and Phan 2007, Fu et al. 2011). The intrinsic factors (original compressive strength, water-cement ratio, high moisture content of concrete, low permeability) also contribute to concrete spalling (Fu et al. 2011).

It is now well established that inclusion of mineral admixtures result in to improvements in various mechanical properties of Portland based concrete at ambient temperature conditions. The high performance concrete is not so advantageous and increases the chance to spalling compared to conventional concrete, when subjected to high temperatures. During heating, in normal strength concrete, the water is vaporized easily from the surface and some part of the water or moisture is transported to the surface through inter connected micro channels and the part of the moisture moves towards the core. But in the case of high strength or high performance concrete, the moisture remains trapped and develops very high pressure near the surface of concrete due to dense microstructure which aggravates the spalling beyond the limit of maximum tensile strength of concrete (Figure 2.5 (a)-(b)). The addition of mineral admixtures results in improvements of various mechanical properties and also modifies the microstructure of concrete at ambient temperature condition. On the contrary a review of the existing literature shows that high performance concrete has a higher spalling potential and the chances of temperature induced explosive spalling compared to the case of normal strength concrete (NSC) (Willam et al. 2009).

The spalling in normal strength concrete isn't common practice and occurs very rarely. However, it was seen in the event of rapidly heating temperature typically at the rate of 20 °C/min (Khoury 2000). On the other hand, the high performance concrete (HPC) faces higher potential of explosive spalling than the normal strength concrete (NSC) due to its dense micro-structure and low permeability. The literature indicates that the explosive spalling in HPC may occur even at low heating rate (Bezant 1997, Fu et al. 2011). i.e. 1 °C/min (Hertz 2003), less than 5 °C/min (Phan et al. 2001).

Usually the high strength concretes, when exposed to temperatures above 300 °C, develops more spalling tendency than normal strength concrete. This is due to adverse combinations of low permeability, low porosity, high thermal transmission, high moisture content and high pore pressure (Sideris et al. 2009, Chan et al. 1999[b]). The recent studies have been shown a few effective measures to improve spalling resistance and fire performance of high performance concrete (Kalifa 2001). To prevent such problems, now-a-days polypropylene and steel fibers are being included in high performance concrete to mitigate the explosive spalling behavior under high temperature exposures (Kalifa et al. 2001, Bayasi et al. 2002, Noumowe 2003, Han et al. 2005, Xiao et al. 2006, Khoury et al. 2008). Polypropylene fibers are typically used in high performance concrete to improve its permeability in the extreme events like fire. During a fire attack at relatively low temperatures, approximately 160 °C the polypropylene fibres melt and micro pores (channels) are formed in a porous mass of concrete, the high pressure vapors escape out through these channels and relieve the pressure inside the concrete, thus avoiding high pore pressures and consequently avoiding the spalling failure of concrete (Yoo et al. 2006, Khoury et al. 2008, Behnood and Ghandehari 2009).

Effects of mineral admixtures: It is now well established that inclusion of many suitable natural or artificial waste by-products as partial replacement of cement in the concrete improves its various mechanical properties at ambient temperature conditions. However, the strength and material properties of such concrete, at high temperature also gets changed due to the presence of such binder materials. There are many such binder materials that have been used for concrete and studied by a number of researchers. There is a large amount of research data available on the usage of single pozzolanic admixtures in concrete exposed to high temperatures (Diederichs et al. 1989, Khoury 1992, Sullivan et al. 1992, Sarshar et al. 1993, Saad et al. 1996, Poon et al. 2001, Ravindraraja et al. 2002, Fu et al. 2005, Behnood et al. 2008, Tanyildizi et al. 2008, Demirel et al. 2010, Ghandehari et al. 2010). The results of pozzolonic concretes revealed that pozzolonic concretes perform better and show higher residual compressive strength compared to concretes prepared without any pozzolana (Khoury 1992, Poon et al. 2001).

At elevated temperatures, the concretes made with fly ash and GGBS have performed better as compared to silica fume and OPC concretes and showed reduced deterioration at elevated temperature and also after cooling by air and water. The heat

exposure of HPC mixes made with silica fume based concrete further increase the spalling potential (Hertz 1992, Sanjayan and Stocks 1993, Phan et al. 1998, Hertz 2003, Poon 2001). The heated silica fume concrete show poor performance compared to other concretes. The literature concluded that, the addition of silica fume highly densifies the pore structure of the concrete, which results in explosive spalling due to rapid increase in pressure at high temperatures (Behnood et al. 2008).

Effect of moisture in the concrete: The moisture content of the concrete has a significant influence on its various properties under different exposure conditions. Moisture is an integral part of concrete and the variation in moisture content of concrete depends on ambient environmental conditions throughout its lifetime. At early ages, the moisture is helpful for hydration of cement particles; in hardened state, it is responsible for changes in dimensions and other properties such as strength, temperature distribution and other thermal properties of concrete in a complex manner (Hilsdorf 1967). During fire situations, the moisture offers both constructive and detrimental effects. Many studies have reported the role of moisture content of concrete at elevated temperatures (Sanjayan et al. 1993, England et al. 1995, Chan et al. 1999[b], Luccioni et al. 2003, Zhang 2011, Van Der Heijden et al. 2012). The above studies concluded that the spalling of concrete depends on the moisture content and the grade of concrete. Usually in the normal strength concretes, the moisture content prevents the development of higher thermal gradients at initial stage of heating up to 250 °C (Bentz 2000), as the temperature rises beyond 250 °C it develops thermo-physical changes in normal strength concrete. For high strength or high performance concretes, the moisture content has dominant influence on dense micro-structure of the concrete at elevated temperatures. In case of rapid heating, the dense micro-structure of concrete develops pore pressure very quickly and subsequently causes violent spalling as the pore pressure exceeds the limit of tensile strength of concrete.

Effects of heating and cooling regimes: The concrete structure, subjected to high temperatures, can experience thermo-physical changes, severe degradation of mechanical and transport properties that may lead to expeditious reduction of its service life. The previous studies have shown keen interest to know the behavior of different heating and cooling regimes (Mohamedbhai 1986, Sarshar et al. 1993, Nassif et al. 1999, Luo et al. 2000, Chan et al. 2000, Hager et al. 2005, Lee et al. 2008, Bingol et al. 2009, Zaidi 2011).

Above cited literature reveals that, detrimental effect on the concrete depends on the size of the elements and the environmental conditions such as maximum temperature; heating rate (fast or slow), exposure time, and cooling rate (fast or slow) and the above factors hasten the damage level of residual properties of post fired concrete. The heating rate of concrete is highly responsible for major strength loss and spalling when exposed to different heating rates and exposure for long durations (Mohamedbhai 1986). The experimental results showed that the heating and cooling rates hardly matters the residual strength of concrete for exposure temperatures above 600 °C and 800 °C. However, the said variable has a very significant effect on the residual compressive strength of concrete at lower temperature levels. Water cooling of concrete results in greater loss of strength compared to air cooling.

Effects of high temperature on steel reinforcement: The steel reinforcement is supplemented to the concrete mass in appropriate positions to cater primary or secondary tensile stresses in a structural member made up of concrete. When the reinforced concrete structures are subjected to elevated temperatures, both concrete and steel may undergo considerable deterioration in their strength, physical properties and stiffness of the materials due to the effects of heating. The changes are not recoverable in concrete after subsequent cooling but, it is possible in steel. The mechanical properties of steel rebars have been investigated by a few researchers in the past (Schneider et al. 1981, Takeuchi et sl. 1993, Topcu et al. 2008[b], Prasad et al. 2009, Kodur et al. 2010, Zaidi 2011, Kumar et al. 2013). A few studies expressed that concrete cover layers may protect the steel bars in reinforced concrete against fire as well as from harmful environment effects (Unluoglu et al. 2007, Topcu et al. 2008[a]). The overall performance of reinforced concrete depends on the various aspects such as tensile strength; rebar diameter, bond strength, manufacturing process (CTS, TMT), hardness of steel, steel making constituents, surface grip for bonding, thickness of concrete cover, strength of concrete, application of load, placement of bars, etc.

2.2.5 Thermal behaviour of reinforced concrete columns

The HPC in buildings may be used for structural framings consisting of beams and columns, which are the primary load bearing elements. Hence those need appropriate fire safety measures to avoid high temperature adversity. Many research studies were performed on the behaviour of columns under extreme fire conditions and it was shown that the columns' behaviour at elevated temperature is quite different than the ambient

temperature conditions. A review of previous literature indicated that a lot of experimental and numerical studies were done in recent years on the behaviour of reinforced columns in real fire situations. (Lie et al. 1986, Lie and Celikkod 1991, Dotreppe et al. 1996, Sidibe et al. 2000, Usmani et al. 2001, Ali et al. 2001, Kodur et al. 2003[a], Kodur et al. 2003[b], Ali et al. 2004, Benmarce et al. 2005, Tenchev and Purnell 2005, Ali et al. 2010, Raut et al. 2010, Khaliq et al. 2012, Zaidi et al. 2012). The above mentioned studies investigated the effect of elevated temperature on various parameters, such as residual compressive strength, cover thickness, size and shape of column, reinforcement ratio, lateral reinforcement configuration, load intensity, load eccentricity, presence of fibres etc. for the fire performance (Kodur et al. 2003[b]). These studies pointed out that, the columns made of conventional normal strength concrete (NSC) were showed good fire resistance under extreme fire situations. However, the HSC columns may not exhibit a satisfactory and the same level of fire resistance as that of NSC (Kodur et al. 2006). The cross-section of RC column on fire exposure may experience high thermal gradients which in turn can significantly influence the high temperature behaviour of structural elements. The development of thermal gradients in the column cross section can be moderate to highly steep, depending up on thermal properties of concrete such as hardened microstructure, moisture content, grade, size of structural member, placement of reinforcement and load level on column. The high thermal gradients resulting from high and rapid rising temperature on the surface of structural members lead to quick increase in the pore pressure and internal thermal stresses. When the pore pressure and thermal stresses exceed the maximum allowable tensile strength of concrete, it could result in explosive spalling. The explosive spalling could seriously affect the stability and durability of the reinforced concrete columns because of the extensive removal of concrete from reinforced concrete structural elements. This may result in severe reduction of fire resistance of the structure and also create the threat on the integrity of whole structure. Eventually, the whole structural collapse may occur. (Dotreppe et al. 1996, Sidibe et al. 2000, Ali et al. 2001, Kodur et al. 2003[a], Kodur et al. 2003[b], Ali et al. 2004, Benmarce et al. 2005, Ali et al. 2010, Raut et al.2010, Khaliq et al. 2012).

Lateral reinforcement of columns: The data in the previous studies are documented on material parameters and mechanical properties of unconfined concrete that deteriorate very rapidly with increase in temperature under uni-axial compression testing conditions (Castillo and Durani 1990, Wu et al. 1992, Felicetti and Gambarova

1998, Phan et al. 2002, Wu et al. 2002, Cheng et al. 2004, Fu et al. 2005, Kodur and McGrath 2006, Youssef et al. 2007, Sideris et al. 2009, Knaack et al. 2011, Sharma et al. 2012). However, to avoid such malfunctioning of unconfined concrete, the concept of effective confinement has been employed by many researchers to improve the structural capability as well as ductility of concrete at elevated temperatures under axial compression (Terro and Hamoush 1997, Wu et al. 2002, Kodur and McGrath 2003[b], Kodur and McGrath 2006, Zaidi et al. 2011, Sharma 2011, Sharma 2012). Wu et al. (Wu et al. 2002) studied behaviour of residual mechanical properties of confined and unconfined high strength concrete at high temperatures. The results indicate that the ties were helpful in preventing the spalling of high strength concrete under elevated temperatures(Wu et al. 2002). The thermally induced damage was less pronounced in confined concrete specimens than unconfined concrete. Kodur and McGrath (Kodur and McGrath 2003[b]), their results showed that tie configuration (bending of ties at 135° ties and provision of cross ties) and closer tie spacing has a significantly beneficial effect on the fire resistance of HSC columns. The limited numbers of studies are available on this matter and these indicate that properly designed lateral confinement can enhance the fire endurance of the reinforced concrete columns and also contribute to minimize the spalling of HPC columns (Kodur 2005, Kodur and Phan 2007, Kodur and McGrath 2006). Terro and Hamoush (Terro and Hamoush 1997) revealed the improvement of 20 to 30% in residual compressive strength of confined concrete specimens at 400 °C. The confined concrete has shown higher compressive strengths and maximum post peak strain at elevated temperatures compared to unconfined concrete.

Fire performance of columns under loading: Structural fire safety is a primary concern in the design of all types of buildings. The structural members with heavy service loads may face unpredictable failure or total collapse of the whole structure due to continuous fire for longer time. Load levels are considered as major factor that influences the behaviour of structural elements subjected to high temperatures. The structural capacity of RC member decreases with increases of fire exposure duration and loss of integrity occurs when the imposed service load becomes comparable or exceeds the reduced strength of the member due to fire (Kodur et al. 2010).

Effects of axial restraints: Lie and Lin (Lie and Lin 1985) studied the influence of heating on axially restrained RC columns and found that the restraint against thermal expansion of RC columns has insignificant effect on the fire performance. A parametric

study was conducted by Ali et al. to investigate the effect of restraint degree, loading level (0 to 60% of ultimate load) and heating rates(slow and fast) on fire performance of high and normal strength columns (Ali et al. 2004). He concluded that additional forces due to application of preload could accelerate the failure of reinforced concrete columns under severe fire. Wu et al. investigated the effects of different degrees of axial restraint on special shaped RC columns during expanding and contracting phases both, at elevated temperatures (Wu et al. 2009).

2.2.6 Stress-strain behaviour

The effects of elevated temperatures on the mechanical properties and load-deformation behavior of high strength and normal strength concrete have been investigated by many researchers in the past using various testing methods and different testing conditions (Castillo and Durani 1990, Felicetti et al. 1998, Fu et al. 2005, Xiao et al. 2006, Babu Narayan et al. 2010). The behavior of stress-strain relationship of concrete becomes poor at elevated temperatures and the elastic modulus reduces to a greater extent. Generally, small strain conditions involve elastic analysis procedures, where the concrete modulus of elasticity and strength is sufficient. When a concrete is subjected to elevated temperature, elastoplastic analysis procedures are required to analyze the stress-strain relations obtained by heated concrete. Typical load-deformation curves for normal and high strength concrete exposed to different temperatures are shown in Figure 2.8 (Castillo and Durani 1990).

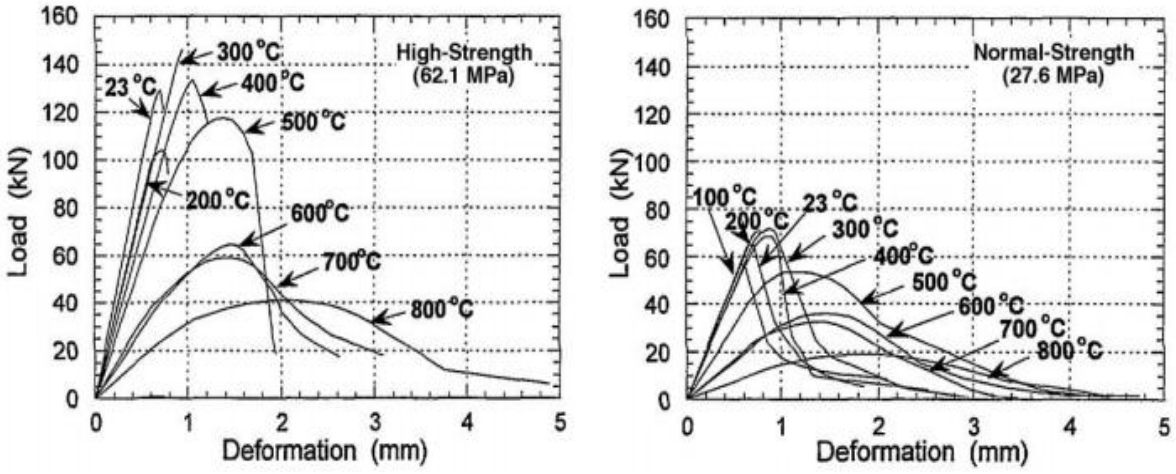

Fig. 2.8 The load-deformation behavior of normal and high strength concretes at high temperatures (Castillo and Durani 1990)

The typical curves of both normal strength and high strength concretes show the same load-deformation behavior in the range of room temperature to 400 °C and the strain values are not significantly changed. Further increase in temperature to a range from 600 °C to 800 °C, the specimens undergo large deformations along with controlled gradual failure. The high strength and normal strength concretes were noticed to show brittle failure mode soon after reaching the peak strength up to 250 °C (Castillo and Durani 1990, Felicetti et al. 1998). The failure mode was more controlled and the specimens undergo large strains before failure while the temperature increases to 300 °C to 800 °C.

2.3 THERMAL PROPERTIES OF CONCRETE SUBJECTED TO ELEVATED TEMPERATURES

The concrete structures usually behave well and exhibit reasonably high resistance to temperature dynamics. At high temperatures, the concrete shows complex behavior because of multi-phase nature of hardened concrete. However, the global and local behavior of structure is wholly governed by coupled actions of thermo-hydro-mechanical behavior as the physical and chemical changes are realised by the material constituents of concrete mixture subjected to elevated temperatures (Noumowe et al. 2009). Therefore adequate knowledge of thermal properties and thermal analysis are of fundamental interest for calculation and evaluation of overall thermal behavior and fire endurance of concrete both at room temperature and at elevated temperatures.

Concrete is a multi phase composite material, its thermal properties are more complex in nature than other building materials. The experimental data on thermal properties of normal strength and high strength concrete are available in plenty in the range of ambient temperatures. These properties show different behavior at various ambient temperature conditions due to different mix proportions of concrete, type of ingredients, type and amount of aggregates, type and percentage replacement of cement with mineral admixtures and water content and age of test specimens and type of testing methods and instruments (Xu et al. 2000[a], Xu et al. 2000[b], Demirboga 2003[a], Demirboga 2003[b], Demirboga et al. 2003[a], Demirboga et al. 2003[b], Uysal et al. 2007, Bentz et al. 2011). The results of the above literature indicated that, mineral admixture incorporated concrete showed reduction in thermal conductivity values than the plain cement concrete and increased thermal conductivity values were observed with increase in moisture

content. The aggregate type and their mineral composition are highly influenced by the thermal conductivity of concrete (Neville 2009).

The interest behind thermal properties of concrete is to study the thermodynamic changes and reactions occurring in concrete subjected to elevated temperatures. The concrete is a poor conductor of heat. However, the heat leads to significant changes in physical, chemical and mechanical properties of concrete and causes phase transformations, moisture movement, spalling of concrete, reduction of strength and stiffness. Such degradation processes have come to the forefront in the safety assessment of structures. Hence, fire safety assessment is the foremost consideration for new structures and heat exposed structures, when concrete is a favorable material choice to the designers.

The review of previous literature shows that very few experimental programs have been performed for characterizing thermal properties of normal strength and high strength concretes at elevated temperatures (Norton 1912, Carmen et al. 1925, Harmathy 1964, Harmathy 1970, Harmathy and Allen 1973, Hertz 1981, Hu et al. 1993, Lie and Kodur 1995[a], Lie and Kodur 1995[b], Lie and Kodur 1996, Kassir et al. 1996, Van Geem et al. 1997, Shin et al. 2002, Kodur and Sultan 2003, Jansson 2005, Khaliq et al. 2011[a], Kodur and Khaliq 2011, Khaliq et al. 2011[b]). The reported studies reveal that, normal strength concretes have shown high resistance to fire among the various construction materials. However, the recent studies pointed out that the new types of concretes like high performance and high strength concretes did not perform and posses the same level of fire resistance (Kodur and Sultan 2003). Those concretes have shown poorer fire performance and faster degradation of mechanical properties because of high compactness and reduced permeability (Hertz 2003). However, inferior thermal behavior and poor fire behavior of concrete may be attributed to the different thermal response of constituent materials.

The thermal properties like thermal conductivity, specific heat capacity governs the temperature rise and its distribution in the structural members. The other thermal properties, such as thermal expansion and mass loss influence the thermal stresses and volume changes in the structural members. A few high temperature studies have been undertaken in the past to investigate the influence of thermal conductivity on concrete (Harmathy 1970, Harmathy and Allen. 1973, Lie and Kodur 1996, Lie and Kodur 1995, Lie and Kodur 1996, Kassir et al. 1996, Van Geem et al. 1997, Shin et al. 2002, Kodur

and Sultan 2003, Khaliq et al. 2011[a], Khaliq et al. 2011[b], Kodur and Khaliq 2011). The thermal conductivity of concrete as a function of temperature gradually decreases with increase in temperature and this trend may be attributed mainly to the role of moisture content at high temperature in the concrete and partly to the thermal behavior of other constituents i.e. aggregates and mineral additives. Figure 2.9 (a) shows the variation of thermal conductivity of normal strength concrete at elevated temperatures. It can be noted that the high performance concrete (HPC) usually made with low w/c ratio, higher binder content, different pozzolanic additions, may yield relatively lower variation of thermal conductivity as a function of temperature compared to NSC. It can be observed from the above studies that there is a large variation in the experimental data of thermal conductivity with temperature, which may be attributed to the use of different measuring methods and different test conditions (Phan 1996, Kodur et al. 2003, Kodur and Khaliq 2011).

The specific heat capacity of concrete as a function of temperature was studied by many researchers (Harmathy 1970, Harmathy and Allen 1973, Kassir et al. 1996, Lie and Kodur 1996, Phan 1996, Van Geem et al. 1997, Shin et al. 2002, Kodur and Sultan 2003, Naus 2010, Shui et al. 2010, Khaliq et al. 2011[a], Khaliq et al. 2011[b], Kodur and Khaliq 2011). At elevated temperatures, the specific heat capacity increase with increase of temperature. The specific heat capacity of any type of concrete is greatly influenced by moisture content (Phan 1996, Kodur and Khaliq 2011) as well as type of aggregate and density of concrete (Harmathy 1970, Phan 1996, Kodur and Sultan 1998). Figure 2.9 (b) shows the variation of specific heat capacity of normal strength concrete at elevated temperatures. In the above figure the shaded portion indicates the range of values of experimental data presented by different researchers (Harmathy and Allen. 1973, Shin et al. 2002, Kodur and Sultan 1998). The deviation of results are due to different measuring techniques, moisture content, type of aggregates and their mineral composition used in the experiments (Kodur and Khaliq 2011). The coefficient of linear thermal expansion represents the change in volume of material due to rise in temperature and it is expressed as the percentage change in length of test specimen per degree rise of temperature. At elevated temperatures, the thermo-physical changes in concrete result in to non-uniform thermal stresses between aggregate and cement matrix. The above phenomenon is termed as the thermal strain due to change in temperature (Naus 2010). Figure 2.9 (c) shows the variation of linear thermal expansion of normal strength concrete at elevated temperatures.

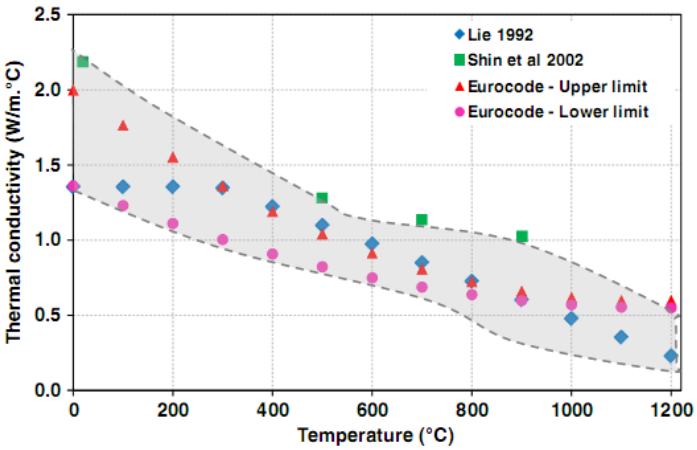

(a)

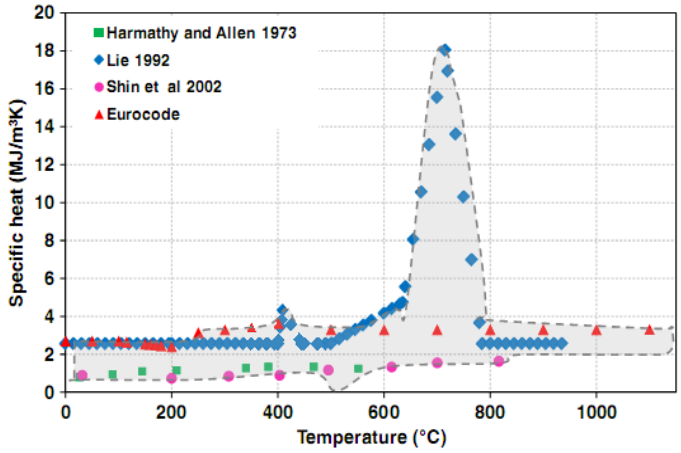

(b)

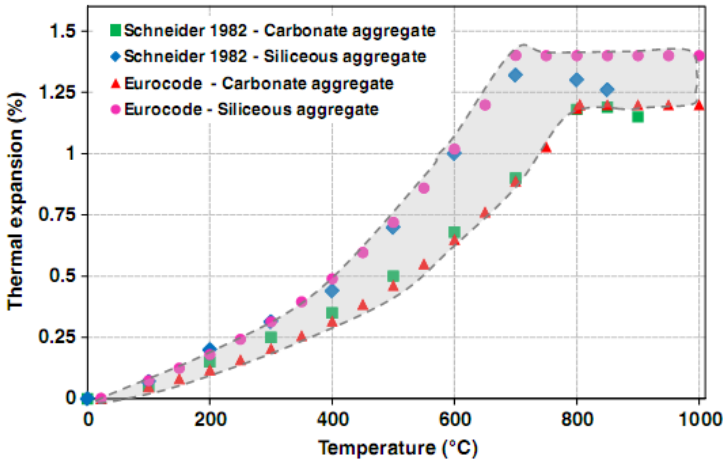

(c)

Fig. 2.9 (a)-(c) Variation of thermal conductivity, specific heat capacity and linear thermal expansion of NSC as a function of temperature (Kodur and Khaliq 2011)

The thermal expansion of concrete is generally influenced by cement type, water content, aggregate type, temperature variation, and age (Harmathy and Allen 1973, Cruz and Gillen 1980, Freskakis 1984, Kodur and Sultan 1998, Kodur and sultan 2003, Naus 2010). The volume changes of concrete are caused by driven off moisture and also by chemical reactions (dehydration, change of composition etc.).

Mass loss is a temperature dependent property and generally represented by the thermo-gravimetric curves of concrete which also indicates the progress of decomposition reactions within the concrete at elevated temperatures. Such curves are very useful in assessing the advantages and drawbacks of materials to be used in fire resistance applications. The previous studies presented experimental data of thermo-gravimetric curves of aggregates have indicated that the type of aggregate has a strong influence on the mass loss of concrete at elevated temperatures (Harmathy and Allen 1973, Lie and Kodur 1995, Lie and Kodur 1996, Uygunoglu et al. 2009, Shui et al. 2010). The loss of weight of concrete increases with increase in temperature, because of the physio-chemical changes and driven off moisture existing in various form (free water and chemically combined water) in the concrete (Shin et al. 2002).

2.4 MIX PROPORTIONING OF HPC

There is no ideal method to fix up the best combination for mixture proportions for high performance concrete. Although, the existing methods of mix proportioning are required, more number of trial mixes are required to fix the desired combination of materials. However, a good mix proportioning procedure has to minimize the number of trial mixes and achieve an economical and satisfactory mixture with desired properties. The fabrication of a HPC is based upon the selection of materials and optimization of ingredients is more of an art than a science (Rougeron et al. 1994). Now-a-days, more sophisticated mix proportioning techniques have been employed to arrive at suitable mix proportions of high quality high performance concrete. Long lasting efforts have been devoted by many research scholars in last three decades to produce excellent high performance concrete, proportioning method to improve the performance of fresh as well as hardened concrete. A modified mixture design method based on ACI method (Bharathkumar et al. 2001), Artificial neural networks (Mukherjee et al. 1997, Yeh 1999, Oh et al. 1999, Cheng Yeh 2003, Tao Ji et al. 2006, Jamil et al. 2009, Khan 2012), Densified mixture design algorithm (Chang et al. 2001, Chang 2004), Concept of

densified system with ultra fine particles (Sobolev 2004), An expert system for mix design of high performance concrete (Zain, 2005), Genetic algorithm (Lim et al. 2003, Rajasekaran 2006), concrete mixture optimization using statistical methods (Simon et al. 1997) and response surface method (Simon et al. 1999). These studies, which dealt with designing of successful mixture proportion of high performance concrete. The above reference studies revealed that mixture proportions of HPC have been well documented.

2.4.1 Optimization of material parameters of HPC

A large number of trial experiments are usually required to fix-up a suitable mixture combination for getting the targeted requirements. The continuous revolutionary developments in the field of concrete technology, the ideas of statistical methods have been conceived to be significant in improve the motherhood properties of concrete through optimized mix proportions of constituents. The process of optimization of concrete mixture proportion involves the adaptation of available resources to meet varying engineering criteria, construction operations, and economic needs. The optimization techniques like, statistical methods were also employed to obtain optimum content of concrete mix proportions. However lot of attempts have been made by many researchers in the past to make use of optimization techniques to obtain best optimum content of concrete mix proportions at ambient temperature conditions to achieve best mechanical properties for a given set of materials and exposure conditions. The optimization techniques like, statistical methods were employed earlier to optimize the content of concrete mix proportions to achieve best mechanical properties for a given set of materials, exposure conditions and user defined constrains (Simon et al. 1999, Rougeron et al. 1994, Aitcin 1998, Soudki et al. 200, Ayen et al. 2011, Komeili et al. 2012, Modirzadeh et al. 2012) adopted full factorial design methods in their experimental programs to optimize the material and economical (cost) parameters in the production of the optimized HPC mix proportions. In full factorial experiments, to study the factors and their interactions numerous numbers of experiments are required and it is practically not possible to carry out the experiments in most of the cases (shariq et al. 2012). Because of that the fractional factorial experimental procedure has been applied, when the experiments minimum numbers of experimental trials are needed to study the main effects and desired parameter interactions (Soudki et al. 2001, Antony 2003). The fractional factorial designs are widely and commonly used types of optimization techniques in production and manufacturing design industry to simplify the experimental

procedure and to investigate only a fraction of all the possible combinations. These types of designs are very useful in specifically identifying the important process parameters to determine the influence of the factors and their levels and identify the best combination of process parameters (Roy 1988, Abbasi 1987). The experimental design methodology of fractional factorial experiments had been implemented extensively in his experimental design procedures by Taguchi (Roy 1988).

Taguchi's philosophy emphasis on quality improvement in places a great detail of emphasis on variation reduction in design and processes. Mainly the Taguchi's procedure focuses on off-line experimentations of single quality characteristic optimization for a product or a process that needs improvement leading to controlling factors determination and subsequent regulation, managing to adjust their influence even under a very noisy environment. The survey of existing literature indicates that Taguchi method has been extensively and successfully employed to optimize various parameters mix design that affect the performance of concrete under very noisy conditions (Yang et al. 2009, Ibrahim et al. 2008, Narendra et al. 2008, Nuruddina et al. 2008, Haiwidodo et al. 2010).

Most of the real situations have multiple characteristics or responses of interest. The result of Taguchi technique is best suited for products with a single quality response or characteristic optimization. The particular single quality response optimized by Taguchi technique, may not give desired results for other parameters of the products response. In such cases, multi response optimization may be the solution to obtain a single optimal setting of the process parameters. In multi-response problems the objective is to determine the optimal settings factors or process variables which will simultaneously optimize several responses (Antony 2000). Most of the published literature available reveals that the multiple response characteristics have been investigated by number of researchers by different of methods, the Response surface method (Myers et al. 2004), Taguchi's quality loss function (Antony 2000, Gaitonde 2006) and robust design method of experiments (Ramakrishnan and Karunamoorthy 2006), Principle component analysis (Su and Tong 1997, Antony 2000, Gaitonde et al. 2006), Fuzzy logic (Tong et al. 1997, Amiri et al. 2008, Antony et al. 2006), Utility concept (Yang, 2004 Hari Singh and Kumar 2006, Kansal 2006, Gaitonde 2009, Garg 2010, Baddkar et al. 2011), Artificial neural networks (Al-Refaie et al. 2008, Noorossana et al. 2009), Grey relational analysis (Lin et al., 2006), Data envelope method (Liao et al. 2002) and Regression techniques followed soft computing approaches (Baykasoglu et al. 2009) were engaged for solving the multi-response characteristics problems according to their product requirements.

Among the variety of approaches and methods intended to use the simplified methodology of utility concept was implemented for determining the optimal settings of the process parameters for simultaneous optimization (Kumar et al. 2000, Singh et al. 2006, Garg et al. 2010).

2.5 SUMMARY OF LITERATURE REVIEW

In this chapter, the research outcome of pervious experimental and analytical data has been discussed. The high temperature behavior of unreinforced and reinforced concrete test specimens at the material and structural levels has been presented. Based on this review of literature, the following concluding remarks have been made:

- The studies established that the conventional normal strength concrete (NSC) exhibits good fire resistance. However, structures made of pozzolana added concretes such as HPC may not provide similar level of fire performance.
- The physical and chemical changes strongly affect the behavior of concrete subjected to fire or high temperatures and these changes are also responsible for degradation of mechanical and thermal properties of concrete. The deterioration of concrete mainly depends upon the mix proportions of concrete, properties of constituents, mineral admixtures, moisture content and environmental parameter (heating rate, cooling rate and duration of heat exposure etc). The mechanical properties of concrete and steel rebars have been explored and appropriate constitutive relationships were also developed.
- The available literature indicates that only few studies have been performed on effects of mix proportions of concrete on the residual compressive strength and other mechanical properties of concrete exposed to high temperatures.
- No data is available to assess the residual strength properties and spalling behavior of confined reinforced high performance concrete columns subjected to high temperatures in the presence of preload.
- More data is required on the comparative performance and fire behavior of different pozzolana added concretes at material level and structural level.
- The literature indicated that a detailed study is required to explore the spalling behavior of high performance concretes incorporating different mineral admixtures and subjected to high temperatures.
- At elevated temperatures, the computational modeling is a challenging task to

reproduce real behavior of concrete. It requires more precise temperature dependent thermal properties of concrete materials to simulate the thermo-mechanical performance of concrete.

- Further research work is needed to generate data on thermal properties for high strength or high performance concretes at high temperatures.

CHAPTER - 3

MULTI-RESPONSE OPTIMIZATION OF RESIDUAL COMPRESSIVE STRENGTH OF HEATED HIGH PERFORMANCE CONCRETE

3.1 GENERAL

Concrete is the most versatile material for making any kind of structure and is employed to fabricate a variety of structures like buildings and other built infrastructures. Fire is one of the most serious potential hazards to concrete buildings, though it is believed that the concrete is an excellent thermal resistant building material due to its thermal properties to endure high temperature and fires. When the concrete is exposed to fire or high temperatures, the significant changes in physical and chemical composition of concrete occur, which leads to progressive degradation of mechanical properties and durability of concrete. The extent of degradation in properties of concrete due to high temperature depends on many material and fire parameters such as constituents of concrete mix, properties of the constituents, grade of concrete, heating rate, peak temperature, cooling rate, shape and size of member, methods of heating and cooling etc. As the use of mineral admixtures in high performance concrete production is becoming common now days, it becomes important to investigate the influence of material parameters on the residual (post-fire) behaviour of such concretes. It is generally believed that the most influencing mix design parameters of high performance concrete are water-cement ratio (W/C), water content, cementitious material content, mineral admixture content, chemical admixture content, fine aggregate content, coarse aggregate content and binder to aggregate ratio etc.

The present study is aimed to investigate the role of various concrete mix parameters on the residual compressive strength of different high performance concrete mixes after exposing to various elevated temperatures. A large number of trial experiments are usually required to deal with such cases where the number of variables and mix combinations become worth investigating. In view of this the design of experiment (DoE) methods and optimization tools are generally used to fix-up a suitable mixture combination for getting the targeted requirements. Thus a lot of attempts have been made by many researchers in the past to make use of optimization techniques to

obtain optimum levels of various concrete mix proportions at room temperature for a given set of materials and exposure conditions (Turkmen et al. 2003, Ozbay et al. 2003). The pervious literature indicates that Taguchi method has been successfully employed to optimize the various parameters that affect the performance of concrete under ambient conditions (Turkmen et al. 2003, Hinislioglu et al. 2004, Ozbay et al. 2006, Tan et al. 2005, Chaulia and Das 2008, Ozbay et al. 2009, Turkmen et al. 2009, Usyal et al. 2012) and to a very limited extent at elevated temperatures (Tanyildizi et al. 2008, Tanyildizi 2008[b,] Tanyildizi et al. 2008a[a], Tanyildizi et al. 2008[b], Bastami et al. 2011, Chaboki-khiabani et al. 2011). Further, the Taguchi scheme of practice is best suited for situations with a single quality response or characteristic optimization. However, most of the real situations have multiple characteristics or responses of interest. In such cases multi response optimization may be the solution to obtain a single optimal setting of the process parameters. In view of this the present study on one hand attempts to establish the most influencing mix parameters at different temperatures using Taguchi method and on the other hand utility concept is proposed to be used for obtaining the best possible mix conditions for achieving best residual compressive strength of heated high performance concrete.

3.2 DESIGN OF EXPERIMENTS

The design of experiments is formulated using the statistical techniques. The statistical knowledge can play an important role in planning, conducting, analyzing and interpreting data for engineering experiments. In the design of experiments (DoE), the influencing factors can be applied effectively to adjust the output of experiments. This section describes a methodology for the design of experiments to determine the optimum mix proportions of high performance concrete for obtaining best residual compressive strength and minimum deterioration effect when heated to elevated temperatures ranging from room temperature to 800 °C.

3.2.1 Process parameters optimization-Taguchi's methodology

The design of experiments (DoE) is a powerful systematic and scientifically appropriate statistical approach for determining the optimal factor settings of process parameters and thereby achieving improved process performance, reduced process variability and improved manufacturability of products and processes (Antony 2003). The outcome indicated from the properly designed, implemented and analyzed experiments can improve functional performance of the product, reduction in the excessive variability

in the production process, minimizing the product develop cycle time and reducing the scrape rate and rework rate. Dr. Genichi Taguchi developed new successful design application methods to optimize the process of high quality engineering experimentation and the developed techniques are known as Taguchi method (Roy 1988). However, he also introduced several unique and powerful statistical concepts, which have been found as valuable tools to improve the product quality, minimize variability from target value of the product. Taguchi used a fractional factorial experimental design approach instead of full factorial experiments to simplify the experimental procedure using orthogonal arrays (OA) and thereby investigating only a fraction of all possible combinations which saves the product development cycle time, scrap rate, rework rate and cost of materials.

3.2.1.1 Design strategy-orthogonal array

Taguchi constructed a special set of orthogonal array (OA) for layout of his experiments. These arrays are often employed in experimental programs to study the effect of several control factors and subsequently results in reduction of the number of experiments. The purpose of conducting an orthogonal experiment is to determine the optimum level for each controllable parameter and to establish the relative significance of individual parameters in terms of their main effects on the response. The appropriate selection of an orthogonal array is significant step in Taguchi experimental design strategy to study the experimental parameters of interest. Before selection of an appropriate orthogonal array for a particular experimental investigation, it is mandatory to assign the number of factors, their levels and the possible interactions to be accommodated and included in the Taguchi's experimental design.

3.2.1.2 Parameter design

Parameter design is intended as a cost-effective approach for reducing variation in and around products and processes. Taguchi's philosophy on quality improvement paid a lot of emphasis on variation reduction; which is caused by the uncontrollable or noise factors while keeping the quality characteristic of interest on target. Taguchi formulated some techniques to eliminate the causes of variation, which could be achieved by adjusting the levels and controlling the variation of other factors in the experimental procedure. The inner fractional factorial orthogonal arrays settings are to be employed in experimentation to minimize the variation causes due to noise factors on responses of control factors.

3.2.1.3 Optimization technique by Taguchi - signal to noise (S/N) ratio

Signal to noise ratio (S/N) is a desirable feature to measure sensitivity of the quality characteristic being investigated under the controlled experimental conditions. Signal is a product's response of desired effect in the experimental design. When the experiments are conducted, lot of external factors not considered earlier into experimental design may influence the outcome. Noise factors are the factors that cannot be controlled or are difficult to control by the designer during the execution of experiment. These external forcing factors are called noise factors.

There are three categories of performance characteristics based on signal to noise ratios for evaluating the performance of parameters namely larger the better, smaller the better and nominal the better (Roy 1989).

$$\text{Larger the better S/N (db)} = -10\times\log_{10}\left(\frac{1}{n}\sum_{i=1}^{n}\frac{1}{y_i^2}\right) \quad (3.1)$$

$$\text{Smaller the better S/N (db)} = -10\times\log_{10}\left(\frac{1}{n}\sum_{i=1}^{n}y_i^2\right) \quad (3.2)$$

$$\text{Nominal the best S/N (db)} = -10\times\log_{10}\left(\frac{1}{n}\sum_{i=1}^{n}(y_i-y_0)^2\right) \quad (3.3)$$

where, y_i is a performance value of the i^{th} trial and n is the number of repetitions for an experimental combination.

The aim of the present study is to determine the best possible highest ratio for the experimental results. The high values of S/N indicate signal much higher than the allied effects of the noise factors and yield probable optimum condition with minimum variance.

3.2.1.4 Analysis of results

Using the Taguchi's method, the results obtained from experiments were analyzed to achieve following objectives:

1. To find the best possible optimum condition for a given range of product process.
2. To estimate the individual responses of control factors under optimum conditions.
3. To estimate contribution of individual factors.

A simple arithmetic manipulation of the numerical results has been employed to identify and study the main effects of each process parameters. The main effects indicate the general behavior of control factors present in the experimental program. The analysis of variance (ANOVA) is a statistical approach most commonly applied to the experimental results to explore the contribution of each parameter.

3.2.1.5 Steps

Taguchi suggested certain steps to conduct the experimental study for optimizing the process parameters using robust design approach (Phadke 1989), which are discussed as follows:

1. *Problem formulation:* This is the first step in the experimental investigation. A clear and complete understanding of problem makes easy way to find the best answer.
2. *Identification of the objective function:* The selection of quality characteristics or parameters is to select the best combination of the control parameters so that the product or process is most robust with respect to noise factors. Generally, the optimum conditions were arrived using the loss function as larger-the better, which is a quality characteristic function to maximize the compressive strength of concrete.
3. *Selection of parameters:* This is the most important step of the experimental design procedure. Taguchi believes that it is generally preferable to include as many factors as possible for the initial screening. The information required can also be obtained from the already available literature or research data.
4. *Design of experiment:* The selection of appropriate experimental design is done by assigning the levels of the design factors and their interactions in the columns of orthogonal array.
5. *Classifying factors:* The next step is to classify the contributing factors as control, noise and signal factors. Control factors are those factors that can be controlled by experimenter during manufacturing process. Noise factors are the external factors that cannot be controlled and are difficult to control in actual production environments. Signal factors are those that affect the target performance of the characteristics but generally have no influence on variability in the performance characteristics of the product or process.

6. *Determining levels and orthogonal array:* A level is the value that a factor holds in an experiment. The number of levels depends on the requirement of selected orthogonal array and the levels need to be in an operational range of the product or process. The orthogonal arrays are a set of tables of numbers created by Taguchi that allow experimenters to study the effect of a large number of control and noise factors on the quality characteristic in a minimum number of trials.
7. *Conducting the experiment:* Perform the experimental trials, preferably conduct the experiments replicating each trial to minimize the effect of experimental error. The experimental results are collected and recorded.
8. *Analysis of data:* After the experiment, the recorded and collected experimental results are put to the statistical analysis by the experimenter to understand the responses of control parameters.
9. *Confirmation experiment:* To validate the conclusions from the experiment, a confirmatory experiment should always be performed.

3.2.2 Multi characteristic response optimization model

In today's complex manufacturing processes we often have to optimize several responses simultaneously rather than optimizing one response at a time. But most of the products have several quality features of interest. The conventional trial and error method cannot be implemented in order to obtain the best combination of process parameters, since there are multi-response parameters that are to be optimized. A single setting of process parameters may be optimal for one response but the same setting may yield detrimental results for other responses. In such cases, a need arises to obtain an optimal setting of the process parameters so that the product can be produced with optimum or near optimum responses. In multi-response problems the objective is to determine the optimal settings factors or process variables, which will simultaneously optimize several responses (Antony 2000). The published literature reveals that many researchers had investigated the multiple response characteristics by using various methods. The Response Surface Method (Myers et al. 2004), Taguchi's quality loss function (Antony 2000, Gaitonde 2006), robust design method of experiments (Ramakrishnan and Karunamoorthy 2006), Principle component analysis (Su and Tong 1997, Antony 2000, Gaitonde et al. 2006), Fuzzy logic (Antony 2006, Tanyildizi 2009[a]), Utility concept (Kumar et al. 2000, Yang 2004, Singh and Kumar 2006, Kansal 2006, Gaitonde 2009, Garg 2010), Artificial neural networks (Al-Refaie et al. 2008, Noorossana et al. 2009),

Grey relational analysis (Lin et al. 2006) and Data envelope method (Liao et al. 2002) are a few notable methods employed in experimental investigations. Regression techniques were used in the various methods for solving the multi-response characteristic problems according to the product requirements. Among the variety of approaches and methods, the simplified methodology of utility concept for determining the optimal settings of the process parameters for simultaneous optimization was considered to be more appropriate (Kumar et al. 2000, Singh et al. 2006, Garg et al. 2010). In view of this, the present work attempts to employ Taguchi's technique to determine the most optimum mix proportions for maximizing the residual compressive strength of heated high performance concrete, while the utility concept has been used for determining the optimal setting of the process parameters for multiple temperature responses.

3.2.2.1 The utility concept

In multi-response problems, the objective is to determine the optimal settings of factors or process variables which will simultaneously optimize several responses. As mentioned earlier the Taguchi technique and utility concept have been employed simultaneously to optimize the multiple responses of HPC mix parameters exposed to different temperatures. In order to optimize the multiple responses, Taguchi design cannot be applied directly for each performance characteristic, which does not have the same dimensional units. Hence, the evaluations of different characteristics should then be combined to give a composite index. Such a composite index represents the utility of a product. It is assumed that the overall utility is the sum of utilities of individual quality characteristics.

The present experimental work is aimed and designed with an objective of arriving at optimum proportions of mix parameters for maximum residual compressive strength of HPC at all Target temperatures. These mix parameters can be determined by applying the utility concept. In the application of utility concept all S/N ratios of mix parameters, optimized at different temperatures, are computed for larger the better optimization criterion. Assuming equal weights at all temperatures, the weighted S/N ratios obtained for different temperatures are summed up and with these data the mean process parameters are determined. Using the significant contribution of mean utility values of main effects, the optimal setting process parameters are determined.

The above mentioned concepts were applied to the present problem and absolute optimum proportions of mix parameters for HPC were obtained at various elevated temperatures. The methodology can be explained as follows:

If *Mi* represents measure of mix parameters of i^{th} mix proportion level and *n* represents number of mix proportion levels, then the overall utility function can be expressed as (Kumar et al. 2000):

$U(M_1, M_2, \ldots, M_n) = f(U_1(M_1), U_2(M_2), \ldots, U_n(M_n))$ (3.4)

where $U_i(M_1, M_2, \ldots M_n)$ is the overall utility of *n* parameter responses.

The earlier utility function may be rewritten to optimize the proportion of mix parameters and the weights are assigned according to their responses for the individual utility index. So, the general form of weighted utility equation can then be written as:

$$U(M_1, M_2, \ldots\ldots, M_n) = \sum_{i=1}^{n} W_i U_i(M_i) \quad (3.5)$$

where, W_i is the weight assigned to the mix parameters *i* and the sum of the weights for all the mix parameters is equal to 1.

The utility function is also a "larger-the-better" type composite measure. When Utility function is maximized, the quality characteristics being considered are collectively optimized.

3.2.2.2 Construction of preference scale

A preference scale is constructed for determining the utility value of HPC for each temperature. The mix proportion parameters are assigned as preference number of 9 for best optimal values of mix parameters. If a logarithmic scale is chosen, then the preference number (P_i) is given as (Kumar et al. 2000):

$$P_i = C \log \frac{M_i}{M_i'} \quad (3.6)$$

where M_i is the value of mix proportion parameter *i*, M_i' is the minimum acceptable value of the mix proportion level *i* and *C* is a constant of preference scale number equal to 9.

Subjectively, we may choose such that $P_i = 9$ at $M_i = M^*$, where M^* is the optimum value of M_i assuming such a number exists.

So, $$C = \frac{9}{\log \frac{M_i^*}{M_i'}} \quad (3.7)$$

The next step is to assign weights to the responses of high temperatures. Moreover, this assignment is subjective and based on experience. The weights should be assigned such that the following condition holds good:

$$\sum_{i}^{n} W_i = 1 \quad (3.8)$$

3.2.2.3 Calculation of utility value

The overall utility function relation mentioned below was deployed to calculate the utility value data of HPC at various temperatures of exposure:

$$U = \sum_{i=1}^{n} W_i P_i \quad (3.9)$$

$$U\,(n, R) = P_{(Room)}(n, R) \times W + P_{(200\,^{\circ}C)}\,(n, R) \times W + \ldots\ldots P(n, R) \times W \quad (3.10)$$

where, n = trial number, R = replication number, x = no. of quality characteristics.

Thus, the data obtained by transforming the experimental results for various mix proportions is known as utility data. This data is subsequently analyzed by appropriate statistical techniques for arriving at the optimal setting of mix proportions.

3.2.2.4 Computation of confidence interval

The estimate of mean responses is a point-based estimate on the average results obtained from the utility values of the experiment. The confidential value is a maximum and minimum value between which proper average value falls at some stated percentage of confidence. This result statistically provides 50% chances for true mean being greater than the estimated mean value and vice versa. The confidence interval (CI) at a chosen error level may be estimated by the following equation (Ross 1998):

$$\mathrm{CI} = \sqrt{F\ \alpha, 1, fe\ Ve\left[\frac{1}{N_{eff}} + \frac{1}{R}\right]} \quad (3.11)$$

where F (α,1, fe) is the F value from the F table from any statistical book at the required confidence level and at a degree of freedom (DOF) of 1, Ve is the variance error, R is the number of replications and N_{eff} is the effective number of replications.

3.2.3 Data analysis- Analysis of Variance (ANOVA)

Analysis of variance (ANOVA) is a standard statistical technique, which is routinely used to provide a measure of confidence from the factors of responses. It provides the variance of controllable factors and noise factors. Generally, this technique does not involve the analysis of the data of factor response directly, but to find out the results as how much variation each factor causes relative to the total variation in the whole results. The confidence level of the data is measured from the data itself (Roy 1990).

3.2.4 Confirmation experiment

The confirmation experiment is the final step and a crucial step in Taguchi's experimental methodology and as well as for the multi-characteristic optimization of utility concept for validating the predicted results (Ross 1998). This important requirement is purposely conducted to verify that the optimum conditions suggested by the experimental methods do indeed give the projected improvement. Usually the optimum conditions are derived from significant parameters and their levels along with the selected numbers of test runs under controlled conditions.

3.3 EXPERIMENTAL PROGRAM

This section describes an experimental program designed to determine the optimum mix proportions of high performance concrete for obtaining maximum residual compressive strength and minimum deterioration effect of heat when exposed to elevated temperatures ranging from room temperature to 800 ℃.

3.3.1 Material properties

The present investigation considers three different high performance concrete mixes made with three different pozzolanas or mineral admixtures in addition to a non-pozzolanic control HPC mix. The cubes were cast using locally available Ordinary Portland Cement (OPC), fine aggregate, coarse aggregate, pozzolana, super plasticizer and tap water.

3.3.1.1 Cement

A commercially available 43 grade OPC cement complying with IS 8112: 1989 from single lot was used for preparing concrete mixes throughout the course of this investigation. The collected cement samples, before their use, were thoroughly tested in the laboratory to establish their feasibility according to the appropriate Indian standards.

All the cement tests were carried out as per the guidelines of IS 4031: 1988 and IS 4032: 1985. Table 3.1 shows the physical properties of the cement. The value are found to be acceptable and in conformity with the Indian standard IS 8112: 1989. The chemical properties of cement are tabulated in Table 3.2. The cement was carefully stored in the airtight silos to prevent deterioration in its properties due to atmospheric exposure. Figure 3.1 presents the cementing materials i.e. cement and various mineral admixtures used in this experimental research study.

Table 3.1 Physical properties of cement

S. No	Characteristics	Units	Results obtained	Recommended values as per IS 8112: 1989
1	Blaine's fineness	m^2/kg	280	225 (minimum)
2	Specific gravity	-	3.16	-
3	Le-Chatelier test for Soundness	mm	2	10 (maximum)
4	Autoclave expansion	%	0.078	0.8 (maximum)
5	Normal consistency (percent of cement by weight)	%	28	30
6	Setting (i) Initial (ii) Final	minutes	95 182	30 (minimum) 600 (maximum)
7	Compressive strength (i) 3-days (ii) 7-days (iii) 28-days	MPa	27.28 36.91 44.10	23.0 33.0 43.0

Table 3.2 Chemical composition of OPC 43 cement

S. No	oxide	Test results (%)	Limiting % values specified as per IS 8112: 1989
1	Silica dioxide (SiO_2)	21.6	-
2	Alumina (Al_2O_3)	5.20	3-6
3	Ferric oxide (Fe_2O_3)	3.90	1-4
4	Sodium oxide (Na_2O)	0.23	≤ 0.6
5	Potassium oxide (K_2O)	0.18	-
6	Calcium oxide (CaO)	61.70	59-64
7	Magnesia oxide (MgO)	2.40	≤ 6
8	Sulphuric anhydride	1.50	≤ 3
9	Insoluble residue	1.20	≤ 2
10	Loss of ignition	1.10	≤ 5

Fig. 3.1 OPC and the other supplementary cementitious materials used in this study

3.3.1.2 Silica fume (or) micro-silica

Silica fume (SF) is a by-product of the smelting process in the silicon and ferro-silicon industry. American Concrete Institute defines the silica fume as very fine non-crystalline silica produced in electric furnaces as a by-product of the elemental silicon or alloys containing silicon (ACI 211.4R-2008). Silica fume has been well recognized as a pozzolanic admixture that is effective in enhancing the mechanical properties to a great extent. Addition of silica fume to concrete improves the durability of concrete through reduction in the permeability, refined pore structure leading to a reduction in the diffusion of harmful ions, reduced calcium hydroxide content, which results in a higher resistance to sulfate attack (Siddique, 2011). In the present investigation, silica fume of grade 920 U (including the silica content of more than 90 %) was used in the high performance concrete as the cement replacement. The physical and chemical properties of the chosen silica fume are presented in Table 3.3. It satisfied the requirements of relevant Indian standard IS 15388: 2003.

3.3.1.3 Fly ash

The finely divided residue that results from the combustion of ground or powdered coal and that is transported by flue gases from the combustion zone to the particle removal system is called fly ash. It is also known as pulverized fuel ash and is

Table 3.3 Physical and chemical properties of silica fume, fly ash and GGBFS

S. No	Properties	Results obtained		
		Silica fume	**Fly ash**	**GGBFS**
1	Blaine's fineness (cm^2/gm)	-	5280	6420
2	Specific gravity	2.25	2.25	2.71
3	Silicon dioxide (SiO_2), % by mass	92.40	68.10	26.30
4	Alumina (Al_2O_3),%	3.80	20.80	19.57
5	Ferric oxide (Fe_2O_3),%	1.20	0.90	2.07
6	Sodium oxide (Na_2O),%	0.45	0.09	1.20
7	Potassium oxide (K_2O) ,%	0.32	0.23	0.92
8	Calcium oxide (CaO) ,%	3.16	2.50	32.30
9	Magnesia oxide (MgO) ,%	2.60	0.98	7.90
10	Sulphuric anhydride,%	1.23	0.24	1.88
11	Insoluble residue,%	11.1	0.24	1.88
12	Loss of ignition,%	3.07	2.18	0.88

produced from burning pulverized coal in electric power generating plants. It is a fine grained, powdery particulate material that is collected from the exhaust gases by electrostatic precipitators or bag house filters. Fly ash properties may also vary within the same plant because of several factors. These factors are the type and mineralogical composition of the coal, degree of coal pulverization, type of furnace and oxidation conditions, the collection systems (bag-house collection system, electrostatic precipitator).

Normally, the fly ash particles are spherical in shape and the size of particles ranges from 1 to 150 μm. It is generally finer than Portland cement and the size primarily depends upon the type of collection equipment system. The use of this waste by-product produces economical concrete mixes and stabilizes the environmental system as well. However, fly ash has also been incorporated in concrete production with the purpose to produce good impermeable and durable concrete. When fly ash is added to concrete, it fills in voids between cement particles and reduces the permeability. Since its particle shape is spherical, the spheres act as ball bearings and increases workability in fresh concrete. In mass concrete operations, decreased heat of hydration is another advantage. The fly ash added concrete creates stronger concrete, but the strength develops slowly than Portland cement concretes. In the present experimental study, indigenously available fly ash from Panipat thermal power plant was used as the mineral admixture to prepare the high performance concrete. The physical and chemical properties and the chemical

composition of fly ash are presented in Table 3.3. The fly ash satisfied the requirements of relevant Indian standard IS 3812 (Part2): 2003.

3.3.1.4 Ground granulated blast furnace slag

Blast furnace slag, a non-metallic product consisting of silicates and alumino-silicates of calcium, is an outcome from the blast furnace of iron and steel factories where processing of natural ores are done. The process involves cooling of the molten blast furnace slag through water jetting or water-immersion for granulation. The large size granules are then grounded to at least cement particle size, which is named as ground granulated blast furnace slag (GGBFS). The concrete containing GGBFS greatly influences the pore sizes and results in reduction of cumulative volume considerably. In the present experimental study, indigenously available Ground granulated blast furnace slag (GGBFS) from nearby steel making plant was used as mineral admixture to prepare the high performance concrete. The physical and chemical properties and chemical composition are presented in Table 3.3. The GGBFS satisfied the requirements of relevant Indian standard IS 12089:1987.

3.3.1.5 Fine aggregate

Locally available river sand was used as fine aggregate. The particle size distribution and other physical properties of the fine aggregate are listed in Table 3.4 and Table 3.5 respectively. The fine aggregate was first sieved through 150 micron sieve to make it free from lumps of clay and other foreign matter.

Table 3.4 Sieve analysis of fine aggregates

S. No	Size of sieve in (mm)	Weight retained (gm)	Cumulative % weight retained	Cumulative % weight Passing	% Passing for grading zone- II IS 383:1970
1	10.00	-	-	100	100
2	4.75	12	1.21	98.80	90-100
3	2.36	148	16.13	84.00	75-100
4	1.18	160	32.26	68.00	55-90
5	600µ	192	51.61	48.80	35-59
6	300µ	294	81.25	19.40	8-30
7	150µ	154	96.77	4.00	0-10
8	Residue	32	100.00	0.00	
	Total	1000	279.23		

Table 3.5 Physical properties of fine aggregates

S. No	Characteristics	Requirement as per IS 383: 1970	Fine aggregate
1	Fineness modulus	2.0 to 3.5	2.79
2	Specific gravity	2.6 to 2.7	2.67
3	Water absorption (%)	-	1.41
4	Moisture content (%)	-	1.40

3.3.1.6 Coarse aggregate

The coarse aggregates occupy about 60 to 70% of the total volume of concrete. Because of this large volume fraction, the properties of concrete depend on the type of aggregate, shape and size of aggregate used. In this study, locally available crushed calcareous type aggregate of maximum nominal size of 12.5 mm brought from a single source was used as coarse aggregate. Sieve analysis and other physical properties of the aggregate are listed in the Table 3.6 and Table 3.7 respectively.

Table 3.6 Sieve analysis of coarse aggregates

S. No	Size of sieve in (mm)	Weight retained (gm)	% Weight retained	Cumulative % weight retained	Cumulative % Passing	Range Specified for 12.50 mm downgraded coarse aggregate of IS 383:1970
1	20.00	-	-	-	-	100
2	16.00	-	-	-	-	-
3	12.50	0.20	2.00	2.00	98.00	90-100
4	10.00	3.28	32.77	34.77	65.23	40-85
5	4.75	5.80	58.47	99.23	6.77	0-10
6	2.36	0.73	0	0	0	0
7	Residue	0.00	0	0	0	0

Table 3.7 Physical properties of coarse aggregates

S. No	Characteristics	Coarse aggregate
1	Fineness modulus	6.30
2	Specific gravity	2.69
3	Water absorption (%)	0.87
4	Moisture content (%)	0.67

3.3.1.7 Water

The water to be used both for mixing and curing of concrete should be free from deleterious materials. Potable water is usually used for this purpose. In the present investigation, potable tap water was used. The physical and chemical properties of the tap water are given in Table 3.8 and the water met the requirements of IS 456: 2000.

Table 3.8 Physical and chemical tests results of water

S. No	Chemical oxide	Units	Results obtained	IS 456: 2000 permissible limits
1	pH	-	7.23	Not < 6.00 (max)
2	Alkanity	mg/l	248	250 mg/l (max)
3	Acidity	mg/l	16	50 mg/l (max)
4	Total suspended solids	mg/l	6	2000 mg/l (max)
5	Total organic solids	mg/l	2	200 mg/l (max)
6	Total inorganic solids	mg/l	1540	3000 mg/l (max)
7	SO_2	mg/l	25	400 mg/l (max)
8	Chlorides	mg/l	468	2000 mg/l for concrete (max)

3.3.1.8 Super-plasticizer

A commercially available high range water-reducing admixture namely Glenium-51 based on modified poly-carboxylic ether (PCE) polymer confirming to IS 9103: 1999, with specific gravity 1.10 and pale colour was used to prepare the high performance concrete of the required workability. Poly-carboxylic ether polymer is a third generation high range water-reducing super-plasticizer. The carboxylic ether polymer with long lateral chains greatly improves the cement dispersion and reduces the requirement of water. The properties of super-plasticizer are presented in Table 3.9. The dosage of super plasticizer was decided according to the percentage of total cementitious materials to be used for preparing concrete and to maintain the required workability.

Table 3.9 Properties of chemical admixture

S. No	Properties	Results obtained
1	pH	6.70
2	Specific gravity	1.10
3	Turbidity (NTU/JTU)	33.72
4	Ash content %	0.20
5	Solid content (mg)	9.2

3.4 DESIGN OF EXPERIMENT (DoE)

The behaviour of concrete subjected to high temperature depends on many internal and external parameters, such as properties of constituents of concrete, concrete mix design, and environmental factors etc. The present study attempts to investigate the importance of various concrete mix parameters on the post-heat compressive strength of concrete. The basic influential mix parameters identified in this context are:

a. Water content
b. Binder content
c. Mineral admixture content
d. Water /binder ratio
e. Fine and coarse aggregate content
f. Dosage of super plasticizer

3.4.1 Selection of Orthogonal Array

The first step in Taguchi's approach is the selection of levels and their factors. The determination of factor and their levels influencing the residual compressive strength of high performance concrete were chosen to investigate the response upon the process performance characteristics. The factors in terms of experimental parameters of high performance concrete are water-cement ratio, cement content, mineral admixture content, super-plasticizer content and fine aggregate content. Based on the available literature and laboratory trials, different levels of the above mentioned mix parameters were chosen. The design of experiment was formulated based on Taguchi's standard orthogonal array L_9 (3^4) considering four parameters (mix constituents) at three levels with a maximum of nine mixture trials. The variation of levels in the experiments represents the possible unique combinations involved. Usually, the letters *A, B, C* and *D* represent the factors. The subscripts 1, 2 and 3 represent the factor level value at one, two and three respectively of the Taguchi's fractional factorial orthogonal array experiments. Generally, it is desirable to have minimum levels of parameters to reflect the true behaviour of the output data of the study. The general form of the Taguchi's standard orthogonal array L_9 (3^4) is shown in Table 3.10. In this experimental study, no interaction effects of parameters were considered.

The experimental trials were carried out according to OA and the results obtained were put to further statistical analysis to find out the significant mix parameters that

improve the residual compressive strength of HPC. The details of experimental test runs, optimization procedure, casting of concrete and the results obtained are discussed in the following sections.

Table 3.10 Standard L_9 (3^4) orthogonal array of Taguchi experimental design

Mixes	Factors			
	Factor (A)	**Factor (B)**	**Factor (C)**	**Factor (D)**
	Code	Code	Code	Code
1	A1	B1	C1	D1
2	A1	B2	C2	D2
3	A1	B3	C3	D3
4	A2	B1	C2	D3
5	A2	B2	C3	D1
6	A2	B3	C1	D2
7	A3	B1	C3	D2
8	A3	B2	C1	D3
9	A3	B3	C2	D1

3.4.2 Design and preparation of various HPC mixes

Four types of high performance concretes were investigated in this study. Three high performance concrete mixes were developed by adding three types of pozzolanic mineral admixtures individually (i.e. silica fume, fly ash, GGBFS) apart from designing a non-pozzolanic control mix. The initial trial proportions were designed using the guidelines of ACI-211.4R: 2008 and IS 10262: 2009. Each mineral admixture (silica fume, fly ash and GGBFS) was taken as cement replacement at three levels by weight and most suitable cement replacement were found to achieve the desired compressive strength and workability. Investigations on four different mixes were carried out under four different modules as explained below.

Module 1: Control High Performance Concrete

In case of non-pozzolanic HPC control mix, water binder ratio, cement content, super plasticizer dosage and fine aggregate content were considered as parameters. Table 3.11 shows the factors and chosen levels. A standard L_9 (3^4) Orthogonal Array (OA) was selected for the design of the experimental trial runs with four factors and three levels, giving rise to a total of 9 trials of mixes as shown in the Table 3.12. The code numbers and absolute values of all the four factors are also shown in the Table 3.12.

Table 3.11 Mix parameters and their levels of control HPC

Levels	Water-Cement ratio (A)	Cement content (B) (kg/m^3)	Super plasticizer content (C) (l/m^3)	Fine aggregate content (D) (kg/m^3)
1	0.29	543.062	3.530 (0.65%)	654.124
2	0.30	525.960	3.150 (0.60%)	668.375
3	0.31	508.025	2.794 (0.55%)	681.708

Table 3.12 Experimental design matrix of control HPC

Mixes	Factors and their coded (levels) and absolute values							
	Water-cement ratio (A)		Cement content (B) (kg/m^3)		Super-plasticizer content (C) %		Fine aggregate content (D) (kg/m^3)	
	Code	Absolute	Code	Absolute	Code	Absolute	Code	Absolute
HPC C-1	1	0.28	1	543.062	1	0.65	1	654.124
HPC C-2	1	0.29	2	525.960	2	0.60	2	668.375
HPC C-3	1	0.29	3	508.025	3	0.55	3	681.708
HPC C-4	2	0.30	1	543.062	2	0.60	3	681.708
HPC C-5	2	0.30	2	525.960	3	0.55	1	654.124
HPC C-6	2	0.30	3	508.025	1	0.65	2	668.375
HPC C-7	3	0.31	1	543.062	3	0.55	2	668.375
HPC C-8	3	0.31	2	525.960	1	0.65	3	681.708
HPC C-9	3	0.31	3	508.025	2	0.60	1	654.124

Module 2: Fly ash High Performance Concrete

In case of fly ash based HPC mix, cement content, fly ash content (FA), super-plasticizer dosage and fine aggregate content were considered as control parameters. Table 3.13 shows the chosen factors and their levels. The experimental trial runs with four factors and three levels provided nine combinations of trial mixes as shown in Table 3.14.

Table 3.13 Mix design parameters of fly ash HPC and their levels

Parameters				
Levels	**Cement content (A) (kg/m^3)**	**Fly Ash content (B) (kg/m^3)**	**Super plasticizer content (C) (l/m^3)**	**Fine aggregate content (D) (kg/m^3)**
1	434.449 (80%)	108.612 (20%)	4.888 (0.80%)	619.919
2	393.720 (75%)	131.240 (25%)	5.512 (0.95%)	627.045
3	355.618 (70%)	152.408 (30%)	6.096 (1.10%)	633.711

Table 3.14 Experimental design matrix of fly ash HPC with parameters and their coding

Mixes	Factors							
	Cement content (A) (kg/m^3)		**Fly ash content (B) (kg/m^3)**		**Super-plasticizer content (C) (l/m^3)**		**Fine aggregate Content (D) (kg/m^3)**	
	Code	Absolute	Code	Absolute	Code	Absolute	Code	Absolute
HPC F-1	1	434.449	1	108.612	1	4.888	1	619.919
HPC F-2	1	434.449	2	131.240	2	5.512	2	627.045
HPC F-3	1	434.449	3	152.408	3	6.096	3	633.711
HPC F-4	2	393.720	1	108.612	2	5.512	3	633.711
HPC F-5	2	393.720	2	131.240	3	6.096	1	619.919
HPC F-6	2	393.720	3	152.408	1	4.888	2	627.045
HPC F-7	3	355.618	1	108.612	3	6.096	2	627.045
HPC F-8	3	355.618	2	131.240	1	4.888	3	633.711
HPC F-9	3	355.618	3	152.408	2	5.512	1	619.919

Module 3: Ground granulated blast furnace slag (GGBFS) High Performance Concrete

Table 3.15 shows the factors and levels chosen for the GGBFS based mix. The cement content, ground granulated blast furnace slag content (GGBFS), super-plasticizer dosage and fine aggregate content were considered as processing parameters. The design of the experimental plan with four factors and three levels provided nine combinations of trial mixes as shown in the Table 3.16.

Table 3.15 Mix design parameters of GGBFS HPC and their levels

Parameters				
Levels	**Cement Content (A) (kg/m^3)**	**GGBFS content (B) (kg/m^3)**	**Super-plasticizer content (C) (l/m^3)**	**Fine aggregate content (D) (kg/m^3)**
1	380.143 (70%)	162.919 (30%)	2.172 (0.40%)	633.298
2	314.976 (60%)	209.984 (40%)	2.362 (0.45%)	641.534
3	254.013 (50%)	254.013 (50%)	2.540 (0.50%)	649.238

Module 4: Silica Fume High Performance Concrete

In silica fume based HPC, the cement content, silica fume content (SF), super-plasticizer content and fine aggregate content were considered as significant parameters for making the high performance concrete. Table 3.17 shows the factors and levels chosen in this context. The experimental trial runs with four factors and three levels provided nine combinations of trial mixes as shown in the Table 3.18.

Table 3.16 Experimental design of GGBFS HPC with parameters and their coding

Mixes	Factors							
	Cement content (A) (kg/m^3)		**GGBFS content (B) (kg/m^3)**		**Super-plasticizer content (C) (l/m^3)**		**Fine aggregate Content (D) (kg/m^3)**	
	Code	Absolute	Code	Absolute	Code	Absolute	Code	Absolute
HPC G-1	1	380.143	1	162.919	1	4.888	1	633.298
HPC G-2	1	380.143	2	209.984	2	5.512	2	641.534
HPC G-3	1	380.143	3	254.013	3	6.096	3	649.238
HPC G-4	2	314.976	1	162.919	2	5.512	3	649.238
HPC G-5	2	314.976	2	209.984	3	6.096	1	633.298
HPC G-6	2	314.976	3	254.013	1	4.888	2	641.534
HPC G-7	3	254.013	1	162.919	3	6.096	2	641.534
HPC G-8	3	254.013	2	209.984	1	4.888	3	649.238
HPC G-9	3	254.013	3	254.013	2	5.512	1	633.298

Table 3.17 Mix design parameters of silica fume HPC and their levels

Parameters				
Levels	**Cement content (A) (kg/m^3)**	**Silica fume content (B)(kg/m^3)**	**Super plasticizer content (C) (l/m^3)**	**Fine aggregate Content (D) (kg/m^3)**
1	488.731 (90%)	54.303 (10%)	2.987 (0.55%)	637.063
2	446.199 (85%)	78.740 (15%)	3.150 (0.60%)	643.619
3	406.400 (80%)	101.600 (20%)	3.302 (0.65%)	649.751

Table 3.18 Experimental design matrix of silica fume HPC with parameters and their coding

Mixes	Factors							
	cement content (A) (kg/m^3)		**Silica fume content (B) (kg/m^3)**		**Super-plasticizer content (C) (l/m^3)**		**Fine aggregate Content (D) (kg/m^3)**	
	Code	Absolute	Code	Absolute	Code	Absolute	Code	Absolute
HPC S-1	1	488. 731	1	54.303	1	2.987	1	585.687
HPC S-2	1	488. 731	2	78.740	2	3.150	2	591.740
HPC S-3	1	488. 731	3	101.600	3	3.302	3	597.352
HPC S-4	2	446. 199	1	54.303	2	3.150	3	597.352
HPC S-5	2	446. 199	2	78.740	3	3.302	1	585.687
HPC S-6	2	446. 199	3	101.600	1	2.987	2	591.740
HPC S-7	3	406.400	1	54.303	3	3.302	2	591.740
HPC S-8	3	406.400	2	78.740	1	2.987	3	597.352
HPC S-9	3	406.400	3	101.600	2	3.150	1	585.687

3.4.3 Mixing, casting and curing

In this experimental study casting of the test specimens were done under the laboratory condition using the above indicated mix combinations. The cubic specimens of size 100 mm × 100 mm × 100 mm were cast for heating and then for monotonic concentric compression testing. Before each casting, the quantities of various ingredients i.e. cement, fine aggregate, coarse aggregate, water, mineral admixture and super plasticizer were kept ready in required proportions. Initially, the mixer drum was wetted thoroughly; the coarse aggregate and cementitious materials were added together in the mixer drum in dry state while keeping the drum in motion. About more than half of the water added super-plasticizer was poured slowly to get a uniform mix. The uniformity of the mix was indicated by its uniform colour when the colours of individual materials got suppressed. Following the mix became uniform; the mixing was further continued for about two minutes. Subsequently, the fine aggregate was added to the mixing drum while the drum was in motion. Finally, the remaining water was added to mix, and the mixing operation was continued for about five minutes. Simultaneously, the steel moulds for casting the specimens were cleaned, brushed, oiled and placed on a vibrating table with a speed range of 12000 ± 400 RPM and an amplitude range of 0.055 mm. A desired level of workability was achieved for all types of high performance concretes. To achieve the required workability, a commercially available super-plasticizer was used for preparing the high performance concrete mixes. The workability of concrete was measured using the slump cone and compaction factor test. The slump values ranging from 150 to 180 mm were obtained in all the mixes, which seem to be quite satisfactory for high performance concrete mixes. The concrete specimens were cast for each test variable investigated as shown in the Figure 3.2.

Fig. 3.2 Casting and curing of cube test specimens

3.4.4 Thermal testing

After a total of 28 days of ageing, the specimens were dried in an oven at 105 ± 5 °C for 24 hrs to remove excess moisture in order to avoid undue thermal spalling during heating to the target temperatures. Figure 3.3 shows an inside view of hot air oven with specimens. Subsequent to that the specimens were heated in an electric high temperature muffle furnace to the desired target temperatures. The said high temperature muffle furnace had a maximum operating temperature of 1200 °C and any temperature could be maintained up to ± 1 °C accuracy. The furnace was controlled by programmable microprocessor based temperature controller with feedback temperature from a K-type Thermocouple located in the furnace chamber. The outer dimensions of the furnace were 192 cm wide × 105 cm deep × 105 cm high. The furnace compartment was completely closed except for two 25 mm holes, which were also liable to be sealed with porcelain stopper. One hole was used to insert thermocouples in the furnace and another hole for monitoring the specimens in the furnace during heating. These holes provided the air circulation within the furnace and also acted as exhaust during heating operations. However, these holes were generally closed during the heating process. It was possible to accommodate 18 test samples of concrete cubes in the furnace chamber

Fig. 3.3 A view of hot air oven

simultaneously with satisfactory temperature homogeneity during the heating process. An additional protective measure was also adopted to avoid damage to the unprotected heating elements in the event of spalling, if any, during the heating process. It was achieved by enclosing the specimens in a specially fabricated steel cage. At the same time, it was also ensured that enclosing the cage did not obstruct the heating of the specimens. Figure 3.4 shows the inside view of the muffle furnace.

Fig. 3.4 Inside view of high temperature muffle furnace

The testing was planned to be performed at five different temperatures i.e. room temp., 200 °C, 400 °C, 600 °C and 800 °C. The test specimens were subjected to target temperatures after the attainment of age of 28 days. All cubic specimens were heated without preload. The rate of heating was kept at 5 °C/min with each temperature level maintained for 2 hours and then the furnace was switched off. The heating rate was chosen on the basis of the fact that normally for fire protection, a heating rate of 5 °C/ minute is adopted (Zaidi 2011, Zaidi et al. 2012). On completion of the exposure time the furnace was switched off and it was kept in closed condition for 1 hour before opening the door of the furnace to allow natural cooling up to room temperature. The heating rate of 5 °C/minute was the rate of rise inside the furnace and not the temperature rise of inside of the concrete specimens. Subsequent to a single cycle of heating and cooling, the conventional uni-axial destructive compressive strength tests were conducted on the test specimens.

3.4.5 Details of test specimens

Four different series of cubic specimens (100 mm × 100 mm × 100 mm) for the three types of pozzolanic high performance concrete mixes along with the non-pozzolanic HPC mix were cast to achieve objectives of research. The test specimens of plain and fly ash HPC were tested under full range of target temperatures namely room temp., 200 °C, 400 °C, 600 °C and 800 °C. However, the GGBFS HPC and silica fume HPC experienced spalling before reaching the target temperatures of 600 °C and 400 °C respectively. Therefore, the original test plan was customized to avoid the spalling of test specimens and these GGBFS HPC and silica fume HPC were finally exposed to lower range of temperatures.

Four types of concrete specimens were cast for each test variable investigated as shown in the Table 3.19 and Figure 3.2. Three specimens were cast in order to get the average of three results. Thus, 162 control HPC and 594 pozzolanic HPC specimens were cast to examine the residual compressive strength behavior of concrete both at ambient temperature and after subjecting to target temperatures. The specimens were de-moulded after 24 hrs and placed in the water tank for curing. After 13 days of water curing the cubes were removed from the curing tank and stored for another 14 days in the laboratory at ambient condition before testing. The details of the specimen's type, its number and target temperatures of exposure are summarized in the Table 3.19.

Table 3.19 Characteristics of specimens

Mixes	Target temperatures					Confirmation test	Total
	Room Temp.	200 °C	400 °C	600 °C	800 °C		
	Control HPC						
HPC C-1	3	3	3	3	3	3	18
HPC C-2	3	3	3	3	3	3	18
HPC C-3	3	3	3	3	3	3	18
HPC C-4	3	3	3	3	3	3	18
HPC C-5	3	3	3	3	3	3	18
HPC C-6	3	3	3	3	3	3	18
HPC C-7	3	3	3	3	3	3	18
HPC C-8	3	3	3	3	3	3	18
HPC C-9	3	3	3	3	3	3	18
Fly ash HPC							
HPC F-1	3	3	3	3	3	3	18
HPC F-2	3	3	3	3	3	3	18
HPC F-3	3	3	3	3	3	3	18
HPC F-4	3	3	3	3	3	3	18
HPC F-5	3	3	3	3	3	3	18
HPC F-6	3	3	3	3	3	3	18
HPC F-7	3	3	3	3	3	3	18
HPC F-8	3	3	3	3	3	3	18
HPC F-9	3	3	3	3	3	3	18
	Silica fume HPC						
Mixes	**Room Temp.**	**100 °C**	**200 °C**	**300 °C**	**350 °C**	**400 °C**	**Confirmation test**	**Total**
HPC S-1	3	3	3	3	3	3	3	21
HPC S-2	3	3	3	3	3	3	3	21
HPC S-3	3	3	3	3	3	3	3	21
HPC S-4	3	3	3	3	3	3	3	21
HPC S-5	3	3	3	3	3	3	3	21
HPC S-6	3	3	3	3	3	3	3	21
HPC S-7	3	3	3	3	3	3	3	21
HPC S-8	3	3	3	3	3	3	3	21
HPC S-9	3	3	3	3	3	3	3	21
	GGBFS HPC								
Mixes	**Room Temp.**	**100 °C**	**200 °C**	**300 °C**	**400 °C**	**500 °C**	**600 °C**	**800 °C**	**Confirmation test**	**Total**
HPC G-1	3	3	3	3	3	3	3	3	3	27
HPC G-2	3	3	3	3	3	3	3	3	3	27
HPC G-3	3	3	3	3	3	3	3	3	3	27
HPC G-4	3	3	3	3	3	3	3	3	3	27
HPC G-5	3	3	3	3	3	3	3	3	3	27
HPC G-6	3	3	3	3	3	3	3	3	3	27
HPC G-7	3	3	3	3	3	3	3	3	3	27
HPC G-8	3	3	3	3	3	3	3	3	3	27
HPC G-9	3	3	3	3	3	3	3	3	3	27

3.5 ANALYSIS OF RESULTS

3.5.1 Module 1: Control HPC

The strength testing of specimens was carried out at room temperature conditions after a complete cycle of heating and cooling. This section presents the analysis of results for the non-pozzolanic control concrete specimens.

Figure 3.5 shows the specimens of plain HPC after exposing to a cycle of heating and cooling. The conventional uni-axial destructive compressive strength tests were conducted on the specimens using Amsler make compression testing machine (CTM) (Figure 3.6). Three specimens were tested for each result and the average values are given in the Table 3.20.

Fig. 3.5 Control HPC specimens exposed to different temperatures

3.5.1.1 Parameter optimization by Taguchi technique

A statistical analysis was performed to determine the statistically significant factors. In the present study, the aim was to determine the best possible concrete mix proportions in order to achieve the maximum residual compressive strength of heated

concrete. Generally, the optimum conditions were arrived using the loss function as larger-the better, which is a quality characteristic function to maximize the compressive strength of concrete. The compressive strength is always larger the better criterion. So, the 'larger the better' type of quality characteristic situation was evaluated in terms of Signal to Noise ratio (S/N) by using the equation (3.1).

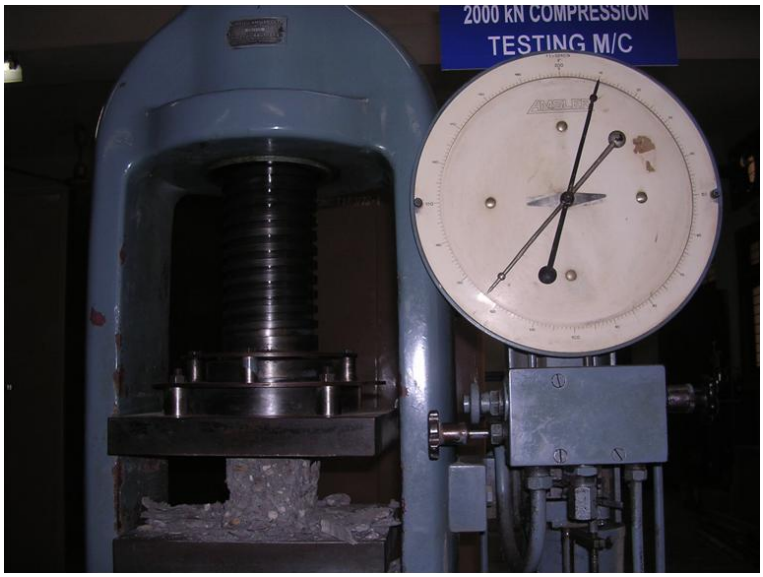

Fig. 3.6 Testing of heated cubes in compressive testing machine

Table 3.20 Results of residual compressive strength of control HPC

Mixes	**Residual Compressive Strength, MPa (% of room temperature strength)**				
	Room Temp.	**200 °C**	**400 °C**	**600 °C**	**800 °C**
HPC C-1	77.00 (100%)	87.33 (113.42%)	67.33 (87.45%)	46.67 (61.40%)	20.83 (27.06%)
HPC C-2	71.33 (100%)	79.33 (111.21%)	67.00 (93.93%)	47.33 (66.36%)	24.50 (34.35%)
HPC C-3	73.33 (100%)	78.33 (106.82%)	71.6 (97.72%)	42.33 (57.73%)	21.50 (29.32%)
HPC C-4	74.33 (100%)	88.67 (119.28%)	67.33 (90.58%)	44.67 (58.26%)	21.17 (28.48%)
HPC C-5	76.67 (100%)	84.67 (110.43%)	72.00 (89.67%)	49.33 (64.35%)	22.67 (29.57%)
HPC C-6	75.83 (100%)	88.00 (116.04%)	68.00 (92.10%)	48.33 (63.74%)	24.17 (31.87%)
HPC C-7	78.00 (100%)	76.33 (97.86%)	71.00 (91.03%)	48.33 (61.97%)	22.33 (28.63%)
HPC C-8	78.00 (100%)	92.00 (117.95%)	77.33 (99.15%)	44.83 (57.48%)	21.17 (27.14%)
HPC C-9	85.50 (100%)	80.67 (94.35%)	59.33 (69.40%)	47.67 (55.75%)	22.33 (26.12%)

The mean numerical values of signal to noise ratio (S/N) of each parameter and temperature of exposure are given in Table 3.21. The variation of S/N ratio with the three levels of each parameter was also plotted according to the values given in Table 3.21. Figure 3.7 shows the effects of effective performance factors analysis of signal to noise ratio (S/N) at all the three levels for the various chosen factors i.e. water-cement ratio (W/C), cement content, super-plasticizer content and fine aggregate content. From the Figure 3.7 (a), the maximum values of signal to noise (S/N) ratio at room temperatures was obtained for water- cement ratio at Level A_3 (0.31), for cement content at Level B_3 (508.025 kg/m^3), for super-plasticizer dosage at Level C_1 (3.530 L/m^3 (0.65% dosage of content of cement)) and for fine aggregate content at Level D_1 (654.124 kg/m^3). It can be observed that the water–cement ratio and fine aggregate content acted as main influencing factors at room temperature. The cement content and super plasticizer content did not seem to have shown significant effect at room temperature conditions.

The parameters appeared to change their influence on the residual compressive strength of concrete with the change in temperature of exposure. At 200 °C exposure, the optimum values were obtained for water- binder ratio at Level A_2 (0.30), for cement content at Level B_2 (524.960 kg/m^3), for super-plasticizer at Level C_1 (3.530 L/m^3 (0.65% dosage of total cementitious materials)) and for fine aggregate content at Level D_3 (681.708 kg/m^3). The results indicate that the residual compressive strength of concrete exposed to 200 °C increased compared to the respective room temperature strength irrespective of the level of any parameter. This strength gain may be due to the formation of tobermorite gel and dehydration of water and moisture (Chan 1999[a]).

Table 3.21 Signal to noise (S/N) ratio values of heated Control HPC

Mixes	Room Temp.	200 °C	400 °C	600 °C	800 °C
HPC C-1	37.730	38.824	36.565	33.380	26.375
HPC C-2	37.066	37.989	36.521	33.503	27.783
HPC C-3	37.306	37.879	37.106	32.534	26.649
HPC C-4	37.424	38.955	36.565	33.000	26.513
HPC C-5	37.692	38.554	37.147	33.863	27.108
HPC C-6	37.597	38.890	36.650	33.685	27.664
HPC C-7	37.842	37.654	37.025	33.685	26.979
HPC C-8	37.842	39.276	37.767	33.032	26.513
HPC C-9	38.639	38.134	35.466	33.564	26.979

The optimum values were obtained for water- binder ratio at Level A_3 (0.31), for cement content at Level B_2 (524.960 kg/m^3), for super-plasticizer at Level C_3 (2.794 L/m^3 (0.55% dosage of total cementitious materials)) and for fine aggregate content at Level D_3 (681.708 kg/m^3) for specimens exposed to 400 °C temperature. At 400 °C temperature, the values of residual compressive strength reduced and stabilized at around their original room temperature strength. However, the residual strength values reduced sharply for all the mixes as the temperature of exposure increased to 600 °C. The W/C ratio and fine aggregate content were observed to be the most influencing parameters at 600 °C as shown Figure 3.7 (d). The optimum residual strength of concrete was obtained for water-binder ratio at Level A_2 (0.30), for cement content at Level B_2 (524.960 kg/m^3), for super-plasticizer at Level C_3 (2.794 L/m^3 (0.55% dosage of total cementitious materials)) and for fine aggregate content at Level D_2 (668.375 kg/m^3) for the specimens exposed to 600 °C.

A severe strength loss was observed as the temperature of exposure increased to 800 °C for all the mixes of control HPC. The fine aggregate content seemed to be the main influencing parameter at 800 °C (Figure 3.7 (e)). The optimum conditions at 800 °C exposure were obtained for water- binder ratio at Level A_2 (0.30), for cement content at Level B_2 (524.960 kg/m^3), for super-plasticizer at Level C_2 (0.60% dosage of content of cement) and for fine aggregate content at Level D_2 (668.375 kg/m^3). Table 3.22 displays the individual optimal values and the corresponding optimal settings of process parameters for the entire range of heated concrete.

3.5.1.2 Application of the utility concept for multi temperature responses

The present experimental study was aimed and designed with an objective of arriving at optimum proportions of mix parameters for maximum residual compressive strength of HPC at all target temperatures. The Taguchi off-line approach is employed to obtain best-suited mono characteristic response optimization of concrete mix proportions. From the results of Taguchi's technique, five dissimilar optimum mix proportions were obtained for maximum post fire residual compressive strength of control HPC corresponding to different target elevated temperatures. The five dissimilar optimum mix proportions obtained are shown in the Table 3.23. The utility concept was applied to the test results to obtain single optimized set of mix proportions for achieving maximum residual strength of concrete heated to any elevated temperature up to 800 °C. The application of utility concept requires the computation of all S/N ratios of mix parameters

optimized at different temperatures for larger the better optimization criterion. Assuming equal weights at all temperatures, the weighted S/N ratios obtained for different temperatures were summed up and with these data the mean process parameters were determined. Using the significant contribution of mean utility values of main effects, the optimal setting process parameters were determined. These concepts were applied to the present problem and absolute optimum proportions of mix parameters for HPC were obtained at different exposures temperatures. The methodology applied can be explained as follows:

Table 3.22 Mean S/N ratios for various parameters at different temperatures (Main effects raw data)

Level No	Factor A	Factor B	Factor C	Factor D
		Room temperature		
1st Level	73.899	76.444	**76.944***	**79.722***
2nd Level	75.611	75.333	77.056	75.056
3rd Level	**80.500***	**78.222***	76.000	75.222
		200 ˚C temperature exposure		
1st Level	81.667	84.111	**89.111***	84.222
2nd Level	**87.111***	**85.333***	82.889	81.222
3rd Level	83.000	82.333	79.778	**86.333***
		400 ˚C temperature exposure		
1st Level	68.667	68.556	70.889	66.222
2nd Level	69.111	**72.111***	64.556	68.667
3rd Level	**69.222***	66.333	**71.556***	**72.111***
		600 ˚C temperature exposure		
1st Level	45.444	46.566	46.611	47.889
2nd Level	**47.444***	**47.167***	46.556	**48.000***
3rd Level	46.944	46.111	**46.667***	43.994
		800 ^{o}C temperature exposure		
1st Level	22.278	21.444	22.056	21.994
2nd Level	**22.667***	**22.778***	**22.667***	**23.667***
3rd Level	21.944	22.667	22.167	21.278

***** Indicates optimum level of values for a given temperature of exposure

(i) Construction of preference scale

A preference scale is constructed for determining the utility value of HPC for room temperature using the equation (3.6). Following are the details of calculations for

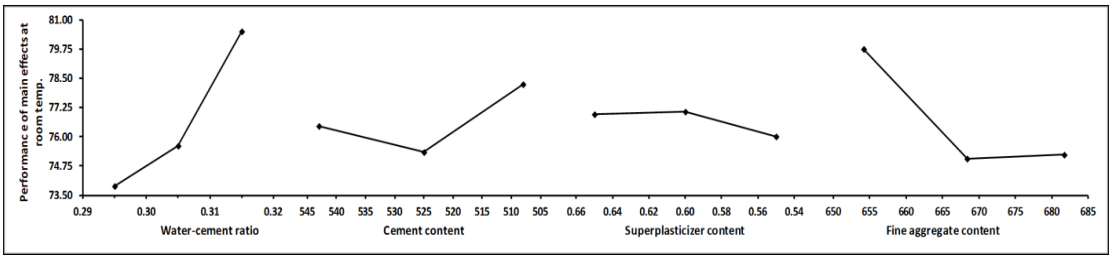

(a) Room temperature

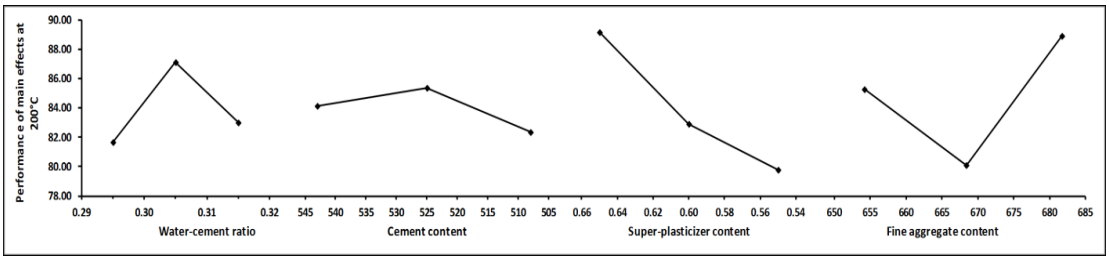

(b) 200 °C

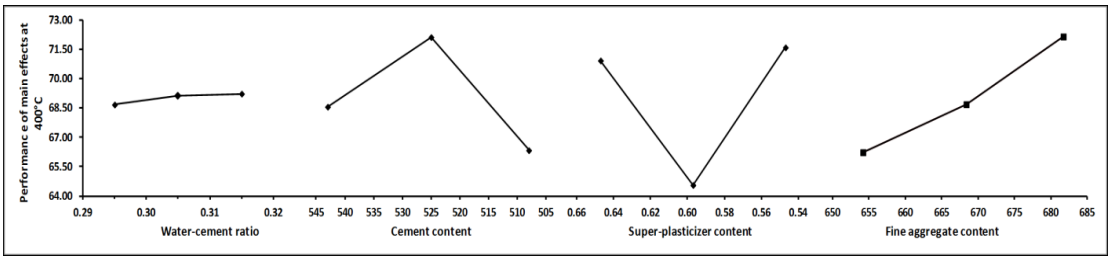

(c) 400 °C

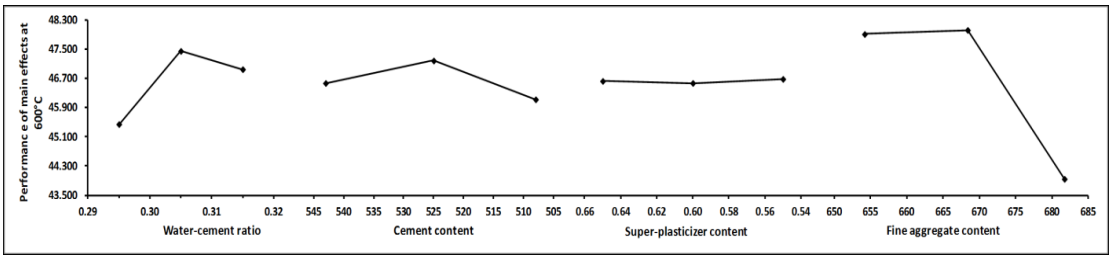

(d) 600 °C

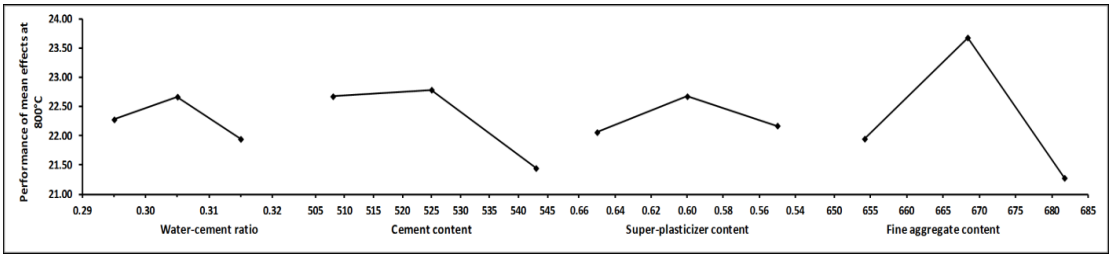

(e) 800 °C

Fig. 3.7 (a)-(e) Mean values of main effect of parameters on the performance characteristic of heated concrete

Table 3.23 Optimal setting of process parameters (phase I) and optimal values of individual quality characteristics

No.	Quality characteristics	Optimum setting of process parameters	Predicted optimum value	95% of Predicted confidence intervals of quality characteristics
1	Room Temp.	A_3, B_3, C_1, D_1	84.667	$81.339 < \mu_{\text{Room temp.}} < 87.995$
2	200 °C	A_2, B_2, C_1, D_3	88.815	$80.157 < \mu_{200\,^{o}C} < 97.472$
3	400 °C	A_3, B_2, C_3, D_3	77.333	$75.646 < \mu_{400\,^{o}C} < 79.020$
4	600 °C	A_2, B_2, C_3, D_2	48.611	$47.306 < \mu_{600\,^{o}C} < 49.917$
5	800 °C	A_2, B_2, C_2, D_2	23.815	$22.623 < \mu_{800\,^{o}C} < 25.006$

the preference scale value $P_{(Room\ temp.)}$ expressed on a logarithmic scale for compressive strength of concrete at room temperature.

M_i^* = optimum value of room temperature is 84.667 (refer Table 3.24)

M_i' = minimum acceptable value at room temperature is 60 MPa (all the observed values in Table 3.20 lie between 67 MPa and 74 MPa)

Using the above values and the equations (3.6) and (3.7), the preference scale for room temperature is constructed as

$$P_{(Room\ Temp.)} = 60.176 \times \log\left(\frac{X_{Room\ Temp.}}{60}\right) \tag{3.12}$$

In a similar way, the preference scale values for other temperatures, namely 200 °C, 400 °C, 600 °C and 800 °C were also calculated.

(ii) Weightage of quality characteristics

The concrete responses of five different target temperatures were assumed as equally important for optimizing the compressive strength of heated concrete. As a result in the equation (3.8), the selected temperatures were assigned equal weights,

$W_{(Room\ Temp)}$ = Weight assigned to room temperature as 0.2

$W_{(200\,^{o}C)}$ = Weight assigned to 200 °C as 0.2

$W_{(400\,^{o}C)}$ = Weight assigned to 400 °C as 0.2

$W_{(600\,^{o}C)}$ = Weight assigned to 600 °C as 0.2

$W_{(800\,^{o}C)}$ = Weight assigned to 800 °C as 0.2

(iii) Calculation of utility value of control HPC

The utility value of the composite measure was then calculated using the equations (3.9 and 3.10):

The below mentioned overall utility function was employed to calculate the utility value data of control HPC at various temperatures of exposure:

$$U(n, R) = P_{(Room\ temp)}(n, R) \times W + P_{(200\ ^oC)}(n, R) \times W + P_{(400\ ^oC)}(n, R) \times W + P_{(600\ ^oC)}(n, R) \times W + P_{(800\ ^oC)}(n, R) \times W \quad (3.13)$$

where, *n* is the trial number, = 1, 2,..... 9; R is the replication of samples = 1, 2, 3. The calculated utility data are reported in Table 3.24.

Table 3.24 Utility data based on quality characteristics raw data: (Room temp., 200 °C, 400 °C, 600 °C and 800 °C)

Mixes	1	2	3	Mean	S/N ratio
HPC C-1	6.812	7.455	6.866	7.044	16.957
HPC C-2	6.613	7.061	6.119	6.597	16.387
HPC C-3	6.037	5.698	5.640	5.792	15.256
HPC C-4	7.630	5.633	7.105	6.789	16.637
HPC C-5	9.072	6.513	7.399	7.661	17.686
HPC C-6	8.136	7.942	7.422	7.833	17.879
HPC C-7	7.073	6.625	6.614	6.771	16.613
HPC C-8	7.888	8.071	7.788	7.915	17.969
HPC C-9	6.041	6.930	7.585	6.852	16.717

3.5.1.3 Data analysis and estimation of optimal mix proportions

The utility values were analysed using the larger the better quality characteristic type and were calculated using equation (3.1). The calculated values of mean responses (mean utility value) and the signal to noise ratios (S/N ratio) are given in Tables 3.25 and Table 3.26 respectively, and the mean responses of mix proportions of utility values are plotted in Figure 3.8. This figure depicts clearly that the second level of water-cement ratio A_2 (0.30), the second level of cement content B_2 (524.960 kg/m^3), the first level of super-plasticizer content C_1 (3.530 L/m^3 (0.65% of total cementitious materials)) and the first level of fine aggregate content D_1 (654.124 kg/m^3), shall yield the best optimal performance value of the utility function, i.e., the residual compressive strength of high performance concrete exposed to different temperatures. Table 3.27 shows absolute values of optimal values of mix proportions for optimized high performance concrete mix parameters and their levels of multi-response optimization using the utility concept.

Table 3.25 Mean utility vales of main effects of raw data

Levels	Cement content (A)	Fly ash content (B)	Super-plasticizer content (C)	Fine aggregate content (D)
1	6.478	6.868	**7.598***	**7.186***
2	**7.428***	**7.391***	6.746	7.067
3	7.179	6.826	6.741	6.832

***** Indicates the best performance of utility values for different temperature of exposures

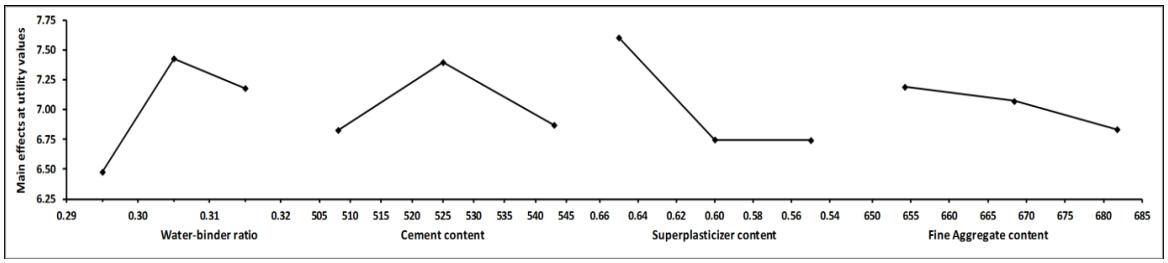

Fig. 3.8 Mean responses of main effects of process parameters of utility values

Table 3.26 Mean utility vales of signal to noise (S/N) ratio of raw data

Levels	Cement content (A)	Fly ash content (B)	Super-plasticizer content (C)	Fine aggregate content (D)
1	16.200	16.735	**17.602***	**17.120***
2	**17.401***	**17.348***	16.580	16.960
3	17.100	16.167	16.518	16.621

***** Indicates the best performance of signal to noise (S/N) ratio values for different temperature of exposures

Table 3.27 Optimal setting of process parameters utility values (phase II)

S. No.	Process parameter	Level	Optimal values
1	Water-cement ratio	A_2	0.30
2	Cement content (kg/m^3)	B_2	524.960
3	Super-plasticizer content %	C_1	0.65
4	Fine aggregate content (kg/m^3)	D_1	654.194

3.5.1.4 Predicted means (optimal values) of mix proportion parameters

The optimum value of utility ($U_{\text{Room Temp},200\ ^oC,\ 400\ ^oC,\ 600\ ^oC,\ 800\ ^oC}$) was predicted at the selected levels of variables as stated above viz. Water-cement ratio (A_2), cement content (B_2) and super-plasticizer content (C_1). The estimated mean of the response of mix proportion parameters ($U_{\text{Room Temp.,}\ 200\ ^oC,\ 400\ ^oC,\ 600\ ^oC,\ 800\ ^oC}$) can be determined as (Garg 2010):

$$\mu_{\text{Room Temp.,}200\ ^oC,\ 400\ ^oC,\ 600\ ^oC,\ 800\ ^oC} = \overline{A}_2 + \overline{B}_2 + \overline{C}_1 - 2\overline{T} \qquad (3.14)$$

where, $\overline{T}$ = overall mean of utility value = 7.473 which is taken from Table 3.24. The values of $\overline{A}_2, \overline{B}_2, \overline{C}_1$ were taken from Table 3.25.

The utility values of both the main effects and signal-to-noise (S/N) ratio values of raw data were analysed at each level of all the parameters. It is clear from Table 3.27 and Figure 3.8 that the mean utility values of level of second water-cement ratio (A_2), second level of cement content (B_2), first level of super-plasticizer content (C_1) and first level of fine

aggregate content (D_1) would yield best performance in terms of utility value and S/N ratio values for different temperatures of exposure.

Substituting the values of the above mentioned terms in equation (3.12), we get

$\mu_{Room\ Temp.,\ 200\ ºC,\ 400\ ºC,\ 600\ ºC,\ 800\ ºC} = 7.428 + 7.391 + 7.304 + 7.598 - 2\ (7.521) = 7.916$

The 95 % confidence interval of confirmation of experiments (CI_{CE}) was calculated using equation (3.11) and the values are presented in Table 3.27.

f_e = error of DOF = 2; V_e = error variance = 0.097

N = 27; n_{eff} = 27/7 (calculated)

R = 3; $F_{0.05}(1, 02)$ = 18.51 (Tabulated F value)

The confidence interval for confirmation experiments (CI_{CE}) = ± 1.032

The predicted optimal range (for confirmation runs of the experiment) is:

$$(\mu_{Room\ Temp.,\ 200\ ºC,\ 400\ ºC,\ 600\ ºC,\ 800\ ºC} - CI_{CE}) < \mu_{Room\ Temp.,\ 200\ ºC,\ 400\ ºC,\ 600\ ºC,\ 800\ ºC} < (\mu_{Room\ Temp.,\ 200\ ºC,\ 400\ ºC,\ 600\ ºC,\ 800\ ºC} + CI_{CE})$$

$$6.219 < \mu_{Room\ Temp.,\ 200\ ºC,\ 400\ ºC,\ 600\ ºC,\ 800\ ºC} < 8.283$$

3.5.1.5 Analysis of variance (ANOVA)

A statistical analysis of the data was carried out for evaluation of significance of each selected parameter for its contribution towards the optimization of residual compressive strength of high performance concrete. The analysis of variance (ANOVA) and mean responses (mean utility value at each level of desired parameters) were performed to identify the relative significance and future promising direction of the process parameters. Table 3.28 shows the computed results of the ANOVA with 95% confidence for mono characteristics optimization of Taguchi method. The percent contributions of the various parameters as quantified under the respective columns of Table 3.28 reveals that the fine aggregate content shows a significant effect on the residual compressive strength of heated concrete at all the temperatures with a maximum influence at 600 °C of about 77.486%. The water-cement ratio was observed to be the second most influencing parameter with a maximum significance at room temperature. The super plasticizer content showed a significant influence only for temperatures of 200 °C to 400 °C with 51.401% and 46.001% contributions towards the residual strength values respectively. The cement content appeared to be relatively insignificant parameter since its F- ratios were observed to be lower than the critical values. The F-ratios and

Table 3.28 ANOVA results for control HPC exposed to various temperatures

Factors	Statistical parameters	Room temperature	200 °C	400 °C	600 °C	800 °C
Water-cement ratio (A)	Pooling	No	No	Yes	No	Yes
	Degree of freedom	2	2	(2)	2	(2)
	Sum of square	70.574	48.321	0.519	6.500	0.784
	Variance	35.287	24.160	-	3.250	-
	F-ratio	34.963	3.539	-	7.630	-
	Pure SS	68.556	34.667	-	5.648	-
	(%) contribution	53.816	14.623	-	14.042	-
Cement content (B)	Pooling	Yes	Yes	No	Yes	No
	Degree of freedom	(2)	(2)	2	(2)	2
	Sum of square	12.741	13.654	50.963	1.685	3.284
	Variance	6.370	-	25.481	-	1.642
	F-ratio	6.312	-	4.89	-	4.626
	Pure SS	10.722	-	0.805	-	2.574
	(%) contribution	8.417	-	25.360	-	18.62
Super-plasticizer content (C)	Pooling	Yes	No	No	Yes	Yes
	Degree of freedom	(2)	2	2	(2)	(2)
	Sum of square	2.019	135.506	89.556	0.019	0.636
	Variance	-	67.753	44.778	-	-
	F-ratio	-	9.924	172.714	-	-
	Pure SS	-	121.852	89.037	-	-
	(%) contribution	-	51.401	46.001	-	-
Fine aggregate content (D)	Pooling	No	No	No	No	No
	Degree of freedom	2	2	2	2	2
	Sum of square	42.056	39.580	52.519	32.019	9.117
	Variance	21.028	19.790	26.259	16.009	4.559
	F-ratio	20.832	2.899	101.286	37.587	12.843
	Pure SS	40.037	25.9026	52.000	31.167	8.407
	(%) contribution	31.429	10.936	26.866	77.486	60.831

Table 3.29 shows the computed results of pooled versions of utility values of the ANOVA at 0.05% level of significance with 95% confidence level. For confirmation test results, the F-ratio values were calculated to identify the importance of factors from variance within the confidence level and the percent contributions of the various parameters as quantified under the respective columns of Table 3.29. It reveals that water-cement ratio and super-plasticizer content show a significant effect on the residual compressive strength of heated concrete with 34.075 and 34.101% contributions respectively at all the temperatures. The cement content was observed to be the next influencing parameter with 10. 819% contribution.

Table 3.29 Pooled ANOVA for utility vales of raw data

Factors	Degree of freedom	Sum of squares	Variance	F- ratio	Pure SS	Percentage contribution
Water-cement ratio (A)	2	1.457	0.729	7.489	1.263	34.075
Cement content (B)	2	0.596	0.298	3.060	0.401	10.819
Super-plasticizer content (C)	2	1.458	0.729	7.494	1.264	34.101
Fine aggregate content (D)	(2)	0.195	0.097		---	pooled
Error	2	0.195	0.097			
Total	8	3.706				100.000

3.5.1.6 Confirmation experiments

An important requirement in Taguchi's technique and simultaneous multi-characteristic optimization of utility concept is to conduct confirmation experiments for validating the predicted results. Hence, in order to test the predicted optimized conditions, the confirmation experiments were conducted by running another three replications at the optimal mix proportions as determined from the analysis. Figure 3.9 indicates the experimental test results of nine HPC mixes and their confirmation tests. The confirmation test results are also shown in Table 3.30 along with the predicted results. The 95% confidence interval (CI) for the predicted mean of optimum quality characteristics on confirmation test was estimated using equation (3.11). It can be observed From Table 3.23 that the individual response of residual compressive strength values for the specimens tested at room temperature and those exposed to 800°C fall within the predicted 95% confidence interval of optimal range. The utility values obtained at different temperatures of exposure of concrete were analyzed for different levels of mix

parameters. The experimentally obtained utility values are shown in Table 3.31. The values are observed to be lying above the predicted 95% confidence interval of optimal range of utility values calculated for the utility function.

Table 3.30 Confirmation test results of specimens utility values

Temperature ranges	Confirmation test results (in MPa)			
	1	2	3	Mean
Room temperature	77.830	78.540	78.690	**78.353**
200 °C	98.460	105.000	100.230	**101.230**
400 °C	89.000	98.000	94.000	**93.667**
600 °C	57.500	55.500	58.060	**56.687**
800 °C	23.000	25.500	24.000	**24.167**

Table 3.31 Results of confirmation experiments for utility values

No.	Quality characteristics	Optimum setting of process parameters	Predicted optimum value	95% of Predicted confidence intervals of quality characteristics	Mean value of confirmation
1	Room Temp., 200 °C, 400 °C, 600 °C, 800 °C	A_2, B_2, C_1, D_1	**7.916**	$7.659 < \mu_{\text{Room temp., 200 °C, 400 °C, 600 °C, 800 °C}} < 8.172$	**11.263**

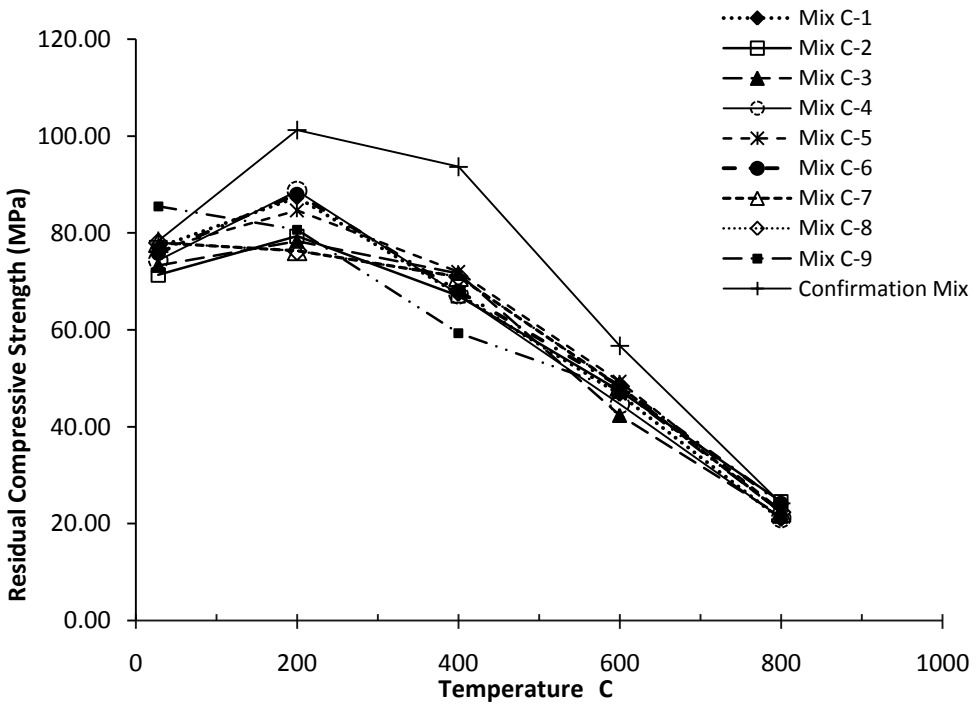

Fig. 3.9 Test results of various confirmation mixes with respect to initial mixes heated concrete

3.5.2 Module 2: Fly ash HPC

After a complete cycle of heating and cooling, fly ash incorporated HPC specimens were tested for compressive strength. Three specimens were tested for each result and the average values of the compressive strength are given in the Table 3.32. The Figure 3.10 shows heated fly ash HPC specimens before compression testing.

Table 3.32 Observed results of residual compressive strength of fly ash HPC

Mixes	Room temperature	200 ˚C	400 ˚C	600 ˚C	800 ˚C
HPC F-1	64.17 (100.00%)	87.83 (136.88%)	75.33 (117.40%)	44.67 (69.61%)	20.33 (31.69%)
HPC F-2	74.67 (100.00%)	85.83 (114.96%)	79.50 (106.47%)	43.83 (58.71%)	20.50 (27.46%)
HPC F-3	73.17 (100.00%)	86.00 (117.54%)	78.83 (103.74%)	44.33 (60.59%)	22.17 (30.30%)
HPC F-4	67.50 (100.00%)	86.33 (127.90%)	68.67 (101.73%)	45.50 (67.41%)	22.83 (33.83%)
HPC F-5	65.33 (100.00%)	80.33 (122.96%)	79.17 (121.17%)	46.17 (70.66%)	21.50 (32.91%)
HPC F-6	62.67 (100.00%)	85.17 (122.96%)	78.83 (125.80%)	47.33 (75.53%)	23.83 (38.03%)
HPC F-7	62.67 (100.00%)	82.50 (131.62%)	77.00 (122.87%)	44.17 (70.48%)	22.33 (35.64%)
HPC F-8	58.50 (100.00%)	85.83 (146.72%)	77.50 (132.48%)	44.17 (75.50%)	21.00 (35.90%)
HPC F-9	58.17 (100.00%)	84.17 (144.70%)	79.50 (136.48%)	44.50 (76.50%)	20.50 (35.24%)

3.5.2.1 Selection of optimal levels using Taguchi technique

Following the procedure described earlier in section 3.5.1.1, the results of fly ash HPC were also processed. The analysis of the results using ‘larger the better’ type of quality characteristic situation was evaluated in terms of Signal to Noise ratio (S/N). The computed values of signal to noise ratio (S/N) of each parameter and temperature of exposure are given in Table 3.33. A statistical data analysis was performed to determine the significant factors statistically. The optimum conditions were arrived using loss function as larger-the better, which is a quality function to maximize the residual compressive strength of heated concrete specimens. The mean numerical values of main effects of each parameter and temperature of exposure are given in Table 3.34 and Figure 3.11 (a) shows the effects of mean values. The maximum of mean values of main effects at room temperature was obtained for cement content at Level A_1 (434.449 kg/m^3), for fly ash content at Level B_2 (131.240 kg/m^3), /m^3), for super-plasticizer dosage at Level C_3

(6.056 L/m^3) and for fine aggregate content at Level D_2 (627.045 kg/m^3). The most influencing parameters as identified through ANOVA are presented in Table 3.35. According to the results of ANOVA, the cement content is observed to be acting as main influencing parameter at room temperature with 65.128% contribution. The strength decreased with increase in the fly ash content and fly ash content did not show any significant effect at room temperature conditions.

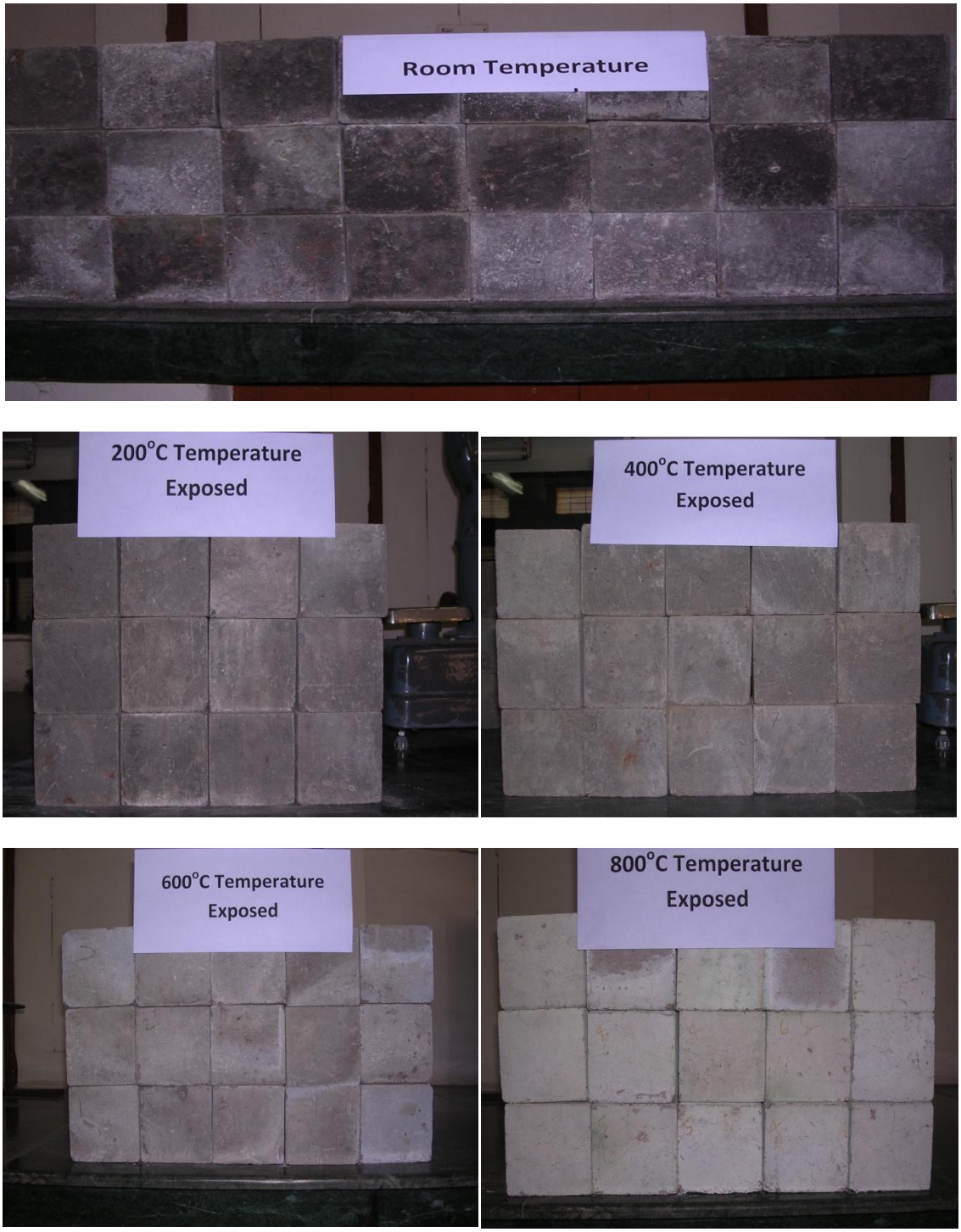

Fig. 3.10 Fly ash HPC specimens exposed to different temperatures

Table 3.33 A computed signal to noise (S/N) ratio values of post fire fly ash HPC

Mixes	Room temperature	200 ˚C	400 ˚C	600 ˚C	800 ˚C
HPC F-1	36.146	38.873	37.540	32.999	26.164
HPC F-2	37.462	38.673	38.007	32.836	26.235
HPC F-3	37.286	38.690	37.934	32.935	26.914
HPC F-4	36.586	38.724	36.735	33.160	27.171
HPC F-5	36.302	38. 098	37.971	33.287	26.649
HPC F-6	35.940	38.605	37.934	33.503	27.544
HPC F-7	35.940	38.329	37.730	32.636	26.979
HPC F-8	35.343	38.673	37.786	32.902	26.444
HPC F-9	35.293	38.503	38.007	32.967	26.235

Table 3.34 Mean values of quality characteristics at different temperatures

Level No	Factor A	Factor B	Factor C	Factor D
		Room temperature		
1st Level	**70.667***	64.778	61.778	62.556
2nd Level	65.167	**66.167***	66.778	**66.667***
3rd Level	59.778	64.667	**67.056***	66.389
		200 °C temperature exposure		
1st Level	**86.556***	**85.556***	**86.278***	84.111
2nd Level	83.944	84.000	85.444	84.500
3rd Level	84.167	85.111	82.944	**86.056***
		400 °C temperature exposure		
1st Level	77.889	73.667	77.222	78.000
2nd Level	75.556	78.722	75.889	**78.444***
3rd Level	**78.000***	**79.056***	**78.333***	75.000
		600 °C temperature exposure		
1st Level	44.278	44.778	**45.389***	**45.111***
2nd Level	**46.333***	44.722	44.611	44.667
3rd Level	44.278	**45.389***	44.444	44.667
		800 °C temperature exposure		
1st Level	21.000	21.833	21.722	20.778
2nd Level	**22.722***	21.000	21.278	**22.222***
3rd Level	21.278	**22.167***	**22.000***	22.000

***** Indicates optimum level of values for a given temperature of exposure

The parameters appeared to change their influence on the residual compressive strength of fly ash HPC with the change in temperature of exposure. At 200 °C exposure, the optimum values were obtained for cement content at Level A_1 (434.449 kg/m^3), for fly ash (FA) content at Level B_1 (108.612 kg/m^3), for super-plasticizer content at Level C_1 (4.888 L/m^3) and for fine aggregate content at Level D_3 (633.711 kg/m^3). The main influencing parameters at 200 °C exposure were super-plasticizer content, cement content and fine aggregate content as evident from Figure 3.11 (b). The increased dosage of the super-plasticizer shows relatively negative effects at this temperature condition. The residual strength of high performance concrete decreased with increase in the amount of fly ash content. However, the residual compressive strength of concrete exposed to 200 °C increased in the range of 15-46 % compared to room temperature strength irrespective of the level of any parameter. It is believed that this strength gain may be due to the formation of tobermorite gel, due to reaction between the unhydrated fly ash particles and calcium at elevated temperatures (Poon et al. 2001). The increase in compressive strength may also be due to the hardening of the cement paste during the evaporation of free water, which attenuates surface (Van der Waal's) forces between the cement gel particles, making the particles closer to each other (Xu et al. 2001, Aydin et al. 2007). The optimum conditions for specimens exposed to 400 ºC temperature were obtained for cement content at Level A_3 (355.618 kg/m^3), for fly ash content at Level B_3 (152.408 kg/m^3), for super-plasticizer dosage at Level C_3 (6.096 L/m^3) and for fine aggregate content at Level D_2 (627.045 kg/m^3). Fly ash content and the fine aggregate content were observed to be the main influencing parameters on the compressive strength at 400 °C exposure as shown in Figure 3.11 (c) and Table 3.35. It is evident that the higher strength was retained by the high performance concrete containing 30% of fly ash. At 400 °C temperature, all the fly ash concrete mix specimens exhibited much better fire resistance and the residual strength compared to their performance under room temperature. However a strength reduction was observed for all the specimens heated at 400 °C compared to the corresponding strengths at 200 °C. This may be due to the pore structure coarsening and complete dehydration of concrete when exposed to high temperatures (Aydin et al. 2007). Mild hairline cracks were also observed on the surface of specimens heated to 400 °C.

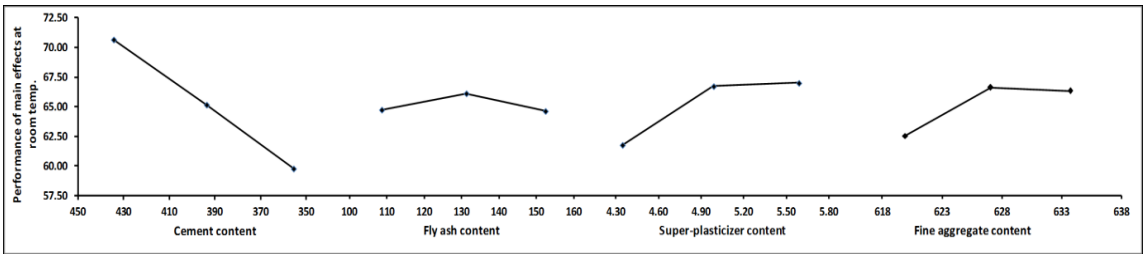

(a) Room temperature

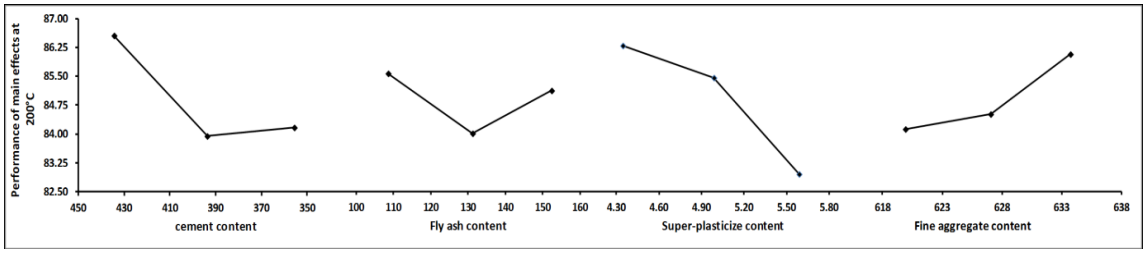

(b) 200 °C

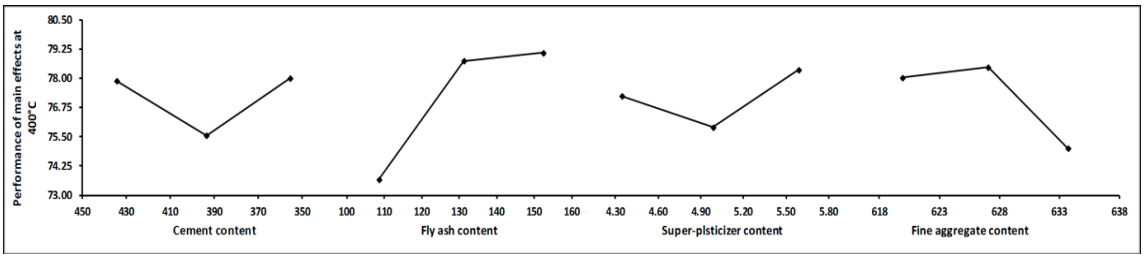

(c) 400 °C

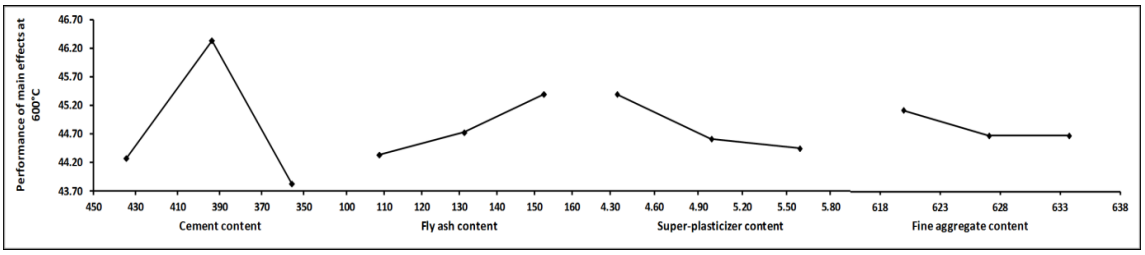

(d) 600 °C

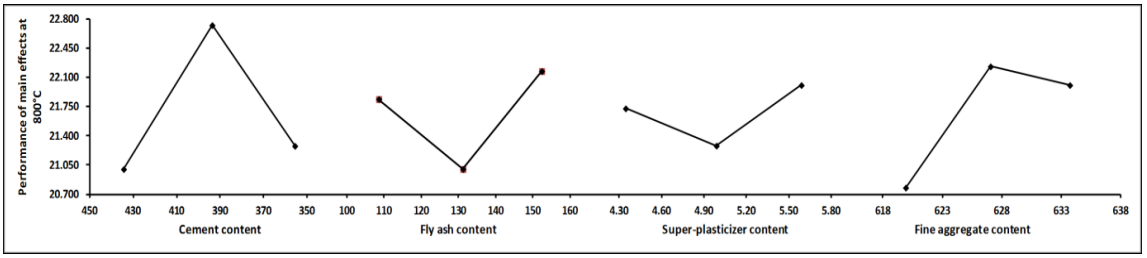

(e) 800 °C

Fig. 3.11 (a)-(e) Mean values of main effect of parameters on the performance characteristic of heated concrete

Table 3.35 ANOVA results for fly ash concrete exposed to various temperatures

Factors	Statistical parameters	Room temp.	200 °C	400 °C	600 °C	800 °C
Cement content (A)	Pooling	No	No	No	No	No
	Degree of freedom	2	2	2	2	2
	Sum of square	177.858	12.574	11.432	10.673	5.130
	Variance	88.929	6.287	5.716	5.336	2.565
	F-ratio	42.434	3.264	1.272	15.211	6.442
	Pure SS	173.667	8.722	2.444	9.971	4.333
	(%) contribution	65.128	21.361	2.541	69.717	36.967
Fly ash content (B)	Pooling	Yes	Yes	No	Yes	No
	Degree of freedom	(2)	(2)	2	(2)	2
	Sum of square	4.191	3.852	54.710	1.710	2.167
	Variance	-	-	27.355	-	1.083
	F-ratio	-	-	6.087	-	2.721
	Pure SS	-	-	45.722	-	1.370
	(%) contribution	-	-	47.533	-	11.690
Super-plasticizer content (C)	Pooling	No	No	Yes	Yes	Yes
	Degree of freedom	2	2	(2)	(2)	(2)
	Sum of square	52.932	18.056	8.988	1.525	0.769
	Variance	26.466	9.028	-	-	-
	F-ratio	12.629	4.687	-	-	-
	Pure SS	48.741	14.204	-	-	-
	(%) contribution	18.279	34.785	-	-	-
Fine aggregate content (D)	Pooling	No	No	No	Yes	No
	Degree of freedom	2	2	2	2	2
	Sum of square	31.673	6.352	21.062	0.395	3.630
	Variance	15.836	3.176	10.531	-	1.815
	F-ratio	7.557	1.649	2.343	-	4.558
	Pure SS	27.481	2.500	12.074	-	2.833
	(%) contribution	10.306	6.122	12.552	-	24.171

The post fire residual strength values severely reduced for the various mixes as the temperature of exposure increased to 600 °C. The maximum residual strength of concrete at this temperature was obtained for cement content at level A_2 (393.720 kg/m^3), for fly ash content at level B_3 (152.408 kg/m^3), for super-plasticizer content at level C_1 (4.888 L/m^3) and for fine aggregate content at level D_1 (619.919 kg/m^3). The cement content was observed to be the most influencing parameter and the fly ash content, super-plasticizer dosage and fine aggregate content were observed to be relatively less effective. Overall at 600 °C, the fly ash high performance concrete performed better and showed reduced cracking and spalling. The average loss of residual strength was in the range of 23.5-41% for fly ash based high performance concrete exposed to 600 °C. It is believed that at temperature as high as 600 °C, the major hydrates of concrete known as C–S–H gel decompose and cause the loss of cementing ability of binding material.

At 800 °C temperature exposure, a severe strength loss and deterioration was observed in all the specimens due to further decomposition of the C-H-S gel and disintegration of concrete at such high temperatures. The optimum conditions at 800 °C exposure were obtained for cement content at level A_2 (393.720 kg/m^3), for fly ash content at Level B_3 (152.408 kg/m^3), for super-plasticizer content at level C_3 (6.096 L/m^3) and for fine aggregate content at level D_2 (627.045 kg/m^3). The cement content and fine aggregate content were observed to be the main influencing parameters as shown in Figure 3.11 (e) and Table 3.35. It is observed that the increased amount of cement content and fine aggregate content leads to reduction of strength at such high temperatures. It is therefore noticed that all nine trial mixes could only maintain a minor part of their original compressive strength after exposure to 800 °C. Table 3.36 displays the individual optimal values and the corresponding optimal settings of process parameters for the entire range of heated fly ash HPC.

Table 3.36 Optimal setting of process parameters of fly ash HPC (phase I) and optimal vales of individual quality characteristics

No.	Quality characteristics	Optimum setting of process parameters	Predicted optimum value	95% of Predicted confidence intervals of quality characteristics
1	Room Temp.	A_1, B_2, C_3, D_2	73.537	$68.740 < \mu_{\text{Room temp.}} < 78.334$
2	200 °C	A_1, B_1, C_1, D_3	88.667	$84.069 < \mu_{200\,^\circ C} < 93.265$
3	400 °C	A_3, B_3, C_3, D_2	80.759	$73.735 < \mu_{400\,^\circ C} < 87.783$
4	600 °C	A_2, B_3, C_1, D_1	47.037	$45.249 < \mu_{600\,^\circ C} < 48.232$
5	800 °C	A_2, B_3, C_3, D_2	23.333	$20.755 < \mu_{800\,^\circ C} < 25.541$

3.5.2.2 Estimation of optimum response parameters using utility concept

As observed earlier, the application of utility concept can provide an absolute optimum set of mix parameters for varying exposure temperatures. Therefore, the same was followed with an aim to arrive at single optimum mix proportions that maximize the residual compressive strength of fly ash HPC at all the temperatures. The optimum mix conditions corresponding to various target temperature was obtained per Taguchi's approach and the resulting five dissimilar optimum mix proportions are shown in Table 3.36. The utility concept was then applied to obtain absolute optimum mix combination as larger the better optimization criterion. Assuming equal weights at all temperatures, the weighted S/N ratios obtained for different temperatures were summed up and with this data the mean process parameters were determined. Using the significant contribution of mean utility values of main effects, the optimal setting process parameters were determined. The sums of composite measures of overall maximized signal-to-noise ratio values are summarized in Table 3.37.

Table 3.37 Utility data based on quality characteristics (utility values: room temp., 200 ℃, 400 ℃, 600 ℃ and 800 ℃)

Mixes	1	2	3	Mean	S/N ratio
HPC F-1	6.468	7.403	7.371	7.081	17.001
HPC F-2	8.288	7.106	7.950	7.781	17.821
HPC F-3	7.727	8.761	7.666	8.052	18.118
HPC F-4	8.238	7.594	6.114	7.315	17.285
HPC F-5	7.071	7.281	7.072	7.141	17.075
HPC F-6	8.034	7.270	8.531	7.945	18.002
HPC F-7	6.787	7.038	6.332	6.719	16.546
HPC F-8	7.001	7.349	5.610	6.653	16.461
HPC F-9	6.626	6.584	6.493	6.568	16.348

(i) Formulation of Preference Scale

A preference scale is constructed for determining the utility value of HPC for each target temperature using the equation (3.6). Following are the details of calculation for the preference scale value $P_{(Room\ Temp)}$ expressed on a logarithmic scale for compressive strength of concrete at room temperature.

M_i^* = optimum value of room temperature is 73.537 MPa (refer Table 3.36)

M_i' = minimum acceptable value at room temperature is 50 MPa (all the observed values in Table 3.32 lie between 57 MPa and 78 MPa)

Using the above values and the equations (3.6) and (3.7), the preference scale for room temperature was constructed as

$$P_{(Room\ Temp.)} = 53.72 * \log\left(\frac{X_{Room\ Temp.}}{50}\right) \quad (3.15)$$

In a similar way, the preference scale values were calculated for other temperatures, namely 200 °C, 400 °C, 600 °C and 800 °C.

The selected mix design parameters were assigned equal weights, $P_{(Room\ Temp.)}$, $P_{(200^{o}C)}$, $P_{(400^{o}C)}$, $P_{(600^{o}C)}$, and $P_{(800^{o}C)}$ respectively.

(ii) Calculation of utility Value of fly ash HPC

The overall utility value of the amalgamated measure is calculated using the equations (3.9 and 3.10). The same equation (3.13), was used to calculate the utility data of fly ash HPC at various temperatures of exposure. Using the above equation, the calculated utility data are reported in Table 3.37.

3.5.2.3 Data analysis and estimation of optimal mix proportions

The data was further analyzed for mean responses of utility values at each level of selected parameters and signal to noise ratio. The quality characteristics utility values are a larger the better quality characteristic type and were calculated using equation (3.1). The calculated values of mean responses (mean utility value) and the signal to noise ratios (S/N ratio) are given in Tables 3.38 and 3.39 respectively, and the mean responses of mix proportions of utility values are plotted in Figure 3.12.

Table 3.38 Fly ash HPC's mean utility values of main effects of raw data

Levels	**Cement content (A)**	**Fly ash content (B)**	**Super-plasticizer content (C)**	**Fine aggregate content (D)**
1	**7.638***	7.038	7.226	6.930
2	7.467	7.192	7.221	**7.482***
3	6.647	**7.521***	**7.304***	7.340

***** Indicates the best performance of utility values for different temperature of exposures

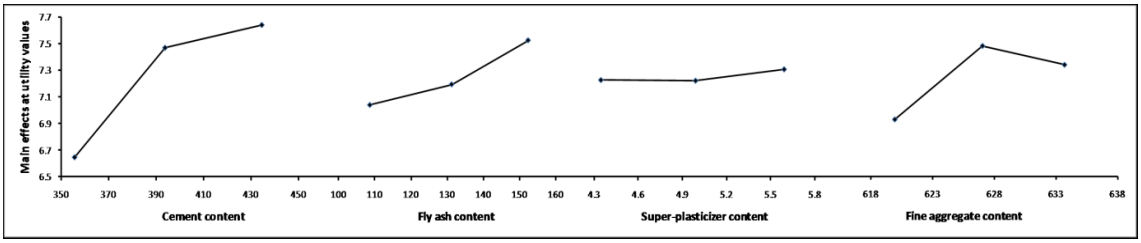

Fig. 3.12 Mean responses of main effects of process parameters of utility values

Table 3.39 Fly ash HPC mean utility vales of signal to noise (S/N) ratio of raw data

Levels	**Cement content (A)**	**Fly ash content (B)**	**Super-plasticizer content (C)**	**Fine aggregate content (D)**
1	**17.647***	16.944	17.155	16.808
2	17.454	17.119	17.151	**17.456***
3	16.452	**17.489***	**17.246***	17.288

***** Indicates best performance of signal to noise (S/N) ratio values for different temperature of exposures

This figure depicts clearly that the first level of cement content (A_1= 434.449 kg/m^3), the third level of fly ash content (B_3= 152.408 kg/m^3), the third level of super-plasticizer content (C_3= 6.096 L/m^3) and the second level of fine aggregate content (D_2= 627.045 kg/m^3) shall yield a best optimal performance value of the utility function i.e. the residual compressive strength of fly ash based high performance concrete exposed to different temperatures. Table 3.40 indicates absolute optimal values of mix proportions for optimized high performance concrete mix parameters and their levels of multi-response optimization using the utility concept.

Table 3.40 Optimal setting of process parameters utility values (phase II)

S. No.	**Process parameter**	**Level**	**Optimal values**
1	Cement content (kg/m^3)	A_1	434.449
2	Fly ash content (kg/m^3)	B_3	152.408
3	Super-plasticizer content (l/m^3)	C_3	6.096
4	Fine aggregate content (kg/m^3)	D_2	627.045

3.5.2.4 Optimal values of mix proportions parameters of fly ash HPC

The optimum value of utility ($U_{\text{Room temp, } 200\ ^oC, 400\ ^oC, 600\ ^oC, 800\ ^oC}$) was predicted at the selected levels of variables as stated above viz. cement content (A_1), fly ash content (B_3), super-plasticizer content (C_3) and fine aggregate content (D_2). The estimated mean of the responses of mix proportion parameters ($U_{\text{Room Temp., } 200\ ^oC, 400\ ^oC, 600\ ^oC, 800\ ^oC}$) can be determined as:

$$\mu_{\text{Room Temp.,}200\ ^oC, 400\ ^oC, 600\ ^oC, 800\ ^oC} = \overline{A}_1 + \overline{B}_3 + \overline{C}_3 + \overline{D}_2 - 3\overline{T} \quad (3.16)$$

where, $\overline{T}$ = overall mean of utility value = 7.473 which is taken from Table 3.37. The values of $\overline{A}_1, \overline{B}_3, \overline{C}_3, \overline{D}_2$ were taken from Table 3.38.

The utility values of both the main effects and signal-to-noise (S/N) ratio values of raw data were analyzed at each level of all the parameters. It is clear from Table 3.39 and Figure3.12 that the mean utility values of first level of cement content (A_1), third level of fly ash content (B_3), third level of super-plasticizer content (C_3) and second level of fine aggregate content (D_2) would yield best performance in terms of utility value and S/N ratio values for different temperatures of exposure. Substituting the values of the above mentioned terms in equation (3.16), we get

$\mu_{\text{Room Temp., 200ºC, 400ºC, 600ºC, 800ºC}} = 7.638 + 7.521 + 7.304 + 7.482 - 3\,(7.473) = 7.526$

The 95 % confidence interval of confirmation of experiments (CI_{CE}) was calculated using equation 3.3 and the values are presented in Table 3.40.

f_e = error of DOF = 2; V_e = error variance = 0.016

N = 27; n_{eff} = 27/7 (calculated)

R = 3; $F_{0.05}(1, 02) = 18.51$ (Tabulated F value)

The confidence interval for confirmation experiments (CI_{CE}) = ± 0.420

The predicted optimal range (for confirmation runs of the experiment) is:

$(\mu_{\text{Room Temp., 200 ºC, 400 ºC, 600 ºC, 800 ºC}} - CI_{CE}) < \mu_{\text{Room Temp., 200 ºC, 400 ºC, 600 ºC, 800 ºC}} < (\mu_{\text{Room Temp., 200 ºC, 400 ºC, 600 ºC, 800 ºC}} + CI_{CE})$

$7.230 < \mu_{\text{Room Temp., 200 ºC, 400 ºC, 600 ºC, 800 ºC}} < 8.067$

3.5.2.5 Analysis of variance (ANVOA)

An analysis of variance (ANOVA) was performed to identify the relative significance and future promising direction of the process parameters. Table 3.35 shows the computed results of pooled versions of utility values of the ANOVA at 0.05% level of significance with 95% confidence level. The fisher ratios (F-ratio) were calculated to identify the importance of factors from variance within the confidence level and the percent contributions of the various parameters as quantified under the respective columns of Table 3.41. It reveals that cement content showed a significant effect on the residual compressive strength of heated concrete with 65.41% contribution at all the temperatures with a maximum influence. The fine aggregate content was observed to be the second most influencing parameter with respect to residual compressive strength of heated concrete.

Table 3.41 Pooled ANOVA for utility vales of raw data

Factors	Degree of freedom	Sum of squares	Variance	F- ratio	Pure SS	Percentage contribution
Cement content	2	1.685	0.842	130.749	1.672	65.409
Fly ash content	2	0.366	0.183	28.372	0.353	13.798
Super-plasticizer content	(2)	0.013	0.006	---	pooled	pooled
Fine aggregate content	2	0.493	0.246	38.274	0.480	18.777
Error	2	0.013	0.006			2.016
Total	8	2.556				100.000

3.5.2.6 Confirmation experiments

It is a final step in the experimental design to verify results obtained from the previous trials of experiments. Hence, in order to verify the predicted optimized conditions, confirmation experiments were conducted. Figure 3.13 indicates the experimental test results of nine HPC mixes and their confirmation test. The confirmation test results are also shown in Table 3.42 along with the predicted results. It can be observed From Table 3.36 that the individual response of residual compressive strength values for the specimens tested at room temperature and those exposed to 800 $^{\circ}$C, fall within the predicted 95% confidence interval of optimal range. The utility values obtained at different temperatures of exposure of concrete were analyzed for different levels of mix parameters. The experimentally obtained utility values are shown in Table 3.43. The values are observed to lie above the predicted 95% confidence interval of optimal range utility calculated for the utility function.

Table 3.42 Confirmation test results of specimen's values

Temperature ranges	Confirmation test results (in MPa)			
	1	2	3	Mean
Room temp.	78.000	77.000	82.000	**79.000**
200 °C	98.000	99.000	96.000	**97.667**
400 °C	88.000	86.000	83.000	**85.667**
600 °C	54.000	52.000	55.500	**53.833**
800 °C	22.000	20.500	21.000	**21.167**

Table 3.43 Results of confirmation experiments for utility values

No.	Quality characteristics	Optimum setting of process parameters	Predicted optimum value	95% of Predicted confidence intervals of quality characteristics	Mean value of confirmation
1	Room Temp.	A_1, B_3, C_3, D_2	7.524	$7.261 < \mu_{28°C, 200°C, 400°C, 600°C, 800°C} < 7.792$,	11.302
2	200 °C				
3	400 °C				
4	600 °C				
5	800 °C				

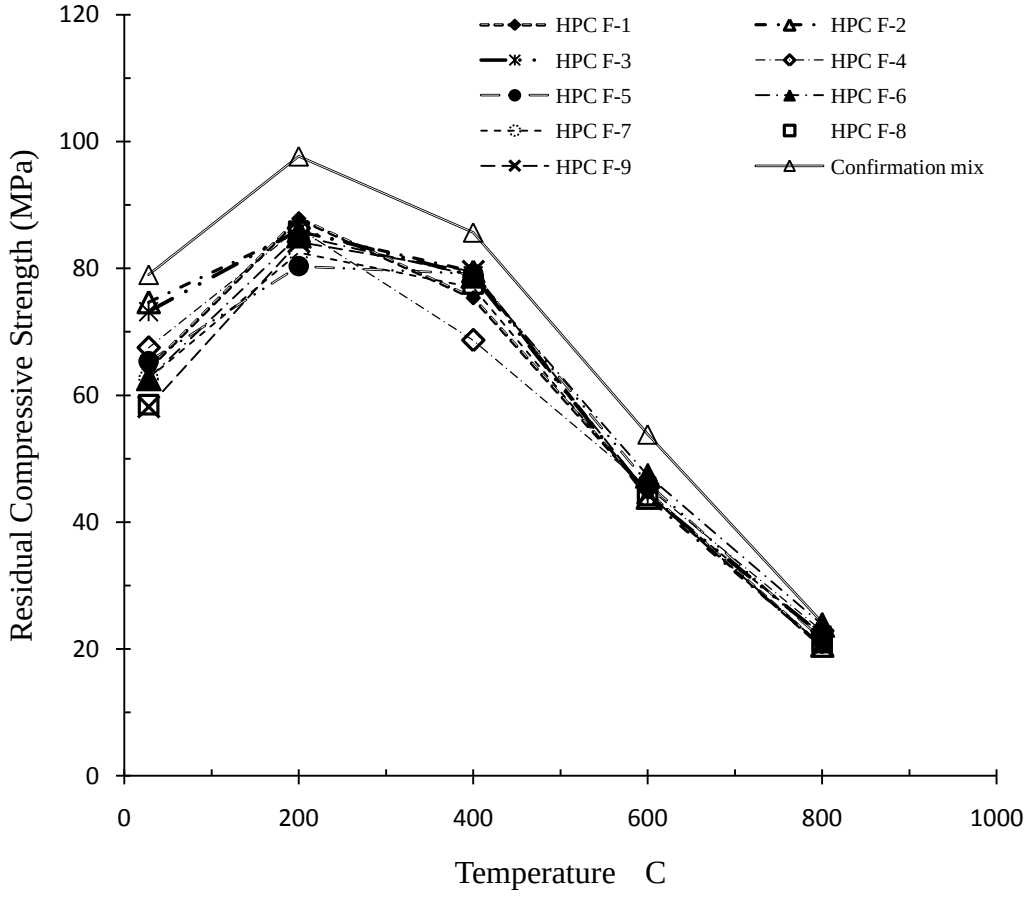

Fig. 3.13 Mix trials and their confirmation test results of fly ash HPC specimens subjected to elevated temperatures

3.5.3 Module 3: GGBFS HPC

The measured average residual compressive strength values of various trial mixes of GGBFS based HPC are shown in Table 3.44. The Figure 3.14 shows the appearance of the specimens after heating.

Table 3.44 Measured residual compressive strengths of concrete mixes

Mix Trials	**Room temp.**	**100 °C**	**200 °C**	**300 °C**	**400 °C**	**500 °C**	**600 °C**	**800 °C**
HPC G-1	77.50 (100%)	71.00 (91.61%)	77.33 (99.78%)	84.17 (108.60%)	78.50 (101.29%)	70.33 (90.75%)	51.00 (65.81%)	24.00 (30.97%)
HPC G-2	76.67 (100%)	71.83 (93.70%)	75.67 (98.70%)	97.67 (127.39%)	82.67 (107.83%)	68.00 (88.70%)	55.50 (72.39%)	23.000 (30.00%)
HPC G-3	80.50 (100%)	69.00 (85.71%)	78.67 (97.72%)	95.67 (118.84%)	83.67 (103.93%)	69.00 (85.71 %)	***	***
HPC G-4	79.50 (100%)	70.33 (88.47%)	73.17 (92.03%)	85.67 (107.76%)	85.00 (106.92%)	64.33 (80.92%)	***	21.750 (27.36%)
HPC G-5	74.67 (100%)	63.67 (85.27%)	75.50 (101.12%)	79.00 (105.80%)	72.00 (96.43)	66.67 (89.29)	54.67 (73.21)	21.00 (28.13)
HPC G-6	77.33 (100%)	66.17 (85.56%)	75.67 (97.84%)	79.67 (103.02%)	89.33 (115.52%)	66.67 (86.21%)	45.00 (58.19%)	24.000 (34.91%)
HPC G-7	70.67 (100%)	57.00 (80.66%)	74.33 (105.19%)	77.67 (109.91%)	73.33 (103.77%)	63.67 (90.09%)	45.17 (63.92%)	24.66 (34.97%)
HPC G-8	67.33 (100%)	61.83 (91.83%)	74.50 (110.64%)	84.00 (124.75%)	84.00 (124.75%)	63.33 (94.06%)	***	***
HPC G-9	77.50 (100%)	59.50 (76.77%)	76.00 (98.06%)	85.00 (109.68%)	85.33 (110.11%)	64.83 (83.66%)	46.167 (59.57%)	24.00 (30.97%)

*** Indicates the test specimens spalled during thermal load application

3.5.3.1 Analysis of data by Taguchi technique

The residual compressive strength results of various mixes were analysed by Taguchi's technique as described earlier in context with control HPC and fly ash HPC. The S/N ratios for optimum conditions were arrived at using the loss function as larger-the better. The signal to noise (S/N) ratios of the residual compressive strength results are tabulated in Table 3.45 up to 500 °C temperature. It is important to note here that some of the specimens exposed to 600 °C and 800 °C temperatures got spalled during heating and hence no subsequent statistical data analysis was possible for the concrete mixes subjected to these temperatures. Therefore, the analysis was applied only up to 500 °C temperature and some additional target temperatures namely 100 °C, 300 °C and 500 °C were also chosen here.

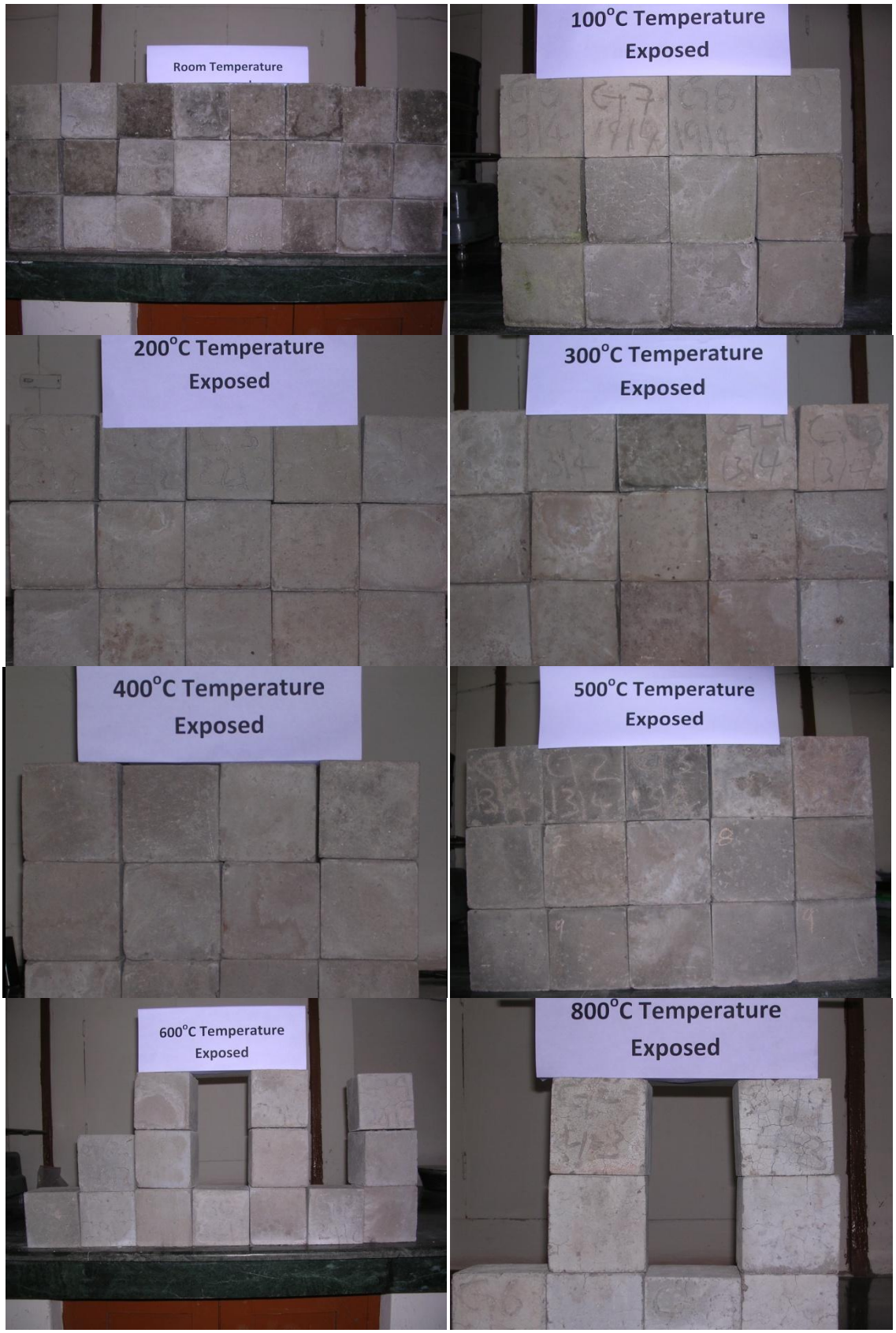

Fig. 3.14 Test specimens of GGBFS HPC subjected to different elevated temperatures

Table 3.45 Signal to noise (S/N) ratio values of post fire compressive strength of concrete

Mixes	Room temperature	100 °C	200 °C	300 °C	400 °C	500 °C
HPC G-1	37.786	37.025	37.767	38.503	37.897	36.943
HPC G-2	37.692	37.127	37.578	39.795	38.276	36.650
HPC G-3	38.116	36.777	37.915	39.615	38.451	36.777
HPC G-4	38.007	36.943	37.286	38.656	38.588	36.169
HPC G-5	37.463	36.078	37.559	37.952	37.147	36.478
HPC G-6	37.767	36.413	37.578	38.026	39.020	36.478
HPC G-7	36.984	35.118	37.423	37.805	37.306	36.078
HPC G-8	36.565	35.824	37.443	37.486	37.635	36.033
HPC G-9	37.786	35.490	37.616	38.588	37.654	36.236

It can be observed from Table 3.46 and Figure 3.15 (a) that at room temperature the maximum values of mean effects were obtained at Level A_1 (380.143 kg/m^3) for cement content, at Level B_3 (254.013 kg/m^3) for GGBFS content, at Level C_2 (2.362 L/m^3) for super-plasticizer dosage and at Level D_1 (633.298 kg/m^3) for fine aggregate content. The results show that an increase in the amount of cement content and GGBFS content increases the strength of concrete under room temperature conditions. The most influencing factors as identified through the ANOVA results are shown in Table 3.47. The cement content is observed to be the most influencing parameter for the compressive strength of concrete with 45.99% contribution. The second most influencing parameter is found to be GGBFS content with 29.33% contribution followed by the remaining two parameters. It is now well established that the use of GGBFS as cement replacement in concrete mixture improves the strength of concrete due to the occurrence of complex hydration reactions in the presence of water and calcium hydroxide. Further, the secondary pozzolanic reactions also result in a denser microstructure of matrix because of the consumption of calcium hydroxide and the generation of CSH (Chidiac, et al., 2008).

In case of HPC specimens heated at 100 °C exposure, The maximum values of residual strength were obtained at Level A_1 (380.14 kg/m^3) for cement content, at Level B_1 (162.919 kg/m^3) for GGBFS content, at Level C_2 (2.362 L/m^3) for super-plasticizer content and at Level D_3 (649.238 kg/m^3) for fine aggregate content. It can be noticed that the cement content parameter showed its importance at this temperature condition as well. The results presented in Table 3.46 and Figure 3.15 (b) illustrate that the cement content

acted as the main influencing parameter with 80.690% contribution. The GGBFS content and fine aggregate content were considered as relatively insignificant at 100 °C exposure and were pooled. The results indicate that the residual compressive strength of concrete heated at 100 °C decreased in the range of 10-25 % compared with the room temperature strength irrespective of the level of any parameter. The fall in strength at 100 °C is consistent with the observations of some earlier studies.

Table 3.46 Mean values of quality characteristics at different temperatures (Main effects)

Level No	Factor A	Factor B	Factor C	Factor D
		Room temperature		
1st Level	**78.222***	75.889	74.056	**76.556***
2nd Level	77.167	72.889	**77.889***	74.889
3rd Level	71.833	**78.444***	75.278	75.778
		100 °C temperature exposure		
1st Level	**70.611***	**66.111***	66.333	64.722
2nd Level	66.772	65.778	**67.222***	65.000
3rd Level	59.444	64.889	63.222	**67.056***
		200 °C temperature exposure		
1st Level	**77.222***	74.944	75.833	**76.278***
2nd Level	74.778	75.222	74.944	75.222
3rd Level	74.944	**76.778***	**76.167***	75.444
		300 °C temperature exposure		
1st Level	**92.500***	82.500	82.611	82.722
2nd Level	81.444	**86.889***	**89.444***	85.000
3rd Level	82.222	86.778	84.111	**88.444***
		400 °C temperature exposure		
1st Level	81.389	78.944	**81.333***	75.611
2nd Level	**82.111***	76.722	81.111	81.556
3rd Level	75.278	**83.111***	76.333	**81.611***
		500 °C temperature exposure		
1st Level	**69.111***	66.111	**66.778***	**67.278***
2nd Level	65.889	66.000	65.722	66.111
3rd Level	63.944	**66.833***	66.444	65.556

***** Indicates the optimum level of values for a given temperature of exposure

Dias et al. (Dias et al. 1990) reported that this reduction in strength is due to the moisture movement from inside of concrete when temperature reaches about 100 °C resulting into softening of paste. The observed strength reduction of heated concrete is also reported to be due to the outcome of thermally energized swelling between the inter layers of physically bound water which causes the disjoining pressure (Castillo and Durrani, 1990; Dias et al. 1990).

The cement content, GGBFS content and fine aggregate content were observed to be the most influencing parameters at 200 °C exposure as evident from Table 3.46 and Figure 3.15 (c). The optimum values for the specimens exposed to 200 °C temperature were obtained at Level A_1 (380.14 kg/m^3) for cement content, at Level B_3 (254.01 kg/m^3) for GGBFS content, at Level C_3 (2.540 L/m^3) for super-plasticizer dosage and at Level D_1 (633.298 kg/m^3) for fine aggregate content. An increase in the amount of cement content and GGBFS content tends to improve the residual strength of heated concrete. Among the various factors, the ANOVA results reveal in Table 3.47 that the cement content again showed the highest influence with a contribution of 41.292% followed by GGBFS content with a contribution of 16.256%. When the temperature increased from 100 °C to 200 °C, a small gain in residual strength of concrete was observed in most of the cases and the residual strength regained to its room temperature value. It is believed that in this temperature range, the entire heat supplied to the concrete layers is used for evaporation of moisture till the layers become dry. As a result of drying, the possible physico-chemical changes could generate the stresses (Van der Wall's forces) between the interfacial zones of hardened cement-slag concrete and the paste layers come closer to each other (Dias et al. 1990).

When the concrete was heated at 300 °C temperature, the residual compressive strength increased with respect to its room temperature value in all the cases. This may be attributed due to the partial penetration of moisture into the concrete core, which activates further hydration of unhydrated GGBFS particles (Aydin et al. 2007). This would react with calcium hydroxide and it's consequential product that is C-S-H, additionally strengthens the micro structure of heated concrete. According to Castillo and Durrani (Castillo and Durrani 1990), this is also attributed to the stiffening of cement gel, in other words it means increase in the surface forces between the gel particles due to removal of adsorbed moisture. At 300 °C temperature, the maximum values were obtained

corresponding to Level A_1 (380.14 kg/m^3) for cement content, Level B_2 (209.98 kg/m^3) for GGBFS content, Level C_2 (2.362 L/m^3) for super-plasticizer dosage and Level D_3 (649.238 kg/m^3) for fine aggregate content. The analysis of ANOVA data as shown in Table 3.47 reveals that cement content was observed as the most significant parameter with highest percentage of contribution of 48.54%. The GGBFS content did not seem to contribute towards the increase in the strength of concrete heated at 300 °C and therefore it was pooled.

The optimum conditions for specimens exposed to 400 °C temperature were obtained at Level A_2 (314.98 kg/m^3) for cement content, at Level B_3 (254.01 kg/m^3) for GGBFS content, at Level C_1 (2.17 L/m^3) for super-plasticizer dosage and at Level D_3 (649.238 kg/m^3) for fine aggregate content. The cement content followed by fine aggregate content and GGBFS content were the main influencing parameters with respect to the residual compressive strength of concrete heated at 400 °C temperature. It can be observed from the results that the concrete mix containing 60% of cement content and 50% of cement replacement with GGBFS retained the highest residual compressive strength. The results further show that at 400 °C temperature the cement content was again found to be the most effective parameter influencing the residual compressive strength of concrete with a percentage contribution of 13.745%. Fine aggregate content with a contribution of 8.79% was the next most influencing parameter at 400 °C temperature. Though there was a slight decrease in residual strength as the temperature of exposure increased from 300 °C and 400 °C, it is interesting to note that all the concrete mixes retained their room temperature strength when heated at a temperature of 400 °C with all the strength values well above the respective room temperature strengths. In fact the residual strengths for concrete specimens heated at 300 °C and 400 °C temperatures were more than the strength achieved in specimens heated at both 100 °C and 200 °C temperatures. On the contrary, the residual compressive strength of concrete without any pozzolanic addition such as GGBFS has been reported to deteriorate at an exposure at 400 °C (Sarshar et al. 1993). At this temperature range, the presence of calcium hydroxide in the matrix leads to various adverse effects of elevated temperature on concrete (Aydin et al. 2007). However, these effects of calcium hydroxide are eliminated by the addition of pozzolanic admixtures such as GGBFS to the concrete. The pozzolanic reactions between calcium hydroxide and cement paste consume the calcium hydroxide and convert to

useful calcium silicate hydroxide (C-S-H). Hence the depleted level of calcium hydroxide in concrete is helpful in improving the strength of heated concrete (Sarshar et al. 1993, Aydin et al. 2007 and Demirel et al. 2010). This shows that the GGBFS addition helps in reducing the detrimental effects of elevated temperature on the strength of concrete.

The influence of elevated temperatures on concrete began to appear when the specimens were exposed to 500 °C temperature. The residual strength of various concrete mixes heated at 500 °C lost their room temperature compressive strength in the range of 6 to 20%. The different mixes cast by using various levels of the chosen mix parameters showed varying degrees of loss in their respective room temperature strength. For cement content parameter, the maximum residual strength was achieved at level A_1 (380.143 kg/m^3), while for GGBFS content at level B_3 (254.013 kg/m^3) gave the maximum effect. The maximum strengths were obtained for super-plasticizer content at level C_1 (2.172 L/m^3) and for fine aggregate content at level D_1 (633.298 kg/m^3) in this case. The ANOVA data as presented in Table 3.47 reveals that the cement content was the main influencing parameter with a contribution of 14.751%, while all other chosen parameters were considered to be relatively insignificant and were therefore pooled. The results from Figure 3.15 (f) however indicates that the fine aggregate content appeared to be slightly more influential compared to GGBFS content and super-plasticizer dosage. It is observed that the increased amount of cement content leads to a reduction in the strength of concrete subjected to 500 °C temperature. The test results presented in Table 3.44 indicate that the heated test specimens at higher temperatures i.e. 600 °C and 800 °C resulted into a considerable reduction in the residual compressive strength. A few test specimens even got burst. Thus, the further analysis of the results of specimens heated at 600 °C and 800 °C temperatures was not possible. Figure 3.16 shows the specimens heated at temperatures 600 °C and 800 °C.

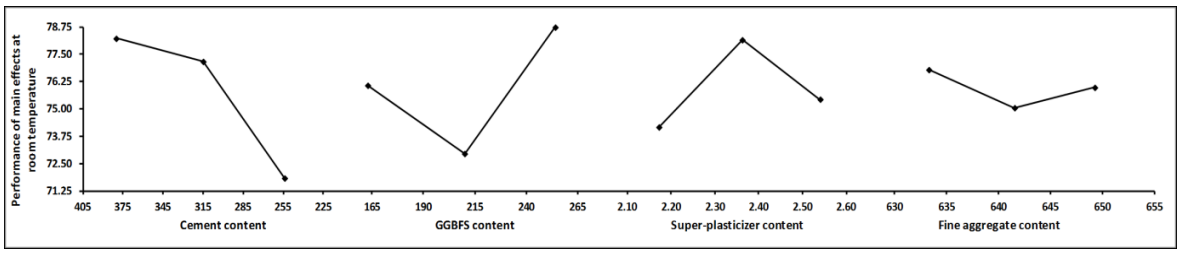

(a) Room temperature

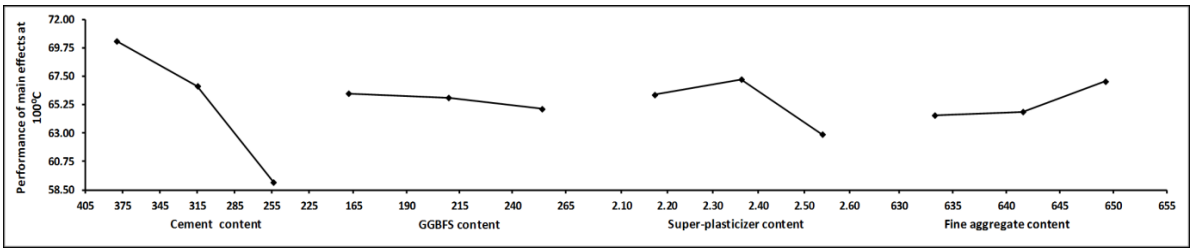

(b) 100 ℃

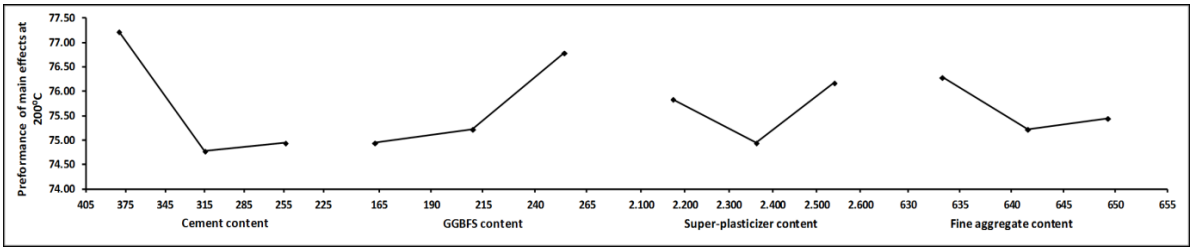

(c) 200 ℃

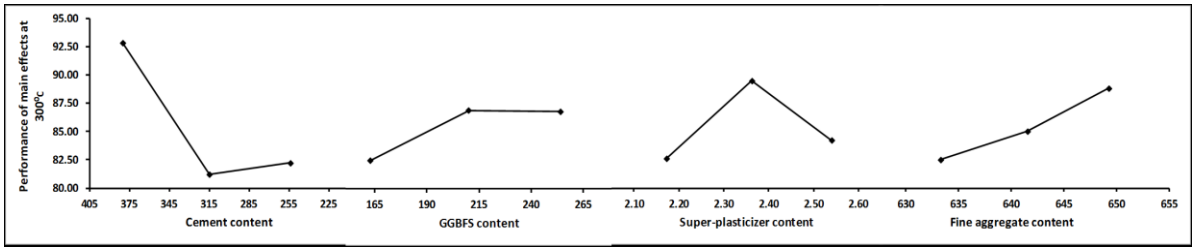

(d) 300 ℃

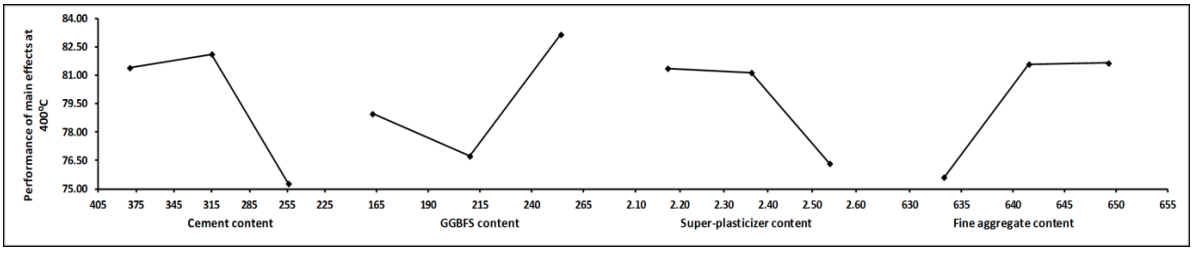

(e) 400 ℃

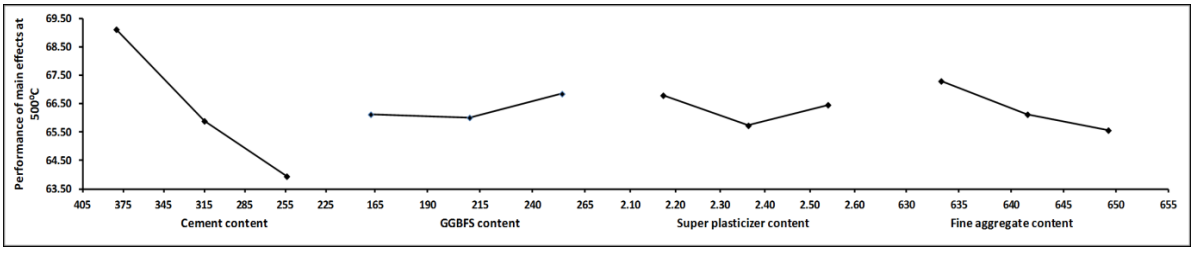

(f) 500 ℃

Fig. 3.15 (a)-(f) Mean values of main effect of parameters on the performance characteristic of heated concrete

Table 3.47 ANOVA results for concrete exposed to various temperatures

Factors	Statistical parameters	Room temp.	100 °C	200 °C	300 °C	400 °C	500 °C
Cement content (A)	Pooling	No	No	No	No	No	No
	Degree of freedom	2	2	2	2	2	2
	Sum of square	70.377	192.784	11.191	228.463	84.562	40.858
	Variance	35.188	96.392	5.596	114.231	42.281	20.429
	F-ratio	16.865	31.755	4.673	6.080	1.766	27.465
	Pure SS	66.204	186.713	8.796	190.889	36.685	39.370
	(%) contribution	45.991	80.690	41.292	48.545	13.745	14.751
GGBFS content (B)	Pooling	No	Yes	No	Yes	No	Yes
	Degree of freedom	2	(2)	2	(2)	2	2
	Sum of square	46.395	2.395	5.858	37.574	63.117	1.228
	Variance	23.198	-	2.929	-	31.559	-
	F-ratio	11.118	-	2.446	-	1.318	-
	Pure SS	42.222	-	3.463	-	15.241	-
	(%) contribution	29.331	-	16.256	-	5.710	-
Super-plasticizer content (C)	Pooling	No	No	Yes	No	Yes	Yes
	Degree of freedom	2	2	2	2	2	2
	Sum of square	23.006	26.469	2.395	77.389	47.877	1.747
	Variance	11.503	13.235	-	38.694	-	-
	F-ratio	5.513	4.360	-	4.119	-	-
	Pure SS	18.833	20.398	-	39.815	-	-
	(%) contribution	13.083	8.815	-	10.125	-	-
Fine aggregate content (D)	Pooling	Yes	No	Yes	No	No	No
	Degree of freedom	(2)	(2)	2	2	2	2
	Sum of square	4.173	9.747	1.858	49.796	71.340	4.636
	Variance	-	-	-	24.898	35.670	2.318
	F-ratio		-	-	2.651	1.490	3.116
	Pure SS	-	-	-	12.222	23.463	3.148
	(%) contribution	-	-	-	3.108	8.791	1.180

Fig. 3.16 Bursted test specimens subjected to thermal loading at 600 °C and 800 °C

3.5.3.2 Evaluation of optimum response parameters of the utility concept

The utility concept has been utilized to obtain a single best mix combination out of the chosen slag concrete mixes exposed to different elevated temperatures. The utility concept, as described in the earlier sections was applied here also to achieve the single optimum proportions of mix parameters for maximum residual compressive strength of GGBFS HPC subjected to elevated temperatures. The larger the better optimization criterion was applied to all S/N ratios of mix parameters optimized at room temperature to 500 °C. The Table 3.48 shows the optimized mix proportions of different mix proportions derived from Taguchi technique.

Table 3.48 Optimal setting of process parameters (phase I) and optimal vales of individual quality characteristics

S. No.	Quality characteristics	Optimum setting of process parameters	Predicted optimum value (MPa)	95% of Predicted confidence intervals of quality characteristics
1	Room Temp.	A_1, B_3, C_2, D_1	82.630	$78.152 < \mu_{\text{Room Temp.}} < 87.107$
2	100 °C	A_1, B_1, C_2, D_3	72. 019	$62.86 < \mu_{100\,^{o}C} < 75.751$
3	200 °C	A_1, B_3, C_3, D_1	78.130	$74.504 < \mu_{200\,^{o}C} < 81.755$
4	300 °C	A_1, B_2, C_2, D_3	99.167	$84.806 < \mu_{300\,^{o}C} < 113.527$
5	400 °C	A_2, B_3, C_1, D_3	80.815	$65.646 < \mu_{400\,^{o}C} < 95.983$
6	500 °C	A_1, B_3, C_1, D_1	69.852	$61.968 < \mu_{500\,^{o}C} < 77.736$

(i) Construction of preference scale

A preference scale was constructed for determining the utility value of slag concrete for each target temperature from room temperature to 500 °C. Following are the details of calculations for the preference scale value, $P_{(Room\ Temp.)}$ expressed on a logarithmic scale for compressive strength of concrete at room temperature.

M_i^* = optimum value at room temperature, 82.630 MPa (refer Table 3.48)

M_i' = minimum acceptable value at room temperature, 60 MPa (all the observed values in Table 3.44 lie between 62 MPa and 70 MPa)

Using the above values and the equation 3.6, the preference scale for room temperature was constructed as

$$P_{Room\ temp} = 82.630 * \log\left(\frac{M_{Room\ temp}}{60}\right) \quad (3.17)$$

In a similar way, the preference scale values for other temperatures, namely 100 °C, 200 °C, 300 °C, 400 °C and 500 °C were also calculated.

(ii) Weightage of quality characteristics

The concrete responses of six different target temperatures are assumed as equally important for optimizing the compressive strength of heated concrete. As a result, in the equation (3.8), the selected temperatures were assigned equal weights as 0.1667.

(iii) Computation of utility value of slag HPC

The experimental results as given in Table 3.44 and the subsequent signal to noise ratio values using Taguchi's larger-the-better criterion as presented in Table 3.45 were processed and the sum of composite measures of overall maximized signal-to-noise ratio values were obtained. The utility values of the composite measure were then calculated using the equations 3.9 and 3.10. Table 3.49 shows the results of computed utility data of slag HPC.

Table 3.49 Utility data based on quality characteristics (raw data: Room temp., 100 °C, 200 °C, 300 °C, 400 °C and 500 °C)

Mixes	1	2	3	Mean	S/N ratio
HPC G-1	7.016	8.018	7.939	7.658	17.682
HPC G-2	8.670	8.248	7.722	8.214	18.291
HPC G-3	9.423	8.234	8.538	8.731	18.822
HPC G-4	8.141	7.514	6.451	7.369	17.348
HPC G-5	5.164	5.783	6.025	5.657	15.052
HPC G-6	8.109	7.260	7.164	7.511	17.514
HPC G-7	4.034	5.738	3.941	4.571	13.200
HPC G-8	4.806	6.754	4.211	5.257	14.415
HPC G-9	6.409	6.439	5.534	6.127	15.745

3.5.3.3 Multiple response data analysis and estimation of optimal mix parameters

The utility values were further analyzed using the larger the better criterion characteristic type using equation (3.1). The calculated values of mean responses (mean utility value) and the signal to noise ratios (S/N ratio) are given in Tables 3.50 and 3.51 respectively, and the mean responses of mix proportions of utility values are plotted in Figure 3.17. The Figure 3.17 clearly represents that the first level of cement content (A_1= 380.143 kg/m^3), the third level of GGBFS content (B_3= 254.013 kg/m^3), the second level of super-plasticizer content (C_2= 2.362 L/m^3) and the third level of fine aggregate content (D_3= 649.238 kg/m^3) shall yield the best optimal performance value of the utility function i.e. residual compressive strength of concrete exposed to different elevated temperatures. Table 3.52 presents absolute optimal values of mix ingredient proportions for achieving the maximum residual compressive strength of heated slag based concrete.

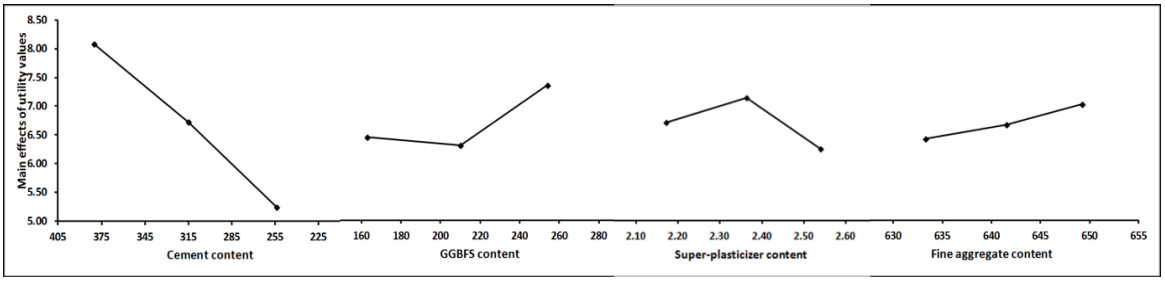

Fig. 3.17 Mean responses of main effects of process parameters of utility values of GGBFS HPC

Table 3.50 Mean utility vales of main effects of raw data

	Cement content (A)	**GGBFS content (B)**	**Super-plasticizer content (C)**	**Fine aggregate content (D)**
1	**8.201***	6.532	6.809	6.481
2	6.846	6.376	**7.236***	6.765
3	5.318	**7. 456***	6.320	**7.119***

***** Indicates best performance of utility values for different temperatures of exposure

Table 3.51 Mean utility vales of signal to noise (S/N) ratio of raw data

	Cement content (A)	**GGBFS content (B)**	**Super-plasticizer content (C)**	**Fine aggregate content (D)**
1	**18.265***	16.076	16.537	16.160
2	16.638	15.919	**17.128***	16.335
3	14.453	**17.360***	15.691	**16.861***

***** Indicates the best performance of S/N ratio values for different temperatures of exposure

Table 3.52 Optimal setting of process parameters utility values (phase II)

S. No.	Process parameter	level	Optimal values
1	Cement content (kg/m^3)	A_1	380.143
2	GGBFS content (kg/m^3)	B_3	254.013
3	Super-plasticizer content (kg/m^3)	C_2	2.362
4	Fine aggregate content (kg/m^3)	D_3	649.238

3.5.3.4 Predicted means (optimal values of mix proportion parameters)

The optimum utility values ($U_{\text{Room Temp},100\ ^oC,200\ ^oC,\ 300\ ^oC,\ 400\ ^oC,\ 500\ ^oC}$) were predicted at the selected levels of variables as stated above viz. cement content (A_1), GGBFS content (B_3), super-plasticizer content (C_2) and fine aggregate content (D_3). The estimated mean of the response of mix proportion parameters ($U_{Room\ Temp.,\ 100\ ^oC,\ 200\ ^oC,\ 300\ ^oC,\ 400\ ^oC,\ 500\ ^oC}$) can be determined as:

$$\mu_{Room\ Temp.,\ 100\ ^oC,\ 200\ ^oC,\ 300\ ^oC,\ 400^oC,\ 500\ ^oC} = \overline{A}_1 + \overline{B}_3 + \overline{C}_2 - \overline{2T} \quad (3.18)$$

where, $\overline{T}$ = overall mean of utility value = 7.010, which is taken from Table 3.49. The values of $\overline{A}_1, \overline{B}_3, \overline{C}_2$ were taken from Table 3.50.

The utility values of both the main effects and the signal-to-noise (S/N) ratio values of raw data were analyzed at each level of all the parameters. It is evident from Table 3.51 and Figure 3.17 that the mean utility values of first level of cement content (A_1), third level of GGBFS content (B_3), second level of super-plasticizer content (C_2) and the third level of fine aggregate content (D_3) would yield absolute performance in terms of utility value and S/N ratio values corresponding to different temperatures of exposure. Substituting the values of the above mentioned terms in equation (3.18), we get:

$\mu_{Room\ Temp.,\ 100\ ^oC,\ 200\ ^oC,\ 300\ ^oC,\ 400\ ^oC,\ 500\ ^oC}$ = 8.201+ 7.456+7.236– 2(7.010) = 8.981

The 95% confidence interval for utility values (CI_{CE}) was calculated using equation (3.11) and the values are presented in Table 3.55.

f_e = error of DOF = 2; V_e = error variance = 0.270

N = 27; n_{eff} = 27/7 (calculated)

R = 3; $F_{0.05}(1, 02)$ = 18.51 (Tabulated F value)

The confidence interval for confirmation experiments (CI_{CE}) = ± 1.835

The predicted optimal range (for confirmation runs of the experiment) is:

$(\mu_{Room\ Temp.,\ 100\ ^oC,\ 200\ ^oC,\ 300\ ^oC,\ 400\ ^oC,\ 500\ ^oC} - CI_{CE}) < \mu_{Room\ Temp.,\ 100\ ^oC,\ 200\ ^oC,\ 300\ ^oC,\ 400\ ^oC,\ 500\ ^oC} < (\mu_{Room\ Temp.,\ 100\ ^oC,\ 200\ ^oC,\ 300\ ^oC,\ 400\ ^oC,\ 500\ ^oC} + CI_{CE})$

$$7.146 < \mu_{Room\ Temp.,\ 100\ ^oC,\ 200\ ^oC,\ 300\ ^oC,\ 400\ ^oC,\ 500\ ^oC} < 10.817$$

3.5.3.5 Analysis of variance (ANOVA)

Table 3.47 shows the computed results of pooled version of ANOVA for slag concrete exposed to various target temperatures analysed by Taguchi technique. The Table 3.54 shows the computed results of pooled versions of utility values of the ANOVA at 0.05% level of significance with 95% confidence level. The fisher ratios (F-ratio) were calculated to identify the importance of factors from variance within the confidence level and the percent contributions of the various parameters as quantified under the respective columns of Table 3.53. It can be observed that the cement content showed the most significant effect on the residual compressive strength of heated concrete at all the temperatures with 72.343% contribution. The GGBFS content was observed to be the second most influencing parameter followed by the dosage of super plasticizer.

Table 3.53 Pooled ANOVA for utility vales of raw data

Parameters	Degree of freedom	Sum of squares	Variance	F-ratio	Pure SS	Percentage contribution
Cement content (A)	2	12.478	6.239	20.331	11.864	72.343
GGBFS content (B)	2	2.046	1.023	3.334	1.432	8.735
Super-plasticizer content (C)	2	1.262	0.631	2.056	0.648	3.953
Fine aggregate content (D)	2	0.614	0.307	-	pooling	pooling
Error	2	0.641	0.307			14.969
Total	8	15.721				100.000

3.5.3.6 Confirmation experiment

In order to validate the predicted optimized conditions, confirmation experiments were conducted by running another three replications at the optimal mix proportions as determined from the analysis. Figure 3.18 shows a comparison of the experimental results of selected nine mixes with their confirmation test. The numerical values of confirmation test results are also shown in Table 3.54. It can be observed From Table 3.44 that the individual response of residual compressive strength values for the specimens tested at room temperature and those exposed to 500 °C, fall within the predicted 95% confidence interval of optimal range. The experimentally obtained utility value is shown in Table 3.55. The values are observed to be lying above the predicted 95% confidence interval of optimal range utility calculated for the utility function.

Table 3.54 Confirmation test results of specimens for utility values

Temperature ranges	Confirmation test results			
	1	2	3	Mean
Room temp.	89.935	84.316	91.238	**88.497**
100 °C	85.361	91.221	92.467	**89.683**
200 °C	102.392	95.489	101.697	**99.859**
300 °C	109.358	101.602	104.135	**105.032**
400 °C	102.5	101.069	98.6	**100.723**
500 °C	85.625	83.159	80.542	**84.392**

Table 3.55 Results of confirmation test for utility values

No.	Quality characteristics	Optimum setting of process parameters	Predicted optimum value	95% of Predicted confidence intervals of quality characteristics	Mean value of confirmation results
1	Room Temp.	A_1, B_3, C_2, D_3	**8.981**	**7.146< μ Room temp, 100 °C, 200 °C, 300 °C, 400 °C, 500 °C < 10.816**	**13.521**
	100 °C				
3	200 °C				
4	300 °C				
5	400 °C				
6	500 °C				

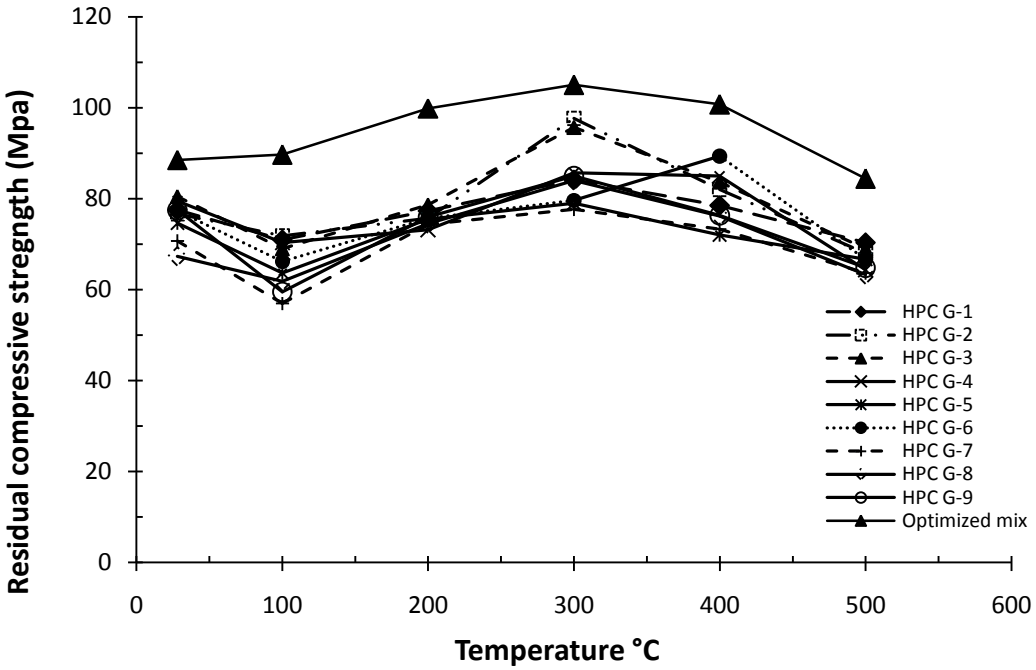

Fig.3.18 Comparisons of experiment results of trials mixes and confirmation test of GGBFS specimens subjected to elevated temperatures

3.5.4 Module 4: Silica Fume HPC

The average residual compressive strength values of various trial mixes of silica fume HPC are shown in Table 3.56. It can be observed that the silica fume HPC could be exposed to temperatures up to 400 °C only. All the specimens exposed to higher temperatures spalled. The appearance of various specimens after heating is shown in Figure 3.19.

Table 3.56 Measured residual compressive strengths of concrete mixes

Mixes	Room temperature	100 °C	200 °C	300 °C	350 °C	400 °C
HPC S-1	87.67 (100.00%)	82.33 (93.92%)	103.00 (117.49%)	109.33 (124.71%)	98.833 (112.74%)	***
HPC S-2	88.33 (100.00%)	82.33 (93.21%)	104.67 (118.49%)	112.33 (127.17%)	98.667 (111.70%)	***
HPC S-3	88.00 (100.00%)	84.33 (95.83%)	112.67 (128.037%)	112.33 (127.65%)	92.83 (105.49%)	102.5
HPC S-4	92.00 (100.00%)	90.33 (98.19%)	101.00 (109.78%)	107.67 (117.03%)	99.667 (108.33%)	***
HPC S-5	91.67 (100.00%)	82.00 (89.45%)	104.17 (113.64%)	106.18 (101.33%)	98.00 (106.91%)	***
HPC S-6	88.33 (100.00%)	87.33 (98.87%)	108.67 (123.02%)	114.17 (129.25%)	99.00 (112.08%)	113.5
HPC S-7	91.67 (100.00%)	81.83 (89.27%)	105.33 (114.91%)	114.00 (124.36%)	94.667 (103.27%)	***
HPC S-8	90.00 (100.00%)	84.33 (93.70%)	108.00 (120.00%)	110.00 (122.22%)	92.67 (102.96%)	101.5
HPC S-9	88.33 (100.00%)	80.33 (90.94%)	104.667 (118.49%)	105.33 (119.25%)	89.83 (101.70%)	***

*** indicates the test spalled during subjected to thermal loading

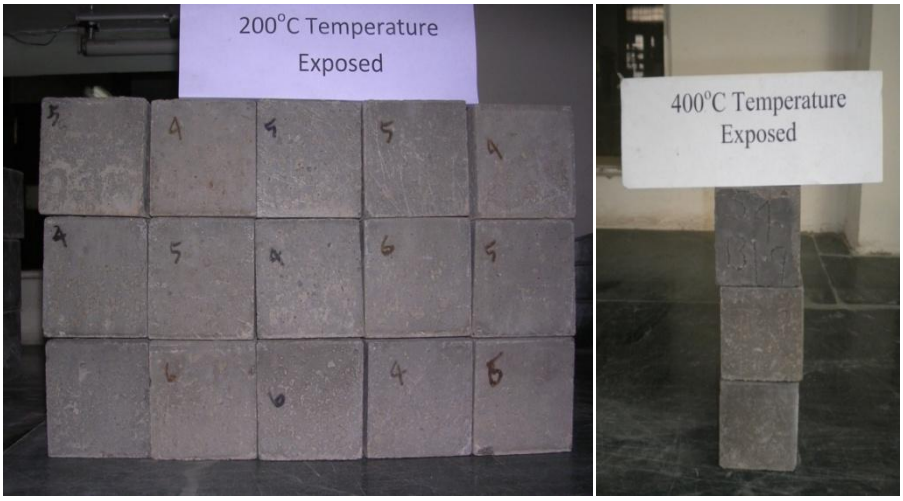

Fig. 3.19 Test specimens of silica fume HPC subjected to different elevated temperatures

3.5.4.1 Analysis of data by Taguchi technique

The results of residual compressive strength of various mixes of silica fume HPC were also first evaluated by Taguchi's technique. The signal to noise ratios for optimum conditions were arrived using equation 3.1. It is important to mention here that the silica fume HPC specimens exposed to temperatures of 400 °C and above spalled drastically during thermal heating (Figure 3.20). In the view of this no subsequent data analysis was possible for the specimens subjected to such heating conditions. Therefore, the investigations were carried out by taking exposure temperatures ranging from room temperature to 350 °C.

The computed S/N ratios of the residual compressive strength results are shown in Table 3.57. This data was used to get optimum mix conditions. The mean numerical values of main effects of each parameter and temperature of exposure are given in Table 3.58. Figure 3.21(a-e), demonstrates the variation of mean values of main effects with the three levels of each parameter. It can be observed that the optimum cement content is at Level A_2 (446.193 kg/m^3), silica fume content is at Level B_1 (54.303kg/m^3), the super-plasticizer dosage is at Level C_3 (3.302 L/m^3) and the fine aggregate content is at Level D_3 (649.751 kg/m^3). At room temperature, the most effective parameters were observed to be cement content and silica fume content. The fine aggregate content did not show statistically significant effect at room temperature conditions.

Table 3.57 Signal to noise (S/N) ratio values of residual compressive strength of silica fume HPC

Mixes	Room temperature	100 °C	200 °C	300 °C	350 °C
HPC S-1	38.857	38.312	40.257	40.775	39.898
HPC S-2	38.922	38.312	40.396	41.010	39.883
HPC S-3	38.890	38.520	41.036	41.010	39.354
HPC S-4	39.276	39.117	40.086	40.642	39.971
HPC S-5	39.244	38.276	40.355	40.547	39.824
HPC S-6	38.922	38.824	40.722	41.151	39.913
HPC S-7	39.244	38.259	40.451	41.138	39.524
HPC S-8	39.085	38.520	40.668	40.828	39.338
HPC S-9	38.922	38.098	40.396	40.451	39.069

Fig. 3.20 Spalling of test specimens during thermal loading

At 100 °C, a marginal strength loss of about 2-11% of reference strength at room temperature was noted. The optimum level of ingredients corresponding to 100 °C temperature were cement content at Level A_2 (446.193 kg/m^3), the silica fume (SF) content at Level B_1 (54.303 kg/m^3), the super-plasticizer at Level C_1 (2.987 L/m^3) and the fine aggregate content at Level D_3 (649.751 kg/m^3). The main influencing parameters at 100 °C exposure are observed to be the cement content followed by fine aggregate content and super-plasticizer content. The analysis of ANOVA data as shown in Table 3.59 reveals that fine aggregate content was the most significant parameter with highest contribution of 35.626% followed by cement content with a contribution of 33.518%. The silica fume and super-plasticizer content were not that significant at 100 °C and therefore these factors were pooled.

The optimum values were obtained for cement content at Level A_3 (406.400 kg/m^3), silica fume (SF) content the Level B_3 (101.600 kg/m^3), super-plasticizer at Level C_3 (3.302 L/m^3) and for fine aggregate content at Level D_3 (649.751 kg/m^3) for specimens subjected at 200 °C temperature. It can be observed from Figure 3.21 (c) that, the increased levels of the cement content had shown negative effect in this temperature range. The parameters like super-plasticizer content and the silica fume content were found to be the major influencing parameters on the compressive strength at 200 °C. The results indicated that all the silica fume high performance concrete mix specimens exhibited much better fire resistance compared to those at 100 °C and room temperatures. A strength increase of 9 to 28% with reference to room temperature strength was observed at 200 °C. Literature indicates that other researchers had also reported similar trends (Phan et al. 2001, Kim et al. 2009). Such strength gain is reported to be greatly

influenced by moisture of concrete (Aydın et al. 2007). The continuous heating accelerates the escape of moisture from concrete and could be helpful in drying the inner layers of core concrete. As a result of drying, the possible physico-chemical changes occur and the stiffening of cement gel could generate the stresses (Van der Wall's forces) between the interfacial zone of aggregate cement paste of silica fume concrete (Behnood et al. 2008). However, no cracks and colour changes were observed on the surface of specimens at this temperature.

Table 3.58 Mean values of quality characteristics at different temperatures (Main effects)

Level No	**Factor A**	**Factor B**	**Factor C**	**Factor D**
		Room temperature		
1st Level	88.000	**94.444***	88.667	89.222
2nd Level	**90.667***	90.000	89.556	89.444
3rd Level	90.000	88.222	**90.444***	**90.000***
		100 ˚C temperature exposure		
1st Level	83.000	**84.833***	**84.667***	81.556
2nd Level	**86.556***	82.889	84.333	83.833
3rd Level	82.167	84.000	82.722	**86.333***
		200 ˚C temperature exposure		
1st Level	106.778	103.111	106.556	103.944
2nd Level	104.611	105.611	103.444	106.222
3rd Level	**106.000***	**108.667***	**107.389***	**107.222***
		300 ˚C temperature exposure		
1st Level	**111.333***	110.333	**111.167***	107.056
2nd Level	109.444	109.611	108.444	**113.50***
3rd Level	109.778	**111.278***	110.944	110.000
		350 ˚C temperature exposure		
1st Level	96.778	97.722	**96.833***	95.556
2nd Level	98.889*	96.444*	96.056	**97.444***
3rd Level	92.389	93.889	95.167	95.056

***** Indicates optimum level of values for a given temperature of exposure

The residual strength of silica fume HPC increased further when temperature of exposure increased to 300 ˚C. The optimum residual strength was obtained for cement

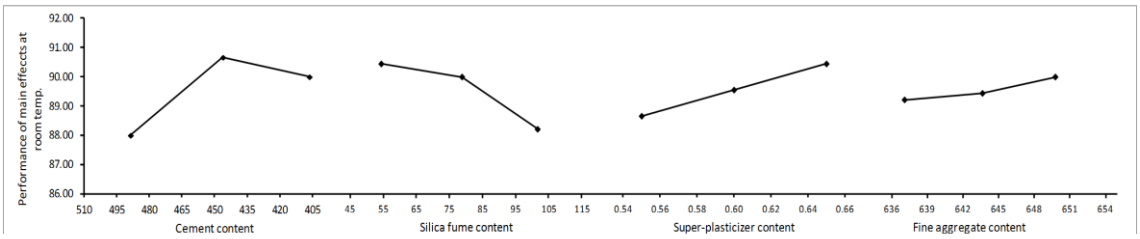

(a) Room temperature

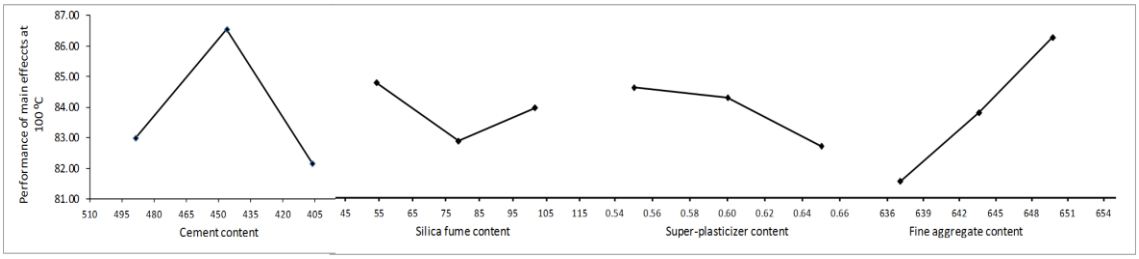

(b) 100 °C

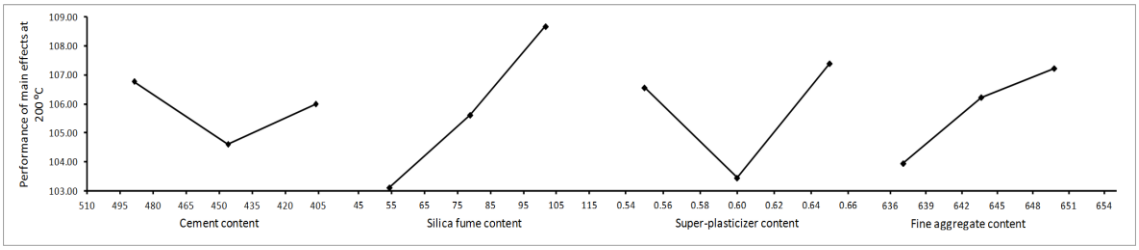

(c) 200 °C

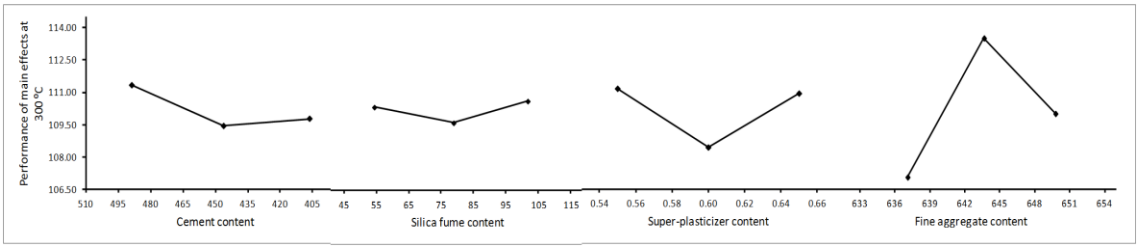

(d) 300 °C

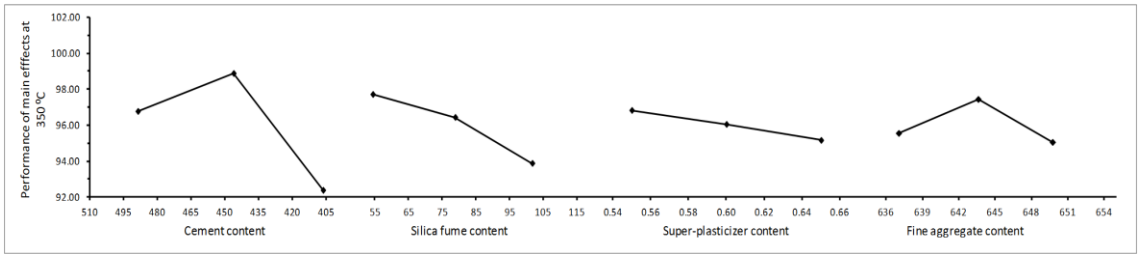

(e) 350 °C

Fig. 3.21 (a)-(e) Mean values of main effect of parameters on the performance characteristic of silica fume HPC

Table 3.59 ANOVA results for silica fume HPC exposed to various temperatures

Factors	Statistical parameters	Room temperature	100 °C	200 °C	300 °C	350 °C
Cement content (A)	Pooling	No	No	Yes	Yes	No
	Degree of freedom	2	2	2	2	2
	Sum of square	11.556	32.599	11.056	6.099	65.969
	Variance	5.778	16.299	-	-	32.985
	F-ratio	12.000	5.345	-	-	15.809
	Pure SS	10.593	26.500	-	-	61.796
	(%) contribution	41.449	33.518	-	-	60.275
Silica fume content (B)	Pooling	No	Yes	No	Yes	No
	Degree of freedom	2	(2)	2	(2)	2
	Sum of square	8.296	5.710	46.451	1.599	22.858
	Variance	4.148	-	23.225	-	11.429
	F-ratio	8..615	-	6.126	-	5.478
	Pure SS	7.333	-	39.222	-	18.685
	(%) contribution	28.696	-	40.627	-	18.225
Super-plasticizer content (C)	Pooling	No	Yes	No	No	Yes
	Degree of freedom	2	2	2	2	2
	Sum of square	4.741	6.488	25.932	13.710	4.173
	Variance	2.370	-	12.966	6.855	-
	F-ratio	4.923	-	1.532	3.562	-
	Pure SS	3.778	-	18.702	9.861	-
	(%) contribution	14.783	-	19.373	11.759	-
Fine aggregate content (D)	Pooling	Yes	No	No	No	No
	Degree of freedom	(2)	(2)	2	2	2
	Sum of square	0.963	34.265	16.932	62.451	9.525
	Variance	-	17.133	8.466	31.225	4.762
	F-ratio		5.618	2.342	16.226	2.283
	Pure SS	-	28.167	9.704	58.602	5.352
	(%) contribution	-	35.626	10.051	69.882	5.220

content at Level A_1 (488.731 kg/m^3), for silica fume (SF) content at Level B_3 (101.600 kg/m^3), for super-plasticizer content at Level C_1 (2.987 L/m^3) and for fine aggregate content at Level D_2 (591.7407 kg/m^3). At this temperature, the fine aggregate content and super plasticizer content were noted as the most influencing parameters. The other constituent parameters such as cement content and silica fume content had practically no effect and hence were pooled. The statistical analysis of ANOVA as given in Table 3.59 shows that the fine aggregate content is the most significant parameter with highest contribution of 69.882%. No cracks and spalling were noted on the surfaces of the test samples even at this temperature. The average residual strength of specimens heated at 300 °C was observed to be 39% more than the strength of room temperature specimens. This strength increase is attributed to additional hydration of unhydrated cement and silica fume grains due to moving of moisture front towards the core. The reaction of silica fume particles with calcium hydroxide in the presence of moisture strengthens the microstructure of heated concrete with relatively lower porosity.

The residual strength values at 350 °C temperature were found to be comparable with those at 300 °C. However, slight reduction in strength was noticed when the temperature increased from 300 °C to 350 °C. The optimum conditions at 350 °C exposure were obtained for cement content at Level A_2 (446.193 kg/m^3), silica fume content at Level B_1 (54.303 kg/m^3), super-plasticizer content at Level C_1 (2.987 L/m^3) and for fine aggregate content at Level D_2 (643.619 kg/m^3). At 350 °C temperature, the cement content and silica fume content were found to be the main influencing parameters as evident from Figure 3.21 (e). The cement content indicated maximum influence with a contribution of 60.275%. The previous literature indicates that the silica fume HPC generally maintains well its residual compressive strength up to 350 °C Hertz 1984). It is reported that the strength is maintained by the additional hydration of silica fume and cement particles with calcium hydroxide, which forms supplementary CSH gel, strengthening the microstructure (Saad et al 1996). The observed slight strength reduction in this study from 300 °C to 350 °C is due to dehydration of cement paste that results as disintegration of bonding between aggregate and cement paste. The thermal mismatch between the cement paste and aggregates also induces some micro cracks around the week transition zone of concrete and it reduces the residual compressive strength of concrete exposed to temperature of 350 °C (Castillo and Durrani 1990). As the

temperature increased to 400 °C, the test specimens spalled during the thermal testing at around 375- 400 °C of furnace temperature. Figure 3.20 shows few of such spalled test specimens during thermal loading. The Table 3.60 shows the optimized mix proportions of different mix proportions derived from Taguchi technique.

Table 3.60 Optimal setting of process parameters of silica fume HPC (phase I) and optimal vales of individual quality characteristics

No.	Quality characteristics	Optimum setting of process parameters	Predicted optimum value	95% of Predicted confidence intervals of quality characteristics
1	Room Temp.	A_2, B_1, C_3, D_3	91.556	$90.072 < \mu_{\text{Room Temp.}} < 93.039$
2	100 °C	A_2, B_1, C_1, D_3	87.093	$83.600 < \mu_{100\,^{\circ}C} < 90.585$
3	200 °C	A_3, B_3, C_3, D_3	110.240	$103.947 < \mu_{200\,^{\circ}C} < 116.534$
4	300 °C	A_1, B_3, C_1, D_2	114.259	$109.663 < \mu_{300\,^{\circ}C} < 118.855$
5	350 °C	A_1, B_1, C_1, D_2	98.259	$95.623 < \mu_{350\,^{\circ}C} < 100.896$

3.5.4.2 Estimation of optimum response parameters using utility concept

In order to get single optimized mix, the test data was further analyzed by using utility concept. The same procedure as mentioned earlier was followed. This enabled to find the optimized mix conditions for achieving maximum residual compressive strength corresponding to various temperatures of exposure. The utility concept was applied here also to solve multiple responses of the mix parameters of heated silica fume based HPC using larger the better optimization criterion. The analysis procedure has already been described in the previous sections. The weightage of 0.2 was assigned equally for all temperatures. The weighted S/N ratios obtained for different temperatures were summed up and with these data and the mean process parameters were determined. The sums of composite measures of overall maximized signal-to-noise ratio values are summarized in Table 3.61.

(i) Formulation of preference scale

A preference scale was constructed for determining the utility value of silica fume HPC for each target temperature using the equation (3.6). Following are the details of

calculation for the preference scale value $P_{(Room\ Temp)}$ expressed on a logarithmic scale for compressive strength of concrete at room temperature.

Table 3.61 Utility data based on quality characteristics (utility values: room temp., 100 °C, 200 °C, 300 °C and 350 °C)

Mixes	1	2	3	Mean	S/N ratio
HPC S-1	5.326	6.990	6.627	39.869	16.006
HPC S-2	7.203	6.166	6.883	45.573	16.587
HPC S-3	21.720	21.451	21.474	464.322	26.668
HPC S-4	21.682	21.276	22.943	482.559	26.836
HPC S-5	21.123	20.880	21.250	444.562	26.479
HPC S-6	21.739	22.908	22.341	498.612	26.978
HPC S-7	20.833	21.904	21.800	462.789	26.654
HPC S-8	21.187	21.103	21.416	450.954	26.541
HPC S-9	19.918	19.025	20.294	389.885	25.909

M_i^* = optimum strength value at room temperature is 91.556 MPa (refer Table 3.60)

M_i' = minimum acceptable value at room temperature is 75 MPa (all the observed values in Table 3.56 lie between 82 MPa and 95 MPa)

Using the above values and the equations (3.6) and (3.7), the preference scale for room temperature was constructed as,

$$P_{(Room\ Temp.)} = 91.556 \times \log\left(\frac{X_{Room\ Temp.}}{75}\right) \tag{3.19}$$

In a similar way, the preference scale values were calculated for other temperatures namely 100 °C, 200 °C, 300 °C and 350 °C. The selected mix design parameters were assigned equal weights, $P_{(Room\ Temp.)}$, $P_{(100^oC)}$, $P_{(200^oC)}$, $P_{(300^oC)}$, and $P_{(350^oC)}$ respectively.

(ii) Calculation of utility value of silica fume HPC

The overall utility value of the amalgamated measure was calculated using the equations (3.9 and 3.10). The overall utility function relation (equation 3.13) was employed to calculate the utility data of silica fume HPC at various temperatures. Using the above equations, the calculated utility data are reported in Table 3.61.

3.5.4.3 Data analysis and estimation of optimal mix proportions

The test results were analysed for mean responses of utility values at each level of chosen parameters and signal to noise ratio. The calculated values of mean responses (mean utility value) and the signal to noise ratios (S/N ratio) are given in Tables 3.62 and

3.63 respectively, and the mean responses of mix proportions of utility values are plotted in Figure 3.22. This figure represents clearly that the second level of cement content (A_2= 446.193 kg/m^3), the third level of silica fume content (B_3= 101.600 kg/m^3), the third level of super-plasticizer content (C_3= 3.302 L/m^3) and the third level of fine aggregate content (D_3= 591.740 kg/m^3) shall yield the best optimal performance. Table 3.64 indicates absolute values of mix proportions for optimized silica fume high performance concrete mix parameters.

Table 3.62 Mean utility values of main effects of raw data

No.	Cement content (A)	Silica fume content (B)	Super-plasticizer content (C)	Fine aggregate content (D)
1	10.477	14.529	14.543	13.704
2	**18.689***	14.313	14.054	14.829
3	17.711	**18.095***	**18.340***	**18.403***

***** Indicates the best performance of utility values for different temperature of exposures

Table 3.63 Mean utility vales of signal to noise (S/N) ratio of raw data

No.	Cement content (A)	Silica fume content (B)	Super-plasticizer content (C)	Fine aggregate content (D)
1	19.288	22.274	22.278	21.872
2	**25.429***	22.293	22.157	22.534
3	24.986	**25.136***	**25.267***	**25.297***

***** Indicates best performance of signal to noise (S/N) ratio values for different temperature of exposures

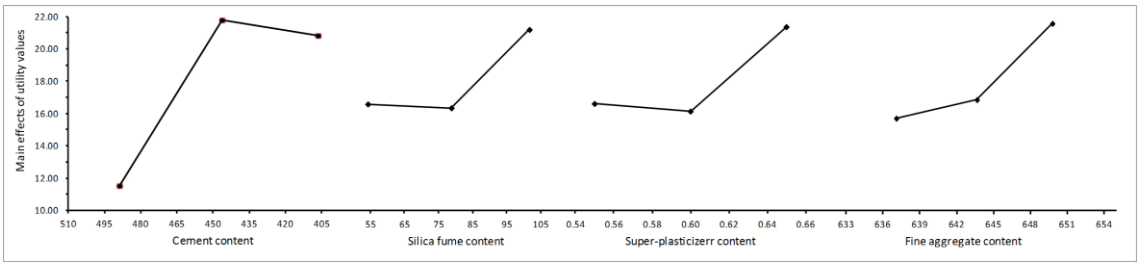

Fig. 3.22 Mean responses of main effects of process parameters of utility values

Table 3.64 Optimal setting of process parameters utility values (phase II)

S. No.	Process parameter	Level	Optimal values (kg/m^3)
1	Cement content	A_2	446.193
2	Silica fume content	B_3	101.600
3	Super-plasticizer content	C_3	3.302
4	Fine aggregate content	D_3	597.710

3.5.4.4 Optimal values of mix proportions parameters of silica fume HPC

The most favorable value of utility ($U_{\text{Room temp, 100 °C, 200 °C, 300 °C, 350 °C}}$) was predicted at the chosen levels of variables as stated above viz. cement content (A_2), Silica fume content (B_3), super-plasticizer content (C_3) and fine aggregate content (D_3). The estimated mean of the response of mix proportion parameters ($U_{\text{Room Temp., 100 °C, 200 °C, 300 °C, 350 °C}}$) can be determined as:

$$\mu_{\text{Room Temp., 100 °C, 200 °C, 300 °C, 350 °C}} = \overline{A}_2 + \overline{B}_3 + \overline{C}_3 - 2\overline{T} \quad (3.20)$$

where, $\overline{T}$ = overall mean of utility value = 18.276, which is taken from Table 3.61. The values of $\overline{A}_2$, $\overline{B}_3$, $\overline{C}_3$ were taken from Table 3.63.

The utility values of both the main effects and signal-to-noise (S/N) ratio values of raw data were analyzed at each level for all the parameters. It is clear from Table 3.62 and Figure 3.21 that the mean utility values of second level of cement content (A_2), third level of silica fume content (B_3), third level of super-plasticizer content (C_3) and third level of fine aggregate content (D_3) would yield best performance in terms of utility value and S/N ratio values for different temperatures of exposure.

Substituting the values of the above mentioned terms in equation (3.20), we get

$\mu_{\text{Room Temp., 100 °C, 200 °C, 300 °C, 350 °C}}$ = 21.794+ 21.208+ 21.382– 2 (18.276) = 27.830

The 95 % confidence interval of confirmation of experiments (CI_{CE}) was calculated using equation 3.11 and the values are presented in Table 3.64.

f_e = error of DOF = 2; V_e = error variance = 13.533

N = 27; n_{eff} = 27/7 (calculated)

R = 3; $F_{0.05}(1, 02)$ = 18.51 (Tabulated F value)

The confidence interval for confirmation experiments (CI_{CE}) = ± 12.188

The predicted optimal range (for confirmation runs of the experiment) is:

$$(\mu_{\text{Room Temp., 100 °C, 200 °C, 300 °C, 350 °C}} - CI_{CE}) < \mu_{\text{Room Temp., 100 °C, 200 °C, 300 °C, 350 °C}} < (\mu_{\text{Room Temp., 100 °C, 200 °C, 300 °C, 350 °C}} + CI_{CE})$$

$$15.642 < \mu_{\text{Room Temp., 100 °C, 200 °C, 300 °C, 350 °C}} < 40.018$$

3.5.4.5 Analysis of variance (ANVOA)

Table 3.59 shows the computed results of pooled versions of utility values of the ANOVA for silica fume HPC exposed to various target temperatures. The 0.05% level of significance with 95% confidence level of computed results of pooled versions of utility data of the ANOVA is shown in Table 3.65. It shows that the cement content indicated a

significant effect on the residual compressive strength of heated concrete with 65.409% contribution at all the temperatures with a maximum influence. The fine aggregate content was observed to be the second most influencing parameter with respect to residual compressive strength of heated silica fume HPC.

Table 3.65 Pooled ANOVA for utility vales of raw data

Factors	Degree of freedom	Sum of squares	Variance	F- ratio	Pure SS	Percentage contribution
Cement content	2	192.485	96.243	7.112	165.149	50.471
Silica fume content	(2)	27.066	13.533	---	pooled	pooled
Super-plasticizer content	2	50.160	25.080	1.853	23.094	7.046
Fine aggregate content	2	58.038	29.019	2.144	30.972	4.450
Error	2		13.55	1.000		2.016
Total	8	327.748				100.000

3.5.4.6 Confirmation experiments

The confirmation experiments were carried out by running another three replications at the optimized mix parameters of the silica fume HPC. The numerical values of confirmation test results are shown in Table 3.66 and the experimentally obtained confirmation utility value is also shown in Table 3.67. The value is observed to be lying above the predicted 95% confidence interval of optimal range utility calculated for the utility function.

Table 3.66 Confirmation test results of specimen's utility values

Temperature ranges	Confirmation test results (in MPa)			
	1	2	3	Mean
Room temperature	89.000	94.000	95.000	**92.667**
100 °C	85.000	77.000	73.000	**78.333**
200 °C	113.500	107.000	109.000	**109.833**
300 °C	113.000	120.00	117.500	**116.833**
350 °C	92.000	97.000	99.000	**96.000**

Table 3.67 Results of confirmation experiments for utility values

No.	Quality characteristics	Optimum setting of process parameters	Predicted optimum value	95% of Predicted confidence intervals of quality characteristics	Mean value of confirmation
1	Room Temp.	A_2, B_3, C_3, D_3	**21.387**	**11.20 < μ** Room temp., **100 °C, 200 °C, 300 °C, 350 °C < 35.576**	**23.891**
2	100 °C				
3	200 °C				
4	300 °C				
5	350 °C				

3.6 INTEGRATIVE ANALYSIS OF COMPRESSIVE STRENGTH OF VARIOUS MIXES

The Table 3.68 and Figure 3.23 presents the comparison of confirmation tests results of residual compressive strength of four different types of high performance concretes exposed to different target temperatures. The specimens of control non-pozzolanic HPC and fly ash HPC were tested under full range of target temperatures i.e. from room temperature to 800 °C with increments of 200 °C. The GGBFS HPC experienced spalling after the attainment of 600 °C temperature and silica fume HPC showed the spalling at 400 °C and beyond. Therefore, the original test plan was modified for these two types of HPCs to avoid the thermal spalling of test specimens and to obtain the residual strength data for further analysis. Thus, the test results of GGBFS HPC were obtained up to 500 °C and the silica fume HPC was tested up to 350 °C temperature.

The residual compressive strength results can be divided into three distinct temperature ranges. Form room temperature to 200 °C, all types of concrete showed increase in strength with the greater increase in fly ash HPC followed by control HPC, silica fume HPC and GGBFS HPC. Nevertheless the silica fume HPC had the maximum strength. However, at 100 °C, the silica fume HPC lost 15.5% of its original room temperature strength.

In 200 °C to 400 °C temperature range; the residual strength of all HPC mixes started reducing gradually though they maintained their residual compressive strength well above their original room temperature compressive strength. The silica fume HPC could not yield the test results beyond 350 °C because of severe spalling of specimens. The control HPC and GGBFS HPC showed 14% higher strength at 400 °C compared to their room temperature strength and both the concretes maintained almost same post fire strength. Among the various types of concrete, the GGBFS HPC showed higher resistance to temperature and lost only about 5% of initial strength at 500 °C. At 800 °C, the plain control and fly ash HPC showed severe strength deterioration. The average residual compressive strength of control plain HPC was 30.85% of its strength at room temperature and that for fly ash HPC was only 26.80% of its room temperature strength.

Table 3.68 Comparison of residual compressive strength of various HPCs

Residual compressive strength					
Target Temperatures (°C)		**Control HPC**	**Fly ash HPC**	**GGBFS HPC**	**Silica fume HPC**
Room temp.	Reading (MPa)	78.35	79	88.5	92.67
	%	100	100	100	100
100	Reading (MPa)	---	---	89.683	78.33
	%	---	---	101.34	84.53
200	Reading (MPa)	96.23	97.67	99.86	109.83
	%	122.82	123.63	112.84	118.52
300	Reading (MPa)	---	---	105.03	116.83
	%	---	---	118.68	126.07
350	Reading (MPa)	---	---	---	96
	%	---	---	---	103.59
400	Reading (MPa)	89.67	85.67	100.72	---
	%	113.81	108.44	113.81	---
500	Reading (MPa)	---	---	84.39	---
	%			95.36	
600	Reading (MPa)	56.69	53.83	---	---
	%	72.35	68.14		
800	Reading (MPa)	24.17	21.17	---	---
	%	30.85	26.80	---	---

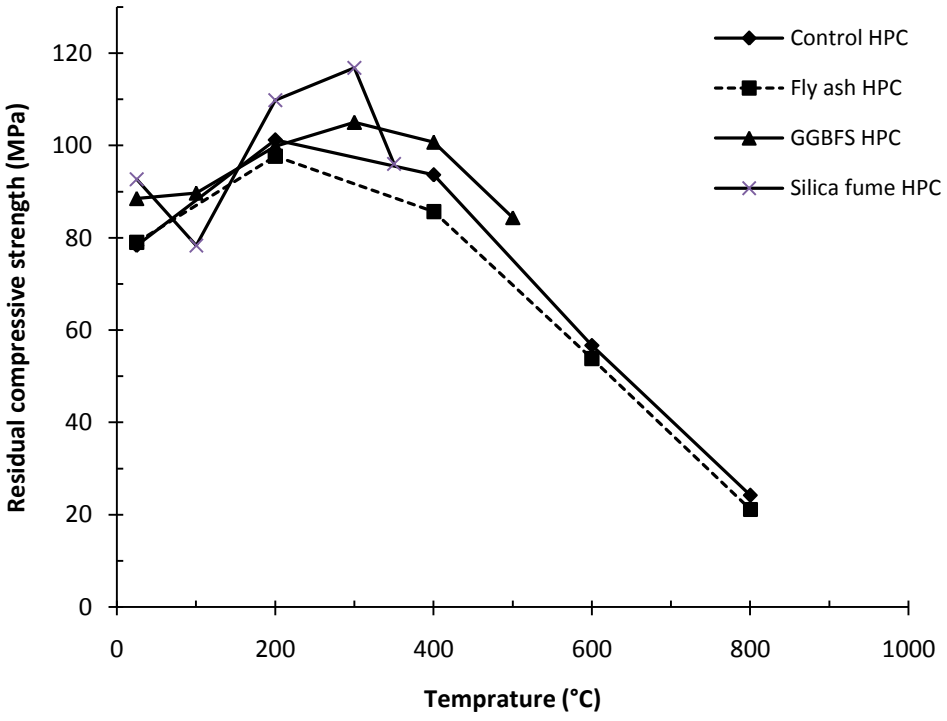

Fig. 3.23 Comparison of confirmation test results of different high performance concretes

3.7 CONCLUDING REMARKS

In this study, two different design of experimental (DoE) techniques have been put into practice to reduce the experimental trial runs and to optimize the residual compressive strength of heated high performance concrete. The research study was focused on the effects of mix constituents or parameters of concrete on the residual compressive strength of various heated high performance concretes mixes and thereby to arrive at an overall optimized mix combination that applies to the entire range of temperatures. In this investigation, three different types of pozzolanic high performance concretes in addition to a plain non-pozzolanic control HPC were prepared and subjected to elevated temperatures. Subsequently, the heated test specimens were tested under axial compression. A total of 756 cubic specimens were tested under this program. While the best mono mix combination for each target temperature was established by Taguchi's technique, an overall most excellent single concrete mix combination was obtained by using the utility concept.

CHAPTER - 4

RESIDUAL MECHANICAL PROPERTIES OF REINFORCED HIGH PERFORMANCE CONCRETE EXPOSED TO ELEVATED TEMPERATURES

4.1 INTRODUCTION

The knowledge of mechanical properties of heated concrete and reinforcing bars is important for evaluating the fire performance of reinforced concrete elements. Mechanical properties of these heated materials are also used in estimating the fire resistance of reinforced concrete structural components. The residual mechanical properties of heated concrete and rebars after subjecting to a complete cycle of heating cooling are always needed to ascertain the post fire condition of structures. Thus investigating the mechanical properties of high performance concrete (HPC) subjected to elevated temperatures becomes necessary. As high performance concretes, especially those containing mineral admixture, are prone to thermal spalling, it also becomes important to investigate the spalling behavior of such concretes. The information concerning spalling of concrete is significant in predicting the fire resistance of high performance concrete structures. The existing literature shows that many studies were undertaken in the past to investigate the spalling and mechanical properties of heated high performance concrete (Khoury 2000, Kalifa et al. 2001, Kodur and McGrath 2006, Kodur and Phan 2007) However, most of the earlier investigations related to fire induced spalling of high performance concrete were undertaken on small scale un-reinforced cubes or cylinders. Only few studies are reported on reinforced and confined high performance concrete columns, which indicate that the lateral confinement enhances the fire endurance of the reinforced concrete columns and can contribute towards minimizing the spalling of high strength and high performance concrete columns (Kodur 2005, Kodur and McGrath 2006, Kodur and Phan 2007).

The earlier studies on residual mechanical properties of heated concrete involved heating of the concrete specimens under unstressed conditions without any pre-load. In realistic situations the columns experience permanent loads (gravity service loads) from upper floors. During fire or unwanted thermal exposure, such structural elements would be exposed to elevated temperatures in the presence of loads. It may be mentioned here

that the presence of a pre-load and the reinforcing bars, especially confining reinforcement, are expected to influence the spalling and other mechanical properties of concrete exposed to fire scenarios. Thus there is a need to investigate the spalling and mechanical properties of reinforced high performance concrete under stressed residual conditions. The conventional unstressed residual and the proposed stressed residual test conditions are schematically shown in the Figure 4.1 (a)-(b). Further as described in the previous chapters, there are very few studies available in the literature on the residual mechanical properties of reinforced HPC containing different types of pozzolanic materials. Therefore, investigating the influence of type of pozzolana on the residual mechanical properties of heated HPC also forms the scope of the present work.

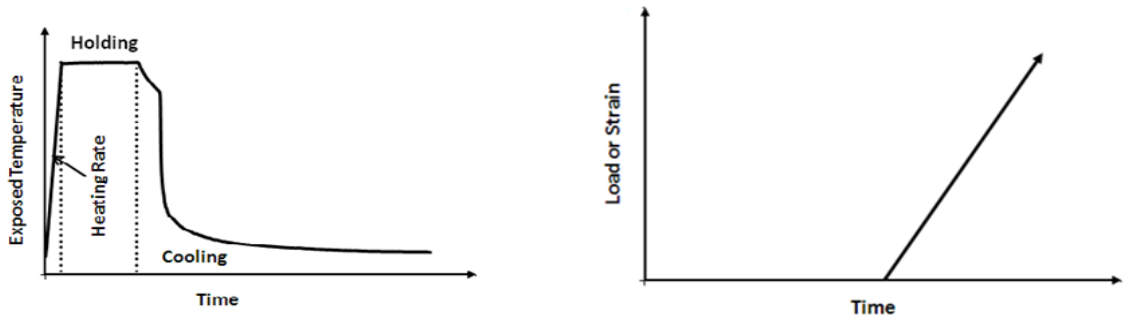

(a) Unstressed residual test method

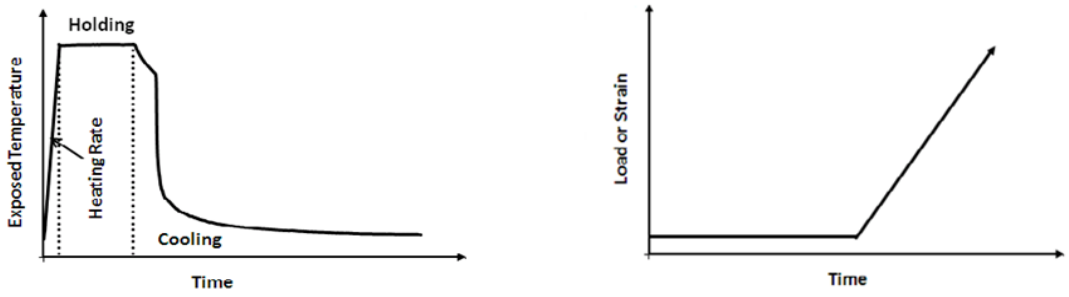

(b) Stressed residual test method

Fig. 4.1 (a)-(b) Schematic representation of two different test methods

4.2 EXPERIMENTAL PROGRAM

This section describes the experimental program planned to explore the effects of high temperatures on the compressive behaviour of reinforced high performance concrete short columns. A total of 108 numbers of reinforced tie confined short cylindrical column specimens of size 150 mm diameter and 450 mm height were cast and tested. Four types of HPC mixes were employed depending on the type of pozzolana. The various relevant

details of high performance concrete specimens are explained in Table 4.1, Table 4.2 and Figure 4.2. The high performance concrete mixes were prepared using ordinary Portland cement, mineral admixtures such as silica fume (SF), or fly ash (FA) or ground granulated blast furnace slag (GGBFS), natural river sand and cursed siliceous aggregate of maximum size 12.5 mm, tap water and water reducing chemical admixture. The three optimized pozzolanic HPC mixes and one optimized non-pozzolanic high performance concrete mix as developed and explained in Chapter 3, were used here to cast the column specimens.

Table 4.1 Test variables and designations of specimens

Type of mix	Temperature (°C)	Test condition	
		Unstressed residual	Stressed residual
Control HPC	Room temperature	CUST0	---
	200	CUST2	CST2
	400	CUST4	CST4
	600	CUST6	CST6
	800	CUST8	CST8
Fly ash HPC	Room temperature	FUST0	---
	200	FUST2	FST2
	400	FUST4	FST4
	600	FUST6	FST6
	800	FUST8	FST8
Silica fume HPC	Room temperature	SUST0	---
	200	SUST2	SST2
	400	SUST4	SST4
	600	SUST6	SST6
	800	SUST8	SST8
GGBFS HPC	Room temperature	GUST0	---
	200	GUST2	GST2
	400	GUST4	GST4
	600	CUST6	GST6
	800	GUST8	GST8

All the HPC confined concrete test specimens were cast and tested in triplicate in order to get the average of three results thus making 27 independent cases. A sufficient numbers of companion cubes (100 mm × 100 mm) were also cast with each series to determine the average compressive strength of the concrete and moisture content on the day of testing of column specimens for a particular set. The experimental variables included type of HPC based on mineral admixture (silica fume (SF), fly ash (FA) and ground granulated blast furnace slag (GGBFS) and control plain HPC), the different target temperatures (Room temperature, 200 °C, 400 °C, 600 °C and 800 °C) and the two

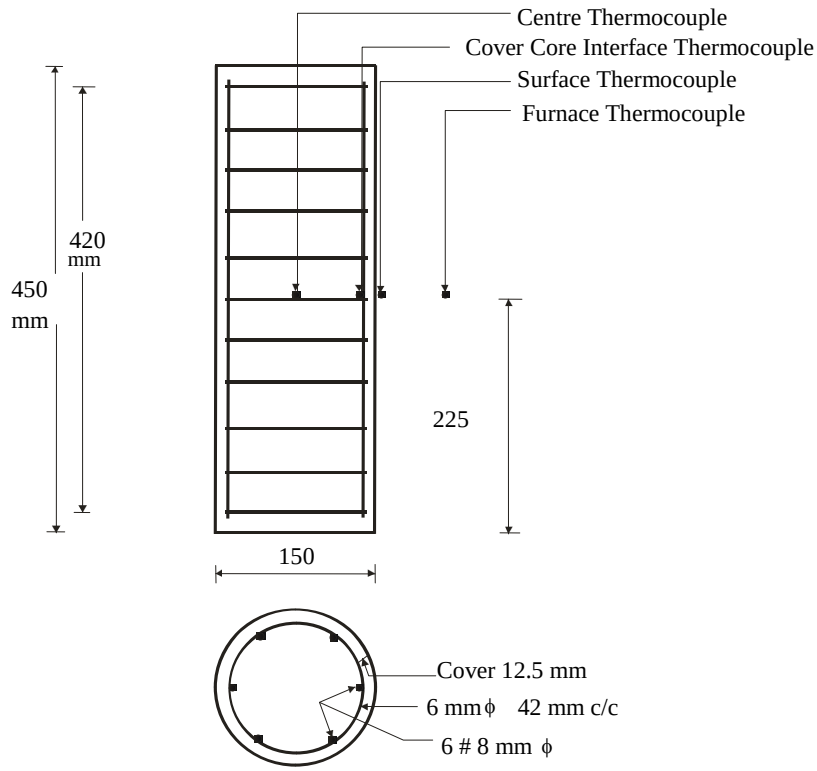

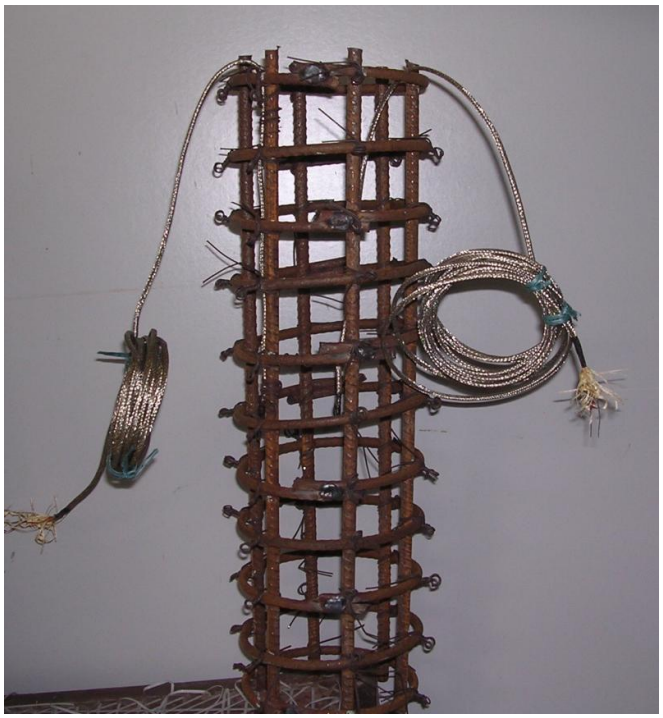

Fig. 4.2 Details of confined HPC cylindrical test specimens and location of thermocouples

test methods (unstressed residual and stressed residual strength test). The specimens were cast in eight dissimilar series (CUST, CST, FUST, FST, SUST, SST, GUST and GST). Each series of specimens consisted of specimens with same longitudinal and confinement reinforcement. The longitudinal reinforcement was in the form of 6 numbers of 8 mm diameter bars of 499.78 MPa yield strength. The lateral hoop ties were of 6 mm diameter with 576.51 MPa yield strength. The spacing of the lateral ties was kept about one third (42 mm) of core dimension of the confined column specimen and was kept constant throughout the investigation. A concrete cover of 12.5 mm was provided in all the specimens. A cover of 15 mm was also provided between the ends of longitudinal bars at top and bottom surfaces of the specimens to prevent direct loading of the bars. The specimens were cast in specially made steel cylindrical moulds in the laboratory.

4.2.1 Concrete mixes

The mix proportions of various HPC mixes corresponding to the optimized proportions as obtained in Chapter 3 are again shown in the Table 4.2. The 28 days and 90 days compressive strengths of mixes are also reported in the Table.

Table 4.2 Details of HPC mixes

Mixes	Water (kg/m^3)	Cement (kg/m^3)	Pozzolana (kg/m^3)	Super plasticizer (l/m^3)	Fine aggregate (kg/m^3)	Coarse aggregate (kg/m^3)	Compressive strength f_{ck} (MPa)	
							28 days	90 days
Control HPC	154.34	524.96	-	3.53	654.194	1031.56	77.90	88.34
Fly ash HPC	152.501	434.45	152.41	5.59	627.045	1031.56	76.03	87.02
Silica fume HPC	154.330	446.19	101.60	3.30	597.352	1031.56	92.69	99.59
GGBFS HPC	155.126	380.14	254.01	2.36	649.238	1031.56	85.93	94.12

4.2.2 The details of mixing, casting and curing

Before each casting, the specified quantities of various ingredients i.e. cement, fine aggregate, coarse aggregate, water, mineral admixture and super-plasticizer were kept ready in required proportions. Initially, mixer drum was wetted thoroughly; the coarse aggregate and cementitious materials were added together in the mixer drum in dry state while the drum was in motion. About more than half of the total water with super-plasticizer was added slowly to get a uniform mixture. The uniformity was indicated by

the uniform colour of the mix and no concentration of any one material being visible. After the mix became uniform, the mixing was continued further for about two minutes. Finally the fine aggregate was added in the mixing drum. After this, the remaining water with super-plasticizer was added, and the mixing was continued for about five minutes. The steel moulds for casting the specimens were cleaned, brushed, oiled and placed on a vibrating table with a speed in the range of 12000 ± 400 RPM and an amplitude of 0.055 mm. The fresh green high performance concrete was placed in the steel moulds in three layers and the moulds were vibrated properly to get a good compaction.

For each test variable investigated, three specimens were cast in order to get the average of three results. Therefore, 27 plain HPC control concrete specimens and 81 pozzolanic high performance concrete specimens were cast to study the residual load-displacement behavior of high performance concrete both at room temperature and predefined target temperatures. The next day after casting of specimens, the specimens were de-moulded, marked and submerged in a fresh water tank for curing. The water curing period continued till 28 days, afterwards the specimens were removed from the curing tank and were kept in laboratory in the ambient conditions for another 62 days to reach the equilibrium moisture content. After the total ageing of 90 days, the specimens were exposed to different target temperatures. In this study, single cycle of heating and cooling was implemented. Subsequently the specimens were tested under monotonic compression. Figure 4.3 shows the various stages of test specimens during casting and curing.

A desired level of workability was achieved for each mix. A commercially available third generation high range water reducing admixture, based on modified poly-carboxylic either (PCE) polymer was used to prepare the high performance concretes for the required workability. The workability of concrete was measured by using slump cone apparatus. The average results of slump cone test for all types of high performance concretes used in the present study are shown in Table 4.3.

Table 4.3 Results of workability test

Mixes	**Slump (mm)**
Control HPC	165
Fly ash HPC	155
Silica fume HPC	175
GGBFS HPC	180

Fig. 4.3 Stages of casting, de-moulding and curing of HPC specimens

4.2.3 Moisture content

The moisture exists in concrete in many forms namely free water, physically and chemically bound water and vapour. This moisture is extremely responsible for thermal softening, developing thermal expansion, drying shrinkage and build-up of pore pressures in concrete. As moisture content of heated concrete influences its mechanical and thermal properties, it is always important to report the moisture content of concrete. Sometimes it is required to eliminate the effect of moisture by keeping approximately similar moisture content in the test investigations unless moisture content itself is a test variable. Thus on the day of thermal testing of specimens, three numbers of companion cubes were dried completely until they achieved a constant mass in an oven at 105 °C ± 2 °C to measure moisture content for each series of HPC specimens. The Figure 4.4 shows the cubic specimens stacked in an oven for measurement of moisture content. The measured values of moisture content of the companion cubes were assumed as the moisture content of the corresponding main specimens. The measured average moisture contents of the concrete specimens are shown in the Table 4.4.

Table 4.4 Moisture content results

S. No.	Type of HPC	Moisture content (% of mass)
1	Control HPC	2.716
2	Fly ash HPC	3.598
3	Silica fume HPC	3.679
4	GGBFS HPC	3.380

Fig. 4.4 A view of cubic specimens in an oven for measurement of moisture

4.2.4 Furnace details

Specially constructed loading reaction frame with vertical split type electrical muffle furnace was used to apply the mechanical load and simultaneous heating to the specimens. The said high temperature furnace had a maximum operating temperature of 1000 ℃ and any temperature could be maintained up to 1 ℃ accuracy. The furnace was controlled by microprocessor based temperature controller with 'K' type thermocouples provided in the furnace chamber. Figure 4.5 shows a view of the complete set up of sustained loading frame with electrical muffle furnace. Though, the furnace was octagonal in appearance, it has an inner compartment of 450 mm height and 210 mm diameter. The furnace had capacity to accommodate single specimen at a time. A protective stainless steel mesh was loosely wrapped on the specimens. This avoided undesirable damage to the unprotected heating zone of refectory materials in the event of spalling during heating. The loading frame was capable of maintaining axial load through 800 kN hydraulic jack. A load cell was also installed to obtain the load data of specimens during heating. The load cell was placed over the hydraulic jack in between bottom of furnace and cross steel beam which was supported by the loading frame.

Fig. 4.5 A view of loading frame with vertical split type muffle furnace

4.2.5 Pre-loading

While some of the specimens were heated in unstressed condition, some specimens were pre-loaded to a defined axial load level before heating them to the various chosen target temperatures. The specimens were mounted on the loading frame to apply the preload. The specimens meant to be heated in stressed conditions were applied with an axial load of 25% of average ultimate load capacity of respective unheated specimen. The ultimate load capacity of unheated specimens was measured beforehand. The preload was applied to the specimens approximately 15 minutes before the start of heating test and was sustained till the end of the thermal test (i.e. for complete heating and cooling cycle of approximately 24 hours duration). No additional load was applied during the test for maintaining the initial load. The loading history of column data was recorded during the heating through the load cell connected to a data logger. The Table 4.5 shows the details of applied preloads on the various high performance concrete specimens.

Table 4.5 Ultimate load and sustained load on the confined high performance columns

Type of concrete	Ultimate load capacity of specimens at room temperature (kN)	Pre-load (kN)
Control HPC	1602.98	**400.75**
Fly ash HPC	1792.65	**448.16**
Silica fume HPC	1720.41	**430.10**
GGBFS HPC	1680.21	**420.05**

4.2.6 Thermal testing

The previous studies show that in the real fire situations, the maximum temperature may reach 1200 ℃ to 1400 ℃ in a compartment. However, such high temperatures may occur at the surface of the structural elements in compartment and that too for an extremely short duration (Purkiss 2007, Zaidi et al. 2012). Therefore, a maximum target temperature of 800 ℃ inside the concrete was considered sufficient in the present investigation. The lower limit of the maximum exposure temperature was taken as 200 ℃, because no significant effects were found on the residual mechanical properties of heated concrete below this temperature (Mohamedbhai et al. 1986, Phan et al. 1998, Arioz 2007). The heating rate was set at 5 ℃ /min, which has been found to be realistic for protected structures exposed to fire. (Phan et al. 2002, Sharma et al. 2011, Zaidi et al. 2012). Each target temperature was maintained for two hours to attain a thermal steady state condition. The temperature histories during the heating and cooling phases were recorded through the embedded K-type thermocouples. Three thermocouples were installed in each test specimen. The first thermo couple was fixed at mid height of the specimen's surface, the second at cover core interface and third thermocouple was installed at centre of the core i.e. 75 mm from the surface. The Figure 4.2 shows the locations of these thermocouples. After heating the specimens to target temperatures for the desired time duration, the furnace was switched off and the specimens were left in the furnace for one hour to allow cooling within the furnace. Thereafter, the furnace was opened and the specimen was left in the furnace to allow further natural cooling to room temperature. The rate of cooling was not controlled but was measured completely during the test duration. The data from the thermocouples was recorded in a computer through an inbuilt data logger mounted in the micro processer unit of furnace. Figure 4.6 shows some views of a typical HPC test specimen before and after application of thermal load with a sustained pre-load.

(a)

(b)

Fig. 4.6 (a)-(b) Views of test setup before and after application of thermal loading

4.2.7 Residual mechanical testing

All the HPC specimens were subjected to uni-axial compression test after a complete cycle of heating and cooling. The load-displacement responses were captured using 2500 kN capacity INSTRON UTM having strain controlled test capabilities. Figure 4.7 shows the UTM for residual compressive testing. The monotonic axial concentric compression was applied at a very slow displacement rate (0.1 mm/minute) to capture the complete load-displacement relationship including the post peak behaviour of the HPC specimens. The axial displacement of the specimens was measured by two linear variable displacement transducers (LVDT), which were attached at opposite faces of the specimens with the help of the steel clamps. The mean displacement of the specimens was measured over the gauge length of 200 mm and was converted into average strain. The load data and LVDT's data were fed into a data acquisition system and stored in a personal computer.

Fig. 4.7 Test setup for uni-axial compression

4.3 OBSERVATIONS DURING HEATING

During heating of concrete, visual observations of colour change, cracking and spalling of concrete provide important information (Short et al. 2001, Yuzer et al. 2004, Arioz 2007). At high temperature exposures, the colour change may be attributed to the changes in the chemical composition of cementing materials and aggregates. The observations of colour change due to the heating and cooling of concrete also gives an idea of the magnitude of temperatures reached. In this test program the concrete specimens exposed to 200 °C did not show any distinguished change in colour of concrete surface. However, at 400 °C temperature, a colour change on the surface of the test samples was observed from dark grey to light brown. The colour of the concrete specimens exposed to 600 °C temperatures was recorded to be light grey. However, ash white colour was seen on all the specimens exposed to 800 °C irrespective of type of HPC. No visible cracks due to temperature effects were seen on the surface of the specimens heated up to 400 °C. The cracks started to appear when the temperature was raised to 600 °C and above. The cracks observed at 600 °C temperature were also not very significant. The number and width of cracks became relatively pronounced only at 800 °C. The Figure 4.8 illustrates the cracks observed on the surface of plain control HPC specimens exposed to 600 °C and 800 °C temperatures. Many specimens of HPC spalled between 350 °C to 500 °C with loud sound. Among all types of plain and pozzolanic concretes, the silica fume HPC experienced maximum spalling. Most of the pre loaded test specimens exposed to 800 °C temperature experienced sudden drop in load after heating. In addition a complete decomposition of materials like concrete and steel was also noticed in these specimens.

4.3.1 Temperature histories

Three thermocouples were positioned in every column specimen at different locations (as explained earlier) to record the thermal histories during heating and cooling. Temperature histories were recorded and monitored and the thermal behaviour of the specimens were carefully studied during complete cycle of heating and cooling. To this end, time temperature curves were plotted for all the test specimens. Some typical average time-temperature curves for only CUST and CST series of non-pozzolanic plain HPC specimens at different target temperatures are being shown here in Figure 4.9 (a)-(h). However, the Table 4.6 reports the temperature histories of the all the test specimens.

The thermal data namely mean temperature difference between the core and the surface, thermal gradients, time and surface temperature at the time of maximum gradients and the description of thermal steady state are provided in this Table.

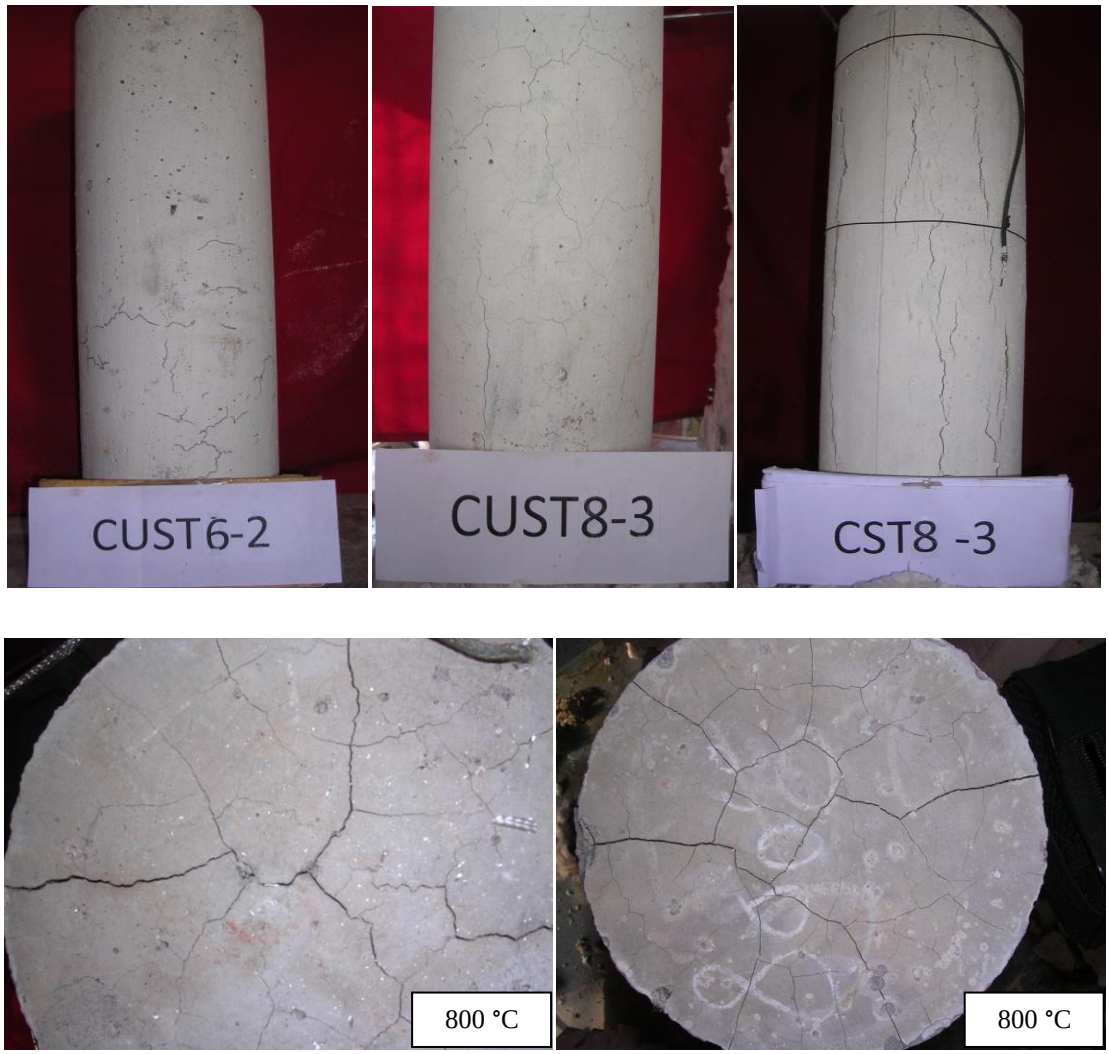

Fig. 4.8 Surface cracking observed in test specimens exposed to 600 °C and 800 °C

The surface temperatures were observed to be higher than the temperatures at the core of all the specimens during the heating phase. The steady state condition at target temperature could not be achieved in any of the specimens irrespective of type of HPC mix and the test methods. Nevertheless the steady state condition was achieved at a lower temperature and that too generally after beginning of the cooling phase in most of the HPC specimens. A maximum cooling deviation with respect to the surface temperature and core was observed between the temperature ranges of 200 °C and 400 °C in all the specimens. This happens in the concrete due to release of free water and later chemically

bound water from the specimens on heating (Phan and Carino 2002, Vorechovska 2008). The difference in the temperature between the core and the surface of the each specimen

Table 4.6 Temperature histories of column specimens

Specimens	Maximum Temperature difference (ΔT °C)		Maximum thermal gradient (°C/cm)		Time at maximum temperature difference (minutes)		Surface temperature at maximum gradient (°C)		Temp. of steady state (minutes)	Time of steady state (°C)
	+ve	-ve	+ve	-ve	+ve	-ve	+ve	-ve		
CUST2	86.8	34.2	11.6	4.9	42	477	145	60.7	174.6	243
SUST2	87.4	32	11.7	4.3	39	473	142	82.5	152.6	222
FUST2	114.4	25.7	15.3	3.4	43	278	168.8	133.8	174.5	181
GUST2	97.9	2.4	13.1	0.3	44	247	154.1	146.6	154.1	232
CST2	82.9	24.5	11.1	3.8	41	303	137.1	121.4	161.6	200
SST2	86.6	12.5	11.6	1.7	42	538	140.4	64.15	134.3	291
FST2	105.2	15.2	14.0	2.0	37	373	153.7	85.1	144.7	229
GST2	86.1	22.5	11.7	3.0	41	298	140.2	146.6	136.4	241
CUST4	162.3	68.4	21.7	9.1	72	480	295.7	131.5	360.64	265
SUST4	187.5	61.6	25.0	8.2	82	348	332.3	232.9	353.4	228.0
FUST4	202.2	60.36	26.9	8.1	79	378	273.2	157.6	312.0	264.0
GUST4	167.5	37.4	22.3	5.0	89	335	306.8	251.1	340.4	248
CST4	169.3	60.3	22.6	8.0	78	293	281.1	257.7	352.48	249
SST4	190.5	34.7	25.4	4.7	76	297	337.1	271.0	338.4	230
FST4	175.3	32.8	23.4	4.4	78	324	313.2	227.2	281.4	302
GST4	184.1	41.7	24.6	5.6	87	392	331.3	171.5	324.6	245
CUST6	300.3	91.5	40.0	12.2	128	346	557.2	295.9	551.2	283
SUST6	313.7	254.9	41.8	34.0	117	399	531.4	208.0	536.0	259
FUST6	337.8	127.0	45.0	16.9	119	342	552.3	252.4	515.2	283
GUST6	347.7	159.6	46.4	21.3	125	425	565.1	225.1	544.8	254
CST6	346.2	71.9	46.2	9.59	129	490	562.3	211.5	471.3	322
SST6	312.7	219.2	41.7	29.2	120	427	572.8	238.9	579.9	246
FST6	338.0	212.6	45.1	28.3	130	357	566.8	245.8	542.3	264
GST6	297.1	206.7	39.6	27.6	122	319	550.8	240.4	539.3	253
CUST8	287.6	128.4	38.4	17.1	126	664	513.2	555.5	790.0	296
SUST8	326.1	144.9	43.5	19.3	117	449	672.1	445.8	771.0	284
FUST8	392.3	265.2	52.3	35.4	136	514	662.2	270.4	739.0	280
GUST8	336.7	275.4	44.9	36.7	125	425	735.9	396.9	776.9	281
CST8	376.3	299.6	50.2	40.0	124	593	579.4	175.8	737.6	287
SST8	370.3	130.3	49.4	17.4	120	449	702.7	583.1	755.4	303
FST8	334.7	211.8	44.6	28.2	151	395	674.5	139.0	755.9	292
GST8	411.5	342.8	54.9	45.7	146	437	717.4	142.7	775.3	294

was also determined to study the nature of thermal gradient for the entire duration of heating and cooling. Figures 4.10 (a)-(h) illustrate the variation of surface-centre temperature difference (ΔT °C) with time for some typical cases. It could be observed that during the heating and cooling cycle, the mean temperature difference between the surface and centre of the specimens first increased and gradually reached a maximum positive value then decreased to attain a maximum negative value during the cooling phase before reaching the ambient temperature.

The maximum positive thermal gradient was noticed at a higher temperature of exposure in pozzolanic high performance concretes specimens than plain high performance concrete. This trend was observed up to 600 °C temperature regardless of the test methods. No clear trend with respect to the type of HPC mix could be marked for maximum positive thermal gradients at 800 °C temperature. At 200 °C temperature, the test results show that the surface temperatures at maximum positive gradient varied from 140.2 to 168.8 °C and the corresponding values at maximum negative gradients varied from 60.7 to 146.6 °C. The unstressed test specimens showed higher thermal gradient values than the stressed test condition specimens in general. This is attributed to the restraining force of preload which influences the moisture movement across the cross section and also induces close contact of concrete mass that reduces thermal gradients during heating. At 400 °C, no clear trend could be marked because of preload. At 600 °C and 800 °C temperatures, the unstressed residual test specimens showed lower thermal gradient values than stressed residual test specimens for most of HPC specimens. At such high temperatures, the damage induced by preload may develop a barrier to flow of heat inside of concrete mass causing higher thermal gradients.

The test data also reveals that the maximum temperature difference and the time of maximum temperature difference are relatively more in pozzolanic high performance concretes compared to non-pozzolanic concrete. Further the results indicate that the maximum temperature difference between the centre of core and the surface during the cooling phase are less in magnitude than the corresponding positive thermal gradients during heating. While a maximum positive thermal gradient of 54.9 °C/cm was observed during heating, a maximum negative cooling thermal gradient 45.7 °C/cm was observed in the slag based HPC specimens of GUST8 series. The heating and cooling gradients increased with the increase in the temperature of exposure.

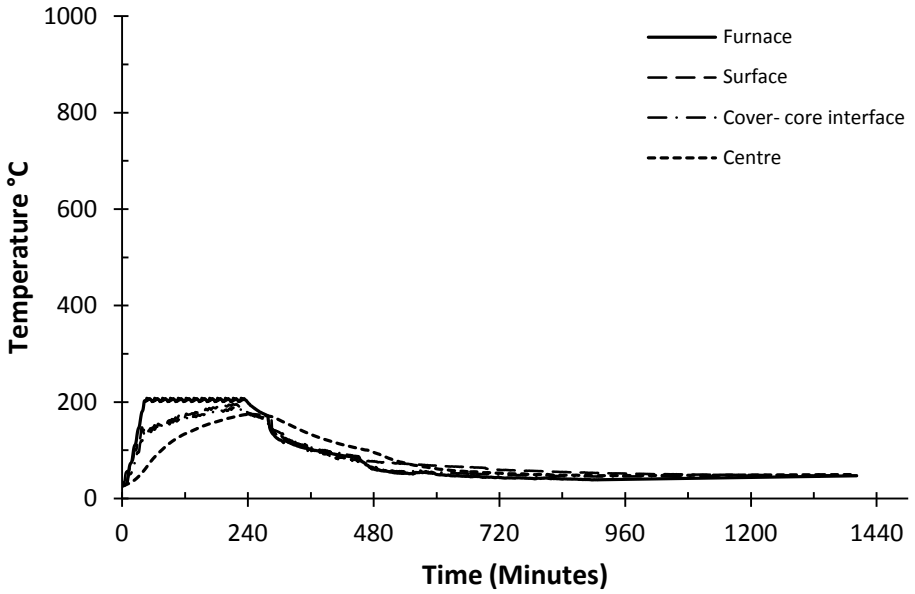

(a) CUST2 Series specimens exposed to 200 ℃

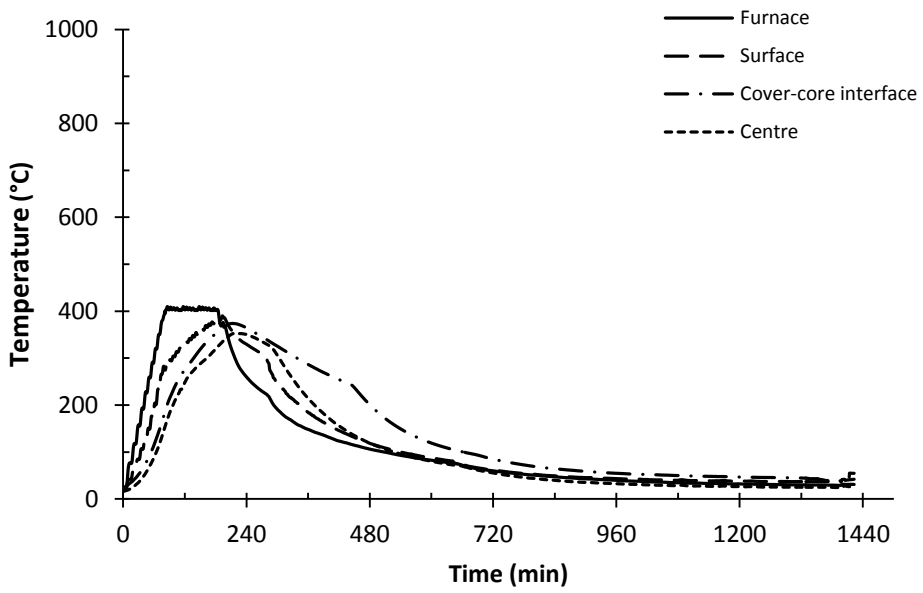

(b) CUST4 Series specimens exposed to 400 ℃

Fig. 4.9 (a)-(h) Typical time-temperature curves for CUST and CST series specimens (contd.)

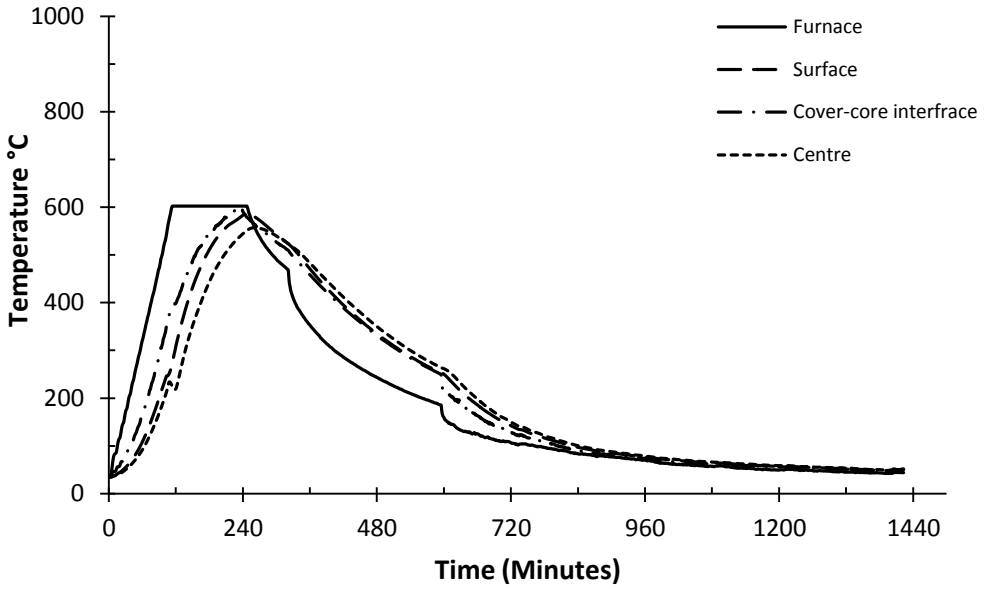

(c) CUST6 Series specimens exposed to 600 °C

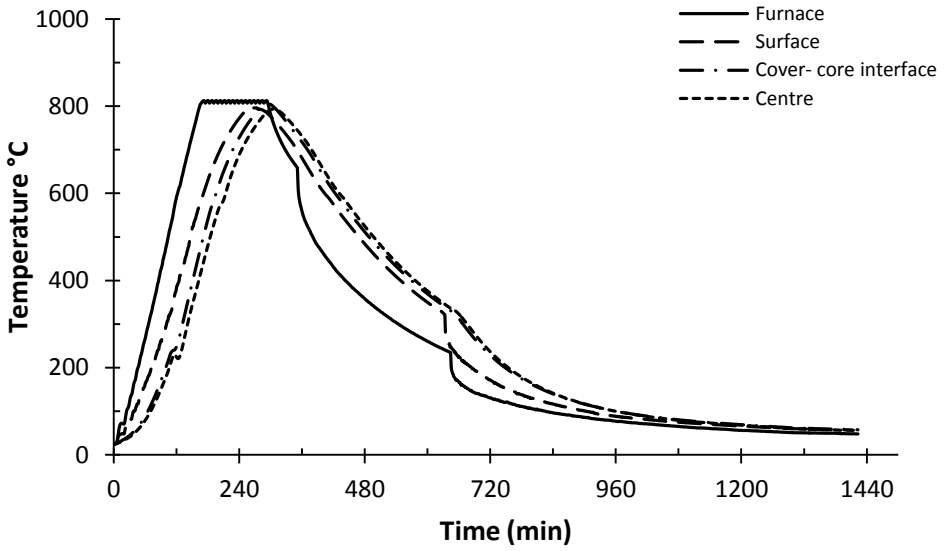

(d) CUST8 Series specimens exposed to 800 °C

Fig. 4.9 (a)-(h) Typical time-temperature curves for CUST and CST series specimens (contd.)

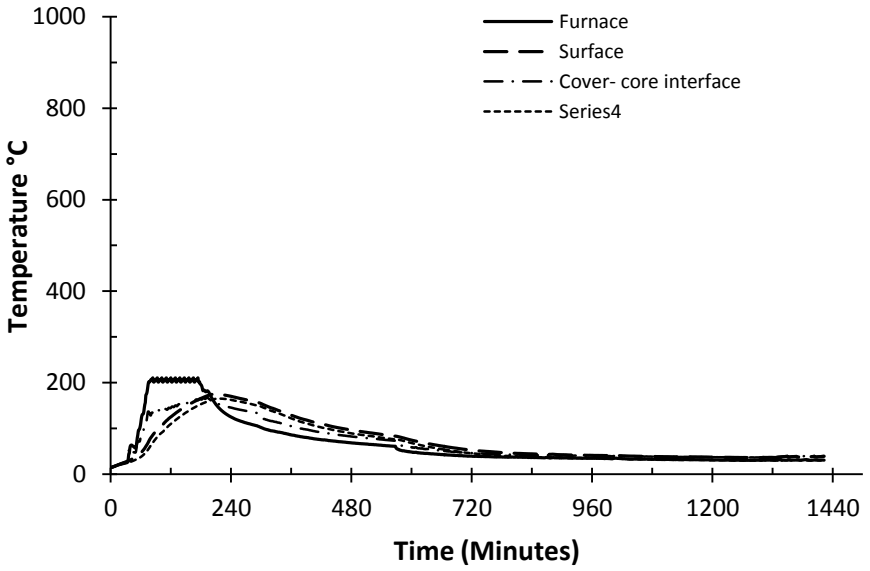

(e) CST2 Series specimens exposed to 200 °C

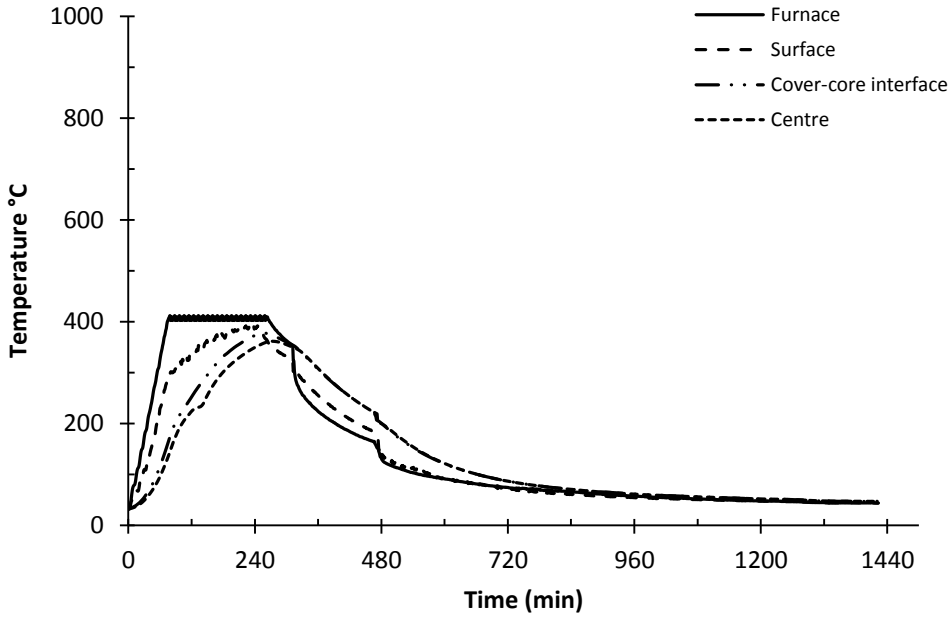

(f) CST4 Series specimens exposed to 400 °C

Fig. 4.9 (a)-(h) Typical time-temperature curves for CUST and CST series specimens (contd.)

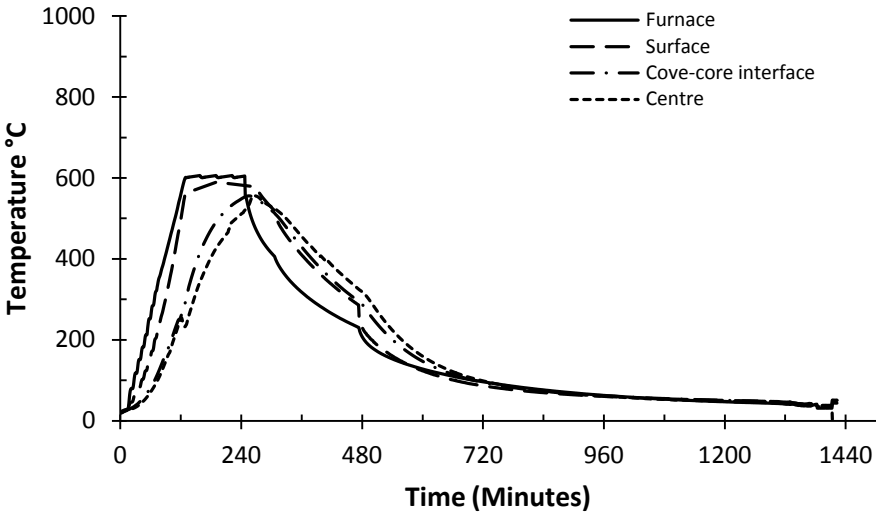

(g) CST6 Series specimens exposed to 600 °C

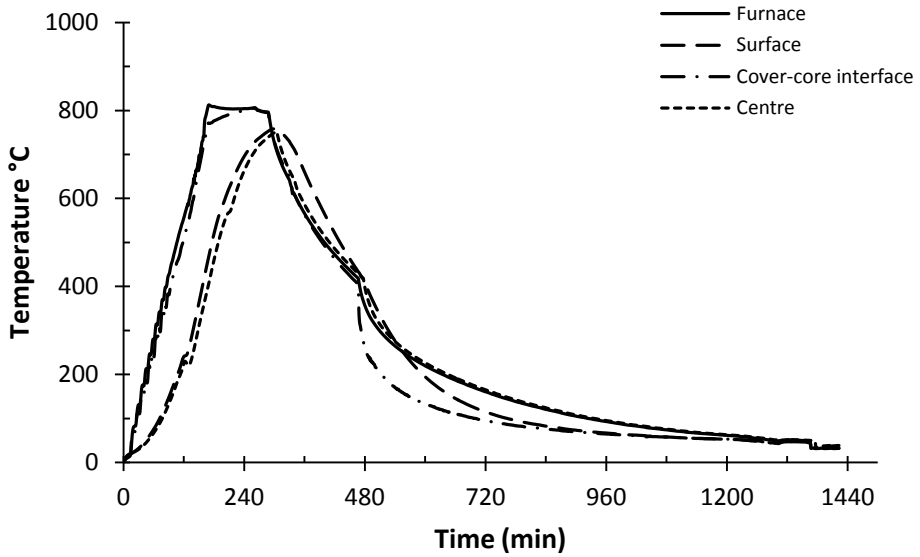

(h) CST8 Series specimens exposed to 800 °C

(i)

Fig. 4.9 (a)-(h) Typical time-temperature curves for CUST and CST series specimens

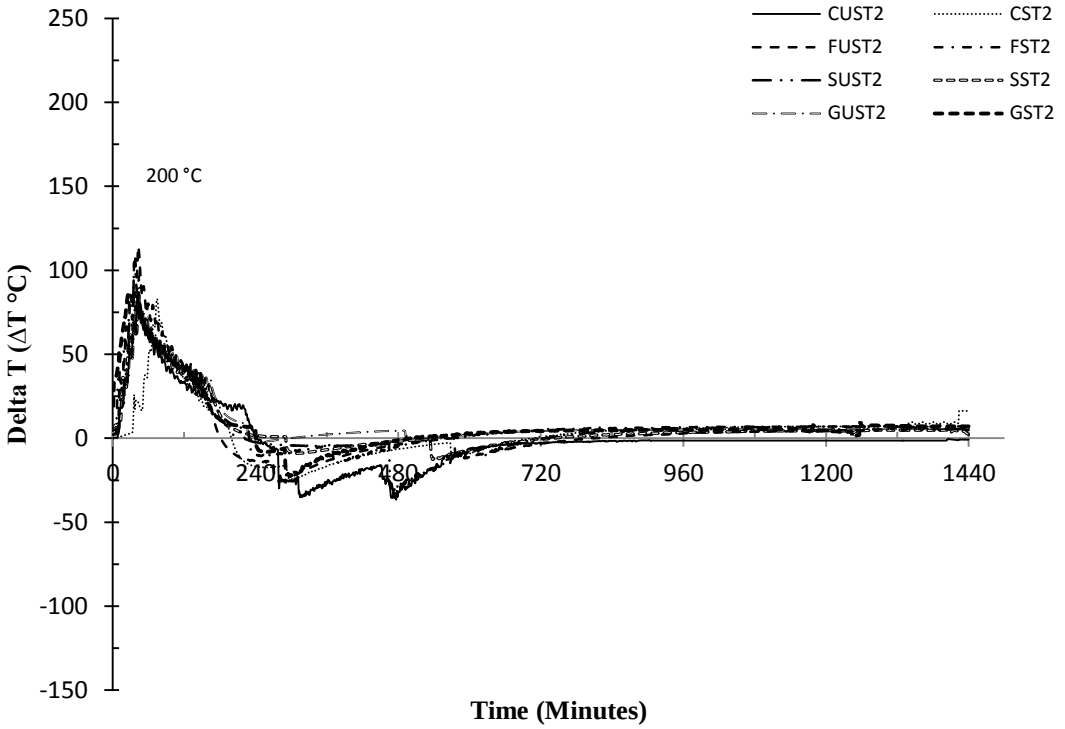

(a) 200 °C

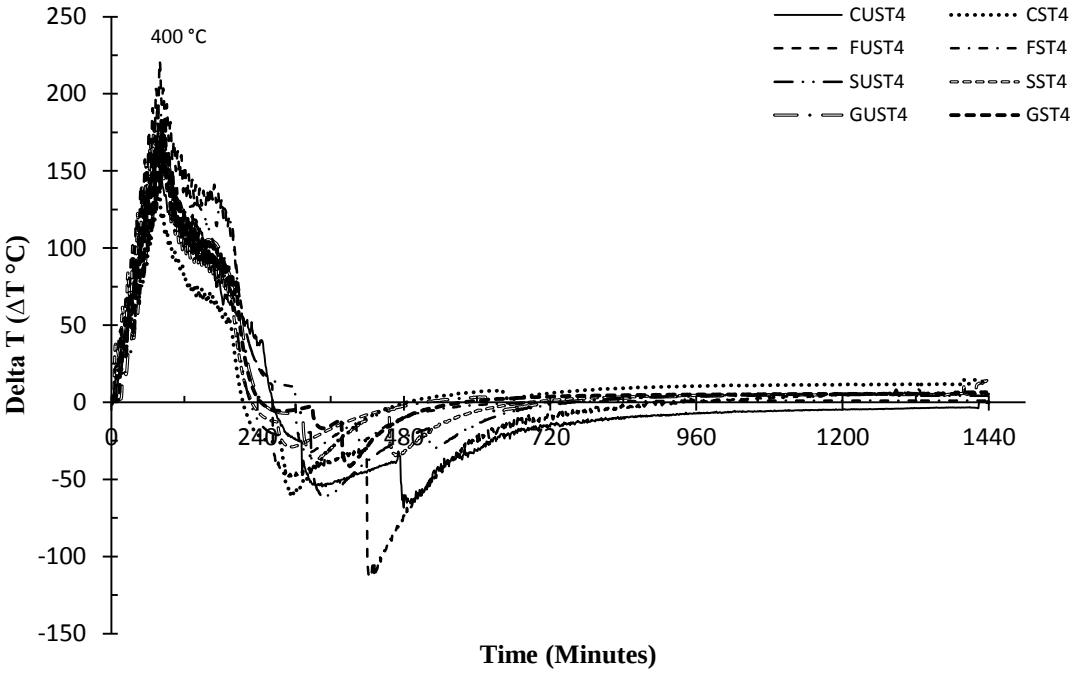

(b) 400 °C

Fig. 4.10 (a)-(d) Temperature difference (Δ T °C) between surface and centre v/s time for some specimens (contd.)

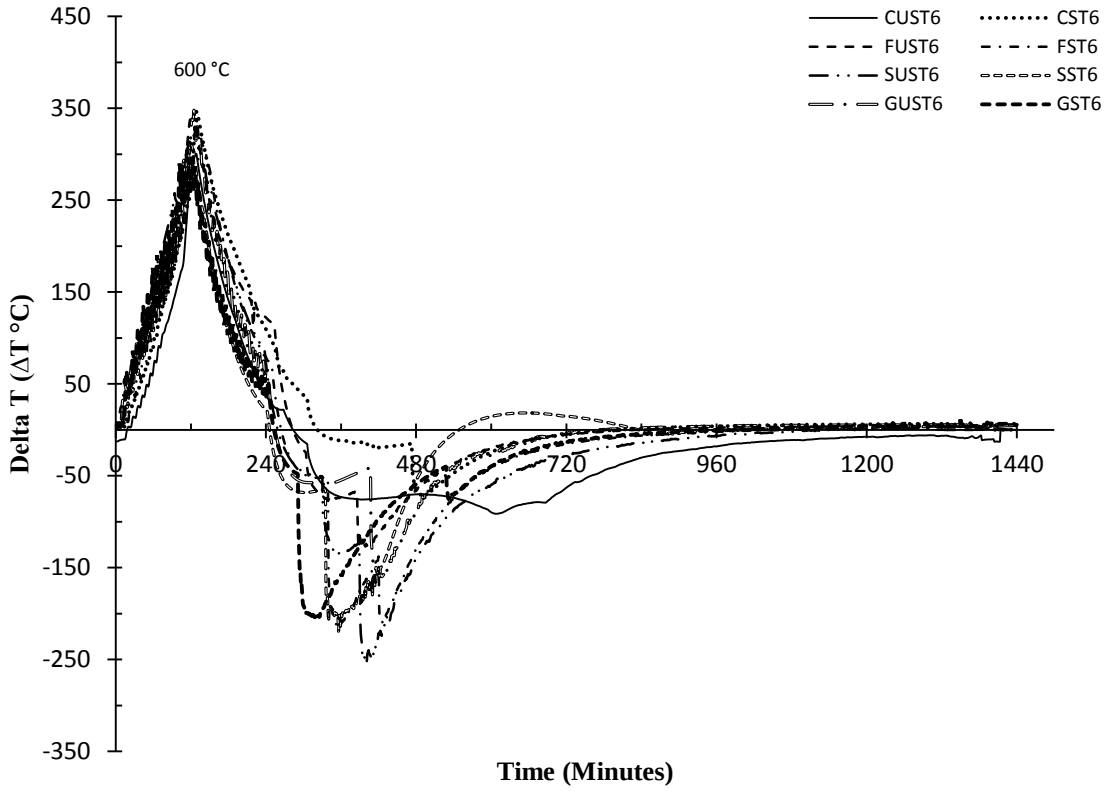

(c) 600 °C

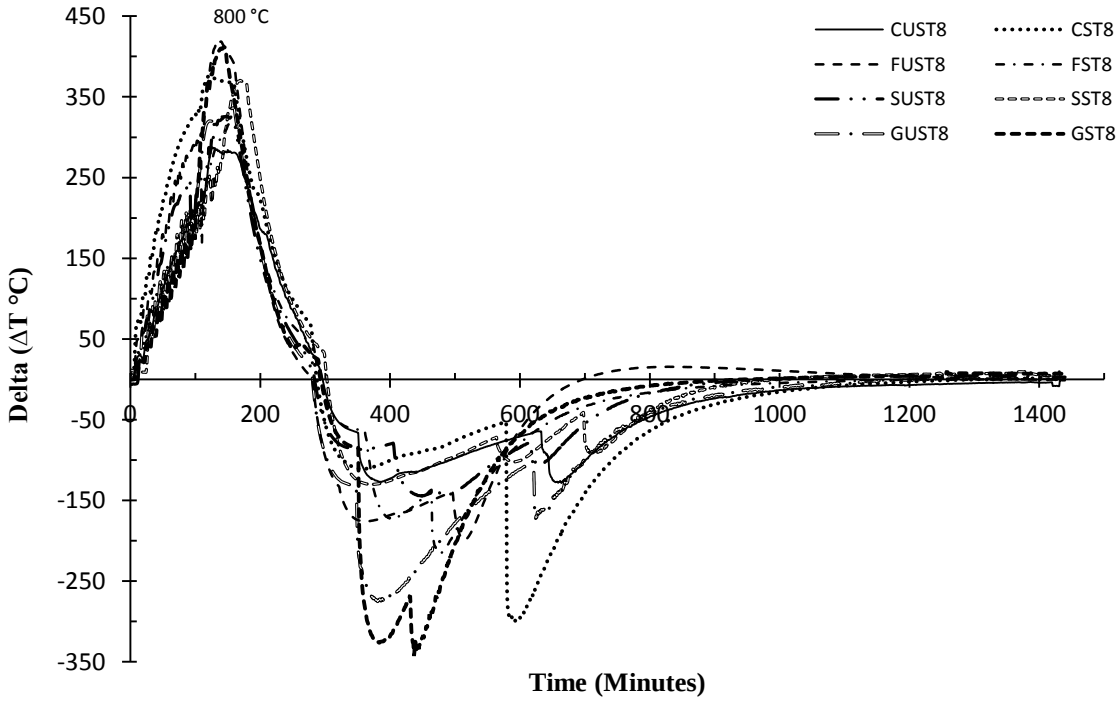

(d) 800 °C

Fig. 4.10 (a)-(d) Temperature difference (Δ T °C) between surface and centre v/s time for some specimens

4.3.2 Spalling behaviour of reinforced HPC during heating

The occurrence of spalling of concrete during heating of various HPC specimens was tracked carefully. The time of spalling since the beginning of heating, temperatures and axial load level at the time of spalling were recorded. While the Table 4.7 reports the specimens experienced explosive thermal spalling, the relevant information of these spalled specimens is provided in Table 4.8. Generally, the severity of spalling of concrete is evaluated on the basis of weight loss of specimen during spalling. The criterion used to assess the degree of concrete spalling is the ratio of weight of concrete lost due to spalling to weight of the specimen before heating. Following this criterion, the degree of spalling was evaluated and the data is shown in Table 4.8. In the spalled specimens, the spalling was observed only in terms of cover spalling either partially or fully up to the reinforcement. Figure 4.11 (a) - (j) shows some instances of explosive thermal spalling in the test specimens. It can be observed that the explosive spalling of the test specimens occurred by separation of the cover concrete from the reinforced core. It was noted that the specimens without any preload showed minor spalling but the preloaded specimens showed higher degree of spalling with complete crushing and separation of cover. It may be mentioned here that though the number of specimens spalled were maximum in silica fume HPC, the degree of spalling was slightly higher in fly ash HPC specimens.

Up to 400 °C, no spalling of concrete was observed except that one pre-loaded cylindrical specimen, SST4 spalled (Figure 4.12). The analysis of the furnace data (Table 4.9) shows that this event of spalling was explosive in nature and occurred at approximately 117 minutes after the start of the test. The test results showed that the temperature history at the surface and centre of the specimen was 249.5 °C and 357 °C and the load on the column was 462.5 kN at the time of spalling. The exposure at 600 °C and 800 °C temperatures caused spalling in most of the HPC specimens. It can be noted from Table 4.8 that all the preloaded specimens of pozzolanic HPCs spalled explosively during heating to 600 °C and 800 °C. The results presented earlier in Table 4.9 indicate that while the spalling of cover concrete occurred between 91 to 103 minutes in specimens heated to 600 °C specimens, the same happened at 89 to 129 minutes in specimens exposed to 800 °C. The results also showed that at 800 °C, the silica fume HPC specimens had taken shorter time duration to spall compared to other concretes. While all the specimens of preloaded pozzolanic HPC specimens spalled when heated to

600 ℃ and 800 ℃, only few such specimens of corresponding series of without preload spalled. The symbol (*) suffixed after name of test sample indicates that test specimen observed spalling during heating.

Table 4.7 Spalling trends of confined high performance concrete test specimens

Mixes	Test method	Room Temp.	200 ˚C	400 ˚C	600 ˚C	800 ˚C
Control HPC	Without preloaded	CUST0-1	CUST2-1	CUST4-1	**CUST6-1***	CUST8-1
		CUST0-2	CUST2-2	CUST4-2	CUST6-2	CUST8-2
		CUST0-3	CUST2-3	CUST4-3	**CUST6-3***	CUST8-3
	preloaded		CST2-1	CST4-1	**CST6-1***	**CST8-1***
			CST2-2	CST4-2	CST6-2	**CST8-2***
			CST2-3	CST4-3	**CST6-3***	CST8-3
Fly ash HPC	Without preloaded	FUST0-1	FUST2-1	FUST4-1	**FUST6-1***	FUST8-1
		FUST0-2	FUST2-2	FUST4-2	**FUST6-2***	**FUST8-2***
		FUST0-3	FUST2-3	FUST4-3	FUST6-3	**FUST8-3***
	preloaded		FST2-1	FST4-1	**FST6-1***	**FST8-1***
			FST2-2	FST4-2	**FST6-2***	**FST8-2***
			FST2-3	FST4-3	**FST6-3***	**FST8-3***
Silica Fume HPC	Without preloaded	SUST0-1	SUST2-1	SUST4-1	**SUST6-1***	**SUST8-1***
		SUST0-2	SUST2-2	SUST4-2	SUST6-2	**SUST8-2***
		SUST0-3	SUST2-3	SUST4-3	SUST6-3	**SUST8-3***
	preloaded		SST2-1	**SST4-1***	**SST6-1***	**SST8-1***
			SST2-2	SST4-2	**SST6-2***	**SST8-2***
			SST2-3	SST4-3	**SST6-3***	**SST8-3***
GGBFS HPC	Without preloaded	GUST0-1	GUST2-1	GUST4-1	GUST6-1	GUST8-1
		GUST0-2	GUST2-2	GUST4-2	GUST6-2	**GUST8-2***
		GUST0-3	GUST2-3	GUST4-3	GUST6-3	**GUST8-3***
	preloaded		GST2-1	GST4-1	**GST6-1***	**GST8-1***
			GST2-2	GST4-2	**GST6-2***	**GST8-2***
			GST2-3	GST4-3	**GST6-3***	**GST8-3***

*****Indicates the specimen observed expolsive spalling during heating

The previous literature shows that the unconfined high strength concrete spalls explosively (Kodur et al. 2006 and Kodur et al. 2008) and the confinement of concrete prevents spalling of concrete (Kodur et al. 2007). However, the results of the present study show that confining reinforcement could save only the core concrete. The cover concrete of confined concrete specimens still spalled irrespective of confinement. The cover spalling would reduce the carrying capacity of concrete columns as the contribution of cover shall no more be available.

Table 4.8 Characterization of spalling of HPC test specimens

Mixes	Test method	Specimens	Time at spalling (minutes)	Temperature (°C)		Pre load (kN) ($0.25*f_{room\ temp.}$)				Degree of spalling (%)
				surface	centre	at beginning	at spalling	Max (+)	Min (-)	
Control HPC	Unstressed	CUST6-1*	98	481.8	241.7	---	---	---	---	28.40
		CUST6-3*	85	401.4	183.5	---	---	---	---	6.09
	Stressed	CST6-1*	109	503.4	215.7	402.35	434.40	434.4	309.5	26.67
		CST6-3*	107	511.2	206.7	401.85	436.90	466.7	287.6	19.06
		CST8-1*	118	499.1	213.5	403.80	442.80	452.9	65.8	25.11
		CST8-2*	103	502.3	211.3	402.69	438.50	470.6	177.6	15.89
Fly ash HPC	Unstressed	FUST6-1*	100	463.5	227.5	---	---	---	---	8.84
		FUST6-2*	102	469.8	205	---	---	---	---	9.38
		FUST8-2*	101	486.9	201.6	---	---	---	---	13.78
		FUST8-3*	98	470.6	197.9	---	---	---	---	14.20
	Stressed	FST6-1*	109	467.7	199.5	448.6	486.20	498.8	304.5	21.81
		FST6-2*	98	455.9	204.8	449.8	485.30	514.0	330.9	22.98
		FST6-3*	110	491	193.9`	449.2	484.00	518.8	327.5	11.51
		FST8-1*	89	486.0	191.8	449.2	476.00	482.5	86.7	31.62
		FST8-2*	109	494.5	219.3	451.2	476.90	478.8	144.4	30.66
		FST8-3*	107	495.1	219.0	449.5	478.00	496.0	86.7	16.28
Silica fume HPC	Unstressed	SUST6-1*	93	399.4	162.6	---	---	---	---	17.11
		SUST6-2*	94	421.4	159.6	---	---	---	---	14.01
		SUST8-1*	92	458.4	175.5	---	---	---	---	11.26
		SUST8-2*	90	454.5	169.4	---	---	---	---	6.17
		SUST8-3*	82	410.3	172.7	---	---	---	---	10.80
	Stressed	SST4-1*	117	357	249.5	433.6	462.50	464.2	371.4	23.17
		SST6-1*	90	448.2	204.9	433.5	458.530	473.7	374.9	18.01
		SST6-2*	93	453.8	208.5	431.5	464.30	488.6	309.9	22.03
		SST6-3*	97	447.3	202.3	433.9	453.30	498.0	343.5	20.56
		SST8-1*	119	488.1	222.8	434.0	453.40	486.5	120.0	22.90
		SST8-2*	129	484.9	233.2	433.6	466.00	491.5	149.3	23.90
		SST8-3*	122	486.3	229.3	434.3	460.80	491.2	158.9	20.48
GGBFS HPC	Unstressed	GUST8-2*	100	461.0	215.6	---	---	---	---	6.22
		GUST8-3*	98	455.7	224.8	---	---	---	---	20.44
	Stressed	GST6-1*	103	405.5	177	422.05	453.00	496.3	302.0	8.37
		GST6-2*	91	408.2	174.2	421.1	449.40	494.1	310.2	38.81
		GST6-3*	91	414.9	175.7	419.0	445.40	480.3	313.3	24.57
		GST8-1*	93	496.5	218.3	420.3	452.60	471.4	93.35	24.49
		GST8-2*	100	485.3	232	419.2	438.60	485.1	173.5	25.50
		GST8-3*	107	479.2	215.7	421.6	456.70	488.5	179.7	14.60

The specimens heated with a pre-load showed variation in the load during heating. The variation of the axial load during heating was measured in all the stressed tests and

(a) FST6 series

(b) FST8 series

(c) FUST6 series

Fig. 4.11 (a)-(j) Explosive spalling of HPC specimens (Contd.)

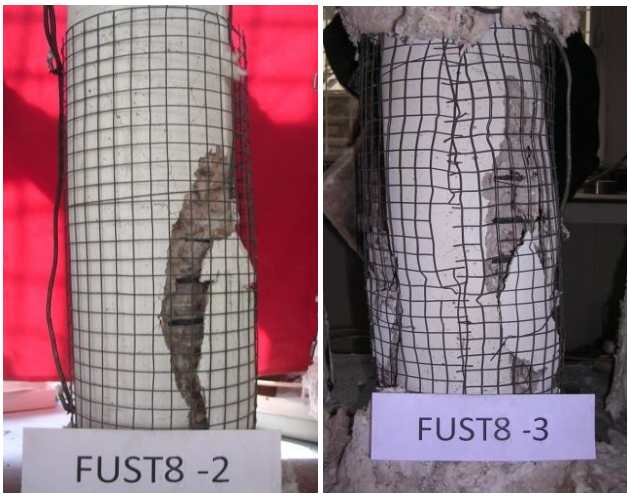

(d) FUST8 series

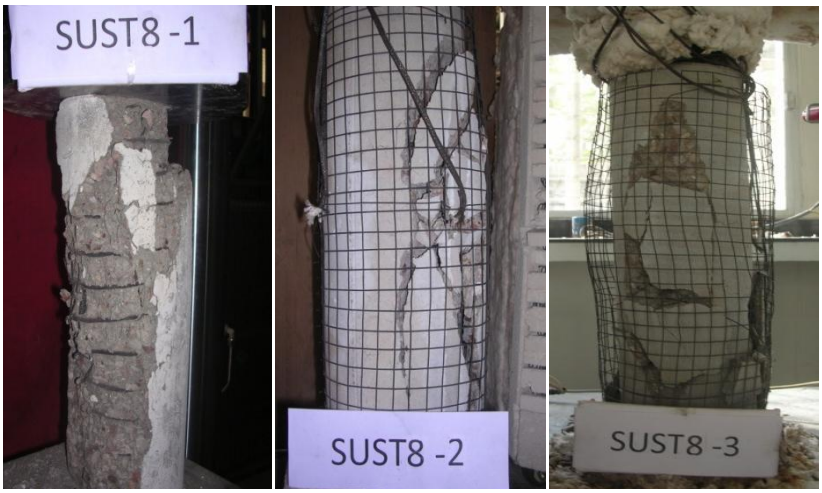

(e) SUST8 series

(e) SST8 series

Fig. 4.11 (a)-(j) Expolsive spalling of HPC specimens (Contd.)

(g) SST6 series

(h) GST6 series

(i) GST8 series

Fig. 4.11 (a)-(j) Expolsive spalling of HPC specimens (Contd.)

(j) Some specimens of control HPC

Fig. 4.11 (a)-(j) Expolsive spalling of HPC specimens

Fig. 4.12 Spalling in the specimen (SST4-1) exposed to 400 °C

The maximum loads (restraining forces) noticed during heating for the various specimens are given in Table 4.9. Fire endurance time was also noted and all values are given in the Table 4.9. Fire endurance was defined as the time between the beginning of heating till the end of test or the moment when the stressed specimen became unstable. The Figure 4.13 (a)-(d) shows the variation of restraining axial force with time in various specimens due to the application of heat. The variation in axial load may be attributed to creep and thermal expansion of the steel and concrete mix constituents. It can be observed that the heat generated axial restraint curves were characterized by two different phases of expansion and contraction.

Table 4.9 Details of axial restraining force development and fire endurance

Maximum restraining force (RF) (kN)							
Sample	**RF**	**Sample**	**RF**	**Sample**	**RF**	**Sample**	**RF**
CST2	15.162	**FST2**	14.951	**SST2**	23.131	**GST2**	16.647
CST4	54.649	**FST4**	50.756	**SST4**	52.106	**GST4**	42.89
CST6	73.992	**FST6**	69.530	**SST6**	57.152	**GST6**	73.049
CST8	49.091	**FST8**	46.527	**SST8**	57.887	**GST8**	75.91
Fire endurance (FE) (minutes)							
Sample	**FE**	**Sample**	**FE**	**Sample**	**FE**	**Sample**	**FE**
CST2	552	**FST2**	579	**SST2**	399	**GST2**	501
CST4	613	**FST4**	529	**SST4**	451	**GST4**	523
CST6	437	**FST6**	372	**SST6**	419	**GST6**	458
CST8	234	**FST8**	250	**SST8**	230	**GST8**	290

During heating the test specimen experienced thermal expansion due to expansion of material at the earlier stages. This caused increase in the load beyond the initially applied preload. At the later stages of heating and then cooling specimens showed decrease in load due to contraction. At 200 °C, the development of axial force was less compared to other temperatures, though the highest relative axial restraint force of about 23.13 kN was noticed in the silica fume HPC specimens. The fly ash HPC specimens showed lower restraint force due to lesser stiffness as well as more softening of concrete. At this temperature the silica fume concrete showed highest fire endurance duration of about 579 minutes. The lowest duration of 399 minutes was observed in fly ash HPC. All types of concretes, except GGBFS HPC, showed reasonable axial restraining force at 400°C. On further rising of temperature to 600 °C, the plain and GGBFS concretes showed maximum restraining forces of about 73.992 kN and 73.049 kN respectively. This indicates that the test specimens developed large amount of restraint forces as the temperatures increased. It is important to mention that most of the pre-loaded test specimens experienced explosive cover spalling in this range of temperature. The results showed that the silica fume HPC showed lesser restraint forces compared to other types of HPC mixes at this temperatures. The GGBFS HPC had the highest endurance of about 458 minutes; on the other hand the fly ash HPC columns indicated lowest heat endurance capacity of about 372 minutes in this temperature range.

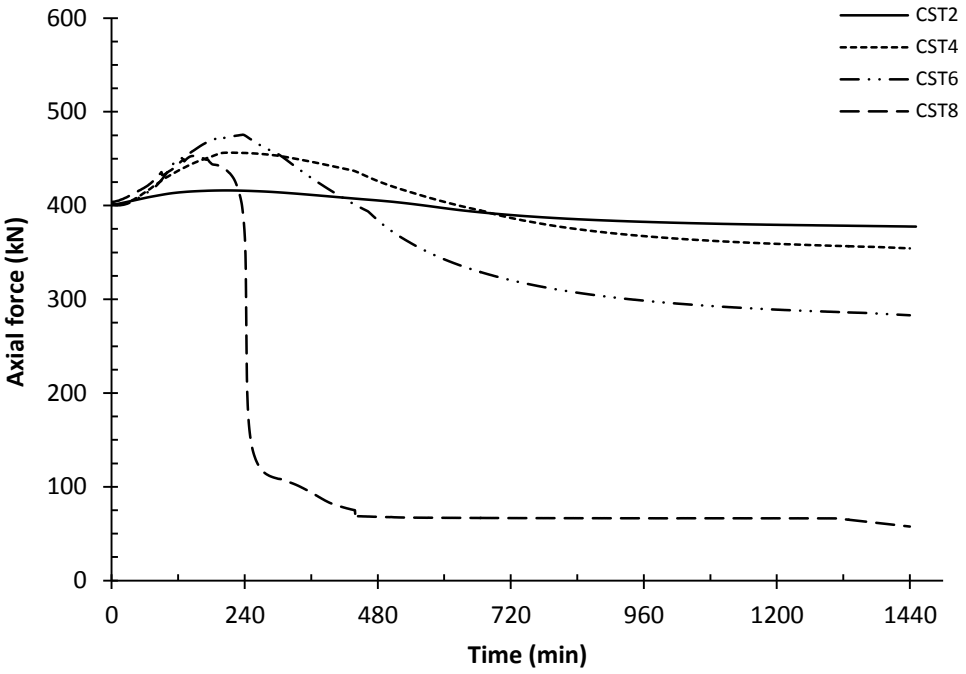

(a) Control concrete

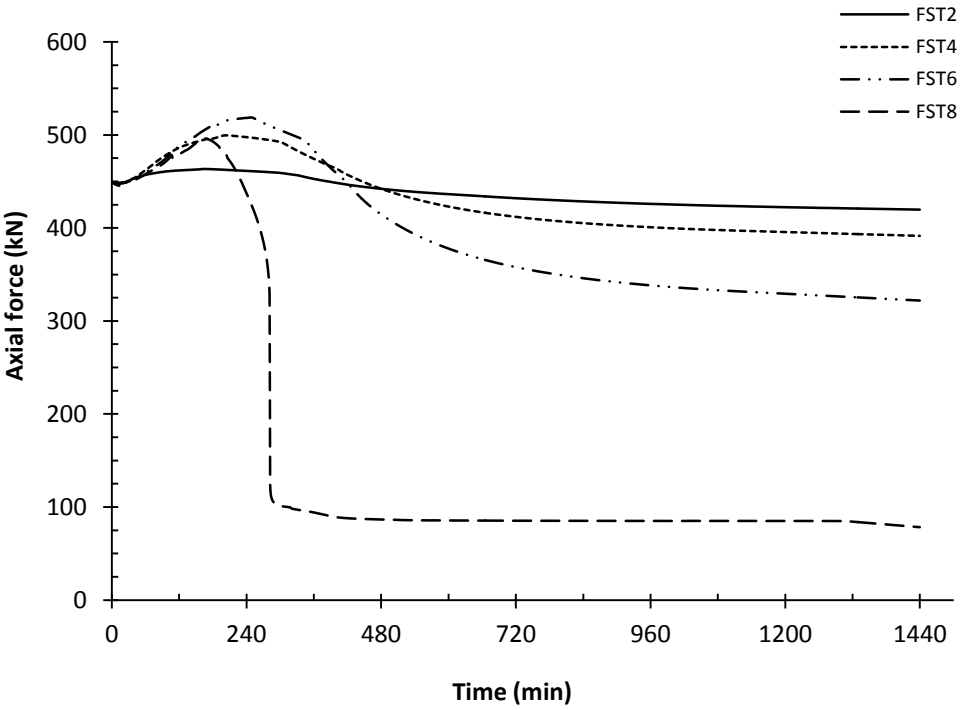

(b) Fly ash HPC

Fig. 4.13 (a)-(d) Variation of preload in stressed specimens during heating (contd.)

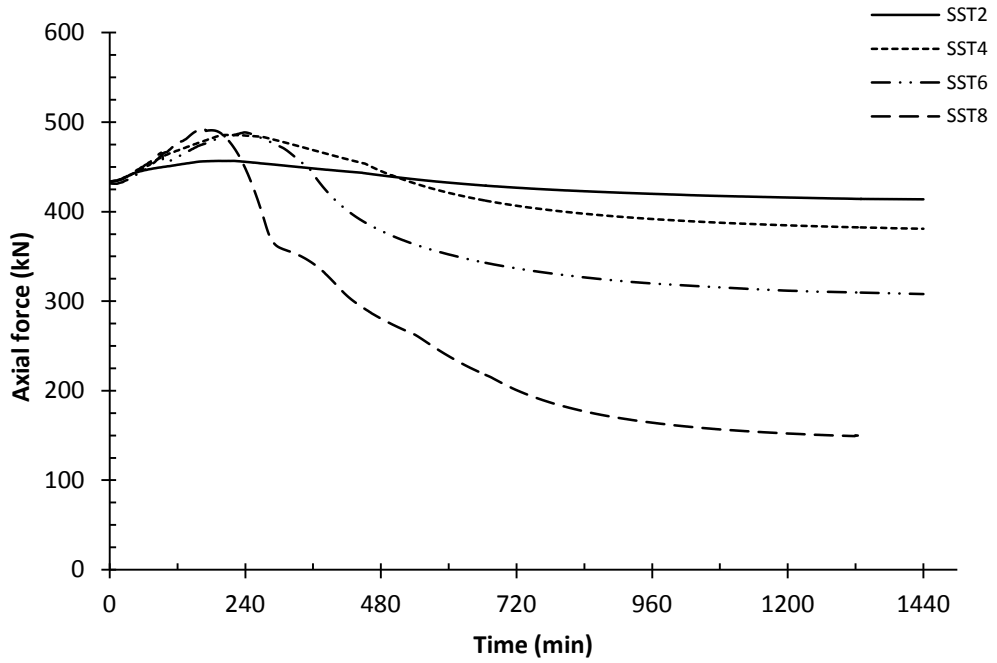

(c) Silica fume HPC

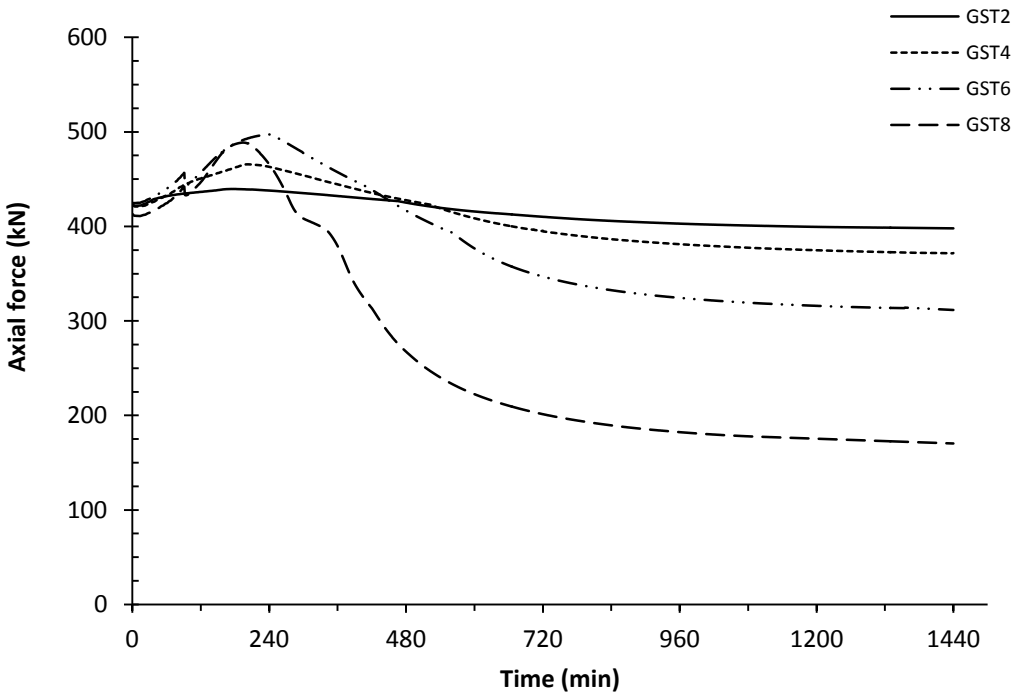

(d) GGBFS HPC

Fig. 4.13 (a)-(d) Variation of preload in stressed specimens during heating

At 800 °C temperature, all HPC specimens showed severe deterioration in load carrying capacity as well as the fire endurance capacity. This may be attributed to the spalling of cover concrete in such preloaded specimens with spalled specimens raising the temperature penetration into the core in the absence of the cover of the concrete and the exposed steel bars conducting the heat directly. Hence, the direct conduction of heat on steel bars and concrete might have deteriorated the material properties of steel and concrete. The increase of temperature as well as progressive increase in the restrain force resulted into continuous decline of the load carrying capacity of these specimens. This behaviour is also due to reduction of section size after severe spalling of cover concrete. The creep strains in concrete as well as in steel due to high temperature will also enhance the contraction before failure of specimens due to high temperatures.

4.4 RESIDUAL LOAD-DISPLACEMENT BEHAVIOUR

The various specimens were submitted to mechanical testing under axial compression to study the residual stress-strain relationships after a complete cycle of heating and cooling. The entire residual mechanical testing program was executed at ambient temperature conditions. The load values of the specimens were directly obtained from the UTM machine. The strain values were obtained from the measured deformation through LVDT's and the adopted gauge length. The results of compressive load-deformation tests are shown in Table 4.10 for all the specimens. The load versus axial strain curves for the test specimens are shown in Figure 4.14 (a)-(d). The curves of specimens exposed to different temperatures are shown by shifting the strain abscissa in order to demonstrate the effects temperature more clearly. Initially all the HPC specimens behaved in the similar manner and exhibited a linear load deformation behavior in the ascending part of the load-displacement curve. The linear ascending portion was longer in the specimens exposed to lower temperature ranges of up to 400 °C than the specimens subjected to higher elevated temperatures. The peak and post-peak behaviour of the reinforced HPC specimens depended upon the type of HPC (such as non-pozzolanic, silica fume, fly ash and GGBFS based mix), the heating test methods (stressed residual and unstressed residual) and temperature of exposure. The residual compressive behaviour of specimens was generally characterized sequentially by the development of surface cracks, cover failure (where cover did not spall during heating), buckling of the longitudinal bars and crushing of the core concrete. The failure of confined HPC specimens under monotonic axial compression was found to be of shear type for the test

Table 4.10 Results of residual compression tests

Type of concrete	Test condition	Name of specimen	Temp. exposure (°C)	P_{max} (kN)	P_{max}/P_o	$\acute{\varepsilon}$	$\acute{\varepsilon}/\acute{\varepsilon}_{(room\ temp.)}$	ε_{c85c}	$\varepsilon_{c85c}/\acute{\varepsilon}_{(room\ temp.)}$	ε_{c50c}	$\varepsilon_{c50c}/\acute{\varepsilon}_{(room\ temp.)}$	A_{cuc}	$A_{cuc}/A_{cuc((room\ temp.)}$
Control HPC	Unstressed	CUST0	Room temp.	1602.98	1.27	0.00247	1.000	0.00983	3.975	0.01641	6.633	19.53	1.000
		CUST2	200	1537.16	1.22	0.00264	1.066	0.00827	3.344	0.01301	5.259	20.55	1.052
		CUST4	400	1804.32	1.43	0.00346	1.397	0.00684	2.766	0.01713	6.927	13.65	0.699
		CUST6	600	1470.67	1.17	0.00457	1.849	0.01135	4.587	0.02006	8.109	21.38	1.095
		CUST6*	600	1031.99	0.82	0.01351	5.464	0.01495	6.042	0.02329	9.415	15.789	0.809
		CUST8	800	965.20	0.77	0.01382	5.587	0.02213	8.946	0.03368	13.615	20.70	1.060
	Stressed	CST2	200	1443.92	1.15	0.00231	0.936	0.00766	3.098	0.01255	5.074	13.16	0.674
		CST4	400	1854.52	1.47	0.00352	1.421	0.01278	5.167	0.01857	7.506	27.20	1.393
		CST6	600	1524.48	1.21	0.00347	1.403	0.00608	2.459	0.01906	7.705	18.83	0.964
		CST6*	600	1241.06	0.99	0.00741	2.997	0.00808	3.266	0.01019	4.118	7.919	0.406
		CST8	800	877.26	0.70	0.01126	4.550	0.01946	7.865	0.02744	11.093	16.33	0.836
		CST8*	800	761.656	0.60	0.01018	4.115	0.01239	5.008	0.01708	6.906	7.877	0.403
Fly ash HPC	Unstressed	FUST0	Room temp.	1792.65	1.44	0.00267	1.000	0.00476	1.783	0.01179	4.419	13.34	1.000
		FUST2	200	1646.52	1.32	0.00270	1.011	0.00567	2.126	0.01475	5.527	17.47	1.310
		FUST4	400	1691.34	1.36	0.00372	1.395	0.01127	4.223	0.01612	6.039	20.65	1.548
		FUST6	600	1240.86	1.00	0.00811	3.041	0.01125	4.218	0.01890	7.084	15.878	1.190
		FUST6*	600*	1076.95	0.87	0.00959	3.593	0.01056	3.959	0.01116	4.182	21.44	1.607
		FUST8	800	760.79	0.61	0.01707	6.397	0.01903	7.133	0.02158	8.085	7.19	0.539
		FUST8*	800*	587.741	0.47	0.01653	6.193	0.02544	9.532	-	-	7.044	0.528
	stressed	FST2	200	1581.54	1.27	0.00293	1.099	0.00440	1.649	0.01293	4.846	13.94	1.045
		FST4	400	1534.74	1.23	0.00352	1.321	0.01129	4.230	0.01627	6.095	20.76	1.556
		FST6*	600*	1397.00	1.12	0.00810	3.035	0.00893	3.348	0.01075	4.029	9.50	0.712
		FST8*	800*	438.17	0.35	0.00352	5.858	0.00892	3.342	0.02462	9.226	8.65	0.649

* indicates the test sample spalled during heating

Type of concrete	Test condition	Name of specimen	Temp. Exposure (°C)	P_{max} (kN)	P_{max}/P_o	$\acute{\varepsilon}$	$\acute{\varepsilon}/\acute{\varepsilon}_{(roomtemp.)}$	ε_{c85c}	$\varepsilon_{c85c}/\acute{\varepsilon}_{(room\ temp.)}$	ε_{c50c}	$\varepsilon_{c50c}/\acute{\varepsilon}_{(roomtemp.)}$	A_{cuc}	$A_{cuc}/A_{cuc(roomtemp.)}$
GGBFS HPC	Unstressed	GUST0	Room temp.	1680.21	1.26	0.00299	1.000	0.00457	1.525	0.01419	4.741	16.89	1.000
		GUST2	200	1685.68	1.27	0.00271	0.905	0.00382	1.277	0.01575	5.262	16.69	0.988
		GUST4	400	1876.38	1.41	0.00345	1.154	0.00736	2.458	0.01384	4.623	17.22	1.020
		GUST6	600	1579.40	1.19	0.00476	1.591	0.00865	2.890	0.01741	5.817	19.09	1.130
		GUST8	600	882.081	0.66	0.01412	4.718	0.01895	6.328	0.01609	5.376	13.96	0.827
		GUST8*	800	720.50	0.54	0.01443	4.821	0.01652	5.518	0.01900	6.348	8.14	0.482
	Stressed	GST2	200	1581.50	1.19	0.00236	0.787	0.00818	2.734	0.01504	5.024	16.89	1.000
		GST4	400	1845.90	1.39	0.00308	1.029	0.01039	3.471	0.01596	5.332	21.78	1.289
		GST6*	600	1374.75	1.03	0.00866	2.893	0.00910	3.039	0.00949	3.170	7.68	0.455
		GST8*	800	550.76	0.41	0.00809	2.369	0.01069	3.572	-	-	4.27	0.253
Silica fume HPC	Unstressed	SUST0	Room temp.	1720.41	1.23	0.00277	1.000	0.00449	1.619	0.01199	4.327	13.77	1.000
		SUST2	200	1754.32	1.25	0.00293	1.056	0.00391	1.411	0.01526	5.506	17.02	1.236
		SUST4	400	1824.43	1.30	0.00288	1.038	0.00747	2.696	0.01334	4.814	17.32	1.258
		SUST6	600	1382.34	0.99	0.01330	4.799	0.01737	6.267	0.02512	9.062	22.08	1.604
		SUST6*	600	872.81	0.62	0.01402	5.059	0.01492	5.382	0.01628	5.873	8.32	0.604
		SUST8*	800	587.13	0.42	0.01675	6.042	0.01986	7.165	0.02528	9.120	9.44	0.685
	Stressed	SST2	200	1813.92	1.29	0.00278	1.002	0.00424	1.530	0.01344	4.847	15.77	1.145
		SST4	400	1871.96	1.34	0.00268	0.969	0.00695	2.508	0.01576	5.686	17.93	1.302
		SST4*	400	1278.10	0.91	0.00782	2.823	0.00903	3.259	0.01133	4.086	10.36	0.752
		SST6*	600	1041.99	0.74	0.00883	3.187	0.01067	3.850	0.01295	4.672	8.71	0.632
		SST8*	800	653.08	0.47	0.00790	2.852	0.01142	4.119	0.01560	5.628	6.68	0.485

* indicates the test sample spalled during heating

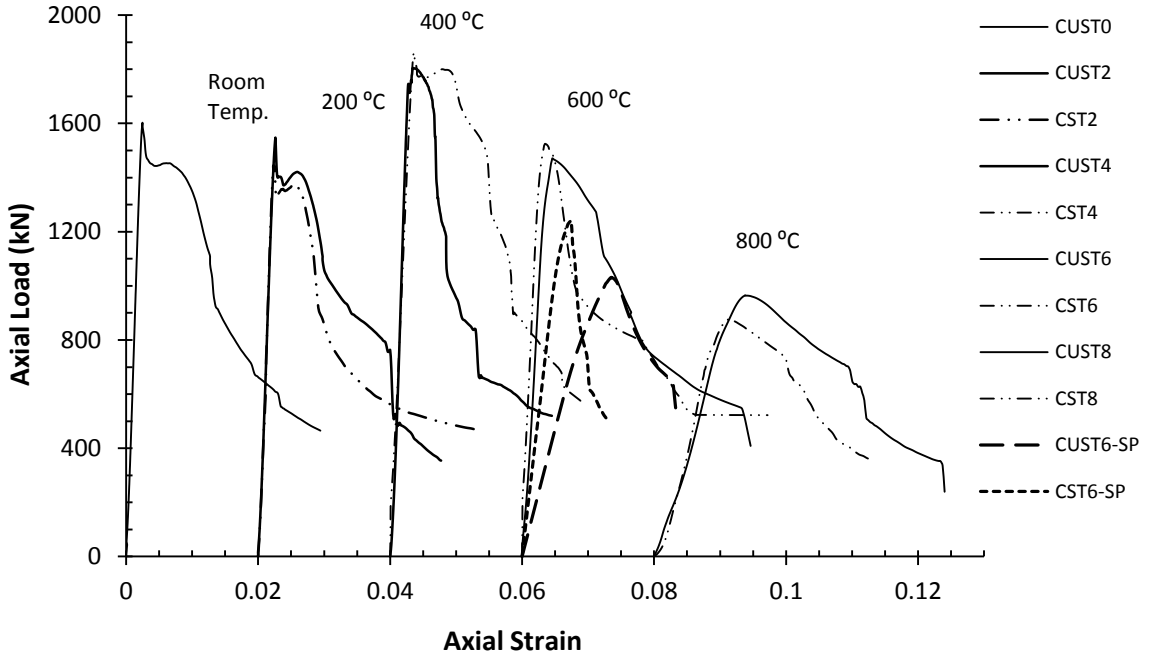

(a) Plain high performance concrete

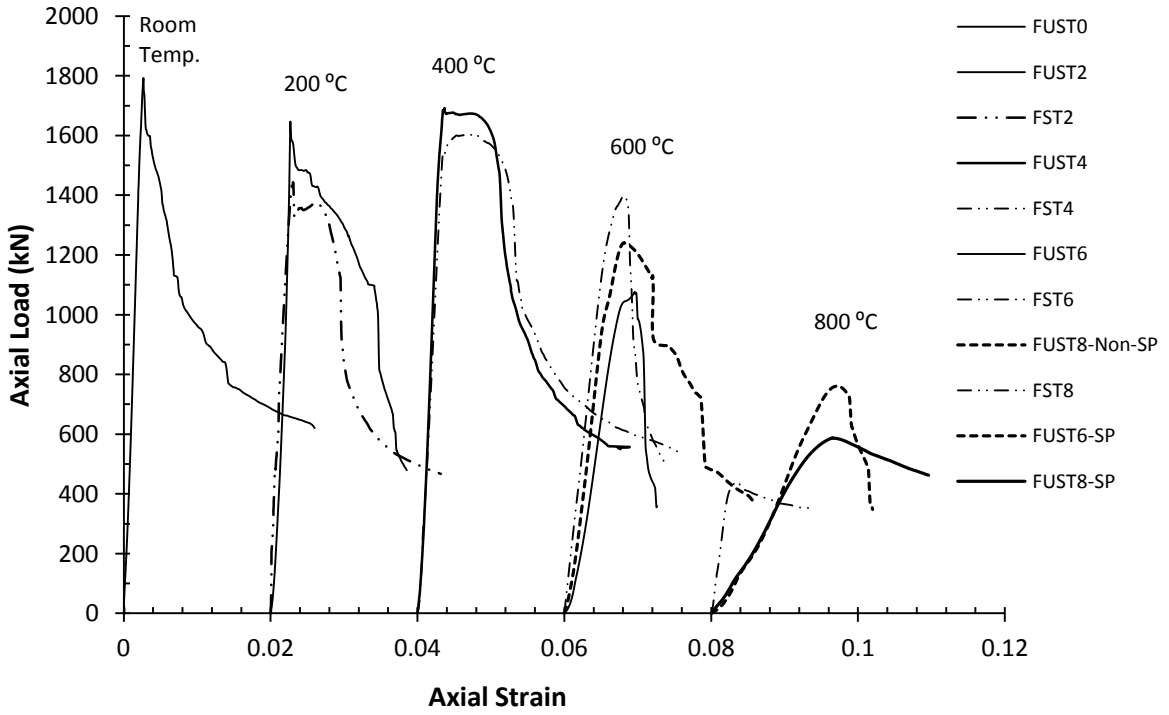

(b) Fly ash high performance concrete

Fig. 4.14 (a)-(d) Relative applied load verses axial strain curves for heated confined HPC columns (contd.)

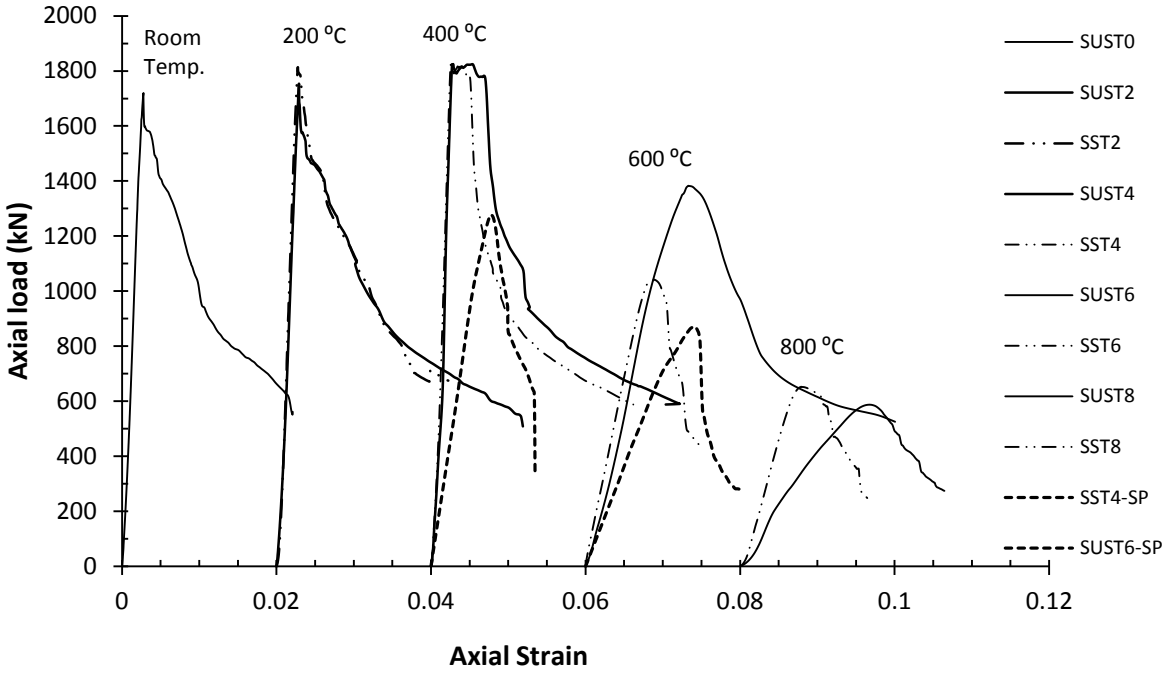

(c) Silicafume high performance concrete

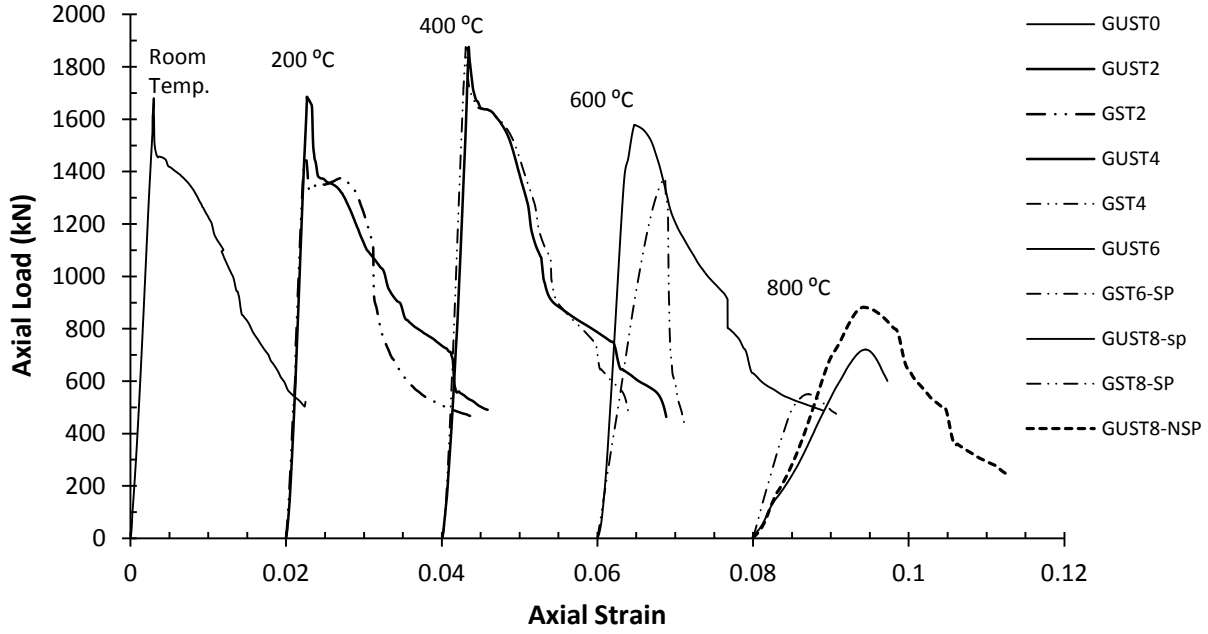

(d) GGBFS high performance concrete

Fig. 4.14 (a)-(d) Relative applied load verses axial strain curves for heated confined HPC columns

samples exposed to temperatures up to 400 °C. At higher temperatures, the axial load-displacement behavior of HPC specimens exhibited comparatively more ductile and soft behaviour irrespective of the nature of the earlier stated variables involved in the test program. At such high temperatures of 600 °C to 800 °C, the failure of the specimens was generally characterised by lateral dilation of concrete and softening.

4.4.1 Residual compressive strength

The effect of high temperatures on the residual compressive load capacity of plain and different pozzolanic high performance concretes are presented in the Table 4.10.The measured residual peak axial load (P_{max}) values obtained from the tests are given in the Table. Further, the peak load, P_{max}, was normalized with respect to theoretically calculated maximum load capacity, P_o, for each case and the resulting ratios are shown in the Table 4.10 (where $P_o = 0.85 f_c^{'}\left(A_g - A_{Ast}\right) + f_y A_{Ast}$). Figure 4.15 illustrates the variation of P_{max}/P_o with temperature. It can be observed that among all types of HPCs, the fly ash concrete has the highest peak compressive strength of 1792.65 kN at room temperature conditions. In the specimens heated at 200 °C temperature, all the GGBFS HPC and silica fume HPC specimens were found to maintain their respective original room temperature strength, while the fly ash HPC lost its residual room temperature compressive strength in the range of 8% for unstressed specimens and 12% for stressed specimens. The residual room temperature strength of plain HPC specimens got reduced by 4% for unstressed specimens and 10% for stressed specimens when heated to 200 °C temperature. All types of pozzolanic concretes (except fly ash concrete) and plain control concrete showed regain in residual strength after heating at 400 °C.

As a result there was no deterioration of residual compressive strength of most of the HPCs with respect to their respective room temperature strengths after exposure at 400 °C. The strength gain of about 6 -12% was noted compared to original compressive strength at room temperature in various pozzolanic and non-pozzolanic mix specimen except fly ash based HPC specimens. The fly ash HPC showed a strength loss of 6% for unstressed specimen's and14% strength loss for stressed test conditions in this temperature range. Some of the plain HPC specimens indicated a gain of 16% in their room temperature strength after heating to 400 °C. Thus the plain and pozzolanic high performance concretes, except fly ash concrete, behaved well at this temperature irrespective of the test methods. On heating of specimens further to 600 °C temperature, it

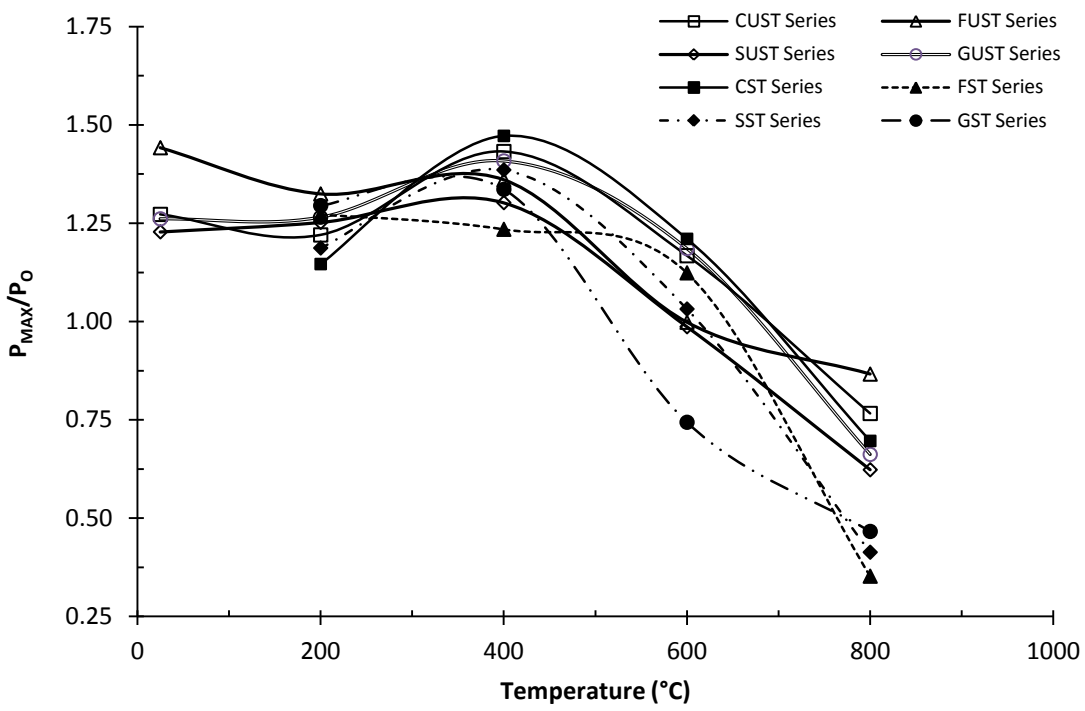

Fig. 4.15 Variation of load ratio (P_{max}/P_o) with temperatures

was observed that most of the specimens experienced thermal spalling of cover concrete and a resulting distinct drop in residual compressive strength. It may be recalled that most of the specimens of various HPC mixes spalled in this temperature range (Table 4.7). The non-spalled test specimens exhibited higher residual strength compared to spalled specimens. The pre-loaded specimens of GGBFS HPC had shown a strength loss of 18% compared to their room temperature strength. The unstressed, non-spalled test specimens of plain HPC and GGBFS HPC showed only a marginal strength deterioration of 6 to 8%. The fly ash HPC, however, indicated a 30% loss in unheated compressive strength after heating to 600 °C temperature. Among all the HPC specimens heated to 600 °C temperature, the spalled and unstressed specimens of plain HPC and fly ash HPC were found to have the highest loss in compressive strength of about 36 to 40% compared to their respective room temperature strengths.

After heating to temperatures of as high as 800 °C, the various HPC specimens showed severe deterioration in their residual strength. The preloaded specimens of all pozzolanic HPCs showed greatest reduction in residual compressive strength and a loss in the range of 62 to 76% in room temperature strength was noticed in these specimens. On the contrary the unstressed plain HPC and GGBFS based concrete specimens showed a

relatively lower strength reduction of about 40% and 48% of their respective unheated strength. The residual load ratio, P_{max}/P_o, ranges from 0.77 to 1.43 in case of unstressed test condition and from 0.60 to 1.47 in case of preloaded test specimens of plain HPC. Similarly fly ash HPC specimens had the load ratio values as 0.47 to 1.44 for unstressed specimens and 0.35 to 1.27 for stressed specimens. However, the GGBFS HPC specimens showed load ratio values of 0.54 to 1. 41 for unstressed and 0.41 to 1.39 for stressed test conditions. Similarly the load ratio values of 0.42 to 1.30 for unstressed specimens and 0.47 to1.34 for stressed test specimens were observed for silica fume HPC specimens. This shows that while the stressed specimens of plain and fly ash HPC mostly had lower residual strength compared to their respective unstressed specimens, the stressed specimens of GGBFS and silica based HPC mixes had more strength compared to their respective unstressed specimens in most of the cases. Despite this, the present results did not show a marked influence of pre-load during heating on the residual strength. At the same time the results definitely show that the thermal spalling was more in pre-loaded specimens compared to the specimens without any pre-load and thus if a comparison of residual strength is made between the unspalled specimen of unstressed condition with the corresponding spalled specimen of stressed test condition of any HPC mix then the presence of preload during heating caused reduction in the residual load carrying capacity.

4.4.2 Residual peak and post-peak strains

The residual strain $\acute{\varepsilon}$, corresponding to the peak load P_{max}, the residual post-peak strains $\varepsilon_{c\ 85c}$ (axial strain at which the load falls to 85% of the peak load) and ε_{c50c} (axial strain at which the load falls to 50% of the peak load) were determined from the recorded load- displacement curves of different series of specimens tested under this experimental study (Table 4.10). To characterize the residual deformability of HPC specimens, these strain values were normalized with respect to the corresponding unheated peak stain values, $\varepsilon'_{Room\ temp.,}$ measured at room temperature. The Figures 4.16, 4.17 and 4.18 show the variation of peak strains, $\acute{\varepsilon}$, ε_{c50c}, *and* ε_{c85c} with temperature. It can be noticed that the strain corresponding to the peak load, $\acute{\varepsilon}$ and the strain ratio $\acute{\varepsilon}/\ \acute{\varepsilon}_{room\ temp}$ remained largely unchanged up to 400 °C temperature for all types of HPC specimens irrespective the test methods. Further increase of temperature from 400 °C to 600 °C, the peak strain increased appreciably in all the HPC specimens and a maximum strain was recorded in unstressed specimens of silica fume HPC. At further high temperatures of 800 °C, the strain, $\acute{\varepsilon}$ and

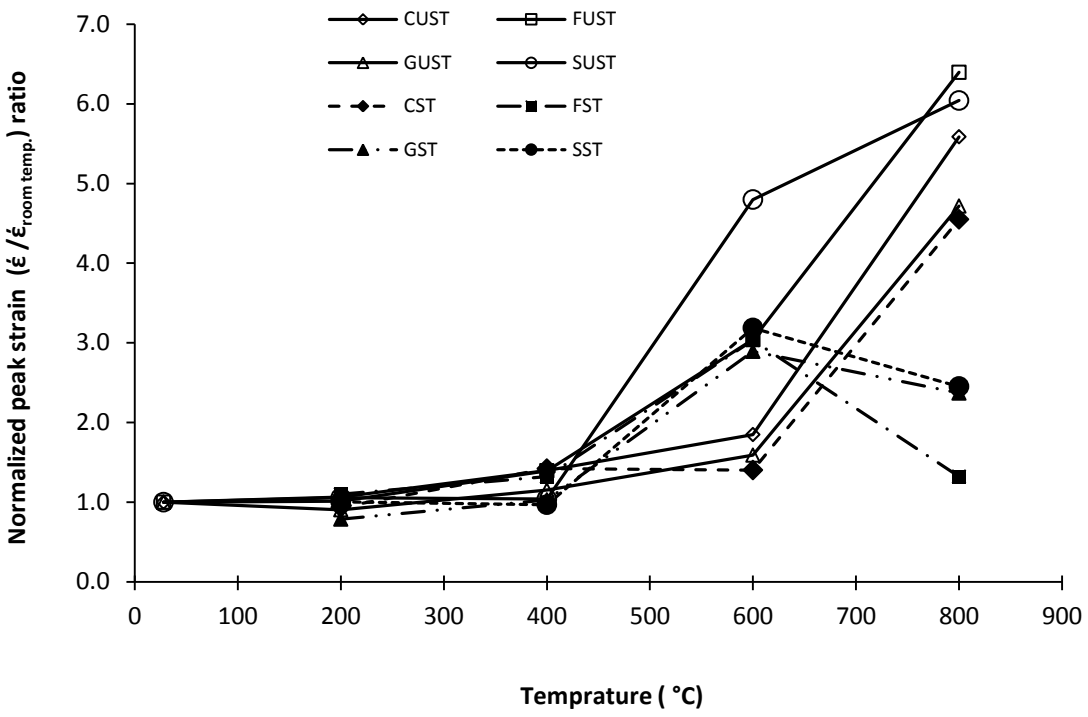

Fig. 4.16 Effect of temperature on peak strain ratio ($\acute{\varepsilon}/\acute{\varepsilon}_{(room\ temp.)}$)

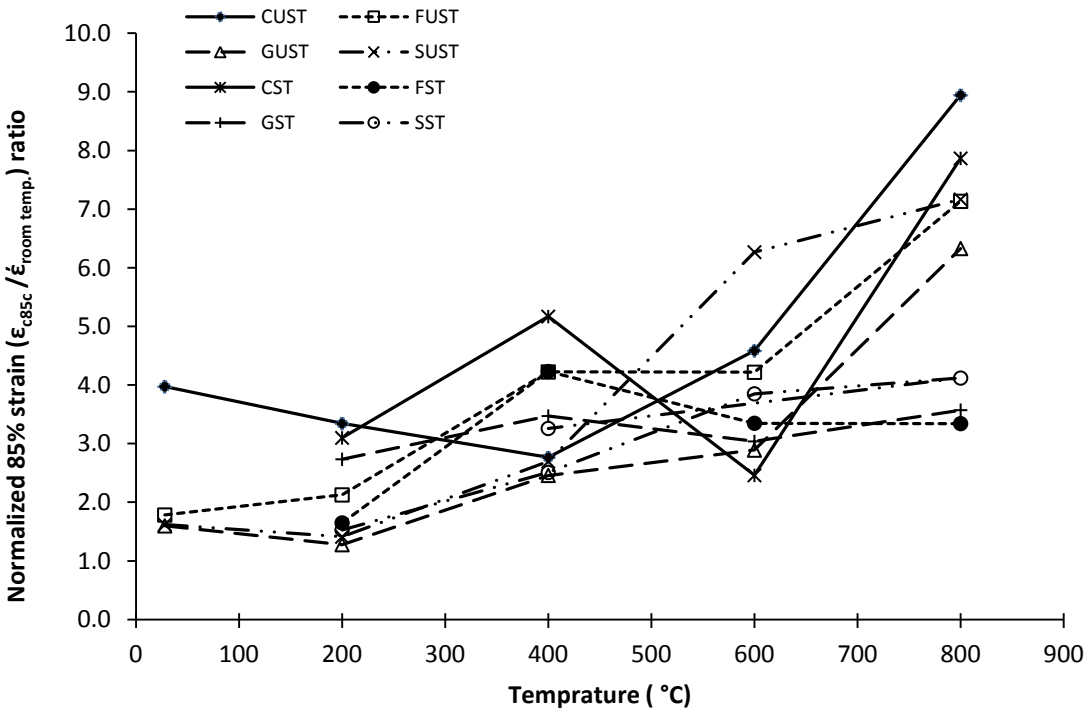

Fig. 4.17 Effect of temperature on post-peak strain ratio ($\acute{\varepsilon}_{c85c}/\acute{\varepsilon}_{(room\ temp.)}$)

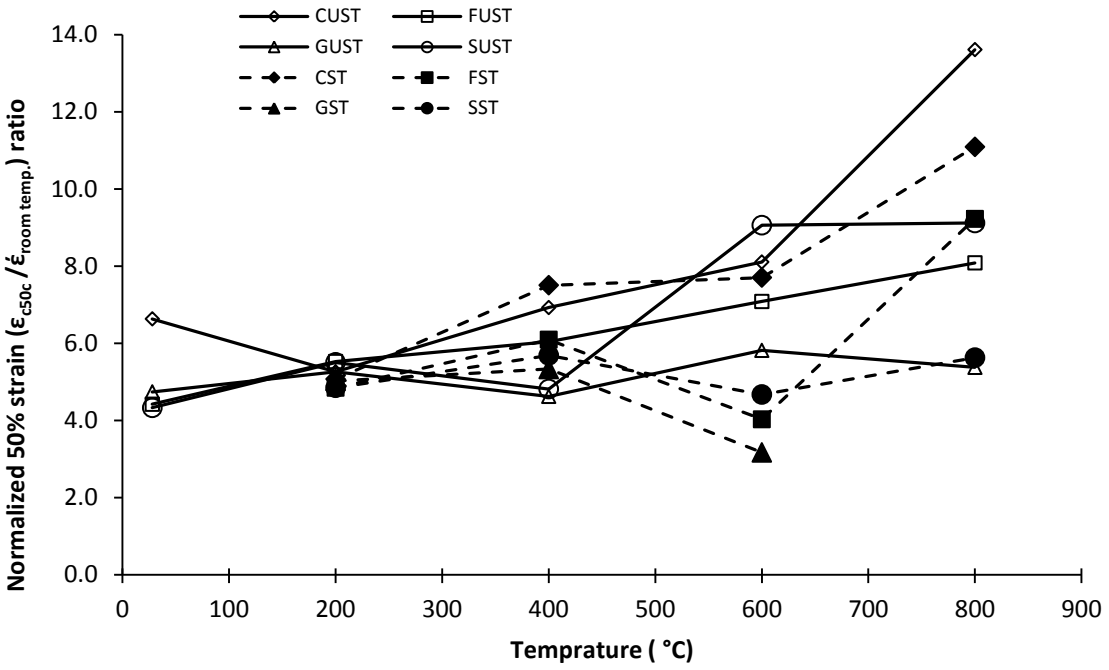

Fig. 4.18 Effect of temperature on post-peak strain ratio ($\acute{\varepsilon}_{c50c}/\acute{\varepsilon}_{(room\ temp.)}$)

the strain ratio, $\acute{\varepsilon}/\acute{\varepsilon}_{room\ temp}$ increased considerably for the unstressed specimens of pozzolanic HPC mixes and both unstressed and stressed specimens of non-pozzolanic HPC mix. On the contrary the strain $\acute{\varepsilon}$ decreased when the temperature was increased from 600 °C to 800 °C for the stressed specimens of pozzolanic HPC mixes. It may be mentioned here that most of the stressed specimens of pozzolanic HPC mixes experienced spalling during heating to 800 °C which resulted into a poor load deformation behavior during residual compression tests. Thus the test results indicated that the unstressed test specimens show higher peak strain values compared to preloaded test specimens at such high temperatures. In order to ascertain the influence of test variables on the residual deformability of heated reinforced HPC, the post peak strains ε_{c85c} and ε_{c50c} and the corresponding strain ratios $\varepsilon_{c85c}/\acute{\varepsilon}_{Room\ temp.}$, $\varepsilon_{c50c}/\acute{\varepsilon}_{Room\ temp}$ were computed. The results show that the strain ratios $\varepsilon_{c85c}/\acute{\varepsilon}_{Room\ temp.}$, $\varepsilon_{c50c}/\acute{\varepsilon}_{Room\ temp}$ increased from 1.277 to 9.532 and from 3.170 to13.615 respectively when the temperature of exposure was increased from room temperature to 800 °C. This shows that the HPC softens as the temperature increases. The results show that plain non-pozzolanic HPC specimens had more post-peak strains and deformability compared to the pozzolanic HPC mixes. This is because many of the pozzolanic HPC specimens suffered thermal spalling which resulted into a deteriorated residual load-deformation behavior and reduced strain capacities. Among the pozzolanic

HPC specimens, the fly ash based HPC specimens had generally more strains than the other two pozzolanic HPC specimens. The stressed specimens of each of the HPC mix showed lower post peak strains than their respective unstressed specimens. This again may be attributed on one hand to the reduced cracking during heating due to the presence of pre-load and on the other had due to the thermal spalling of stressed specimens, which caused reduction in their strain capacities.

4.4.3 Residual compressive toughness

The energy absorption capacity of concrete material in compression is known as its compressive toughness. It is usually described as the area under the load-displacement curve. A convenient way to quantify the ductility of concrete is to use toughness, which is measured as toughness index or toughness ratio (Ezeldin and Balaguru 1992, Barr et al.1996, Bhargava et al. 2006). In this study, the residual compressive toughness was measured as toughness index (T_i), which is the ratio of toughness of heated reinforced high performance concrete to unheated reinforced high performance concrete. The areas, $A_{cuc,}$ and $A_{cuc(room\ temp.)}$ under the load-deformation curves of heated and unheated high performance concrete specimens of each mix were computed and the corresponding toughness indices were found. The values of toughness index are presented in Table 4.10 and the Figure 4.19 shows the variation of T_i with different target temperatures.

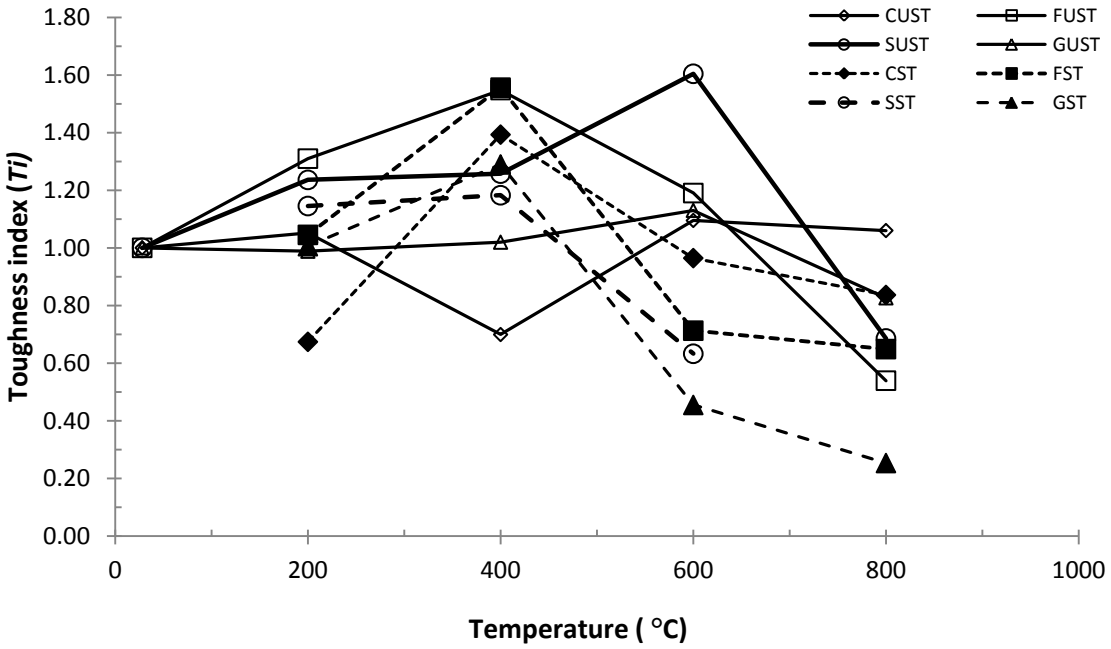

Fig. 4.19 Variation of toughness index with temperatures

The toughness ratio $A_{cuc}/A_{cuc(room\ temp.)}$, gives an idea about the deformation capability of heated high performance concrete. The results show that the toughness index T_i first increased in most of the specimens when the temperature increased to 400 °C, and thereafter lower toughness ratios were noticed for the specimens exposed to higher temperatures beyond 400 °C. The results show that though the strain ductility ratios increased with the increase in temperature, the area under the curve reduced as the temperature of exposure increased.

4.5 CONCLUDING REMARKS

This experimental study reports the results of residual load displacement response of heated reinforced high performance concrete short columns. A total of 108 specimens were tested under this test program. The test variables included type of HPC mix based on the type of pozzolanic admixture (silica fume, fly ash and GGBFS), presence of pre-load during heating and the temperature of exposure. The research program has contributed to the fundamental understanding of the residual compressive behaviour of reinforced HPC exposed to a complete cycle of heating and cooling. The heating and cooling profiles of various HPC specimens were carefully tracked and the resulting observations have been reported. Important observations have been made about the spalling of HPC in the presence of reinforcement and pre-load. The effects of various key variables of study were investigated with respect to residual strength and ductility in reinforced HPC exposed to varying elevated temperatures.

CHAPTER - 5

THERMAL PROPERTIES OF HIGH PERFROMANCE CONCRETE AT ELEVATED TEMPERATURES

5.1 INTRODUCTION

Concrete is an amalgamation of heterogeneous multi-phase composite materials, yet shows good fire resistance properties when subjected to high temperatures or fire. Often the concrete structures are subjected to elevated temperatures due to exposure to an aggressive fire or other heat source. When the concrete is submitted to high temperatures, a series of physical and chemical changes take place leading to degradation in the mechanical and thermal properties of concrete. These changes primarily occur in cement paste and then later in the aggregates. The penetration of heat towards inside of concrete generates temperature gradient and develops thermal stresses, which play an important role in the deterioration of concrete. The adequate knowledge of thermal properties of concrete is of fundamental interest for heat transfer calculations and evaluation of overall thermal behavior of concrete, which helps in assessing the fire endurance of concrete at elevated temperatures.

5.2 THERMAL PROPERTIES OF CONCRETE AT ELEVATED TEMPRATURES

The knowledge of thermal properties is required for numerical fire endurance studies for tracing the fire response of structural elements and determining the fire resistance. To this end, number of thermal properties namely thermal conductivity, specific heat capacity, thermal diffusivity, thermal expansion and mass loss are required as function of temperature. These properties have a direct influence on the temperature rise and its distribution in the concrete at high temperatures. A detailed review of the literature as presented in Chapter 2 indicates that some studies have been undertaken in the past to characterize the thermal properties of concrete at elevated temperatures (Harmathy 1970, Harmathy and Allen. 1973, Hertz 1981, Hu et al. 1993, Lie and Kodur 1996, Van Geem et al. 1997, Shin et al. 2002, Kodur and Sultan 2003, Khaliq et al. 2011, Kodur and Khaliq 2011). These previous studies were conducted mainly on normal strength concrete and to a limited extent on special concretes like high strength concrete, fibre reinforced concrete etc. As the thermal properties of concrete vary considerably

depending on the mix constituents, it becomes important to know the thermal properties of different types of special concretes. High performance concrete is one such type of special concrete, which has found its application in many modern civil structures. There is very little information available on the thermal properties of high performance concrete having different mineral admixtures. In view of the above the present study attempts to investigate the thermal properties of high performance concrete containing different mineral admixtures at elevated temperatures.

5.2.1 Thermal Conductivity (λ)

The thermal conductivity is a measure of the ability of concrete to conduct heat and is defined as the ratio of density of heat flow rate to temperature gradient (IS 1528 (Part 16): 2007, Neville 2009). The unit of measurement of thermal conductivity is watt per meter- Kelvin (W/m-K). This property is used to determine the heat transfer across the materials. It is an important parameter characterizing the thermal performance of any given material. The thermal conductivity of porous material like concrete may be influenced by many factors namely different types of moisture present in concrete medium, type of binder material (cement and type of mineral admixture), types of aggregates and grade of concrete. The above said parameters along with the mineralogical character of aggregate and binder materials have significant influence on thermal conductivity of concrete (Shin et al. 2002, Kodur et al. 2003). The earlier studies show that several methods are available for the measurement of thermal conductivity of concrete materials. Hence, the outcome of results may also vary depending on the test method employed (Harmathy 1964, Shin et al. 2002). Generally steady state and non-steady state methods are employed to determine the thermal conductivity at elevated temperatures. The non-steady state methods may be further divided into two categories, i.e. periodic heat flux method and transient heat flux method (Santos 2007). Now-a-days the transient heat flux method is considered as an effective and an accurate test method for measuring the thermal conductivity of ceramic materials (IS 1528 (Part 16): 2007). The commonly applied steady state methods like hot plate (ASTM C177: 2010) and hot box (ASTM C 1363: 2011) methods do not suit well for measuring thermal properties of porous concrete as the concrete shows variation in physicochemical changes on heating (Shin et al. 2002). Thus for the measurement of thermal properties of concrete at high temperatures, the ‘dynamic or transient state’ methods are preferred, because such methods consider the thermal gradients and overall movement of moisture within the

concrete that would affect the measurements (Shin et al. 2002). Hot wire method (parallel) is a dynamic measuring procedure based on rise in temperature at a certain location and at a specified distance from linear heat source embedded between the set of test specimens (IS 1528 (Part 16): 2007, Shin et al. 2002). The Figure 5.1 illustrates the schematic arrangement of this test method.

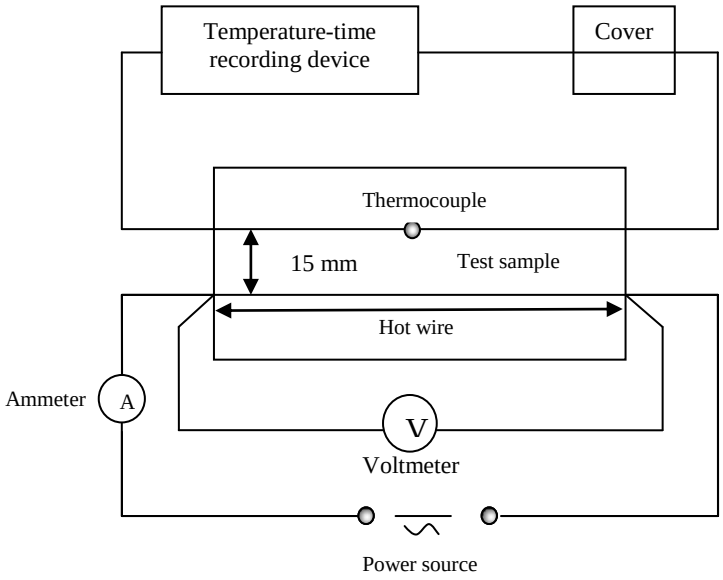

Fig 5.1 Schematic diagram for thermal conductivity test (IS 1528 (Part 16): 2007)

5.2.2 Specific Heat Capacity (C_p)

The specific heat of concrete is defined as the amount of heat energy required to modify the concrete temperature by one degree of per unit mass. It is usually expressed in terms of thermal capacity or heat capacity, which is the product of specific heat and density. Specific heat of concrete represents the energy absorbed by the concrete and it considers the sensible heat and latent heat, which is involved to change the temperature within the concrete mass (Harmathy et al. 1973). While the sensible heat refers to the heat that is involved in changing the body temperature as a part of thermodynamic process, the latent heat is a heat released or absorbed by the mass of body during the process of phase transition due to endothermic or exothermic reactions in the material. The unit of specific heat capacity is Joules per kilogram-Celsius (J/kg-C) or Joules per kilogram-Kelvin (J/kg-K). The specific heat capacity of concrete is highly influenced by the moisture content in the concrete, the type of aggregate, density and grade of concrete (Harmathy et al. 1973, Phan 1996, Kodur et al. 2003, Khaliq et al. 2011[a]). Generally concrete absorbs

considerable amount of energy to achieve the physiochemical changes; hence the numerical heat flow studies require the specific heat values for calculating the phase transition of material.

5.2.3 Coefficient of thermal expansion

The coefficient of thermal expansion is defined as the increase in length of test specimen per unit rise in temperature. At high temperatures, the concrete shows positive coefficient of thermal expansion, which depends on the mix constituents (aggregates, binder material type), their chemical composition and moisture state at the time of temperature variation. This thermal property is important to measure the movement of structural elements and thermal stresses resulting from a temperature change that can lead to cracking and spalling. Usually, the linear thermal expansion of concrete is measured using dilatometric apparatus, which gives the thermal strain resulting due to increased temperature (Harmathy et al. 1970, Cruz et al. 1980). The dilatometric technique is complementary to the thermo-gravimetric analysis and detects the changes of reactions which are not accompanied by change of weight. The thermal expansion of concrete is mainly influenced by hydrated cement matrix (cement type, age, and moisture content), aggregate type (Lie 1992, Kodur and Sultan 2003, Neville 2009), mix proportions and rate of heating (Freskakis 1984).

5.2.4 Mass loss

To know the loss in mass of concrete with heating is always important to track changes in concrete with temperature. Usually mass or weight loss of material clearly indicates the progress of decomposition reactions (Harmathy 1973). The mass loss can also affect the energy requirement and amount of latent heat of thermodynamic system of concrete. The weight loss of concrete at elevated temperatures depends mainly on the constituents of mix (binder type and their content, water content, aggregate type), initial moisture state and degree of hydration (Zhang 2011). At elevated temperatures, the mass loss influences the thermal properties as well as the monarchical properties of concrete too. The mass loss of the concrete at high temperatures can be ascertained through thermo-analytical method called Thermo-gravimetric analysis (TGA). TGA is the measure of change in mass of a specimen as a function of time at a determined temperature or over a temperature range using a predetermined heating rate. At low temperature conditions, this study is conducted purposely to determine the amount of

mass that may be lost through the evaporation of moisture from concrete. TGA curves are also very useful in evaluating the merits or demerits of materials used in fire resistant structures.

5.3 EXPERIMENTAL PROGRAM

This section describes the experimental program planned to investigate the effects of high temperatures on the thermal properties of different types of high performance concretes. Various techniques namely thermogravimetry, differential thermal analysis, differential scanning calorimetry, thermo-mechanical analysis were employed to measure the thermal properties of HPC at elevated temperatures. Table 5.1 illustrates the relevant details of different thermal analysis techniques, sample details, relevant standard codes and other details with reference to various thermal property measurements included in this study.

Table 5.1 Test matrix of thermal properties and their relevant details

S. No.	Property	Method	Apparatus	Temp. Range	Sample description	No of Samples Tested	Reference Code	Test Conducted at
1	**Thermal conductivity**	Non-steady state	Hot wire method	20 ^{o}C to 900 ^{o}C	HPC Bricks 200×100 ×75 mm	3×4=12	IS 1528 (Part 16): 2007	Civil Engg. Dept. at Roorkee
2	**Specific heat**	Differential scanning calorimeter (DSC)	Netzsch, 449C	20 ^{o}C to 1000 ^{o}C	HPC powder	3×4=12	ASTM E 1269:11	CGCRI Kolkata
3	**Thermal Expansion**	Dilatometric apparatus	Netzsch, DIL (402C)	20 ^{o}C to 1000 ^{o}C	HPC cylinder 8mm dia × 25 mm long	3×4=12	ASTM E 831: 12	CGCRI Kolkata
4	**Mass Loss**	Thermo-gravimetric analyser	EXSTAR TG/DTA 6300	20 ^{o}C to 1000 ^{o}C	HPC powder	5×3=15		IIC-Roorkee

5.3.1 Specimens casting and curing

Thermal properties of four different HPC mixes were determined and studied. The four HPC mixes included a plain non-pozzolanic mix, a fly ash based mix, a micro silica based mix and a GGBFS HPC mix. These mixes were the same optimized HPC mixes as reported in the previous chapters of this thesis. Different types of specimens as indicated in Table 5.1 were cast using the various HPC mixes in order to measure the thermal

properties at elevated temperature. Before each casting, the specified quantities of various ingredients i.e. cement, fine aggregate, coarse aggregate, water, mineral admixture and chemical admixture (HAWRA) were kept ready in required proportions. Initially, mixer drum was wetted thoroughly; the coarse aggregate and cementitious materials were added together in the mixer drum in a dry state while the drum was in motion. About more than half of the total water with super-plasticizer was added slowly to get a uniform mixture. The uniformity was indicated by the uniform colour of the mix with no concentration of any one material being visible. After the mix became uniform, the mixing was continued further for about two minutes. Finally the fine aggregate was added in the mixing drum. After this, the remaining water with super-plasticizer was added, and the mixing was continued for about five minutes. The specially made steel moulds were kept ready. The fresh green concrete was placed in these steel molds in three layers and then the moulds were vibrated properly to get a good compaction (Figure 5.2). Further details of casting, curing and testing for a specific thermal property are furnished below:

Fig 5.2 Stages of casting and curing of test specimens

5.3.2 Thermal conductivity

For *thermal conductivity* test, a total of 12 sets of specimens of four different types of high performance concretes were cast under this investigation. The specimens were in the shape of rectangular prisms with size of 200 mm ×100 mm × 75 mm as recommended by IS-1528 (Part 16): 2007. After a day of casting, the specimens were removed from the moulds and identification marks were made on the surface and then they were submerged in a curing tank (Figure 5.2). The water curing period lasted for 14 days after which the specimens were removed from the curing tank, and then kept in the

laboratory at ambient temperature and humidity conditions for another 166 days. After 180 days of total ageing, the specimens were exposed to the target temperatures ranging from room temperature to 700 °C to measure the thermal conductivity of concrete.

Hot wire method was used to determine the thermal conductivity of HPC at elevated temperatures. The transient hot-wire technique (parallel) is a dynamic measuring procedure based on the measurement of temperature at a certain location at a specified distance from the heat source embedded between the two test specimens (IS 1528 (Part 16): 2007). This technique is generally employed to measure the thermal conductivity of refractory materials. An indigenous instrument was fabricated to carry out the experiments in the laboratory as per the specifications of IS 1528 (Part 16): 2007. The device consisted of a 0.5 mm diameter platinum wire as a heating source to raise the temperature during the experiment. Usually the heating wire is placed between the two specimens. To sense the heat form heating source, 0.5 mm diameter K-type ungrounded M.I. thermocouple was used. This thermocouple was set at 15 mm away from the heat source of platinum hot wire to measure the rise in temperature. The equipment consisted of an Ammeter and a Voltmeter to measure and monitor the electrical power supplied through the hot wire circuit. A time-temperature data was continuously recorded using data acquisition system. Figures 5.3 and 5.4 illustrate the details of the instrument.

An electric muffle furnace was used for heating the test specimens to the desired target temperatures. The said furnace had a maximum operating temperature up to 1000 °C and the temperature could be controlled up to 1 °C accuracy. Before the testing operation, the concrete specimen's surfaces were ground smooth for ensuring better contact. The test specimens were placed in the steel holder meant to hold the test setup firmly along with hot wire circuit during the heating operation. The whole assembly was positioned inside the furnace for exposing it to the target temperatures. Subsequently, the furnace was closed and arrangements were made to conduct the experiment. In this experiment, the heating rate was maintained at 1.67 °C/min for measuring the thermal conductivity of concrete samples. The specimens were exposed to eight different target temperatures ranging from room temperature to 700 °C. Each target temperature was kept constant for 20 minutes for achieving thermal equilibrium and the readings were recorded.

Fig. 5.3 Test setup of thermal conductivity measurement apparatus with hot-wire method (parallel).

Fig. 5.4 Complete testing setup of non-steady state hot-wire method (parallel) apparatus with furnace.

Then the temperature in the furnace was increased to the next target temperature level and the same procedure was continued till 700 °C. It took an average of about 60 minutes to attain next target temperature. The average time of running a complete test corresponding to the various chosen temperatures was approximately 11 hours. The thermal conductivity of concrete was determined according to the following equation per IS 1528 (IS 1528 (Part 16): 2007):

$$\lambda = \frac{VI}{4\pi l} \times \frac{-Ei\left(-\frac{r^2}{4at}\right)}{\Delta\theta(t)} \tag{5.1}$$

where

V = is voltage, in Volts.

I = is current, in Amperes,

l= is length of the hot wire (platinum),

$\Delta\theta(t)$ = is the temperature difference, in °C, between the measurement and reference thermocouple at time *t*,

t = is time period, in seconds, between switching on and switching off the heating circuit,

a= is thermal diffusivity, in square meters per seconds,

$-Ei\left(-\frac{r^2}{4at}\right)$ is an exponential integral of the form $\int_x^u \frac{e^{-u}du}{u}$

5.3.3 Coefficient of thermal expansion

In the present experimental program, thermo dilatometric apparatus (Netzsch, Germany, DIL (402C)) was used for measuring the thermal expansion of concrete at high temperatures as per the recommendation of ASTM E 831: 12. This test was conducted in Central Glass and Ceramic Research Institute (CGCRI), Kolkata. This thermo-analytical instrument consists of a sample holder and a pushrod. Both are closely connected to the sample at one end, and the other end is directly connected to linear variable differential transducer (LVDT) which registers the length changes in the test material during heating operation. This type of instrument can be used to measure linear dimensional changes in solids like concrete samples up to temperatures of 1000 °C. When the sample is subjected to high temperature, the sample and the pushrod acquire the same level of controlled temperature. The thermal expansion measurement of instrument is controlled through computer program using predefined parameters such as maximum temperature range, heating rate and atmosphere of testing (type of gas or inert). A total of 12 test specimens

of four different types of high performance concretes were cast and tested under this investigation. Initially the test specimens were cast as 100 mm cubes. After 24 hours, the cubes were removed from the moulds and submerged in the water for curing. The water curing period lasted for 14 days after which the specimens were dried in the laboratory at ambient temperature and humidity conditions for another 76 days. For the coefficient of thermal expansion test, cylindrical cores of 8 mm diameter and 25 mm length were cut from the cubes using special core cutting tool. Thus after 90 days of total ageing, the core specimens were exposed to the target temperatures ranging from room temperature to 1000 ºC to measure the thermal expansion of concrete. Figure 5.5 shows a view of thermo dilatometric apparatus employed in this study.

Fig. 5.5 A view of thermo dilatometric apparatus for thermal expansion test (CGCRI)

As mentioned earlier the cylindrical cores were tested for thermal expansion in the dilatometric apparatus. Before the commencement of the test, the apparatus was calibrated and zeroed to make the instrument ready for the test. Once the sample was placed in sample holder in suitable position, the software supported computer controlled test equipment recorded the initial length of the specimen and other ambient temperature readings. The readings of linear changes occurring in specimen due to the effects of high temperatures were recorded during the experiment. For concrete samples, the selected heating rate was 5 °C/min inside of the furnace. Approximately it took three hours thirty minutes for each test to reach the target temperature of 1000 °C.

5.3.4 Specific heat and mass loss

Many simple methods are available to measure the specific heat capacity of concrete at ambient temperature conditions; however it may be costly and cumbersome, while using the same techniques for measuring the specific heat at the high temperatures. At high temperatures, up to 600 °C, usually differential scanning calorimetry (DSC) is the most common thermo-analytical technique used to measure the specific heat capacity of concrete (Lie et al. 1995). Above 600 °C, differential thermal analyzer (DTA) is generally used. A commercially available instrument STA (Simultaneous Thermal Analyzer, Netzsch, Germany, 449 C) was used in this investigation (Figure 5.6). Figure 5.6 shows a view of the apparatus employed in the test program.

Fig. 5.6 A view of STA apparatus (CGCRI)

This instrument, referred as simultaneous thermal analyzer (STA), was capable of measuring specific heat up to 1000 °C and could also work as thermogravimetre (TG) simultaneously for measuring mass loss. It measures the temperature difference between the sample and the reference material exposed to a given heating thermal schedule and the data relating to differences in temperature are recorded through the computers installed with requisite software. The changes observed in the sample may be exothermic or endothermic; they can be detected with the help of inert reference and are plotted and the

plots are called thermograms. The DSC curve provides information related to phase transformation that has occurred during the thermal loading, such as glass transmission, crystallization, melting and sublimation.

Figure 5.7 showing the Thermogravimetric (TG) instrument used for measuring mass loss of HPC concretes mixes. This instrument consists of a highly sensitive horizontal microbalances surrounded by an electrical furnace. A programmable computer records the changes in mass gains or losses while the concrete specimens are exposed to high temperatures. At high temperatures, this technique is highly useful to monitor heat stability and to detect the degradation mechanisms and their reactions. The weight loss is plotted as a function of temperature for constant heating rate.

Fig 5.7 Thermogravimetric instrument for measuring mass loss of HPC concrete

The powder samples were used to measure the specific heat capacity and mass loss of concrete at elevated temperatures. Powder samples of concrete of approximately 20 to 35 milligrams passing through 75 micron sieve were prepared for the test. The samples were obtained from the test cubes. In all 12 numbers of samples of various chosen high performance concrete mixes were prepared and tested. For the specific heat capacity test, the said instrument consists of two pans (Sample holders) one for testing sample and another one for inert reference material and were internally connected with high-precision balance. The test sample and inert material were tested under controlled heating schedule in the environment of nitrogen. In this investigation, the inert material namely powdered sapphire (AL_2O_3) was loaded as calibration material and another pan

was loaded with testing sample of concrete powder. Subsequently, the loaded pans were placed inside the furnace. The attached programmable device recorded the initial weight, initial temperature and other relevant testing details before the experiment began. During the experiment, a heating rate of 10 °C/minute was kept in the furnace. Each experiment consumed approximately three hours thirty minutes to reach the target temperature of 1000 °C.

5.4 RESULTS AND DISCUSSION

The test results are presented and discussed in the following sections.

5.4.1 Thermal Conductivity

The measured thermal conductivity (TC) data of various pozzolanic HPCs and plain HPC are presented in Table 5.2 and plotted in Figure 5.8 as a function of temperature. It can be observed that the thermal conductivity values of various HPCs vary between 4.578 and 3.347 W/m °C at room temperature. The fly ash HPC had the highest thermal conductivity at room temperature among all the HPCs, while the silica fume HPC had the lowest thermal conductivity value. The thermal conductivity is highly influenced by the amount of binding material content, type of mineral admixture, its chemical composition, mineral characteristics, pore structure, moisture present in the concrete mass etc. The higher thermal conductivity of fly ash HPC at room temperature may be because of higher moisture retained in the concrete mass. The lower conductivity of silica fume HPC at this temperature may be because of the presence of amorphous silica in the silica fume, which introduces thermal barrier in the form of the interface between silica fume particles and the cement matrix compared to crystalline silica in silica fume (Xu et al. 2000).

With an increase in temperature from room temperature to 100 °C, a sharp decrease in thermal conductivity values were observed in all types of concretes except GGBFS HPC. GGBFS HPC in fact indicated a small increase in the thermal conductivity when temperature was increased to 100 °C, may be an experimental anomaly. The decrease of thermal conductivity in most of the HPC mixes was because of the loss of the free water from the concrete up to 100 °C. With further increase in temperature to 200 °C, all high performance concretes had under gone reduction in thermal conductivity due to the dehydration of water from the cement matrix. The loss of remaining free water in the capillary pores takes place in this temperature range and also there may be the loss of

chemically bound water from hydration products. The results presented in Table 5.2 and Figure 5.8 show that the thermal conductivity values remained more or less stable between 200 °C at 300 °C. This may be due to a minimal loss of moisture from the concrete mass in this temperature range. With an increase in temperature to 400 °C, all the concretes showed a further decrease in the thermal conductivity.

Table 5.2 Results of thermal conductivity test for various types of HPC

Temp. (°C)	Thermal conductivity (W/m °C)			
	Plain HPC	Silica fume HPC	Fly ash HPC	GGBFS HPC
28	4.132	3.347	4.578	4.048
100	3.590	2.807	4.060	4.147
200	3.455	2.847	3.146	3.423
300	3.363	2.714	3.400	3.446
400	3.113	2.229	2.696	2.899
500	3.741	2.229	3.422	2.754
600	4.209	2.854	3.852	2.731
700	4.594	3.310	4.588	3.043

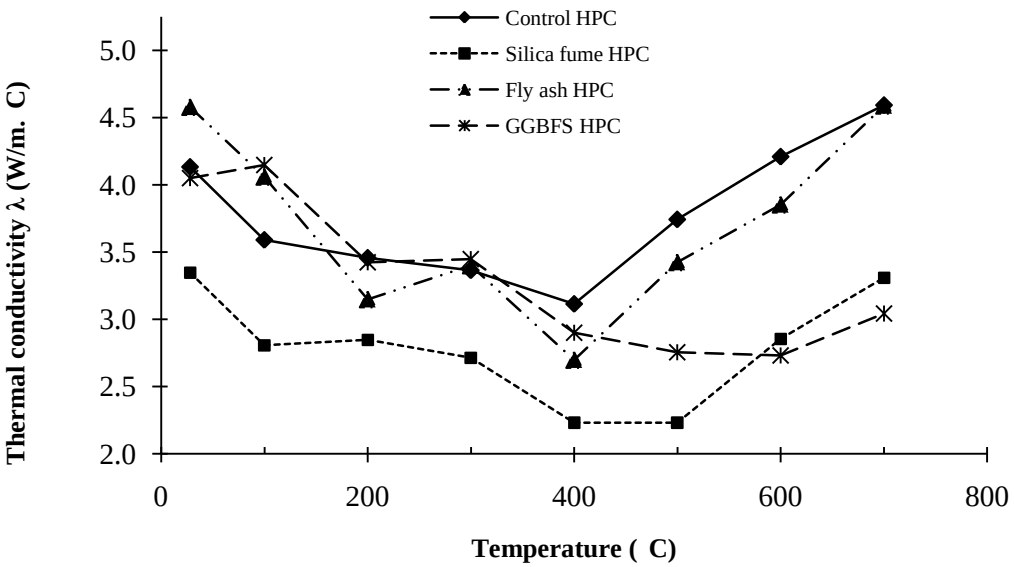

Fig. 5.8 Thermal conductivity of various pozzolanic and plain HPC mixes

This might be due to the micro cracking in the transition zone of aggregate cement matrix inter phase because of dehydration of calcium hydroxide $Ca(OH)_2$. While the silica fume HPC had the lowest thermal conductivity at 400 °C, other HPC mixes had

almost similar values though plain HPC indicated the highest conductivity at this temperature.

In the temperature ranging between 400 °C and 700 °C, all the pozzolanic and non-pozzolanic high performance concretes showed an increase in the thermal conductivity except GGBFS HPC, where thermal conductivity continued decreasing up to 600 °C before showing an increase at 700 °C. The GGBFS HPC showed the lowest thermal conductivity in this temperature range along with silica fume HPC. Plain non-pozzolanic HPC mix and fly ash based HPC had more thermal conductivity values than the other two mixes. This unexpected rising trend of thermal conductivity between 400 °C and 700 °C may be attributed to phase transition of calcareous aggregates used in the concrete mix, the destruction of calcium hydrate silicate (CSH) gel layers and mineral composition of aggregate and pozzolanic admixtures.

5.4.2 Specific heat capacity

The variation of specific heat with temperature for different HPC mixes is shown in Figure 5.9 and the test data is presented in Table 5.3. The results indicate that the specific heat capacity of all types of concretes remained almost constant and indicated similar trends up to 650 °C. However, the silica fume based HPC had maximum specific heat among all the mixes up to 650 °C temperature, followed by fly ash HPC, plain HPC and GGBFS HPC respectively. The highly dense micro structure of silica fume concrete observed to consume extra heat energy for driving off the moisture. There were five endothermic peaks in all types of concrete. These upward peaks indicate endothermic reactions. The first peak was observed at about 100 to 115 °C temperature because of dehydration and loss of water from concrete mass. The second peak was noted at about 160 °C for silica fume HPC (Morsy et al. 2010), at 215 °C for GGBFS HPC and at 226 °C for fly ash HPC. These peaks represent the decomposition of calcium sulpho-aluminate hydrate (gehlenite hydrate). The third endothermic peak was noticed between 411 °C and 426 °C temperature for almost all types of high performance concretes. This peak represents the dehydration of calcium hydroxide $Ca(OH)_2$. The fourth peak was observed at 571 °C for all types of concretes indicating endothermic reactions, decomposition and phase transition of quartz present in the pozzolanic admixture and fine aggregates. While the highest peak was recorded at 731 °C temperature in all types of high performance concretes, the magnitude of peak was different in various HPC mixes. Fly ash HPC

showed a maximum peak at this temperature, which was followed sequentially by plain HPC, silica fume HPC and GGBFS HPC. This peak indicates decomposition of calcite (calcium carbonate ($CaCO_3$)) and second phase of dehydration of CSH gel (Hu et al. 1993, Arioz 2007, Ramachandran et al. 2008, Li et al. 2010).

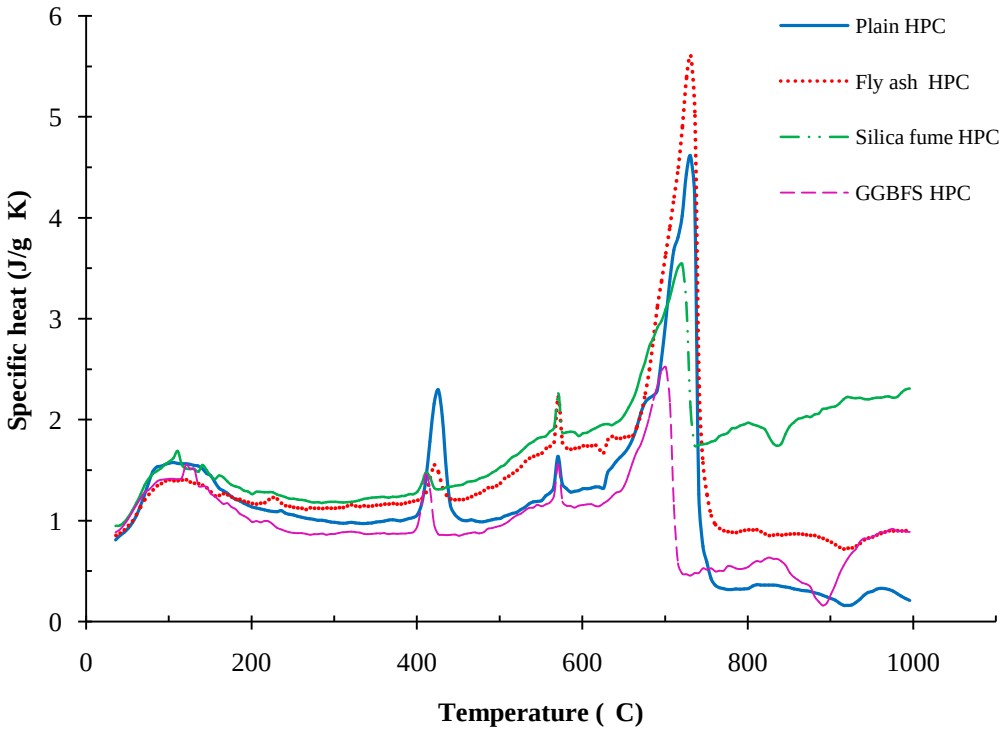

Fig. 5.9 Specific heat capacity of various HPC mixes as function of temperature

The above results indicate that the endothermic peak of plain non pozzolanic HPC has consumed extra heat to dehydrate the calcium hydroxide $Ca(OH)_2$. However, the results clearly indicate that the pozzolanic additives incorporated high performance concretes would have depleted the content of calcium hydroxide during the hydration process. The specific heat values varied for different HPC mixes beyond the temperature of 750°C. Silica fume based HPC showed maximum specific heat in this temperature range up to 1000 °C. The higher value of energy consumption, as noticed in silica fume high performance concrete, may be due to the decaying process of highly reactive silica in silica fume along with siliceous concrete.

Table 5.3 Specific heat capacity data for different HPC mixes

No	Plain HPC		FHPC		SHPC		GHPC		Remarks
	Temp. (°C)	**Cp (J/g-K)**	**Temp. (°C)**	**Cp (J/g-K)**	**Temp. (°C)**	**Cp (J/g-K)**	**Temp. (°C)**	**Cp (J/g-K)**	
1	Room Temp.	0.808	Room Temp.	0.854	Room Temp.	0.949	Room Temp.	0.885	
2	50	0.923	50	0.952	50	1.034	50	1.014	
3	106	1.576	101	1.404	111	1.689	106	1.415	**1st Peak**
4	150	1.448	150	1.284	150	1.444	150	1.268	
5	200	1.134	200	1.172	200	1.262	200	0.987	
6	221	1.098	226	1.230	221	1.282	216	0.996	**2nd peak**
7	250	1.056	250	1.134	250	1.216	250	0.879	
8	300	0.983	300	1.124	300	1.185	300	0.868	
9	350	0.985	350	1.154	350	1.231	350	0.874	
10	400	1.059	400	1.202	400	1.288	400	0.949	
11	426	2.297	421	1.551	411	1.476	411	1.457	**3rd peak**
12	450	1.023	450	1.208	450	1.350	450	0.851	
13	500	1.022	500	1.370	500	1.532	500	0.949	
14	550	1.199	550	1.669	550	1.826	550	1.142	
15	571	1.637	571	2.226	571	2.263	571	1.560	**4th peak**
16	600	1.318	600	1.742	600	1.866	600	1.155	
17	650	1.669	650	1.828	650	2.047	650	1.345	
18	700	2.953	700	3.650	700	3.093	700	2.486	
19	731	4.615	731	5.604	731	3.543	731	2.519	**5th peak**
20	750	0.589	750	1.253	750	1.764	750	0.515	
21	800	0.328	800	0.908	800	1.969	800	0.543	
22	850	0.335	850	0.867	850	1.933	850	0.486	
23	900	0.228	900	0.787	900	2.124	900	0.271	
24	950	0.298	950	0.839	950	2.212	950	0.843	
25	995	0.210	995	0.888	995	2.309	995	0.887	

5.4.3 Thermal expansion

The percentage thermal expansion strains and coefficient of thermal expansion were computed from the test results for all the HPC mixes and are shown in Table 5.4. The variation of thermal expansion strains with temperature for all the HPC mixes are plotted in the Figure 5.10. Figure 5.11 shows the variation of co-efficient of thermal expansion with temperature for different high performance concretes. The results show a steady increase of thermal strain from room temperature to 500 °C in all the HPC mixes. However, up to 200 °C temperature, no significant change was observed in both the thermal strains and coefficient of thermal expansion values because of the moisture release in the interlayer of hydrated products. On increasing the temperature further to 500 °C, variations in thermal strain as well as in the coefficient of thermal expansion were noticed among different concretes.

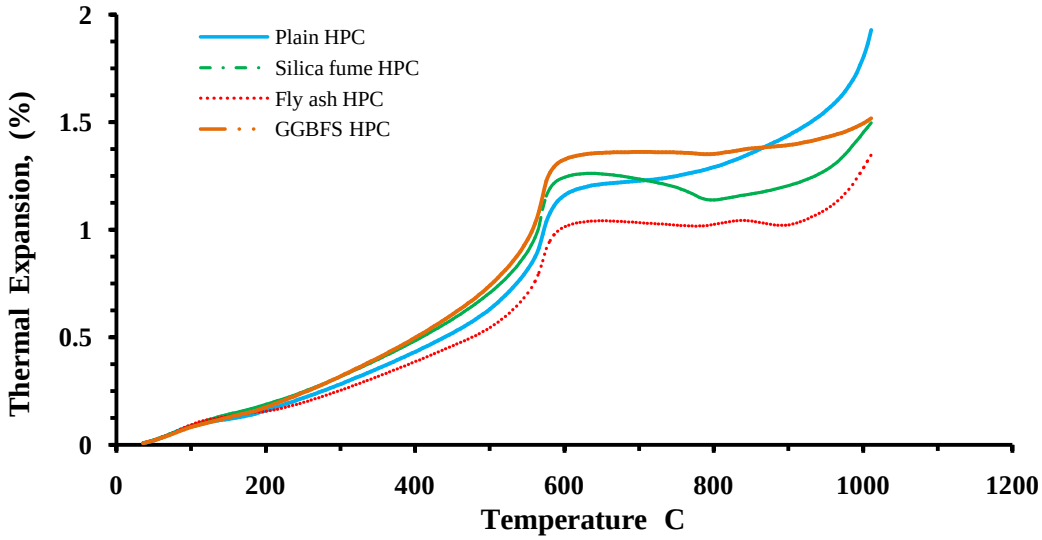

Fig. 5.10 Thermal expansion as a function of temperature

Table 5.4 Thermal expansion strain and coefficient of thermal expansion results

Temp. (°C)	(ΔL/Lo)/%				Coefficient of thermal expansion (CTE)			
	Plain HPC	FHPC	SHPC	GHPC	plain HPC	FHPC	SHPC	GHPC
Room temp.	8.06E-03	8.99E-03	9.01E-03	8.28E-03	0.00E+00	0	0	0
50	2.21E-02	2.39E-02	2.43E-02	2.18E-02	4.42E-09	4.77E-09	4.85E-09	4.36E-09
100	8.99E-02	9.52E-02	8.96E-02	8.36E-02	1.80E-08	1.9E-08	1.79E-08	1.67E-08
150	1.21E-01	1.34E-01	1.43E-01	1.28E-01	2.43E-08	2.68E-08	2.86E-08	2.57E-08
200	1.61E-01	1.57E-01	1.89E-01	1.76E-01	3.22E-08	3.14E-08	3.78E-08	3.52E-08
250	2.19E-01	1.98E-01	2.48E-01	2.44E-01	4.38E-08	3.97E-08	4.96E-08	4.88E-08
300	2.84E-01	2.55E-01	3.19E-01	3.20E-01	5.68E-08	5.1E-08	6.37E-08	6.41E-08
350	3.56E-01	3.20E-01	3.99E-01	4.06E-01	7.12E-08	6.39E-08	7.97E-08	8.11E-08
400	4.34E-01	3.88E-01	4.86E-01	5.00E-01	8.69E-08	7.77E-08	9.72E-08	1E-07
450	5.22E-01	4.62E-01	5.85E-01	6.09E-01	1.04E-07	9.23E-08	1.17E-07	1.22E-07
500	6.34E-01	5.47E-01	7.09E-01	7.43E-01	1.27E-07	1.09E-07	1.42E-07	1.49E-07
550	8.17E-01	7.06E-01	8.99E-01	9.56E-01	1.63E-07	1.41E-07	1.8E-07	1.91E-07
600	1.162	1.015	1.245	1.328	2.32E-07	2.03E-07	2.49E-07	2.66E-07
650	1.213	1.041	1.260	1.358	2.43E-07	2.08E-07	2.52E-07	2.72E-07
700	1.228	1.033	1.235	1.362	2.46E-07	2.07E-07	2.47E-07	2.72E-07
750	1.251	1.021	1.196	1.359	2.50E-07	2.04E-07	2.39E-07	2.72E-07
800	1.292	1.025	1.139	1.353	2.58E-07	2.05E-07	2.28E-07	2.71E-07
850	1.357	1.040	1.167	1.378	2.71E-07	2.08E-07	2.33E-07	2.76E-07
900	1.441	1.023	1.206	1.394	2.88E-07	2.05E-07	2.41E-07	2.79E-07
950	1.555	1.096	1.278	1.430	3.11E-07	2.19E-07	2.56E-07	2.86E-07
1000	1.808	1.291	1.454	1.496	3.62E-07	2.58E-07	2.91E-07	2.99E-07

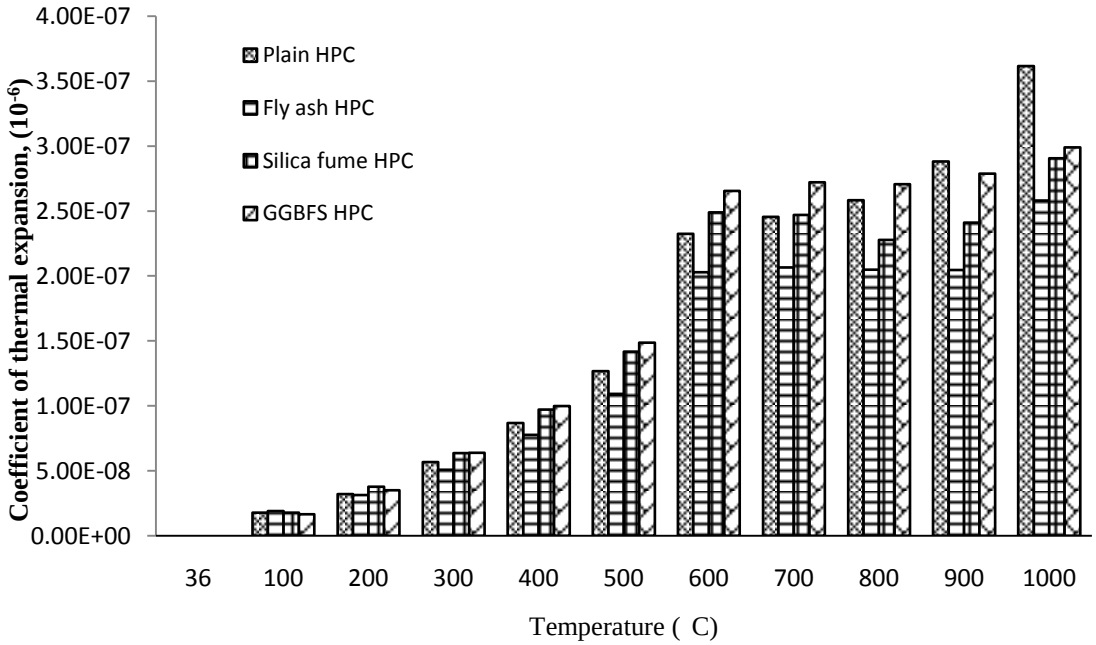

Fig. 5.11 Coefficient of thermal expansion as a function of temperature

Thereafter a steep increase in thermal strain was noticed in the temperature range of 500 °C to 600 °C. This steep rise of thermal expansion may be attributed to the phase transformation of the silica content in pozzolanic admixtures and fine aggregates and also to that of dissociation of dolomite in the carbonate aggregates. The thermal strains remained more or less constant from 600 °C to 1000 °C, though the thermal strains in plain non-pozzolanic HPC continued to increase gently even in this temperature range. Similar trends were noticed with respect to coefficient of thermal expansion. A rise in thermal expansion at 1000°C may be due to complete dehydration and destruction of crystal structure of cement matrix and excessive micro and macro cracks developed in the transition zone between aggregates and paste matrix. The results indicate that the GGBFS based HPC continued to have more thermal expansion than the other mixes though plain HPC indicated highest final expansion at 1000 °C. On the contrary the fly ash HPC had the minimum thermal expansion among the various HPC mixes. The varying values of thermal expansion in different concretes may be explained due to the difference in chemical composition, amount of pozzolanic material and their reactivity with cement by-products during the hydration process. Different types and quantities of pozzolanic materials react differently with Ca $(OH)_2$, which is the main source of the instability and hence volumetric changes. In view of this the results show that the fly ash efficiently reduced the free Ca $(OH)_2$. This reduced content of Ca $(OH)_2$ yielded thermally stable compounds contributing high thermal stability and lower thermal expansion of fly ash

concrete. On the other hand the GGBFS HPC showed a weak pozzolanic activity. The alkalis and sulfates may be possible to increase in the thermal strain and the expansion coefficient of GGBFS HPC.

5.4.4 Mass loss

The mass loss of various HPC mixes after subjecting to various elevated temperatures was determined using thermo gravimetric analysis (TGA) and the data is presented in the Table 5.5. The Figure 5.12 presents the variation of mass of the concrete with temperature based on the thermogravimetric data for different types of HPC mixes.

Table 5.5 Mass loss of HPCs

Temp. (°C)	Plain HPC	Fly ash HPC	Silica fume HPC	GGBFS HPC
Room temperature	0.000	0.000	0.000	0.000
100	-1.917	-3.279	-2.995	-2.621
200	-3.614	-5.093	-5.247	-4.278
300	-4.546	-5.975	-6.303	-5.405
400	-5.220	-6.634	-6.938	-6.316
500	-6.382	-7.381	-7.529	-7.023
600	-7.132	-7.909	-8.371	-7.586
700	-10.332	-10.698	-11.318	-9.722
800	-11.449	-11.077	-11.783	-10.213
900	-11.678	-11.202	-11.968	-10.407
1000	-11.748	-11.217	-12.002	-10.465

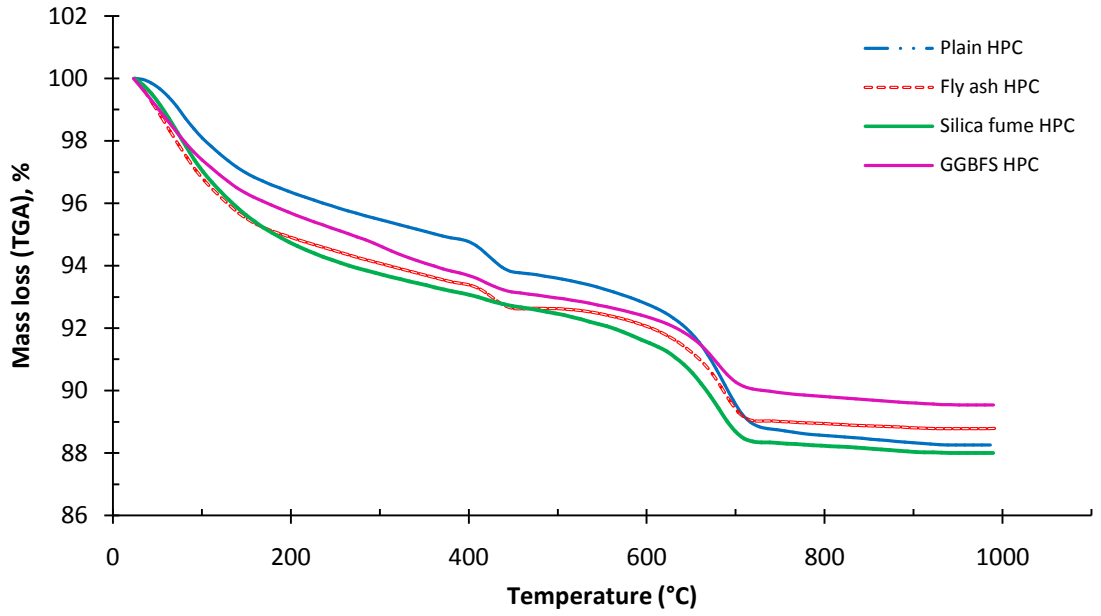

Fig. 5.12 Mass loss for different types of HPCs as a function of temperature

It can be observed that the loss in mass increased and the resulting mass decreased as the temperature increased. All the four HPC mixes showed almost similar kind of behavior. The mass decreased with the increase in temperature up to 700 ℃ and thereafter remained stable at higher temperatures. A perusal of the curves shows that there were three instances when sudden loss in mass was observed. They were approximately in the temperature ranges of 100 to 200 ℃, 400 to 440 ℃ and 600 to700 ℃. The first sudden loss, indicating endothermic peak, occurred when a mass loss of 1.917% for plain HPC, 3.279% for fly ash HPC, 2.995% for silica fume HPC and 2.621% for GGBFS HPC was observed. The pozzolanic concretes retained higher percentage of moisture compared to plain control HPC. The loss of mass is greatly attributed to liberation of moisture present in the concrete. This indicates that the pozzolanic concretes had kept higher percentage of moisture in the concrete. The sudden mass loss at the second instance i.e. second peak corresponding to 400 to 440 ℃ may be due to the decomposition of hydrated product of calcium hydroxide and portlandite. The third endothermic peak i.e. sudden mass loss, which happened at 600 to700 ℃ temperature, shows the major deterioration of all types of high performance concretes due to disassociation of dolomite. It can be noted that the silica fume HPC underwent a maximum mass loss of approximately 11.783 % followed by control HPC (11.449 %), fly ash HPC (11.077%) and GGBFS HPC (10.213%).

5.5 RELATIONSHIPS FOR THERMAL PROPERTIES

In recent years, a number of numerical techniques have been used for assessing the behaviour of concrete structures under extreme fire conditions. Calculation based approaches are also used to estimate the fire resistance of structural elements as experimental investigations entail much cost and effort. To this end the various thermal properties of concrete as a function of temperature are required as input data. Thus the thermal property relationships of HPC shall be required at elevated temperatures to analyze high performance concrete structures and to estimate the fire resistance of HPC elements. In view of this, in the present study, regression equations for different thermal properties of HPC are proposed based on the test data.

The present test results indicate that the thermal properties of high performance concrete depend on the type of mix and the temperature of exposure. To reflect the

influence of these parameters, separate expressions are proposed here for different high performance concrete mixes based on the regression analysis of the test data.

I. Thermal conductivity

a) Plain HPC

$\lambda = 4.0127 - 0.0023T$	Room Temp. $\leq$ 400 °C ($R^2 = 0.86$)	(5.2)
$\lambda = 1.214 + 0.0049T$	400 °C $\leq$ 700 °C ($R^2 = 0.99$)	(5.3)

b) Fly ash HPC

$\lambda = 4.528 - 0.0046T$	Room Temp. $\leq$ 400 °C ($R^2 = 0.86$)	(5.4)
$\lambda = 0.282 + 0.0061T$	400 °C $\leq$ 700 °C ($R^2 = 0.99$)	(5.5)

c) Silica fume HPC

$\lambda = 3.288 - 0.0024T$	Room Temp. $\leq$ 400 °C ($R^2 = 0.83$)	(5.6)
$\lambda = 0.528 + 0.0039T$	400 °C $\leq$ 700 °C ($R^2 = 0.90$)	(5.7)

d) GGBFS HPC

$\lambda = 4.253 - 0.0032T$	Room Temp. $\leq$ 400 °C ($R^2 = 0.88$)	(5.8)
$\lambda = 2.632 + 0.0004T$	400 °C $\leq$ 700 °C ($R^2 = 0.96$)	(5.9)

II. Specific heat capacity

a) Plain HPC

$C_p = 0.0138T+0.266$	Room Temp. $\leq$100 °C ($R^2 = 0.96$)	(5.10)
$C_p = 0.002T+1.665$	100 °C $\leq$400 °C ($R^2 = 0.74$)	(5.11)
$C_p = 0.055T- 20.914$	400 °C $\leq$425 °C ($R^2 = 0.74$)	(5.12)
$C_p = 0.055T+ 25.464$	425 °C $\leq$450 °C ($R^2 = 0.74$)	(5.13)
$C_p = 0.0042T- 1.0681$	450 °C $\leq$680 °C ($R^2 = 0.80$)	(5.14)
$C_p = 0.0462T-29.283$	680 °C $\leq$730 °C ($R^2 = 0.95$)	(5.15)
$C_p = -0.150T+113.66$	730 °C $\leq$760 °C ($R^2 = 0.77$)	(5.16)
$C_p = -0.0005T+0.726$	760 °C $\leq$995 °C ($R^2 = 0.34$)	(5.17)

b) Fly ash HPC

$C_p = 0.0096T+0.4897$	Room Temp. $\leq$100 °C ($R^2 = 0.98$)	(5.18)
$C_p = 0.0007T+1.384$	100 °C $\leq$425 °C ($R^2 = 0.54$)	(5.19)
$C_p = 0.0181T- 6.088$	425 °C $\leq$450 °C ($R^2 = 0.92$)	(5.20)
$C_p = 0.055T+ 25.464$	425 °C $\leq$450 °C ($R^2 = 0.74$)	(5.21)
$C_p = 0.006T- 1.560$	450 °C $\leq$570 °C $R^2 = 0.86$)	(5.22)
$C_p = -0.032T-20.512$	570 °C $\leq$580 °C ($R^2 = 0.70$)	(5.23)

C_p = 0.026T-14.27	680 °C ≤730 °C (R^2 = 0.78)	(5.24)
C_p = -0.150T+113.66	730 °C ≤760 °C (R^2 = 0.77)	(5.25)
C_p = -0.0005T+0.726	760 °C ≤995 °C (R^2 = 0.34)	(5.26)

c) Silica fume HPC

C_p = 0.0107T+0.539	Room Temp. ≤100 °C (R^2 = 0.98)	(5.27)
C_p = 0.0011T+1.570	100 °C ≤450 °C (R^2 = 0.60)	(5.28)
C_p = 0.0051T+ 1.7004	450 °C ≤540 °C (R^2 = 0.974)	(5.29)
C_p = 0.0192T- 8.796	540 °C ≤575 °C (R^2 = 0.70)	(5.30)
C_p = 0.002T+0.855	575 °C ≤640 °C (R^2 = 0.75)	(5.31)
C_p = 0.0213T-11.779	640 °C ≤700 °C (R^2 = 0.99)	(5.32)
C_p = -0.1T-75.555	700 °C ≤725 °C (R^2 = 0. 90)	(5.33)
C_p = -0.0021T+0.163	725 °C ≤995 °C (R^2 = 0.858)	(5.34)

d) GGBFS HPC

C_p = 0.0085T+0.608	Room Temp. ≤100 °C (R^2 = 0.94)	(5.35)
C_p = 0.002T+1.5135	100 °C ≤390 °C (R^2 = 0.70)	(5.36)
C_p = 0.0508T- 19.424	390 °C ≤415 °C (R^2 = 0.99)	(5.37)
C_p = 0.0493T+ 21.765	415 °C ≤425 °C (R^2 = 0.94)	(5.38)
C_p = 0.026T- 0.281	425 °C ≤570 °C (R^2 = 0.89)	(5.39)
C_p =- 0.0182T+ 11.787	570 °C ≤640 °C (R^2 = 0.61)	(5.40)
C_p = 0.0228T-13.441	640 °C ≤700 °C (R^2 = 0.98)	(5.41)
C_p = -0.049T-36.28	700 °C ≤725 °C (R^2 = 0.70)	(5.42)
C_p = -0.0014T-0.5837	725 °C ≤835 °C (R^2 = 0.70)	(5.43)
C_p = -0.0084T+7.62	835 °C ≤ 890°C (R^2 = 0.68)	(5.44)
C_p = -0.007T+5.869	890 °C ≤ 995°C (R^2 = 0. 81)	(5.45)

III. Thermal expansion

(a) Plain HPC

ε_{th} = 3E-10T - 1E-08	Room Temp. ≤500 °C (R^2 = 0.98)	(5.46)
ε_{th} = 1E-09T - 4E-07	500 °C ≤600 °C (R^2 = 0.97)	(5.47)
ε_{th} = 3E-10T - 5E-08	600 °C ≤1000 °C (R^2 = 0.84)	(5.48)

(b) Fly ash HPC

ε_{th} = 3E-10T - 1E-08	Room Temp. ≤500 °C (R^2 = 0.98)	(5.49)
ε_{th} = 1E-09T - 4E-07	500 °C ≤600 °C (R^2 = 0.98)	(5.50)
ε_{th} = 3E-10T - 5E-08	600 °C ≤1000 °C (R^2 = 0.84)	(5.51)

(c) Silica fume HPC

ε_{th} = 3E-10T - 1E-08	Room Temp. ≤500 °C (R^2 = 0.98	(5.52)
ε_{th} = 1E-09T - 4E-07	500 °C ≤600 °C (R^2 = 0.97)	(5.53)
ε_{th} = 3E-11T - 2E-07	600 °C ≤1000 °C (R^2 = 0.84)	(5.54)

(d) GGBFS HPC

ε_{th} = 3E-10T - 2E-08	Room Temp. ≤500 °C (R^2 = 0.98)	(5.55)
ε_{th} = 1E-09T - 4E-07	500 °C ≤600 °C (R^2 = 0.98)	(5.56)
ε_{th} = 6E-11T - 2E-07	600 °C ≤1000 °C (R^2 = 0.81)	(5.57)

IV.Mass loss

a) Plain HPC

M = 99.212- 0.0115T	Room Temp. ≤600 °C (R^2 = 0.95)	(5.58)
M = 112.23- 0.0318T	600 °C ≤700 °C (R^2 = 0.95)	(5.59)
M = 90.77- 0.0027T	700 °C ≤1000 °C (R^2 = 0.86)	(5.60)

b) Fly ash HPC

M = 97.895- 0.0111T	Room Temp. ≤600 °C (R^2 = 0.87)	(5.61)
M = 109.12- 0.0278T	600 °C ≤700 °C (R^2 = 0.96)	(5.62)
M = 89.824- 0.0011T	700 °C ≤1000 °C (R^2 = 0.95)	(5.63)

c) Silica fume HPC

M = 98.074- 0.0121T	Room Temp. ≤600 °C (R^2 = 0.86)	(5.64)
M = 110.06- 0.0303T	600 °C ≤700 °C (R^2 = 0.97)	(5.65)
M = 89.502- 0.0016T	700 °C ≤1000 °C (R^2 = 0.96)	(5.66)

d) GGBFS HPC

M = 98.518- 0.0116T	Room Temp. ≤600 °C (R^2 = 0.92)	(5.67)
M = 105.71- 0.0218T	600 °C ≤700 °C (R^2 = 0.96)	(5.68)
M = 91.43- 0.002T	700 °C ≤1000 °C (R^2 = 0.96)	(5.69)

5.6 CONCLUDING REMARKS

This study reports the test results of thermal properties of high performance concrete (HPC) at elevated temperatures. Four types of HPC mixes based on the type of pozzolana used (plain, silica fume, fly ash and GGBFS) were employed in the study. The thermal properties namely thermal conductivity, specific heat capacity, thermal expansion and mass loss were evaluated experimentally up to a temperature of 1000 °C. For thermal conductivity experiments, eight sets of rectangular prisms were used, while for thermal expansion measurements, 12 numbers of specially made concrete cores were used. The specific heat capacity and mass loss were determined using powdered samples. The results show that though the thermal properties of high performance concrete are definitely influenced by the type of mineral admixture, the elevated temperature has a far more significant influence on the thermal properties of HPC. Based on the test results, simple regression equations have been proposed to estimate the high temperature thermal properties of high performance concrete made with different types of mineral admixtures.

CHAPTER - 6
CONCLUSIONS

6.1 GENERAL

This research focused on the effect of various heating regimes on the residual mechanical and thermal characteristics of high performance concrete (HPC). To this end, the behaviour of both un-reinforced and reinforced high performance concrete containing different types of mineral admixtures has been investigated experimentally. Various parameters related to high performance concrete mix and heating were investigated within the constraints of the available resources and an attempt has been made to draw meaningful conclusions from the investigations. The research program has contributed to the fundamental understanding of the strength and thermal properties of high performance concrete after exposure to elevated temperatures.

6.2 CONCLUSIONS

Within the scope of the present investigation, the following main conclusions may be drawn:

(i) This study establishes a procedure for computing the optimum mix conditions for maximum residual compressive strength of high performance concrete exposed to various elevated temperatures. The test results indicate that the mix parameters change their influence on the residual strength according to the effect of temperature of exposure. These observations can be kept in mind while designing the HPC mix for structures liable to be exposed to elevated temperatures.

(ii) The study further shows that Taguchi method and utility concept can be used efficiently and economically for designing the optimum proportions of concrete mix to achieve a maximum residual compressive strength of heated concrete.

(iii) The detrimental effects of temperature on the residual compressive strength of high performance concrete do not matter much up to a temperature of 400 °C. Rather the strength increases up to a temperature of exposure of 400 °C irrespective of the mix parameters considered in the study. It is only in the

temperature range of 600 to 800 °C that a noticeable degradation in the compressive strength of high performance concrete is observed.

(iv) In non-pozzolanic control HPC, the significant parameter affecting the residual compressive strength of concrete is found to be water cement ratio under room temperature conditions, super-plasticizer dosage at 200 and 400 °C temperatures and fine aggregate content at 600 and 800 °C temperatures. The test results indicate that the overall most influencing parameter with respect to residual compressive strength of heated non-pozzolanic HPC is fine aggregate content followed by water-cement ratio, dosage of super-plasticizer and cement content.

(v) The most influencing parameter affecting the residual compressive strength of fly ash based HPC is found to be cement content under room temperature conditions, super-plasticizer dosage at 200 °C temperature, fly ash content at 400 °C temperature and cement content at both 600 and 800 °C temperatures. The overall most influencing parameter for achieving a maximum residual compressive strength of heated high performance concrete containing fly ash, exposed to any temperature up to 800 °C, is the cement content. The fine aggregate content is found to be the second most influencing parameter, which is followed by fly ash content and super-plasticizer dosage.

(vi) The cement content and slag (GGBFS) content were found to be the important mix parameters at room temperature, 200 °C and at 400 °C temperatures for slag based HPC. While dosage of super-plasticizer appeared to be a significant parameter at 100 °C, 300 °C and 400 °C temperatures, the fine aggregate content was found to be an important parameter only at 400 °C temperature. Within the range of parameters considered in the present study, the cement content followed by GGBFS and super-plasticizer dosage are observed to be the overall most significant parameters influencing the residual compressive strength of slag based HPC.

(vii) The study shows that the cement content is the most significant parameter with maximum influence on the residual compressive strength of heated silica fume HPC. The fine aggregate content is observed to be the second most influencing parameter followed by the silica fume content and the

dosage of super plasticizer with respect to residual compressive strength of heated silica fume HPC.

(viii) Both pozzolanic and non- pozzolanic high performance concretes do not spall when heated to a furnace target temperature of 400 °C. An exposure at higher target temperatures such as 600 °C and 800 °C causes the thermal spalling of HPC irrespective of the type of pozzolana. The silica fume HPC is more vulnerable to spalling than fly ash and GGBFS HPC. Non-pozzolanic HPC is least influenced by spalling. The explosive spalling was observed between 82 to 129 minutes of start of heating for all HPC mixes. The surface temperature at the time of spalling varied from 479.2 °C to 511.2 °C and the core temperature varied from 196.7 to 241.7 °C.

(ix) The presence of axial load on reinforced HPC short columns during heating results in to more severe spalling compared to the reinforced HPC column specimens with no load during heating.

(x) Though the severe explosive spalling of core is saved by providing the confining reinforcement for high performance concrete columns, the cover is still liable to be spalled.

(xi) While the unstressed reinforced HPC column specimens show higher thermal gradient values than the stressed test condition specimens at lower temperatures of less than 400 °C, the unstressed residual test specimens show lower thermal gradient values than stressed residual test specimens at higher temperatures of 600 °C and 800 °C. The test data also reveals that the maximum temperature difference between the surface and centre of specimens and the time of maximum temperature difference are relatively more in pozzolanic high performance concretes compared to non-pozzolanic concrete.

(xii) During exposure to a cycle of heating and cooling, the short reinforced HPC column specimens experience an increase in the load beyond the initially applied preload in the early stages of heating, which is followed at the later stages of heating and then cooling by a decrease in load due to contraction. The test specimens developed large amount of restraint forces as the temperatures increased. It is postulated that this increase in the axial compressive pre load during heating causes more severe spalling of HPC.

(xiii) The residual load carrying capacity of reinforced HPC columns decreases with the increase in the temperature of exposure. Though the exposure temperatures of up to 400 °C do not affect the load capacity much, an exposure at higher temperatures of 600 °C and 800 °C reduces the residual load carrying capacity tremendously. The presence of axial service load during heating of reinforced HPC columns at 600 °C and 800 °C temperatures leads to a more severe reduction in the residual load carrying capacity due to the spalling of cover concrete. The addition of pozzolanic admixtures to HPC mix reduces the loss in the residual strength of HPC due to heating.

(xiv) The peak and post-peak strains of the load-strain behaviour of reinforced HPC column specimens increase with the increase in the temperature of exposure. The plain non-pozzolanic HPC specimens have more post-peak strains and deformability compared to the pozzolanic HPC mixes. The stressed (pre-loaded) specimens of each of the HPC mix show lower peak and post peak strains than their respective unstressed specimens. The results show that though the strains increase with the increase in temperature, the compressive toughness indicated by the area under the load-strain curve reduces as the temperature of exposure increases.

(xv) The thermal conductivity of HPC reduces with the increase in the temperature from room temperature to 400 °C irrespective of the type of HPC mix. In the temperature range of 400 °C to 700 °C, the thermal conductivity of all the HPC mixes, except slag based HPC mix, increases. In slag HPC, the thermal conductivity decreases up to 600 °C before increasing marginally between 600 °C to 700 °C temperature range. Plain non-pozzolanic HPC and fly ash based HPC mixes have more thermal conductivity than the slag HPC and silica fume based HPC mixes in this temperature range.

(xvi) The specific heat capacity of all types of HPC mixes remain almost constant and indicate similar trends up to 650 °C. However, the silica fume based HPC have maximum specific heat among all the mixes up to 650 °C temperature, followed by fly ash HPC, plain HPC and GGBFS HPC. The specific heat of all the HPC mixes increases abruptly to significantly high values after 650 °C temperature and then reduces sharply at around 750 °C temperature. In this temperature range, the fly ash HPC show a maximum value of specific heat

capacity, which is followed sequentially by plain, silica fume and GGBFS HPC mixes. Beyond 750 °C temperature, the specific heat of HPC mixes remain more or less stable with silica fume based HPC having a maximum specific heat in this range of temperatures.

(xvii) The thermal expansion of various types of HPC mixes increases with the increase in the temperature. It first increases steadily up to 500 °C and then rises sharply up to 600 °C. The thermal expansion of various HPC mixes remains almost stable afterwards up to 1000 °C temperature, except non-pozzolanic HPC, where an increase in the thermal expansion is observed even in this temperature range.

(xviii) The mass loss of HPC increases and the resulting mass of HPC decreases as the temperature increases up to 700 °C and thereafter remains stable at higher temperatures. All the chosen four HPC mixes show almost similar kind of trends.

(xix) The relationships have been proposed for estimating the thermal properties of various types high performance concretes. These relationships can be used as input data in computer programs for evaluating the response of high performance concrete structures exposed to fire.

LIST OF PUBLICATIONS

Journals:

1. Abdul Rahim. A., Sharma, U. K., Murugesan K., Sharma, A. and Arora, P. (2012), "Optimization of post-fire residual compressive Strength of concrete by Taguchi method", Journal of Structural Fire Engineering, Vol. 3, No. 2, pp. 169-180.
2. Abdul Rahim. A., Sharma, U. K., Murugesan. K., Sharma, A. and Arora, P. (2013), "Multi-response optimization of post-fire residual compressive strength of high performance concrete", Construction and Building Materials, Vol. 38, pp. 265–273.
3. Abdul Rahim. A., Sharma, U. K., Murugesan K. and Arora, P. "Influence of mix parameters on residual compressive strength of heated slag concrete" Fire Technology-Springer Publications (Under review).

International Conferences:

1. Sharma, U. K., Abdul Rahim. A., Murugesan K. (2013), "Effect of dosage of silica fume on spalling and post fire residual strength of high performance concrete", UKIERI, Concrete Congress, Innovations in concrete constructions, 5-8 March.
2. Abdul Rahim. A., Sharma, U. K., Murugesan K. (2013), "Effect of Load on Thermal Spalling of Reinforced Concrete Containing Various Mineral Admixtures" The 3rd International Workshop on Concrete Spalling due to Fire, Paris (France). (Accepted).

REFERENCES

1. Abbasi, A. F., Munir, A. and Wasim, M. (1987), "Optimization of concrete mix proportioning using reduced factorial experimental technique", ACI Material Journal, 84, pp. 55-63.
2. Abrams, M. S. (1971), "compressive strength of concrete up to 1600 °F (871 °C) in temperature and concrete," ACI SP-25, American Concrete Institute, Detroit, pp. 33-58.
3. ACI 211.4R-08, " Guide for selecting proportions for high-strength concrete using portland cement and other cementitious materials" Reported by ACI Committee, American Concrete Institute .
4. Aitcin, P. C. (1998), "High performance concrete", E & FN Spon, an imprint of Routledge, 11 New Fetter Lane, London SE4P 4EE.
5. Aitcin, P. C. (1995), "Developments the application high-performance concretes", Construction and Building Materials, 9 (1), pp. 13-17.
6. Aldea, C. M., Franssen, J. M., and Dotreppe, J. C. (1997), "Fire test on normal and high-strength reinforced concrete columns", NIST Special Publication 919, Proceeding of International workshop on fire performance of high strength, Gaithersburg.
7. Ali, F., Nadjai, A., and Choi, S. (2010), "Numerical and experimental investigation of the behaviour of high strength concrete columns in fire", Engineering Structures, 32(5), pp. 1236-1243.
8. Ali, F., Nadjai, A., Silcock, G. and Abu-Tair, A. (2004), "Outcomes of a major research on fire resistance of concrete columns", Fire Safety Journal, 39 (6), pp. 433-445.
9. Ali, F., O'Connor, D. and Abu-Tair, A. (2001), "Explosive spalling of high-strength concrete columns in fire", Magazine of Concrete Research, 53 (3), pp.197-204.
10. Al-Refaie, A., Li, M. H., and Tsao, C. W. (2008), "N-G approach for solving the multi-response problem in Taguchi method", Proceedings of the World Congress on Engineering, 1, pp. 1-6.

11. Antony, J. (2000), “Multi-response optimization in industrial experiments using Taguchi’s quality loss function and principal component analysis”, Quality and Reliability Engineering International, 16, pp. 3-8.
12. Antony, J. (2003), “Design of experiments for engineers and scientists”, Butterworth-Heinemann, 200 Wheeler Road, Burlington, MA 01803.
13. Antony, J., Anand, R. B., Kumar, M., and Tiwari, M. K. (2006), “Multiple response optimization using Taguchi methodology and Neuro-fuzzy based model”, Journal of Manufacturing Technology Management, 17(7), pp. 908-925.
14. Arioz, O. (2007), “Effects of elevated temperature on properties of concrete”, Fire Safety Journal, 42 (8), pp. 516-522.
15. Arioz, O. (2009), “Retained properties of concrete exposed to high temperatures: Size effect”, Fire and Materials, 33 (5), pp. 211-222.
16. Armand H. Gustaferro (1966), “Factors influencing the fire resistance of concrete”, Fire Technology, pp. 187-195
17. ASTM C 1363-2011, “Standard test method for thermal performance of building materials and envelope assemblies by means of a hot box apparatus”, ASTM International, American Society for Testing and Materials Standard Practice C1363, Philadelphia, PA.
18. ASTM C177-2010, “Standard test method for steady-state heat flux measurements and thermal transmission properties by means of the guarded-hot-plate apparatus”, ASTM International, American Society for Testing and Materials Standard Practice C 177, Philadelphia, PA.
19. ASTM E 831-2012, “Standard test method for linear thermal expansion of solid materials by thermo-mechanical analysis”, ASTM International, American Society for Testing and Materials Standard Practice E 831, Philadelphia, PA.
20. Ayan, E., Saatcioglu, O. and Turan. L. (2011), “Parameter optimization on compressive strength of steel fiber reinforced high strength concrete”, Construction and Building Materials, 25, pp. 2837-2844.
21. Aydin, S. and Baradan, B. (2007), “Effect of pumice and fly ash incorporation on high temperature resistance of cement based mortars”, Cement and Concrete Research 37, pp. 988–995.
22. Babu Narayan, K. S., Anil Kumar, G., Chandrakala, C., Shashikumar H. M., Katta Venkataramana, Yaragal, S. C., Chinnagiri Gowda, H. C., Reddy, G. R. and Sharma, A. (2010), “Studies on concrete Cylinders Subjected to Elevated

Temperatures", International Journal of Earth Science and Engineering, 3(4), pp. 691-698.

23. Badkar, D. S., Pandey, K. S. and Buvanashekaran, G. (2011), "Parameter optimization of laser transformation hardening by using Taguchi method and utility concept", International Journal of Advance Manufacturing Technology, 52, pp. 1067–1077.
24. Balendran, R. V., Rana, T. M., Maqsood, T. and Tang, W. C. (2002), "Strength and durability performance of HPC incorporating pozzolanas at elevated temperature", Structural Survey, 20(4), pp. 123-128.
25. Barr, B., Gettu, R., Al-Oraimi, S. K. A. and Bryars, L. S. (1996), "Toughness measurement-The need to think again", Cement and Concrete Composites, 18 (4), pp. 281-297.
26. Bastami, M. Khiabani, C. A. Baghabadrani, M. Kordi, M. (2011), "Performance of high strength concretes at elevated temperatures", Scientia Iranica, 18(5), pp. 1028-1036.
27. Basu, P. C. and Mittal, A. (1999), "High performance concrete for Indian nuclear power plants", Transactions of the 15th international conference on structural mechanics in reactor technology (SMiRT-15) Seoul, Korea.
28. Bayasi, Z. and Al Dhaheri, M. (2002), "Effect of exposure to elevated temperature on polypropylene fibre reinforced concrete", ACI Material Journal, 99 (1), pp. 22-26.
29. Baykasoglu, A., Oztas, A., and Ozbay, E. (2009), "Prediction and multi-objective optimization of high-strength concrete parameters via soft computing approaches", Expert Systems with Applications, 36 (3), pp. 6145-6155.
30. Bazant, Z. P. (1997), "Analysis of pore pressure thermal stress and fracture in rapidly heated concrete", Phan, L. T., Carino, N. J., Duthinh, D., Garboczi, E., (Editors), Proceedings of international workshop on fire performance of high-strength concrete, pp. 155-164.
31. Behnood, A. and Ghandehari, M. (2009), "Comparison of compressive and splitting tensile strength of high-strength concrete with and without polypropylene fibers heated to high temperatures", Fire Safety Journal, 44, pp. 4015-1022.
32. Behnood, A. and Ziari, H. (2008), "Effects of silica fume addition and water to cement ratio on the properties of high-strength concrete after exposure to high temperatures", Cement and Concrete Composites, 30 (2), pp. 106-112.

33. Benmarce, A. and Guenfoud, M. (2005), "Experimental behaviour of high-strength concrete columns in fire", Magazine of Concrete Research, 57 (5), pp. 283-287.
34. Bentz, D. P., Peltz, M.A., Duran-Herrera, A., Valdez, P. and Juarez C. A, (2011), "Thermal properties of high-volume fly ash mortars and concretes", Journal of Building Physics 34 (3), pp. 263-275.
35. Bentz, D. (2000), "Fibers, percolations and spalling of high performance concrete", ACI Material Journal, 97 (3), pp. 351-359.
36. Bharatkumar, B. H., Narayanan, R., Raghuprasad, B. K., Ramachandramurthy, D. S. (2001), "Mix proportioning of high performance concrete", Cement & Concrete Composites, 23, pp. 71-80.
37. Bhargava, P., Sharma, U. K., and Kaushik, S. K. (2006), "Compressive stress-strain behavior of small scale steel fibre reinforced high strength concrete cylinders", Journal of Advanced Concrete Technology, 4(1), pp. 109-121.
38. Bingol, A. F., and Gul, R. (2009), "Effect of elevated temperatures and cooling regimes on normal strength concrete", Fire and Materials, 33 (2), pp. 79-88.
39. Buchanan, A. H. (2001), "Structural design for fire safety", John Wiley and Sons, Ltd, West Sussex, U. K., pp.421.
40. Bureau of Indian Standards (1997), "Indian Standard specification for coarse and fine aggregate from natural sources for concrete, code of practice, IS 383: 1970, (Second revision)", BIS New Delhi, pp. 21.
41. Bureau of Indian standards (1999), "Specification for granulated slag for the manufacture of Portland slag cement, I. S. 12089-1987, (first revision)", BIS New Delhi.
42. Bureau of Indian Standards (1999), Recommended guidelines for concrete mix design, IS10262: 1982 (Reaffirmed 2009)", BIS New Delhi, pp. 21.
43. Bureau of Indian Standards (2000), "Indian Standard Plain and Reinforced Concrete, code of practice, IS 456: 2000, (Fourth revision)", BIS New Delhi, pp. 100.
44. Bureau of Indian Standards (2003), "Indian Standard specification for Silica fume, code of practice, IS 15388: 2003", BIS New Delhi, pp. 6.
45. Bureau of Indian Standards (2003), "Indian Standard specification for concrete admixture, code of practice, IS9103: 1999 (Reaffirmed 2004)", BIS New Delhi, pp. 14.

46. Bureau of Indian Standards (2003), “Pulverized fuel ash — Specification: for use as pozzolana in cement, cement mortar and concrete”, IS 3812 (Part 2): 2003, (Second revision)”, BIS New Delhi, pp. 4.
47. Bureau of Indian Standards (2005), “Indian Standard 43 Grade ordinary Portland cement specification, code of practice, IS 8112: 1989, (First revision, Reaffirmed 2005),” BIS New Delhi, pp. 8.
48. Bureau of Indian Standards (2005), “Methods of chemical analysis of Hydraulic cement, code of practice, IS 4031: 1985, (First revision, Reaffirmed 2005)”, BIS New Delhi, pp. 42.
49. Bureau of Indian Standards (2005), “Methods of physical tests for of Hydraulic cement: Part 3 Determination of soundness, IS 4031 (Part 3): 1999, (Reaffirmed 2005)”, BIS New Delhi, pp. 4.
50. Bureau of Indian Standards (2005), “Methods of physical tests for of Hydraulic cement: Part 4 Determination of consistency of standard cement paste, IS 4031 (Part 4): 1988, (Reaffirmed 2005)”, BIS New Delhi, pp. 2.
51. Bureau of Indian Standards (2005), “Methods of physical tests for of Hydraulic cement: Part 5 Determination of Initial and final setting times, IS 4031 (Part 5): 1988, (Reaffirmed 2005)”, BIS New Delhi, pp. 2.
52. Bureau of Indian Standards (2005), “Methods of physical tests for of Hydraulic cement: Part 6 Determination of compressive strength of hydraulic cement (other than masonry cement), IS 4031 (Part 6): 1988, (Reaffirmed 2005)”, BIS New Delhi, pp. 2.
53. Bureau of Indian Standards (2007), “Indian Standard methods of sampling and physical tests for refractory materials, code of practice, IS 1528 (Part 16): 2007: 1990”, BIS New Delhi, pp. 09.
54. Bureau of Indian Standards (2008), “Methods of physical tests for of Hydraulic cement: Part 2 Determination of finesses by specific surface by Blaine air permeability method, IS 4031 (Part 2): 1999, (Reaffirmed 2008)”, BIS New Delhi, pp. 7.
55. Campbell-Allen, D., and Desai, P. M. (1967), “The influence of aggregate on the behaviour of concrete at elevated temperatures”, Nuclear Engineering and Design, 6 (1), pp. 65-77.

56. Carman, A. P. and Nelson, R. A. (1925), "The thermal conductivity and diffusivity of concrete", Engineering Experiment Station, Bulletin No. 122, University of Illinois.
57. Carstensen, J. V. (2011), "Material modelling of reinforced concrete at elevated temperatures", Master thesis, Fire Safety section for Building Design, Department of Civil Engineering, the Technical University of Denmark.
58. Castillo, C. and Durani, A. J. (1990), "Effect of transient high temperature on high-strength concrete", ACI Material Journal, 87 (1), pp. 47-53.
59. Chaboki-Khiabani, A., Bastami, M., Baghbadrani, M. and Kordi, M. (2011), "Optimization of the concrete mix proportions centered on performance after exposure to high temperature", Switzerland Advanced Materials Research, Trans Tech Publications, 268-270, pp. 372-376.
60. Chan, S. Y. N., Peng, G. F., Anson. M. (1999)[b], "Fire behaviour of high performance concrete made with silica fume at various moisture contents", ACI Material Journal, 96 (3), pp. 405-411.
61. Chan, S. Y. N. Peng, G.F and Chan, J. K. W. (1996), "Comparison between high strength concrete and normal strength concrete subjected to high temperature", Materials and Structures, 29, pp. 616-619.
62. Chan, S. Y. N., Luo, X. and Sun, W. (2000), "Effect of high temperature and cooling regimes on the compressive strength and pore properties of high performance concrete", Construction and Building Materials, 14 (5), pp. 261-266.
63. Chan, S. Y. N., Peng, G. F. and Anson, M. (1999)[a], " Residual strength and pore structure of high-strength concrete and normal-strength concrete after exposure to high temperatures", Cement Concrete Composites, 21, pp. 23-27.
64. Chang, P. K. (2004), "An approach to optimizing mix design for properties of high performance concrete", Cement and Concrete Research, 34, pp. 623-629.
65. Chang, P. K., Peng, Y. N. and Hwang, (2001), "A design consideration for durability of high performance concrete", Cement and Concrete Composites, 23, pp. 375-380.
66. Chaulia, P. K. and Das, R. (2008), "Process Parameter Optimization for Fly Ash Brick by Taguchi Method", Materials Research, 11(2), pp. 159-164.
67. Cheng Yeh, (2003), "A mix proportioning technology for fly ash and slag concrete using artificial neural network" Chung Hua Journal of Science and Engineering, 1 (1), pp. 77-84.

68. Chidiac, S.E. and Panesar, D. K. (2008), "Evolution of mechanical properties of concrete containing ground granulated blast furnace slag and effects on the scaling resistance test at 28 days", Cement and Concrete Composites, 30 (2): pp.63-71.
69. Consolazio, G. R., McVay, M. C., and Rish III, J. W. (1998), "Measurement and prediction of pore pressures in saturated cement mortar subjected to radiant heating", ACI, Materials Journal, 95(5), pp.525-536.
70. Cruz, C. R. and Gillen, M. (1980), "Thermal expansion of Portland cement paste, mortar, and concrete at high temperatures", Fire and Materials, 4(2), pp. 66-70.
71. Demirboga, R. and Gul, R. (2003), "Thermal conductivity and compressive strength of expanded perlite aggregated with mineral admixtures", Energy and Building, 35, pp. 1155-1159.
72. Demirboga, R. (2003[a]), "Thermo-mechanical properties of sand and high volume mineral admixtures", Energy and Buildings, 35, pp. 435-439.
73. Demirboga, R. (2003[b]), "Influence of mineral admixtures on thermal conductivity and compressive strength of mortar", Energy and Buildings, 35, pp. 189-192.
74. Demirboga, R. and Gul, R. (2003b), "The effects of expanded perlite aggregate, silica fume and fly ash on the thermal conductivity of lightweight concrete", Cement and Concrete Research, 33, pp. 723–727.
75. Demirel, B. and Kelestemur, O. (2010), "Effect of elevated temperature on the mechanical properties of concrete produced with finely ground pumice and silica fume", Fire Safety Journal, 45 (6), pp. 385-391.
76. Dias, W. P. S., Khoury, G. A. and Sullivan, P. J. E. (1990), "Mechanical properties of hardened cement paste exposed to temperature up to 700 °C", ACI Material Journal, 87(2), pp. 160-166.
77. Diederichs, Jumppanen, U. M. and Penttala, V. (1989), "Behaviour of high strength concrete at high temperatures", Report No.92, Department of Structural Engineering, Helsinki University Technology.
78. Dotreppe, I. C., Franssen, I. M., Bruls, A., Baus, R., Vandevelde, P., Minne, T.R., Nieuwenburgt, D. V. and Lambottet, H. (1996), "Experimental research on the determination of the main parameters affecting the behaviour reinforced concrete columns under fire conditions", Magazine of Concrete Research, 49 (179), pp.117-127.

79. England, G. L. and Khoylou, N. (1995), "Moisture flow in concrete under steady state non-uniform temperature states: experimental observations and theoretical modeling", Nuclear Engineering and Design, 155, pp. 83-107.
80. Ezeldin, A. S. and Balaguru, P. N. (1992), "Normal-and high-strength fiber-reinforced concrete under compression", Journal of Materials in Civil Engineering, 4(4), pp. 415-429.
81. Felicetti, R. and Gambarova, P. G. (1998), "Effects of high temperature on the residual compressive strength of high strength siliceous concretes", ACI Materials Journal, 95 (4), pp. 395-405.
82. Fletcher, I. A., Welch, S., Torero, J. L., Carvel, R. O. and Usmani, A. (2007), "Behaviour of Concrete Structures in Fire", Thermal Science, 11 (2), pp. 37–52.
83. Freskakis, G. N. (1984), "Behaviour of reinforced concrete at elevated temperatures" Report No. DOE/CL/98004-34, Preceding of ASCE conference on Structural Engineering in Nuclear Facilities Raleigh, North Carolina.
84. Fu, Y. and Li, L. (2011), "Study on mechanism of thermal spalling in concrete exposed to elevated temperatures", Materials and Structures, 44, pp. 361-376.
85. Fu, Y. F., Wong, Y. L., Poon, C. S. and Tang, C. A. (2005), "Stress–strain behaviour of high-strength concrete at elevated temperatures", Magazine of Concrete Research, 57 (9), pp. 535–544.
86. Gaitonde, V. N., Karnik S. R. and Davim, J. P. (2009), "Multi-performance optimization in turning of free-machining steel using Taguchi Method and utility Concept", Journal of Materials Engineering and Performance, 18, pp. 231–236.
87. Gaitonde, V. N., Karnik, S. R., Achyutha. B. T. and Siddeswarappa. B. (2006), "Multi-performance optimization in drilling using Taguchi's quality loss function", Indian Journal of Engineering and Materials Sciences, 13, pp. 209-216.
88. Garg, R. (2010), "Effect of process parameters on performance Measures of wire electrical discharge machining", Ph.D Thesis. N.I.T Kurukshetra,.
89. Ghandehari, M., Behnood, A., and Khanzadi, M. (2010), "Residual mechanical properties of high-strength concretes after exposure to elevated temperatures", ASCE, Journal of Materials in Civil Engineering, 22 (1), pp. 59-64.
90. Gillie, M., Usmani, A., Rotter, M., O'Connor, M. (2001), "Modeling of heated composite floor slabs with reference to the Cardington experiments", Fire Safety Journal, 36 (8): pp. 745–67.

91. Hadiwidodo, Y. S. and Mohd, S. B. (2010), "Taguchi Experiment Design for Investigation of Freshened Properties of Self-Compacting Concrete", American Journal of Engineering and Applied Sciences, 3 (2), pp. 300-306.
92. Hager, I., sliwinski, J. and Durica, T. (2005), "The impact of heating conditions on temperature distribution in high performance concrete specimens of various shapes and sizes", Slovak Journal of Civil Engineering, Slovak University of Technology, 2006/2, pp. 8-13.
93. Han, C. G., Han, M. C. and Heo, Y. S., (2008), "Spalling properties of high strength concrete mixed with various mineral admixtures subjected to fire", International Journal of Concrete Structures and Materials, 2 (1), pp. 41-48.
94. Han, C. G., Hwang, Y. S., Yang, S. H, and Gowripalan, N. (2005), "Performance of spalling resistance of high performance concrete with polypropylene fiber contents and lateral confinement", Cement and Concrete Research, 35, pp.1747-1753.
95. Harmathy, T. Z. (1964),"Variable-state methods of measuring the thermal properties of solids", Journal of Applied Physics, 35 (4), pp. 1190-1200.
96. Harmathy, T. Z. (1970), "Thermal Properties of Concrete at Elevated Temperatures", Journal of Materials, JMLSA, 5 (1), pp. 47-74.
97. Harmathy, T. Z., and Allen, L. W. (1973). "Thermal properties of selected masonry unit concretes", Journal of American Concrete Institute, 70, pp. 132–142.
98. Hertz, K. D. (1981), "Simple Temperature calculations of fire exposed concrete constructions", Report No. 160, Institute of Building Design, Technical University of Denmark.
99. Hertz, K. D. (1984), "Heat induced explosion of dense concretes", Report 166. CIB W14/84/33(DK) Institute of Building Design (now Department of Buildings and Energy), Technical University of Denmark, 20p.
100. Hertz, K. D. (1992), "Danish Investigations on Silica Fume Concretes at Elevated Temperatures", ACI Material Journal, 89 (4), pp. 345-347.
101. Hertz, K. D. (2005), "Concrete strength for fire safety design", Magazine of Concrete Research, 57 (8), pp.445–453.
102. Hertz, K.D. (2003), "Limits of spalling of fire-exposed concrete", Fire Safety Journal, 38, pp. 103–116.
103. Hilsdorf, H. K. (1967), "A method to estimate the water content of concrete shields", Nuclear Engineering and Design 6, pp. 251-263.

104. Hinislioglu, S. and Bayrak, O. U. (2004), "Optimization of early flexural strength of pavement concrete with silica fume and fly ash by the Taguchi method", Civil Engineering and Environmental Systems, 21 (2), pp. 79-90.
105. Hu, X. F., Lie, T. T., Polomark, G. M., and MacLaurin, J. W. (1993), "Thermal properties of building materials at elevated temperatures", Internal Report - 643, Institute for Research in Construction, National Research Council Canada, 1-54.
106. Hull, W. A. and Iugberg, S. H. (1925), "Fire resistance of concrete columns", U.S. Bureau of Standards Notes, Technologic Papers, 272, pp. 379-381.
107. Husem, M. (2006), "The effects of high temperature on compressive and flexural strength of ordinary and high performance concrete", Fire Safety Journal, 41, pp. 155-163.
108. Ibrahim, T., Gul. R., and Celik C (2008), "A Taguchi approach for investigation of some physical properties of concrete produced from mineral admixtures", Building and Environment, 43, pp. 1127-1137.
109. Jamil, M., Zain. M. F. M. and Basri. B. H., (2009), "Neural network simulator model for optimization in high performance concrete mix design", European Journal of Scientific Research 34 (1), pp.61-68.
110. Janotka, I., Nurnbergerova, T., and Nad, L. (2000), "Behaviour of high-strength concrete with dolomite aggregate at high temperatures", Magazine of Concrete Research, 52 (6), pp. 399-409.
111. Jansson, R. (2005), "Measurement of Concrete Thermal Properties at High Temperature", Proceedings of the Workshop Fire Design of Concrete Structures: What now? What next? Editors: Gambarova, P. G., Felicetti, R., Meda, A., Riva, P., pp.101-107.
112. Jau, W. C., and Huang, K. L. (2008), "A study of reinforced concrete corner columns after fire", Cement and Concrete Composites, 30 (7), pp. 622-638.
113. Kalifa, P., Chegoire, G and Galle, C. (2001), "High-temperature behaviour of HPC with polypropylene fibres from spalling to microstructure", Cement and Concrete Research, 31, pp. 1487-1499.
114. Kalifa, P., Menneteau, F. D., and Quenard, D. (2000), "Spalling and pore pressure in HPC at high temperatures", Cement and concrete research, 30 (12), pp. 1915-1927.

115. Kanema, M., Pliya, P., Noumowe, A., and Gallias, J. L. (2011), "Spalling, thermal, and hydrous behaviour of ordinary and high-strength concrete subjected to elevated temperature", Journal of Materials in Civil Engineering, ASCE, 23 (7), pp.921-930.
116. Kansal, H. K., Singh, S. and Kumar, P. (2006), "Performance parameters optimization (multi characteristics) of power mixed electric discharge machining (PMEDM) through Taguchi's method and utility concept", Indian Journal of Engineering and Materials Sciences, 13, pp. 209-216.
117. Kaspar, W., Xi, Y., Lee, K. and Kim, B. (2009), "Thermal response of reinforced concrete Structures in nuclear power plants", University of Colorado at Boulder, SESM No. 02-2009.
118. Kassir, M.K., Bandyopadhyay, K. K. and En. Reich (1996), "Thermal degradation of concrete in the temperature range from ambient to 315 ℃ (600 °F)", Engineering Research and Applications Division, Department of Advanced Technology Brookhaven National Laboratory, Associated Universities, Inc. Upton, New York 11973-5000.
119. Khaliq, W. and Kodur, V. K. R. (2011[b]), "High temperature properties of fiber reinforced high-strength concrete", Innovations in Fire Design of Concrete Structures - ACI SP 279, 3-1-42.
120. Khaliq, W. and Kodur, V. K. R. (2012), "Behavior of high strength fly ash concrete columns under fire conditions", Materials and Structures, DOI: 10.1617/s11527-012-9938-7, pp 1-11.
121. Khaliq, W. and Kodur, V.K.R. (2011[a]), "Thermal and mechanical properties of fiber reinforced high performance self-consolidated concrete at elevated temperature", Cement and Concrete Research, 41, pp. 1112-1122.
122. Khan. M. I. (2012), "Mix proportions for HPC incorporating multi-cementitious composites using artificial neural networks, Construction and Building Materials, 28, pp. 14-20.
123. Khoury, G. A. (2000[b]), "Effects of fire on concrete and concrete structures", Progress in Structural Engineering and Materials, 2 (4), pp.429-447.
124. Khoury, G. A. and Anderberg, Y. (2000[a]), "concrete spalling review", A report on Fire Safety Design, Swedish National Road Administration.
125. Khoury. G. A. (1992), "Compressive Strength of Concrete at High Temperature: A Reassessment", Magazine of Concrete Research, 44 (161), pp. 291-309.

126. Khoury. G. A. and Willoughby, B. (2008), "polypropylene fibres in heated concrete. Part 1: Molecular structure and materials behaviour, Magazine of Concrete Research, 60 (2), pp. 125-136.
127. Kim, G. Y., Kim, Y. S. and Lee, T. G. (2009), "Mechanical properties of high strength concrete subjected to high temperature by stressed test", Transactions of Nonferrous Metals Society of China, 19, pp. 128-133.
128. Kim, J. I., Kim, D. K., Feng, M. Q., and Yazdani, F. (2004), "Application of neural networks for estimation of concrete strength", Journal of materials in civil engineering, 16 (3), pp. 257-264.
129. Kmita, A. (2000), "A new generation of concrete in civil engineering", Journal of Materials Processing Technology, 106, pp. 80-86.
130. Knaack, A. M., Kurama, Y. C. and Kirkner, D. J. (2010), "Compressive Strength Relationships for Concrete under Elevated Temperatures", ACI Materials Journal, 107 (2), pp. 164-175.
131. Ko, J., Ryu, D. and Noguchi, T. (2011), "The spalling mechanism of high strength concrete under fire", Magazine of Concrete Research, 63(5), 357-370.
132. Kodur, V. K .R. (2005), "Guidelines for fire resistance design of high-strength concrete columns", Journal of Fire Protection Engineering, 15, pp. 93-106.
133. Kodur, V. K. R. and Sultan, M. A. (1998), "Structural behaviour of high strength concrete columns exposed to fire", International Symposium on High Performance and Reactive Powder Concrete, Sherbrooke, Quebec, Sept. 1998, pp. 217-232.
134. Kodur, V. K. R. and Phan, L. (2007), "Critical factors governing the fire performance of high strength concrete systems", Fire Safety Journal, 42 (6), pp. 482-488.
135. Kodur, V. K. R. and Raut. N, (2010), "Performance of concrete structures under fire hazard: emerging trends", Indian Concrete Journal, 84 (4), pp. 7-18.
136. Kodur, V. K. R. and Sultan, M. A. (2003), "Effect of temperature on thermal properties of high strength concrete", ASCE, Journal of Materials in Civil engineering, 15 (2), pp. 101-107.
137. Kodur, V. K. R. and Sultan, M.A. (1998), "Structural behaviour of high strength concrete columns exposed to fire", NRCC-41736, International Symposium on High Performance and Reactive Powder Concrete, Sherbrooke, Quebec, Sept. 1998, pp. 217-232.

138. Kodur, V. K. R., and McGrath, R. (2003[b]), "Fire endurance of high strength concrete columns", Fire Technology, 39 (1), pp. 73-87.
139. Kodur, V. K. R., and McGrath, R. (2006), "Effect of silica fume and lateral confinement on fire endurance of high strength concrete columns", Canadian Journal of Civil Engineering, 33 (1), pp. 93-102.
140. Kodur, V. K. R., Cheng, F.P., Wang, T.C. and Sultan, M. A. (2003[a]), "Effect of strength and fiber reinforcement on the fire resistance of high strength concrete columns", Journal of Structural Engineering, ASCE, 129 (2), pp. 253–259.
141. Kodur, V. K. R., Dwaikat, M. M. S., and Dwaikat, M. B. (2008), "High temperature properties of concrete for fire resistance modelling of structures", ACI Materials Journal, 105 (5), pp. 517-527.
142. Kodur, V. K. R., Wang, T. C., and Cheng, F. P. (2004), "Predicting the fire resistance behaviour of high strength concrete columns", Cement and Concrete Composites, 26 (2), pp. 141-153.
143. Kodur, V., Dwaikat, M., and Fike, R. (2010), "High-temperature properties of steel for fire resistance modeling of structures", Journal of Materials in Civil Engineering, ASCE, 22 (5), pp. 423-434.
144. Kodur, V.K.R. and Khaliq, W. (2011), "Effects of thermal properties of different types of high-strength concrete", ASCE, Journal of Materials in Civil Engineering, 23 (6), pp.723-801.
145. Komeili, M., Milani, A. S. and Tesfamariam, S. (2012), "Performance based earthquake evaluation of reinforced concrete buildings using design of experiments", International Journal of Materials and Structural Integrity (IJMSI), 6 (1), pp. 1-25.
146. Kumar, P., Barua P. B., Gaindhar J. L. (2000), "Quality optimization (multi-characteristic) through Taguchi's technique and utility concept", Quality Reliability Engineering International, 16, pp. 475-485.
147. Kumar, V., Sharma, U. K., Singh, B. and Bhargava, P. (2013), "Effect of temperature on mechanical properties of pre-damaged steel reinforcing bars", Construction and Building Materials, 46, pp. 19-27.
148. Laskar, A. I. and Talukdar, S. (2008), "A new mix deign method for high performance concrete", Asian Journal of Civil Engineering (Building and Housing) 9 (1), pp. 15-23.

149. Laskar, A. I. and Talukdar, S. (2008), "Rheological behaviour of high performance concrete with mineral admixtures and their blending", Construction and Building Materials, 22 (12), pp. 2345-2354.
150. Lea, F. C. (1920), "The effect of temperature on some of the properties of material", Engineering, London, 110 (3), pp. 293-298.
151. Lea, F. C. and Straddling, R. E. (1922), "The resistance to fire of concrete and reinforced concrete", Engineering, London, 114, pp. 341-344 and pp. 380-382.
152. Lee, J., Xi, Y., and Willam, K. (2008), "Properties of concrete after high-temperature heating and cooling", ACI Materials Journal, 105 (4), pp. 334-341.
153. Li, M., Wu, Z., Qian, C. and Sun, W. (2008), "Strength deterioration of high strength concrete exposed to high temperatures and its prevention and rehabilitation", Advances in Civil Engineering Materials, The 50-yearsTeaching and Research anniversary of Prof. Sun Wei on advances in Civil Engineering Materials, pp. 263-274.
154. Li, M., Wu, Z., Kao, H. and Qian, C. (2010), "Evaluation of the fire-exposed temperature of concrete", Magazine of Concrete Research, 62 (9), pp. 617-624.
155. Liao, H. C., and Chen, Y. K. (2002), "Optimizing multi-response problem in the Taguchi method by DEA based ranking method. International Journal of Quality and Reliability Management, 19 (7), pp. 825-837.
156. Lie, T. T. (1992), "Structural fire protection", ASCE Committee on Fire Protection, Structural division, American Society of Civil Engineers, New York, pp. 225-229.
157. Lie, T. T. and Kodur, V. K. R. (1996), "Thermal and mechanical properties of steel fibre reinforced concrete at elevated temperature", Canadian Journal of Civil Engineering, 23 (2), pp. 511-517.
158. Lie, T. T., and Celikkod, B. (1991), "A method to calculate the fire resistance of circular reinforced concrete columns," ACI Materials Journal, 88 (1), pp. 84-91.
159. Lie, T. T., and Irwin, R. J. (1993), "Method to calculate the fire resistance of reinforced concrete columns with rectangular cross section", ACI structural Journal, 90 (1), pp.52-60.
160. Lie, T. T., and Kodur, V. K. R. (1995), "Thermal properties of fibre-reinforced concrete at elevated temperatures", Internal Report - 683, Institute for Research in Construction, National Research Council Canada, Institute for Research in Construction, pp. 17.

161. Lie, T. T., and Kodur, V. K. R. (1995), "Thermal properties of fibre-reinforced concrete at elevated temperatures", Internal Report - 695, Institute for Research in Construction, National Research Council Canada, Institute for Research in Construction, pp. 19.
162. Lie, T. T., Rowe, T. J. and Lin T. D. (1986), "Residual strength of fire-exposed reinforced concrete columns" Evaluation and Repair of Fire Damage to Concrete, American Concrete institute, ACl- SP- 92-9, pp. 153-174.
163. Lim, C. H., Yoon, Y. S., Kim, J. H. (2004), "Genetic algorithm in mix proportioning of high-performance concrete", Cement and Concrete Research, 34, pp. 409–420.
164. Lin, C. T., Chang, C. W. Chen, C. B. (2006), "A simple approach to solving multi-response quality characteristics problems in CMOS ion implantation", International Journal of Advance Manufacturing Technology, 28, pp. 592-595.
165. Lixian, L., Reddy D.V. and Sobhan K. (2010), "Size effect on fire resistance of reinforced concrete columns and beams", 8th Latin American and Caribbean Conference for Engineering and Technology, (LACCEI'2010) "Innovation and Development for the Americas", June 1-4, Arequipa, Peru.
166. Luccioni, B. M., Figueroa, M. I., and Danesi, R. F. (2003), "Thermo-mechanic model for concrete exposed to elevated temperatures", Engineering Structures, 25 (6), pp. 729-742.
167. Luo, X., Sun, W., and Chan, S. Y. N. (2000), "Effect of heating and cooling regimes on residual compressive strength and microstructure of normal and high performance concrete", Construction and Building Materials, 30, pp. 379-383.
168. Malhotra, H. L. (1956), "The effect of temperature on the compressive strength of concrete", Magazine of Concrete Research, 8 (22), pp. 85-94.
169. Mehta, P. K and Aitcin, P. C. (1990), "Principles underlying the production of high-performance concrete", Cement Concrete and Aggregate, ASTM Journal, 12(2), pp. 70-78.
170. Modirzadeh, M., Tesfamariam, S. and Milani, A. S. (2012). "Performance based earthquake evaluation of reinforced concrete buildings using design of experiments", Expert Systems with Applications, 39(3), pp. 2919-2926.
171. Mohamedbhai, G. T. G (1986), "Effect of Exposure Time and Rate of Heating and Cooling on Residual Strength of Heated Concrete", Magazine of Concrete Research, 38 (136), pp.151-158.

172. Morsy, S. H., Alsayed, S. H. and Aqel, M. (2010), "Effect of elevated temperature on mechanical properties and microstructure of silica flour concrete", International Journal of Civil and Environmental Engineering (IJCEE-IJENS), 10(1), pp. 1-6.
173. Mukherjee, A., and Nag Biswas, S. (1997), "Artificial neural networks in prediction of mechanical behavior of concrete at high temperature", Nuclear engineering and design, 178 (1), pp. 1-11.
174. Myers, R. H., Montgomery, D. C., Vining, G. G., Borror, C. M., and Kowalski, S. M. (2004), "Response surface methodology: a retrospective and literature survey", Journal of Quality Technology, 36 (1), pp. 53-77.
175. Narendra, H., Muthu, K. U., Mattaneh, H., Naidu, N. V. R. and Sowmya B. S. (2008),"Optimisation of SCC mix using Taguchi method", International Conference on Construction and Building Technology (ICCBT 2008-A-(17)), Kualalumpur, Malaysia, June16-20, pp. 191-204.
176. Nassif, A.Y., Rigden, S. and Burley, E. (1999), "The effects of rapid cooling by water quenching on the stiffness properties of fire-damaged concrete", Magazine of Concrete Research, 51 (4), pp. 255-261.
177. Naus, D. J. and Graves, H. L. (2010), "A compilation of elevated temperature concrete material property data and information for use in assessments of nuclear power plant reinforced concrete structures", Prepared by DJ Naus, NUREG/CR-7031, Office of Nuclear Regulatory Research, US Nuclear Regulatory Commission.
178. Naus, D. J. and Graves, H. L. (2006), "The effect of elevated temperature on concrete materials and structures - a literature review", Oak Ridge National Laboratory, U.S. Nuclear Regulatory Commission, Office of Nuclear Regulatory Research, Washington, DC 20555-0001.
179. Netinger, I. I., Kesegic, I. and Guljas, I. (2011), "The effect of high temperatures on the mechanical properties of concrete made with different types of aggregates", Fire Safety Journal, 46, pp .425-430.
180. Neville, A. M. (2009), "Properties of concrete", Pearson Education, Dorling Kindersley (india) Pvt. ltd.4th edition, Delhi.
181. Noorossana, R., Davanloo Tajbakhsh, S., and Saghaei, A. (2009), "An artificial neural network approach to multiple-response optimization", The International Journal of Advanced Manufacturing Technology, 40 (11), pp. 1227-1238.
182. Norton, C. L. (1912), "Some Thermal Properties of Concrete," Proceedings, National Association of Cement Users (ACI), 7, pp. 78-90.

183. Noumowe, A. (2003), "Mechanical properties and microstructure of high strength concrete containing polypropylene fibres exposed to temperatures up to 200 °C", Cement and Concrete Research, 35, pp. 2192 - 2198.
184. Noumowe, A., Siddique, R., and Ranc, G. (2009), "Thermo-mechanical characteristics of concrete at elevated temperatures up to 310 °C", Nuclear Engineering and Design, 239 (3), pp. 470-476.
185. Nuruddina, M. F., and Bayuajia, R. (2009), "Application of Taguchi's approach in the optimization of mix proportion for Microwave Incinerated Rice Husk Ash Foamed Concrete", International Journal of Civil and Environmental Engineering IJCEE, 9 (9), pp.121-129.
186. Oh, J. W., Lee, I. W, Kim, J. T. and Lee, G. W. (1999), "Application of Neural Networks for Proportioning of Concrete Mixes", ACI Materials Journal, 96 (1), pp. 61-67.
187. Ozbay, E., Baykasoglu, A., Oztas, A. and Ozbebek. H. (2006), "An experimental compression of optimum mix proportions of high strength concrete proposed by Taguchi method and genetic algorithm", proceeding of 5th international symposium on intelligent manufacturing systems, pp. 1062-1070.
188. Ozbay, E., Baykasoglu, A., Oztas, A. and Ozbebek. H. (2009), "Investigating mix proportions of high strength self compacting concrete by using Taguchi method", Construction and Building Materials, 23, pp. 694-702.
189. Pan, Z., Sanjayan, J. G., and Kong, D. L. (2012), "Effect of aggregate size on spalling of geo-polymer and Portland cement concretes subjected to elevated temperatures", Construction and Building Materials, 36, pp. 365-372.
190. Papayanni, J. and Valiasis, T. (1991), "Residual mechanical properties of heated concrete incorporating different pozzolanic materials", Materials and Structures, 24 (2), pp. 115-121.
191. Peng , G. F. (2000), Evaluation of fire damage to high performance concrete", Ph. D Thesis, Department of civil Engineering and Structural Engineering, The Hong Kong Polytechnic University, Hong Kong, pp. 213.
192. Peng, G. F., Yang W. W., Zhao, J., Liu, Y. F., Bian, S. H., Zhao, L. H. (2006), "Explosive spalling and residual mechanical properties of fiber-toughened high-performance concrete subjected to high temperatures", Cement and Concrete Research, 36, pp. 723–727

193. Phadke, M. S. (1995), "Quality engineering using robust design", Prentice Hall PTR Upper Saddle River, New Jersey, USA
194. Phan, L. and Carino, N. J. (2001), "Materials properties of high strength concrete at elevated temperatures", NISTIR 6726, US Department of Commerce, National Institute of Standards and Technology, pp. 1-115.
195. Phan, L. T. (1996), "Fire Performance of High-Strength Concrete: A Report of the State-of-the-Art", NISTIR 5934, US Department of Commerce, Technology Administration, National Institute of Standards and Technology, Office of Applied Economics, Building and Fire Research Laboratory, pp. 1-115.
196. Phan, L. T. and Carino, N. J. (2003), "Code provisions for high strength concrete strength temperature relationship at elevated temperatures", Materials and Structures, 36(256), pp. 91-98.
197. Phan, L. T. and Nicholas, J. Carino. (1998), "Review of mechanical properties of HSC at elevated temperature", Journal of Materials in Civil Engineering, ASCE, 10 (1). pp. 58-64.
198. Phan, L. T. and. Carino, N. J (2002), "Effects of test conditions and mixture proportions on behaviour of high strength concrete exposed to high temperatures", ACI Material Journal, 99 (1), pp. 54-66.
199. Phan, L. T., Lawson, J. R. and Davis, F. L. (2001), "Effects of elevated temperature exposure on heating characteristics, spalling, and residual properties of high performance concrete", Materials and Structures, 34, pp. 83-91
200. Prasad, P. D. M. S., Sharma, U. K. and Bhargava, P. (2009), "Effects of elevated temperatures on the properties of reinforcing steel bars", Institutions of Engineers (India), 90, pp. 3-6.
201. Poon, C. S., Azhar, S., Anson, M., Wong, Y. L. (2001 [a]), "Comparison of the strength and durability performance of normal and high-strength pozzolanic concretes at elevated temperatures," Cement and Concrete Research, 31 (9), pp. 1291-1300.
202. Poon, C. S., Shui, Z. H. and Lam, L. (2004), " Compressive behavior of fiber reinforced high-performance concrete subjected to elevated temperatures", Cement and Concrete Research, 34(12), pp. 2215-2222.
203. Purkiss, J. A. (2007), "Fire safety engineering-design of structures", 2nd Edition, Butterworth-Heinemann publications.

204. Rajasekaran, S. (2006), “Optimal mix for high performance concrete by evaluation strategies combined with neural network”, Indian Journal of Engineering & Materials Sciences, 13, pp. 7-17.
205. Ramachandran, V. S., and Beaudoin, J. J. (2008), “Handbook of analytical techniques in concrete science and technology: principles, techniques and applications”, William Andrew Publishing. USA.
206. Ramakrishnan, R. and Karunamoorthy, L. (2006), “Multi response optimization of wire EDM operations using robust design of experiments,” International Journal of Advance Manufacturing Technology, 29, pp. 105–112.
207. Raut, N. K. and Kodur, V. K. R. (2010), “Response of high-strength concrete columns under design fire exposure”, Journal of Structural Engineering, 137 (1), pp. 69-79.
208. Ravindrajah, R. S., Lopez, R. and Reslan, H. (2002, March), “Effect of elevated temperature on the properties of high strength concrete containing cement supplementary materials”, In 9th International Conference on Durability of Building Materials and Components, Brisbane, Australia.
209. Robert, F. and Colinay, H. (2009), “The influence of aggregates on the mechanical characteristics of concrete exposed to fire”, Magazine of Concrete Research, 61 (5), PP. 311–321.
210. Ross, P. J. (1988), “Taguchi techniques for quality engineering: loss function, orthogonal experiments, parameter and tolerance design”, McGraw-Hill book company.
211. Rougeron, P. and Aitcin. P. C. (1994), “Optimization of the composition of a High Performance Concrete.”, Cement, Concrete and Aggregates, ASTM Journal, 16 (2), pp. 115-124.
212. Roy, R. K. (1988), “A primer on the Taguchi method”, Van Nostrand Reinhold International Company Ltd. pp. 1-247.
213. Russell, H. G. (1999), “ACI defines high-performance concrete”, Concrete International-Detroit-, 21, 56-57.
214. Saad, S. A., Eneient, A. E., Hanna, G. B. and Kotkata, M. F. (1996), “Effect of temperature on physical and mechanical properties of concrete containing silica fume”, Cement and Concrete Research, 26 (5), pp. 669-675.

215. Sahin, R., Tasdemi, M. A., Gul, R. and Celik. C. (2007), "Optimization Study and Damage Evaluation in Concrete Mixtures Exposed to Slow Freeze–Thaw Cycles", Journal of Materials in Civil Engineering, ASCE, 19(17), pp. 609-615.
216. Sakr, K. and El-Hakim, E. (2005), "Effect of high temperature or fire on heavy weight concrete properties", Cement and concrete research, 35 (3), pp. 590-596.
217. Sancak, E., Sari, Y. D. and Simsek, O. (2008), "Effects of elevated temperature on compressive strength and weight loss of the light-weight concrete with silica fume and super-plasticizer", Cement and Concrete Composites, 30, pp. 715-721.
218. Sanjayan, G. and Stocks, L. J (1993), "Spalling of high strength silica fume concrete in fire", ACI Material Journal, 90 (2), pp. 170-173.
219. Sarshar, R and Khoury, G. A. (1993), "Material and environmental factors influencing the compressive strength of unsealed cement paste and concrete at high temperatures", Magazine of Concrete Research, 45 (162), pp. 51-61.
220. Schneider, U., Diederichs, U., and Ehm, C. (1981), "Effect of temperature on steel and concrete for PCRV's", Nuclear Engineering and Design, 67 (2), pp. 245-258.
221. Seleem, H. E. H., Rashad, A. M., and Elsokary, T. (2011), "Effect of elevated temperature on physico-mechanical properties of blended cement concrete", Construction and Building Materials, 25(2), 1009-1017.
222. Shariq, M., Prasad, J., Ahuja, A. K. (2012), "Optimization of concrete mix proportioning", International Journal of Emerging Technology and Advanced Engineering, 2 (7), pp. 22-28.
223. Sharma, A., Habib, G. and Matsagar, V. (2013), "Behaviour of High Performance Concrete with Marble Dust at Elevated Temperatures", The International Conference on Trends and Challenges in Concrete Structures, Ghaziabad, NCR Delhi, India, Dec 19 - 21.
224. Sharma, A., Habib, G. and Matsagar, V. (2013), "Durability Study on High Performance Concrete of M80 Grade with Marble Dust", Indian Concrete Institute-Innovative World of Concrete (ICI-IWC), Hyderabad, India, October 23-26.
225. Sharma, U. K., Zaidi, K. A., Bhandari, N. M, and Bhargava. P (2011), "Effect of Heating and Cooling Regimes on Confined Concrete in High Strength Concrete Columns", ACI SP-279-08, pp.1-36.
226. Sharma, U. K., Zaidi, K. A., Bhandari, N. M. (2012), "Strength and deformability of heated confined concrete", Magazine of Concrete Research, 64 (7), pp. 631-646.

227. Shin, K. Y., Kim, S. B., Kim, J. H., Chung, M., and Jung, P. S. (2002), "Thermo-physical properties and transient heat transfer of concrete at elevated temperatures", Nuclear Engineering and Design, 212 (1), pp. 233-241.
228. Short, N. R., Purkiss, J. A. and Guise, S. E. (2001), "Assessment of fire damaged concrete using colour image analysis", Construction Building materials, 15, pp. 9-15.
229. Shui, Z. H., Zhang, R., Chen, W. and Xuan, D. X. (2010), "Effects of mineral admixtures on the thermal expansion properties of hardened cement paste", Construction and Building Materials, 24(9), pp. 1761-1767.
230. Siddique, R., and Khan, M. I. (2011), "Supplementary cementing materials", Springer Heidelberg Dordrecht, London, New York.
231. Sideris, K. K., Manita, P. and Chaniotakis, E. (2009), "Performance of thermally damaged fibre reinforced concretes", Construction and Building Materials, 23 (3), pp. 1232-1239.
232. Sidibe, K., Duprat, F., Pinglot, M. and Bourret, B. (2000), "Fire Safety of Reinforced Concrete Columns", ACI Structural Journal, 97 (4), pp. 642-647.
233. Simon, M. J., Lagergren, E. S. and Snyder, K. A., (1997), "Concrete mixture optimization using statistical mixture design methods", Proceedings of the PCI/FHWA International Symposium on High Performance Concrete New Orleans, Louisiana, Oct. 20-22.
234. Simon, M., Snyder, K. and Frohnsdorff. G (1999), "Advances in concrete mixture optimization", Proceedings of the Concrete durability and repair technology conference, Editor: R. K. Dhir and McCrthy. M. J., University of Dundee, Scotland, U K, Thomas Telford Publishing, September 8-10.
235. Singh, H., and Kumar, P. (2006), "Optimizing multi-machining characteristics through Taguchi's approach and utility concept", Journal of Manufacturing Technology Management, 17 (2), pp. 255-274
236. Sobolev, K., (2004), "The development of a new method for the proportioning of high performance concrete mixtures", Cement and Concrete Composites, 26, pp. 901-907.
237. Soudki, K. A., El-Salakawy, E. F., and Elkum, N. B. (2001), "Full factorial optimization of concrete mix design for hot climates", Journal of Materials in Civil Engineering, ASCE, 13 (6), pp. 427-433.

238. Su and Tong (1997), “Multi-response robust design by principle component analysis”, Total Quality Management, 8(6), pp. 409-416.
239. Sullivan, P. J. E. and Sharshar, R. (1992), “The performance of concrete at elevated temperatures”, Fire Technology, 28 (3), pp. 240-250.
240. Suresh, N. (2002), “Flexural Strength of Concrete subjected to sustained elevated temperature”, Indian Concrete Institute Journal, India.
241. Suresh, N. (2006), “Studies on compressive strength of concrete subjected to sustained elevated temperature”, International Conference on Advances in Concrete Composites Structures (ICACS-2005) Jan 6-8, SERC,CSIR Campus, Taramani, Chennai, India.
242. Takeuchi, M., Hiramoto, M., Kumagai, N., Yamazaki, N., Kodaira, A. and Sugiyama, K. (1993), “Material properties of concrete and steel bars at elevated temperatures”, In 12th International Conference on Structural Mechanics in Reactor Technology, pp. 13-138.
243. Tan, O., Zaimoglu, A. S., Hinislioglu, S. and Altun, S. (2005), “Taguchi approach for optimization of the bleeding on cement-based grouts”, Tunneling and underground space technology, 20 (2), pp.167-173.
244. Tanyildiz, H. (2009), “Fuzzy logic model for prediction of mechanical properties of lightweight concrete exposed to high temperature,” Materials and Design, 30, pp. 2205–2210.
245. Tanyildizi, H. (2008), “Effect of temperature, carbon fibers, and silica fume on the mechanical properties of lightweight concretes”, New Carbon Materials, 23(4), pp. 339-344.
246. Tanyildizi, H. (2009), “Statistical analysis for mechanical properties of polypropylene fibre reinforced lightweight concrete containing silica fume exposed to high temperature”, Materials and Design, 30, pp. 3252-3258.
247. Tanyildizi, H. and Coskun, A. (2008[a]), “Performance of lightweight concrete with silica fume after high temperature”, Construction and Building Materials, 22, pp. 2124-2129.
248. Tanyildizi, H. and Coskun, A. (2008), “An experimental investigation of bond and compressive strength of concrete with mineral admixture at high temperatures”, The Arabian Journal of Science and Engineering, 33 (2B), pp. 443-449.

249. Tanyildizi, H. and Coskun, A. (2008[b]), "The effect of high temperature on compressive strength and splitting tensile strength of structural lightweight concrete containing fly ash", Construction and Building Materials, 22, pp.2269–2275.
250. Tao Ji, Tingwei Lin, Xujian Lin (2006), "A concrete mix proportion design algorithm based on artificial neural networks", Cement and Concrete Research, 36, 1399-1408.
251. Tenchev, R. and Purnell, P. (2005), "An application of a damage constitutive model to concrete at high temperature and prediction of spalling", International Journal of Solids and Structures, 42, pp. 6550–6565
252. Topcu, I. B. and IsIkdag, B. (2008), "The effect of cover thickness on rebars exposed to elevated temperatures", Construction and Building Materials, 22 (10), pp. 2053-2058.
253. Topcu, I. B. and Karakurt, C. (2008), "Properties of reinforced concrete steel rebars exposed to high temperatures", Advances in Materials Science and Engineering, Hindawi Publishing Corporation, pp. 1-4.
254. Turkmen I. Gul R. Celik C. Demrboga, Ramazan (2003), "Determination by the Taguchi method of optimum conditions for mechanical properties of high strength concrete with admixtures of silica fume and blast furnace slag", Civil Engineering and Environmental Systems, 20 (2), pp. 105-118.
255. Turkmen, I., Gul, R. and Celik, C. (2008), "A Taguchi approach for investigation of some physical properties of concrete produced from mineral admixtures", Building and environment, 43 (6), pp.1127-1137.
256. Unluoglu, E., Topcu, I. B. and Yalaman, B. (2007), "Concrete cover effect on reinforced concrete bars exposed to high temperatures", Construction and Building Materials, 21 (6), pp. 1155-1160.
257. Usmani, A. S., Rotter, J. M., Lamont, S., Sanad, A.M. and Gillie, M. (2001), "Fundamental principles of structural behaviour under thermal effects", Fire Safety Journal 36, pp. 721-744.
258. Uygunoglu, T. and Topcu, I. B. (2009), "Thermal expansion of self-consolidating normal and lightweight aggregate concrete at elevated temperature", Construction and Building Materials, 23, pp. 3063-3069.
259. Uysal, H., Demirboga, R., Sahin, R. and Gul, R. (2004), "The effects of different cement dosages, slumps, and pumice aggregate ratios on the thermal conductivity and density of concrete", Cement and concrete research, 34(5), pp. 845-848.

260. Uysal, M. (2012), “Taguchi and Anova approach for optimization of design parameters on the compressive strength of HSC”, Magazine of Concrete Research, 64 (8), pp.1-9.
261. Van Der Heijden, G. H. A., Van Bijnen, R. M. W., Pel, L., and Huinink, H. P. (2007), “Moisture transport in heated concrete, as studied by NMR, and its consequences for fire spalling”, Cement and concrete research, 37 (6), pp.894-901.
262. Van Geem, M. G., Gajda, J. and Dombrowski, K. (1997), “Thermal Properties of commercially available high-strength concretes”, Cement Concrete and Aggregates, 19 (1), pp. 38-53.
263. Vorechovska, D. (2008), “Relation between spalling behaviour and water content of concrete”, Building Research Journal, 56 (4), pp. 229-240.
264. Willam, K., Xi, Y., Lee, K. and Kim, B. (2009), “Thermal response of reinforced concrete Structures in nuclear power plants”, Report No. SESM No. 02-2009, Department of Civil, Environmental and Architectural Engineering, College of Engineering and Applied Science, University of Colorado at Boulder.
265. Wu, B., and Xu, Y. Y. (2009), “Behaviour of axially-and-rotationally restrained concrete columns with ‘+’-shaped cross section and subjected to fire”, Fire Safety Journal, 44 (2), pp. 212-218.
266. Wu, B., Li, Y. H. and Chen, S. L. (2010), “Effect of heating and cooling on axially restrained RC columns with special-shaped cross section”, Fire Technology, 46 (1), pp. 231-249.
267. Wu, B., Su, X. P. Li, H. and Yuan, J. (2002), “Effect of High Temperature on Residual Mechanical Properties of Confined and Unconfined High-Strength Concrete”, ACI Materials Journal, 99 (4), pp. 399-407.
268. Wu, H. J. and Lie, T. T. (1992), “Fire resistance of reinforced concrete columns experimental studies”, Internal Report No. 632, Institute for Research in Construction, NRC, Canada.
269. Xiangjun, D., Yining, D. and Tianfeng, W. (2008), “Spalling and Mechanical Properties of Fiber Reinforced High-performance Concrete Subjected to Fire”, Journal of Wuhan University of Technology-Material Science Edition.
270. Xiao, J., Xie, M. and Zhang, C. (2006), “Residual compressive behaviour of pre-heated high performance concrete with blast-furnace slag”, Fire Safety Journal, 41 (2), pp. 91-98.

271. Xiao, J. and Falkner, H. (2006), "On residual strength of high-performance concrete with and without polypropylene fibres at elevated temperatures", Fire Safety Journal, 41, pp. 115–121.
272. Xiao, J. and Konig, G. (2004), "Study on concrete at high temperatures in China-an overview", Fire Safety Journal, 39(1), pp. 89-103.
273. Xing, Z., Beaucour, A.-L., Hebert, R., Noumowe, A. and Ledesert, B. (2010), "Behaviour at high temperature of concretes prepared with flint, quartzite or limestone aggregates", Structures in fire- proceedings of 6th international conference, SiF'10, June 2-4, pp. 759-766.
274. Xu, Y. and Chung, D. D. L. (2000[a]), "Effect of sand addition on the specific heat and thermal conductivity of cement", Cement and concrete research, 30(1), pp. 59-61.
275. Xu, Y. and Chung, D. D. L. (2000[b]), "Cement of high specific heat and high thermal conductivity, obtained by using silane and silica fume as admixtures", Cement and concrete research, 30 (7), 1175-1178.
276. Xu, Y., Wong**. Y.** L., Poon, C. S. and Anson, M. (2001), "Impact of high temperature on PFA concrete", Cement and Concrete Research, 31, pp.1065–1073.
277. Yan, X., Li, H. and Wong, Y.L. (2007), "Effect of aggregate on high-strength concrete in Fire", Magazine of Concrete Research, 59 (5), pp. 323–328.
278. Yang, E. H., Sahmaran, M., Yang, Y. and Li, V. C. (2009), "Rheological control in production of engineered cementitious composites", ACI Materials Journal, 106 (4), pp. 357-366.
279. Yang, C. Hung, S. W. (2004), "Optimizing the thermoforming process of polymeric foams: an approach by the Taguchi method and the utility concept", International Journal of Advance Manufacturing Technology, 24, pp. 353-360.
280. Yaragal, S. C., Babu Narayan, K. S., Venkataramana, K., Kulkarni, K. S., Chinnagiri Gowda, H. C., Reddy, G. R. and Sharma, A. (2010), "Studies on normal strength concrete cubes subjected to elevated temperatures", Journal of Structural fire Engineering, 1(4), pp. 249-262.
281. Yeh, I. C. (1999), "Design of high-performance concrete mixture using neural networks and nonlinear programming", Journal of Computing in Civil Engineering, 13, (1), pp. 36-42.

282. Yoo, S. H., Shin, S. W. and Kim, I. K. (2006), "Optimum PP fiber dosage for the control of spalling of high strength reinforced concrete columns", International Journal of Concrete Structure and Materials, 18 (2E), pp. 103-109.
283. Youssef, M. A. and Moftah, M. (2007), "General stress–strain relationship for concrete at elevated temperatures", Engineering Structures, 29, pp. 2618-2634.
284. Yuzer, N., Akoz, F. and Ozturkb, L. D. (2004), "Compressive strength-colour change relation in mortars at high temperature", Cement and Concrete Research, 34, pp. 1803-1807.
285. Zaidi, K. A., Sharma, U. K. and Bhandari, N. M. (2012), "Effect of temperature on uni-axial compressive behaviour of confined concrete", Fire Safety Journal, 48, pp. 58–68.
286. Zaidi, S. K. A. (2011), "Residual compressive behaviour of confined concrete subjected to elevated temperatures", Ph. D Thesis, Department of civil Engineering, Indian Institute of Technology Roorkee, Roorkee, India, pp. 219.
287. Zain, M. F. M., Islam, M. N. and Basri. I. H. (2005), "An expert system for mix design of high performance concrete", Advances in Engineering Software, 36, pp.325-337.
288. Zeiml, M., Leithner, D., Lackner, R. and Mang, H. A. (2006), "How do polypropylene fibers improve the spalling behavior of in-situ concrete?", Cement and Concrete Research, 36, pp. 929–942.
289. Zhang, B. (2011), "Effects of moisture evaporation (weight loss) on fracture properties of high performance concrete subjected to high temperatures", Fire Safety Journal, 46 (8), pp. 543-549.